

# STRENGTH AND STRUCTURE OF STEEL AND OTHER METALS

BY

W. E. DALBY, F.R.S.

Assoc. Memb. of Council Inst.N.A., M.Inst.C.E., M.I.Mech.E., M.A., B.Sc.  
London University Professor of Engineering at the City and  
Guilds Engineering College of the Imperial College  
of Science and Technology

LONDON

EDWARD ARNOLD & CO.

1923

*[All Rights Reserved]*

## PREFACE

A few years ago (1911) the idea occurred to me that the usual load-extension diagram of a metal test piece drawn by a pencil on a paper drum could be made a much more valuable record of the quality of metal if the record could be freed from frictional and inertia errors.

On thinking the matter over it occurred to me that photography offered freedom from friction and a steel bar used as a spring offered freedom from inertia. A beam of light focused to a point, moving so that the point of light traces the diagram on a sensitised film, is infinitely delicate compared with a pencil point, however sharp and burnished, rubbing over a sheet of paper however smooth. A steel bar weighs a load by its own extension, and since this extension is only a few hundredths of an inch for the greatest load which it is used to weigh, its inertia is negligible, compared with the inertia of the beam and jockey weight of a testing machine.

I designed a self-contained recording instrument, which combined a steel bar with optical and photographic parts, suitable for placing between the shackles of an ordinary testing machine of the beam type. The first diagram taken with the instrument was good, and subsequent instruments contain only modifications of design to ensure rapidity of setting up and handling. With the instrument records were taken of a large number of metals and these records showed that all expectations were exceeded. The shapes of the load-extension curves proved to be sensitive to quality in a surprising degree.

I next designed and constructed an instrument to record elastic extension. There were many mechanical difficulties, but these were overcome. Recently I have designed a third instrument to record the elastic properties of a metal in torsion. The record is a torque-twist curve.

Thus three recorders have been standardized, namely—



- (1) A recorder giving the complete load-extension diagram from no load to fracture. This record is taken on a  $\frac{1}{2}$ -plate negative and the full 6 in. of the plate corresponds to  $1\frac{1}{2}$  in. extension of the gauge length.
- (2) An elastic recorder showing the first  $\frac{4}{100}$  inch extension of the gauge length on the record.
- (3) An elastic torsion recorder showing a torque-twist curve on the record.
- (4) In addition I have designed a small testing machine suitable for applying an axial pull to the Load Extension Instruments in the simplest way possible and with easy and rapid control. In this machine a test piece can be broken in a fraction of a second and a complete record obtained from no load to fracture. But its special use is for elastic tests made by the elastic recorder.

Many records of metals of all kinds have been taken with this research plant. A comparison of these records led me to the conclusion that the accurate Load Extension and Torque Twist diagrams correlated the properties of metals which now have to be established by a series of separate tests. To take a record with any of these three instruments is a matter of a few minutes only, and these records give information which has hitherto taken hours, or even days, to obtain with the usual instruments. The records have all the accuracy needful in practice.

The correlation of existing tests with the records covers a wide field of research and will take time to explore, but so far the results are most encouraging. A load extension record of a metal is constant so long as the quality is constant. The slightest change in quality, or even a change in a manufacturing process, which is perhaps without detriment to the qualities sought, is made manifest by delicate differences in shape of the load extension curve.

In recent years a new science has come into being, the Science of Metallography. Its frontiers are continually widening, new data are being obtained and new ideas and speculations are being ventilated. There is, however, a bulk of established data at the disposal of the engineer. Metallography gives optical and thermal methods as new tests of quality as well as the constitutional diagram from which so much can be learnt. The standard works on Metallography must be consulted to gain an idea of the extent of the ground already covered by this new science. All I have endeavoured to do in this book is to consider

the subject from the angle of view of an engineer and to discuss it as far as possible in the language of an engineer.

The general plan of this book is to compare methods of testing and to correlate the results by means of the Load Extension diagram, and to record the results of my own researches on the strength and structure of metals with the instruments above mentioned. Although the comparison and correlation is necessarily incomplete, yet the results may be useful to members of the engineering profession and to students of engineering.

Chapter I is a brief review of quality tests in use, including the test of the microscope, but excluding any chemical test.

Chapter II brings before the reader facts about the metals ordinarily in use by engineers. The load extension diagram of each metal chosen for test is shown above a microphotograph of its inner structure magnified 150 times. With few exceptions, the structure seen is that of the everyday metal taken from stock.

In Chapter III attention is concentrated on the Load Extension diagram and the development by its aid of the law of similarity as applied to the testing of metals.

In Chapter IV attention is concentrated on some of the facts and principles of Metallography. By their aid the microphotographs given in Chapter II are interpreted and the Constitutional diagram for iron and steel is explained. The door is only just opened to give the student a glimpse of this wondrous new science whose history is recorded in the Reports of the Alloys Research Committee of the Institution of Mechanical Engineers. The first report is dated 1891 and the eleventh report is dated 1922, and the research is still in progress.

In Chapter V research on the elastic properties of metals are brought together and the looped elastic diagram and its powers are discussed. It is shown that every metal furnishes a characteristic loop after overstrain. The loop is described by merely removing the load and then re-applying it. The area represents work done on the inner structure. The loop area furnishes a new test of quality, and if a succession of loops are taken of the same material the rate of increase of the loop area furnishes a second test of quality. These two new data are characteristic of a metal, and the work correlating them with the quality of the metal is still proceeding.

There is one property of metal which is investigated in this chapter and which exerts a powerful influence on both strength and structure, and that is the power of the metal to re-crystallize.

A breakdown of the inner structure can heal itself by crystal growth. The growth may be rapid or slow ; it may take place at ordinary temperatures or at high temperatures, but the power to grow is latent in the metal and is a vitally important property of the metal.

Chapter VI is added to give useful information to designers. The work was done and communicated to the Sub-Committee on Screw Threads of the British Engineering Standards Association in 1917.

The record of the researches really begins with Chapter II, so that readers who are familiar with the usual methods of testing can omit Chapter I.

My thanks are due to Mr. E. F. D. Witchell for kindly reading the proofs ; to Dr. J. V. Howard and Dr. S. L. Smith for their careful chemical analysis of the metals tested, and to Mr. Orr, who has skilfully reduced the load 'extension diagrams from the originals on a common scale or to the scale shown in the book.

# CONTENTS

## CHAPTER I

### QUALITY TESTS

SECT.	PAGE
1 Introduction . . . . .	1
2 The Tensile Test . . . . .	2
3 The Shock Test . . . . .	5
4 The Notched Test-Piece . . . . .	6
5 The Charpy Shock Testing Machine . . . . .	7
6 The Brinell Test for Hardness . . . . .	9
7 The Shore Scleroscope Test for Hardness . . . . .	11
8 The Scratch Test for Hardness . . . . .	12
9 Wear Test of Hardness . . . . .	13
10 Wear Test by Dry Rolling. The Saniter Test . . . . .	13
11 Wear Test by Dry Sliding . . . . .	14
12 Hardness . . . . .	14
13 The Fatigue Test . . . . .	16
14 The Examination of the Inner Structure of Metals . . . . .	25
15 The Load Extension Diagram . . . . .	30
16 Definition of the Load-extension Diagram . . . . .	31
17 Autographic Recorders . . . . .	31
18 The Dalby Optical Recorder . . . . .	31
19 Description of Standard Type of Dalby Recorder . . . . .	33
20 The Optical Cell . . . . .	35
21 Adjusting the Zero . . . . .	35
22 Calibration of the Weigh Bar . . . . .	36
23 Calibration of the Extensometer . . . . .	36
24 Special Testing Machine for Use with the Instrument . . . . .	37

## CHAPTER II

### LOAD-EXTENSION DIAGRAMS AND INNER STRUCTURE OF METALS IN COMMON USE

25 General Remarks . . . . .	39
26 Swedish Iron . . . . .	40
27 Yorkshire Iron . . . . .	42

SECT.	PAGE
28 Staffordshire Iron . . . . .	43
29 Yorkshire Iron and the Puddling Process . . . . .	43
30 Mild Steel . . . . .	50
31 Steel . . . . .	51
32 Bright Drawn Steel . . . . .	52
33 Bright Drawn Steel Heat-treated . . . . .	54
34 Mild Steel . . . . .	54
35 Pearlite . . . . .	55
36 Heat Treatment reduces the Block Size of Steel . . . . .	57
37 Strength and Inner Structure of Mild Steel . . . . .	57
38 Nickel Steel . . . . .	58
39 Chrome Nickel Steel . . . . .	59
40 Tin and Zinc . . . . .	60
41 Copper . . . . .	61
42 Brass . . . . .	62
43 Gun Metal and Phosphor Bronze . . . . .	64
44 Cast Iron . . . . .	65

## CHAPTER III

COMPARISON OF TABULATED RECORDS OF  
STRENGTH AND DUCTILITY

45 Influence of Gauge Length on the Figures of Strength and Ductility . . . . .	67
46 Form of Test Piece . . . . .	70
47 Ductility and the Principle of Similarity . . . . .	71
48 Ductility Measured by the Percentage Extension produced by the Maximum Load . . . . .	74
49 Approximate Expression for the Extension . . . . .	75

## CHAPTER IV

## THE INNER STRUCTURE OF METALS

50 The Block Structure . . . . .	77
51 The Structure of the Blocks Themselves . . . . .	78
52 Crystalline and Amorphous Material . . . . .	79
53 Permanence of the Crystalline Structure . . . . .	80
54 Recrystallization and Annealing . . . . .	80
55 Change of Inner Structure. Allotropic Modifications . . . . .	84
56 Cooling Curves. Recalescence. . . . .	85
57 Temperature Concentration Diagram of Alloys . . . . .	91
58 Temperature Concentration Diagram of the Iron Carbon Alloys . . . . .	105
59 Interpretation of Microphotographs . . . . .	109
60 The Rate of Cooling . . . . .	117
61 Heat Treatment . . . . .	118

# CONTENTS

ix

## CHAPTER V

### THE ELASTIC AND PLASTIC STATES OF METALS

SECT.	PAGE
62 General Properties . . . . .	122
63 The Dalby Optical Recorder of Load and Elastic Extension . . . . .	123
64 Typical Looped Diagram . . . . .	124
65 Information to be Gained from a Looped Diagram of Material in its Normal State . . . . .	127
66 Looped Diagrams of Various Metals . . . . .	128
67 Loop Area and Permanent Set . . . . .	134
68 Curves of Loop Area and Permanent Set . . . . .	135
69 Influence of Time . . . . .	136
70 Looping under Constant Load . . . . .	139
71 The Practical Utility of the Looped Diagram . . . . .	140
72 Push and Pull Diagrams . . . . .	141
73 The Yield in Compression . . . . .	144
74 Torque Twist Diagram . . . . .	145
75 The Dalby Torque Twist Recorder . . . . .	148
76 Comparisons and Conclusions . . . . .	150
77 Working Stress and Factors of Safety . . . . .	156

## CHAPTER VI

### STRENGTH OF SCREW THREADS

78 The Scope of the Research . . . . .	158
79 Comparison of the Strengths of Threads of Different Lengths : Whit- worth Form . . . . .	159
80 Comparison of the Control Curves . . . . .	165
81 Influence of the Form of Thread on Strength . . . . .	166
82 Manner of Thread Failure . . . . .	169
83 Inner Structure of Deformed Thread . . . . .	173
INDEX . . . . .	174

## PLATES

	FIGS.		TO FACE PAGE
I	4	The Charpy Shock-testing Machine . . . . .	7
II	10	Microphotographic Apparatus . . . . .	29
III	11, 12	The Dalby Recorder . . . . .	34
IV	13	The Recorder in a Testing Machine . . . . .	35
V	14, 15	Load and Extension Scales of 15-ton Recorder . . . . .	36
VI	16-17	Hydraulic Machine for Use with Dalby Recorder . . . . .	37
VII	18-20	Swedish Iron . . . . .	40
VIII	21-23	Yorkshire Iron . . . . .	42
IX	24-26	Staffordshire Iron . . . . .	43
X	27-29	Mild Steel . . . . .	50
XI	30-32	Steel . . . . .	51
XII	33-35	Bright Drawn Steel . . . . .	52
XIII	36-38	Bright Drawn Steel . . . . .	53
XIV	39-42	Bright Drawn Steel. Heat-treated . . . . .	54
XV	43-45	Mild Steel, containing 0.1 per cent. Nickel . . . . .	55
XVI	46, 47	Hadfield Steel (Annealed) . . . . .	57
XVII	48-53	Nickel Steel . . . . .	58
XVIII	54, 55	Chrome Nickel Steel . . . . .	59
XIX	56-59	Tin and Zinc . . . . .	60
XX	60-63	Copper . . . . .	61
XXI	64-68	60-40 Brass . . . . .	62
XXII	69-73	70-30 Brass . . . . .	63
XXIII	74-77	Gun Metal and Phosphor Bronze . . . . .	64
XXIV	78, 79	Cast Iron . . . . .	65
XXV	83	Forms of Test Pieces . . . . .	70
XXVI	84	Effect of Flanges and Shoulders on Extension . . . . .	71
XXVII	88, 89	Swedish Iron . . . . .	80
XXVIII	90-93	70-30 Brass . . . . .	81
XXIX	94, 95	Gun Metal and Phosphor Bronze . . . . .	82

	FIGS.		TO FACE PAGE
XXX	106-109	Carbon Steel . . . . .	110
XXXI	110	Grey Iron . . . . .	111
XXXII	111-114	Pig Iron . . . . .	114
XXXIII	115, 116	Pig Iron . . . . .	115
XXXIV	117, 118	Mild Steel . . . . .	117
XXXV	120	The Dalby Optical Recorder of Load and Elastic Extension . . . . .	123
XXXVI	149	The Dalby Torque Twist Recorder . . . . .	148
XXXVII	151-154	Swedish Iron . . . . .	152
XXXVIII	168, 169	Inner Structure of Deformed Screw Thread . . . . .	173

## FOLDING DIAGRAMS

Figs. 136-139	Curves of Loop Area and Permanent Set . . . . .	136
Fig. 140	Loop Area plotted against Permanent Set . . . . .	136



# STRENGTH AND STRUCTURE OF STEEL AND OTHER METALS

## CHAPTER I

### QUALITY TESTS

**1. Introduction.**—The engineer relies mainly on circumstantial evidence when forming his judgment of the quality of a material. Circumstantial evidence of quality is obtained by cutting a piece from the material and testing the piece to destruction. The evidence is therefore necessarily circumstantial because material used in construction can never itself be tested to destruction. When judging of the quality of the whole from a test made on a small part uniformity of quality is necessarily assumed. A bar of steel is judged to be of good quality if a test piece cut from it is found of good quality. A boiler plate is judged to be of good quality when strips cut from it are found of good quality. In both examples composition, strength, and inner structure are assumed to be uniform throughout the bar and the plate.

Tests of quality are multiplied to give corroborative evidence. For example, if a steel test piece breaks in tension, extends, and reduces in area at fracture according to the quality required of it, the evidence, as far as it goes, is, that the material from which the test piece was cut is good. This evidence may be corroborated by a good "impact number," the number which expresses the resistance of a second test piece to fracture by blows. If the "impact number" is low, notwithstanding that the tensile test is good, the quality of the material is doubtful. Chemical evidence of composition is obtained from the analysis of a few grams of metal drilled from the bar.

Evidence of inner structure is obtained with the microscope. Evidence of hardness is obtained from indentation tests or from various kinds of scratching tests.

I have strong reason to believe that the evidence furnished by these various tests can be correlated by accurate curves of load and extension, giving what are called **Load-extension** and **Torque-twist Diagrams**. This book relates mainly to researches made with the author's **Optical Recorders**, by means of which accurate load-extension or torque-twist diagrams can be taken. Before describing my apparatus and the researches made with it, it will be convenient to bring under brief review some of the methods in common use for testing the quality of materials.

**2. The Tensile Test.**—Tensile strength is tested by stretching a test piece until it breaks.

Figs. 1 and 2 show a testing machine in which load is applied to a test piece *T* by hydraulic power and is measured by a steel-yard. The test piece is held between grips *G G*, the upper one of which hangs from the steel yard, whose fulcrum is *H*. The jockey weight *J* is travelled along the beam by turning the hand-wheel *W* or alternatively by power applied by belts through the pulleys *P* at the top of the machine. A vernier *A* is bolted to the jockey weight, and readings of the load are taken on the scale *C* bolted to the beam.

Let *J* be the weight of the jockey *J* and let  $x_1$  be the distance of its centre of gravity from the fulcrum, when  $F_1$  is the force exerted by the hydraulic cylinders through the test piece on to the beam, and let this force be applied to the beam at a distance of *a* inches from the fulcrum.

Let *B* be the weight of the beam and *b* the distance of its centre of gravity from the fulcrum. Then, when the beam stands level and motionless, the equation of equilibrium is

$$Jx_1 = F_1a + Bb \quad . \quad . \quad . \quad . \quad (1)$$

Also  $Jx_2 = F_2a + Bb \quad . \quad . \quad . \quad . \quad (2)$

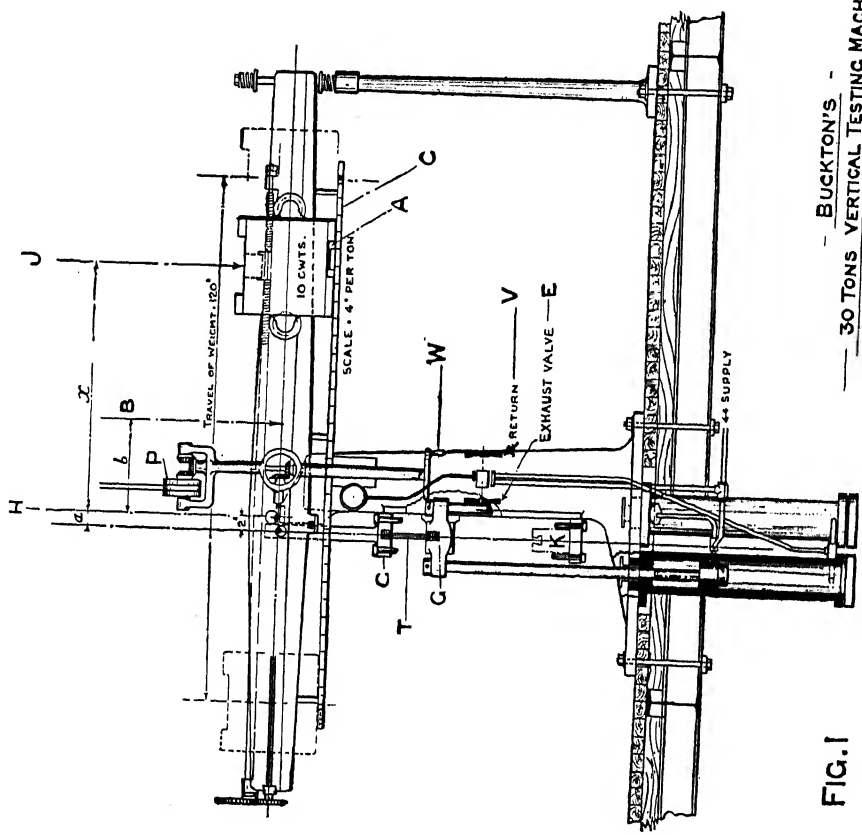
for a distance  $x_2$  and corresponding load  $F_2$ .

So that  $J(x_1 - x_2) = a(F_1 - F_2) \quad . \quad . \quad . \quad . \quad (3)$

From (3) the change of position  $x_1 - x_2$  of the jockey weight, corresponding to a change of load  $F_1 - F_2$ , gives the scale of the steelyard. The distance  $x_0$  of the zero of the scale is found from (1), putting  $F_1 = 0$ , giving

$$x_0 = \frac{Bb}{J} \quad . \quad . \quad . \quad . \quad . \quad (4)$$

In the machine illustrated the beam weighs about 2212 lb. and its centre of gravity is about 20.52 inches from the fulcrum.



— BUCKTON'S —  
— 30 TONS VERTICAL TESTING MACHINE —

FIG. 1

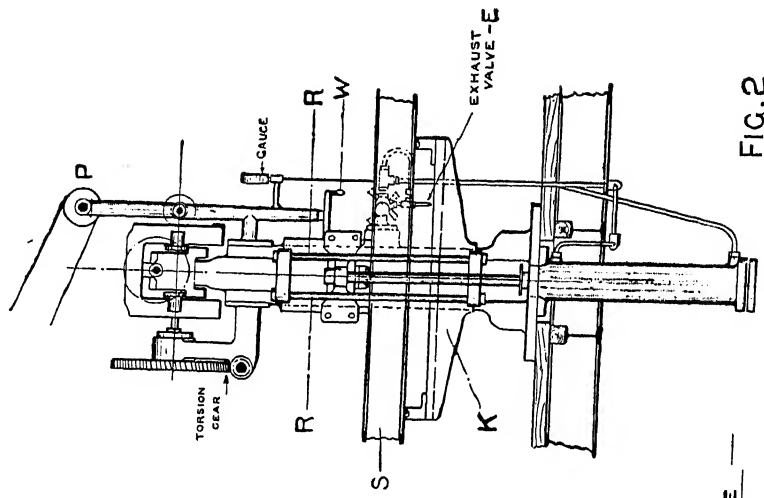


FIG. 2

The jockey weighs 1120 lb. and  $a$ , the distance of the line of load from the fulcrum, is 2 inches. From (3) the scale of graduation is 4 inches per ton, and from (4) the zero of the scale is 40.5 inches to the left of the fulcrum. In practice the beam is balanced before putting in the test piece, after which the vernier on the jockey weight is adjusted to read zero on the scale bolted to the beam.

Load is applied from two hydraulic cylinders each 30.68 square inches area and designed for a water pressure of 1500 lb. per square inch. The piston rods are connected directly to the grip box, and this is guided vertically by a machined vertical bed on the frame of the machine. Loading is controlled by the valves E and V. The top of each cylinder is connected permanently to the hydraulic main, so that pressure is acting all the time to force the pistons down. The bottom of each cylinder is connected through the valve E with the drain or exhaust pipe. With E closed the pressure on top of the pistons merely compresses the water in the bottom of the cylinders. Open E, and the water begins to escape, and the pressure on the top of the pistons then loads the test piece. The rate at which stretching takes place is regulated by the rate at which water is allowed to flow away through the exhaust valve.

X. To bring the pistons up, the exhaust valve E is closed, and an equilibrium valve V is opened. The opening of V puts both sides of the pistons in connection with the water main. The area of the bottom of the piston is greater than the area of the top by the area of the piston rod. The difference is about 5 square inches. This multiplied by the main pressure, 1500 lb., gives an unbalanced upward push of 7500 lb. The pistons are hydraulically locked at any point of the upward stroke immediately the valve V is closed. The control is simple and rapid, and the rate of stretching can be varied within wide limits.

For bending tests a cross girder K (Fig. 2) is slung from the steelyard by four rods, two of which, RR, can be seen. A length of steel joist is seen on the girder, loaded centrally by a pull from the cylinders. A compressive test can be applied to a test block placed in the sling below the crosshead of the hydraulic pistons. Apparatus is also fitted to the machine for torsion-testing and for testing in shear.

Many machines of this type are in use for routine testing in laboratories and factories. A more uniform application of the load can be obtained by interposing an intensifier between the hydraulic cylinders of the machine and a low-pressure water main.

This is often done when the town main is the only source of supply. A finely graduated and steady loading can be obtained by using a water intensifier in which a ram is pushed in by screws turned either by hand or by power. In this apparatus the water is forced from the intensifier cylinder into the machine cylinders uniformly and at as slow a rate as may be desired. As the ram is withdrawn the water is forced back by a weight with which the cylinder ram is loaded permanently.

Water power is in some types dispensed with, and loading is applied through screws turned by hand for small machines and by motors in large machines. Many combinations are possible. What is required in a design is mechanism for stretching the test piece, with power of variation of the rate of stretching within wide limits. In some types of machine the single beam is replaced by a compound steelyard. A compound steelyard is used in the 100-ton horizontal machine made by Messrs. J. Buckton and Co., of Leeds.

The usual tensile test of a piece of mild steel furnishes four data. These are :—

1. The load at which the material passes from a quasi-elastic to a plastic state. This is called the yield load and is indicated by a sudden dropping of the beam towards the stop.
2. The maximum load carried by the test piece.
3. The extension of the gauge length of the test piece.
4. The diameter of the fracture.

The results usually reduced from these data are :—

Yield stress, found by dividing the yield load by the original area of the bar.

The stress corresponding to the maximum load or ultimate stress or tenacity as it is alternatively called, found by dividing the maximum load by the original area of the bar.

Extension, reduced to percentage of the original gauge length.  
Reduction of area reduced to percentage of the original area of the bar.

Example.—Maximum load, 5.75 tons. Yield load, 4.4 tons.

Diameter of bar, 0.447 inch. Diameter of fracture, 0.315 inch. Gauge length, 5 inches; after fracture, 6 inches.

Yield stress = 28 tons per square inch.

Ultimate stress = 36.7 tons per square inch.

Extension, 20 per cent. on 5 inches.

Reduction of area, 50.3 per cent.

**3. The Shock Test.**—The shock-resisting quality of a material is inferred from its resistance to fracture under a blow.

A test piece is supported as a beam under a raised weight, and the weight, when released, falls, hits the piece, and bends or breaks it. The energy of the blow is expended mainly in breaking the test piece and therefore the energy of the blow is taken as a measure of the shock-resisting quality of the test piece. Rails have generally been tested by shock although the blow is regulated to deflect without breaking. A test piece about 5 feet long is cut off a rail and is placed on supports 3 feet 6 inches apart under a raised weight weighing 1 ton. Quality is inferred from the deflections at the centre produced by two successive blows, the first from a height of 7 feet, the second from a height of 20 feet. The central deflection produced by the first blow should be between  $\frac{7}{8}$  and  $1\frac{3}{16}$  inches: from the second blow between 3 and  $4\frac{1}{4}$  inches. These are the heights and deflections prescribed by the Engineering Standards Committee for rails weighing 100 lb. per yard. The height of fall and deflection produced are varied with the weight of the rail per yard.

The tensile test prescribed for this steel is an ultimate strength between 40 and 48 tons per square inch, an elongation of not less than 15 per cent. on a gauge length of 2 inches, when the area of the test piece is  $\frac{1}{4}$  square inch, or on a gauge length of 3 inches when the area of the test piece is  $\frac{1}{2}$  square inch. The prescribed chemical constitution gives carbon between 0.35 and 0.5 per cent.

**4. The Notched Test Piece.**—Shock testing has extended rapidly during recent years to test material used for the parts of machinery subject to vibratory loading. In general the blow given to the test piece is intended to break it. And to localize the blow the test piece is notched at the centre.

The Charpy test piece is a bar 10 × 10 mm. square and 54 mm. long, notched at the centre to a depth of 5 mm. leaving a cross section of half a square centimetre to be broken. The radius of the bottom of the notch is  $\frac{2}{3}$  mm. The notch is made by drilling a hole 1.33 mm. diameter and then sawing down to it. The test piece is shown in Fig. 3.

This test piece, together with a second three times as large in every dimension, was recommended as a standard at the New York meeting of the International Association for Testing Materials in 1912. This test piece is widely though not universally used. Even when a test piece is made to the Charpy dimensions it is frequently notched differently. Probably the difficulty of drilling such a small hole as  $1\frac{1}{3}$  mm. diameter in hard material has led to the use of a V notch with a definite radius at the bottom. The British Engineering Standards

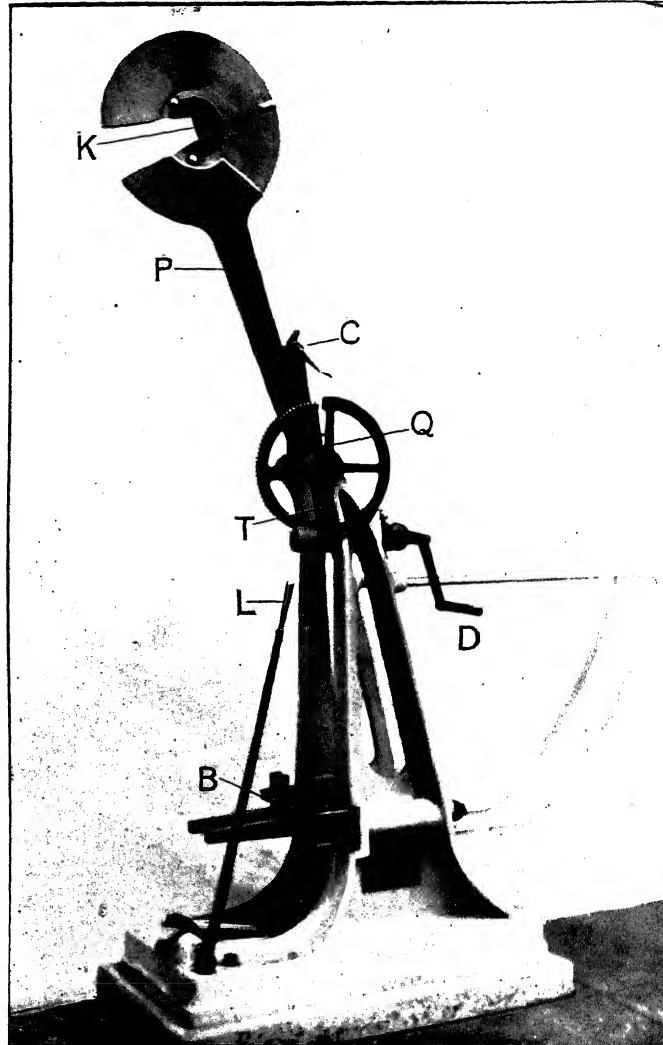


FIG. 4.—Charpy Shock-testing Machine.

Weight of Pendulum =  $W = 22.455$  kilograms.

Radius of C. of Gravity =  $0.692$  metres.

Height of C. of Gravity in initial position =  $H = 1.336$  m =  $(158\frac{1}{2}^\circ)$ .

Energy of Blow = say  $30$  k.m.

Energy expended in breaking the specimen:  $30 - 15.53$  vers. R. Kilogram-metres.

Association recommend a V notch, 45 degrees, finished at the bottom with a radius of 0.25 mm.<sup>1</sup> The test piece is seen in Fig. 3. Experience has shown that the radius of the bottom of the notch has considerable influence on the resistance of the test piece to fracture under the blow.

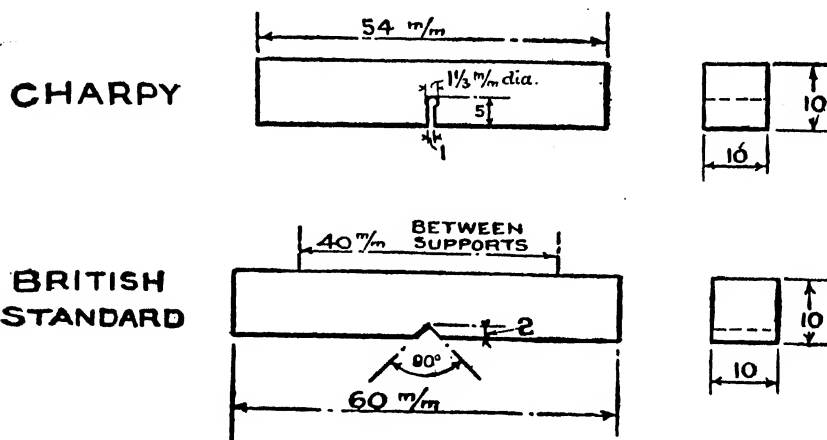


FIG. 3.—Notched Test Pieces.

5. The Charpy Shock-testing Machine.—This is shown in Fig. 4. A pendulum P, mounted in ball bearings, when released by the catch C, swings down on the test piece supported as a beam in the anvil block B, breaks it, passes on, and remounts to a definite height, from which it swings backwards and forwards until brought to rest by the brake strap just beneath it, which is operated by the handle L. The blow is struck by the centre of the blunt knife-edge K, on the side of the test piece opposite the notch, so that the bottom of the notch resists the blow by tension. A short arm ending with a catch C and geared with the handle D is provided for raising the pendulum. D is turned to bring the arm down until the catch C engages the pendulum. D is then turned to raise the arm and with it the pendulum, until the gear runs against a stop, which defines the initial position.

The energy expended in breaking the test piece is  $W(H-h)$ , where  $H$  is the height from which the centre of gravity falls and  $h$  the height to which it remounts after the blow. Both heights are measured from the lowest position of the centre of gravity. The height from which the pendulum falls is constant in its initial angular position, being always  $158\frac{1}{2}$  degrees from the vertical.

<sup>1</sup> Report on British Standard Forms of Notched Bar Test Pieces. Crosby Lockwood & Son, London, 1920.



The height to which the pendulum remounts is calculated from the angle indicated by the pointer T on the scale fixed to the framework. This pointer is loose on its shaft and is engaged by the arm Q and pushed to the highest angular position to which the pendulum remounts.

The pendulum weighs 22.455 kg. Its centre of gravity is 0.692 m. from the axis of suspension. The height H of the centre of gravity in the initial position is 1.336 m. Inserting values corresponding to these data in the expression above, and neglecting small corrections, the energy E absorbed by the test piece is

$$E = 30 - 15.53 \text{ vers } R \text{ kilogram-metres} \quad . \quad . \quad (1)$$

R is the angle of remount in degrees.

The **Impact Number** defined by Charpy is the energy calculated from equation (1) divided by the area of the section broken. The impact number is therefore a quotient giving kilogram-meters per square centimetre. Experiments show that the energy required to break a test piece is not strictly proportional to the area broken, so that it is better to use a standard test piece and record the energy of the blow as the impact number.

The **Izod Shock-testing Machine** is of the pendulum type. It is described in *Engineering*, September 25, 1903. The test piece is held in a vice and resists the blow as a cantilever. The test piece recommended is  $\frac{3}{8}$  inch wide,  $\frac{3}{16}$  inch thick notched with a V to a depth of 0.05 inch: the radius at the bottom of the V is 0.01 inch. The pendulum of the machine described possesses 23 ft.-lb. of energy at the instant of hitting.

Captain Sankey, in *Proc. Inst. Mech. E.*, No. 1, 1904, page 160, gives the results of breaking ninety-eight test pieces in the Izod Machine, and in *Proc. Inst. Mech. E.*, Part 4, 1904, gives the results of breaking test pieces of Chrome Vanadium Steel.

Mr. Seaton<sup>1</sup> and Mr. Jude, advocate breaking the test piece by a succession of blows, the test piece to be turned over after each blow. A vertical rod, freely guided and loaded so that it weighs 6 lb., is lifted through 24 inches and let fall on to the test piece supported as a beam below it. The energy per blow is thus 144 inch-pounds. The test piece is 4 inches long,  $\frac{1}{2}$  inch  $\times$   $\frac{1}{2}$  inch cross-section, and is notched with a V of about 60 degrees to a depth of  $\frac{1}{8}$  inch. The number of blows required to break the test piece is taken to represent the shock-resisting quality of the material. Forged steel of good quality is stated

<sup>1</sup> "Impact Tests on Wrought Steels of Commerce," *Proc. Inst. Mech. E.*, Part 4, 1904,

to take thirty blows. The authors give a table on page 1147 of the paper, stating the number of blows required to break test pieces made of steel of different qualities.

**6. The Brinell Test for Hardness.**—A steel ball placed on a flat surface of a material softer than itself, and pressed into it, makes a saucer-like pit which remains when the pressure is removed provided that the pressure has been sufficient to cause plastic deformation of the material as the ball penetrates into it. The hardness of the material is considered to be proportional to the load and inversely proportional to the size of the pit.

To arrange materials in a scale of hardness either the load must be kept constant and then the size of the pit measured, or the load must be found which produces a pit of specified size. It is usual to keep the load constant. Brinell recommends a standard load of 3000 kilograms for steel, 500 kilograms for softer materials like copper, and 50 kilograms for wood. The load is applied to a hard steel Hoffmann ball 10 mm. diameter. Loading is maintained for 30 seconds on steel. It is necessary to specify a time because plastic deformation creeps slowly under constant load.

The **Brinell Hardness Number** is found by dividing the standard load in kilograms by the area in sq. mm. of the surface of the pit produced. The hardness number is therefore the average stress in kilograms per square mm. between the ball and the surface of the pit produced in a definite time. This hardness number, multiplied by 0.635, gives the average stress in tons per square inch.

It is the practice to consider the area of the surface of the pit as equivalent to the area of a spherical segment of radius equal to the radius of the ball, thus neglecting the slight error due to the compression of the ball itself. This area may be calculated either from a measurement of the depth of the pit, or from a measurement of the diameter of the pit taken at the surface level.

Let  $D$  be the diameter of the ball and  $P$  the load producing a pit,  $h$  mm. deep, and  $d$  mm. diameter. Then the area of the surface of the pit is

$$A = \pi D h = 31.4 h \text{ for a 10 mm. ball,}$$

or alternatively, since  $h = \frac{1}{2} (D - \sqrt{D^2 - d^2})$  mm.

$$A = \frac{1}{2} \pi D^2 \left\{ 1 - \sqrt{1 - \left( \frac{d}{D} \right)^2} \right\} = 157 \left\{ 1 - \sqrt{1 - \frac{d^2}{100}} \right\} \text{ for a}$$

10 mm. ball,

The Brinell hardness number for steel is then

$$N = \frac{3000}{A}.$$

As examples of the order of number found by this test, 0.5 carbon steel gives about 230; mild steel with 0.21 carbon about 115; hardened tool steel about 700.

Brinell noticed a close relation between the hardness number and the tensile strength of steel. For Fagersta steel the ratio between tensile strength in kilograms per square mm. and the hardness number is 0.346, when the hardness number is below 175. The ratio is 0.354 when the hardness number is above 175. Charpy found ratios 0.351 and 0.336. The ratios are remarkably consistent, indicating that the hardness number of a ductile material is really a measure of strength.

The Ball Test was the outcome of M. Brinell's endeavour to devise a test easily applied to steel during the progress of manufacture. A description of M. Brinell's researches is in Volume 2 of the *Congrès International des Méthodes d'Essai des Matériaux de Construction*, Paris, 1901, page 83. The Hoffmann ball is so easily obtained that it bids fair to supersede other forms of indenting tool.

Indentation tests have been made with hatchet-shaped chisels, with conical pointed tools, with a tool ending as a frustrum of a cone and many other shapes.

A ball smaller than the standard 10 mm. ball should be used to make the test on small test pieces. H. Moore<sup>1</sup> has shown that the dimensions of the test piece have no appreciable effect on the hardness number if the size of the ball is selected so that the depth of the pit does not exceed one-seventh of the thickness of the test piece and so that the diameter of the pit does not exceed one-half the distance between the edge of the test piece and the rim of the pit.

The next question to settle is: What load must be applied to the selected ball so that the test gives the same hardness number as would have been obtained with a 10 mm. ball under the standard load? E. Meyer<sup>2</sup> has examined this question, and R. G. C. Batson<sup>3</sup> has demonstrated experimentally that the hard-

<sup>1</sup> "A Small Ball-Hardness Testing-Machine." *Proc. Inst. Mech. Eng.*, Jan. 1921.

<sup>2</sup> "Hardness Testing and Hardness." E. Meyer, *Zeits. Ver. deutscher Ing.*, Vol. 52, 1908, p. 645.

<sup>3</sup> "Static Indentation Tests." *Proc. Inst. Mech. Eng.*, April, 1923.

ness number is independent of the size of the ball if the load is varied as the square of the diameter of the ball. Therefore the load to be used with a ball of diameter  $d$  mm. is

$$P = \frac{3000}{10^2} d^2 \text{ kilograms.}$$

Batson has also shown experimentally that the hardness number is independent of the load on a ball of constant diameter provided that the area  $A$  is calculated from the depth of the pit measured from the original surface of the test piece. If the area  $A$  is calculated from the diameter of the pit the hardness number will vary slightly with the load. This difference is due to the flow of the material round the rim of the pit. An interesting comparison between the hardness numbers derived from the ball test and a test with a  $90^\circ$  conical indenting tool is also given in the paper quoted above.

Dr. Unwin<sup>1</sup> has made indentation experiments with a small square bar of tool steel pressed into the material so that it leaves a  $V$  groove instead of a pit. The depth of indentation is proportional to the load with accuracy over a wide range. This tool can easily be kept sharp by grinding.

Indentation tests are useful only on materials which possess ductility. Brittle materials break down under the test.

**7. The Shore Scleroscope Test for Hardness.**—A small metal weight, diamond-pointed, weighing all together 40 grains, falls from a fixed height inside a glass tube like a gauge glass on to the test piece, dents the surface and rebounds to a height which is observed against a scale inside the glass tube. The height of the fall is about 9 inches, and this height is divided into a scale of 140 parts with zero at the bottom of the fall. The height of the rebound observed against this scale is called the **Scleroscope Hardness Number**.

Tool steel of usual quality is about 100 on the scale. The Brinell hardness number is roughly six times the scleroscope number. A closer comparison is 5.5 for soft steels, increasing to 8 for hard steels with a Brinell number 700. Many tests from which comparisons may be made are recorded in the Report of the Hardness Tests Research Committee, *Proc. Inst. Mech. E.*, Dec. 1916.

Instructions issued with the instrument state that test pieces should be flat and as smooth as possible without actually having a gloss finish, and the surface on which the test is made should

<sup>1</sup> Unwin, *Proc. Inst. C. E.*, Vol. 129, 1897.

be level. The weight is lifted to its small hooks at the top of the glass tube and released from them by pressing a rubber bulb as if working a photographic shutter. The controlling mechanism, operated by air pressure, is contained in a fitting at the top of the glass tube.

**8. The Scratch Test for Hardness.**—The earliest scale of hardness was devised by the mineralogist Moh. He selected ten minerals and placed them in the order in which each would scratch the one below it and would itself be scratched by the one above it. The ten minerals in order are :

Diamond . . . . .	10	
Sapphire, Ruby, Corundum . . . . .	9	
Topaz . . . . .	8	
Quartz . . . . .	7	} Steels ranging Brinell Test, 200 to 700
Felspar . . . . .	6	
Apatite . . . . .	5	
Fluorspar . . . . .	4	
Calcite . . . . .	3	
Selenite . . . . .	2	
Talc . . . . .	1	

Sir Robert Hadfield, in the *Report to the Institution of Mechanical Engineers*, mentioned above, gives the results of scleroscope tests made on these minerals, with the exception of diamond and ruby. The order of hardness is substantially the same on the two scales up to quartz, and then the scleroscope hardness falls as the Moh hardness increases. The range on the Moh scale, fluorspar to quartz, covers the range of Brinell hardness 200 to 700. Sir Robert Hadfield also gives tables comparing scleroscope and scratch hardness of steels, and Brinell and scratch hardness of steels. The Moh scale is in no sense a scale of equal intervals of hardness. The diamond is, according to a diagram given in the Report, 140 times harder than corundum, the next in the scale.

Professor Turner<sup>1</sup> has devised a scratch test in which the scratch is made by a diamond-pointed tool guided mechanically. The tool is loaded until it just scratches the test piece, and the load in grammes is called the hardness number.

Mr. G. A. Hankins<sup>2</sup> has examined experimentally the relation between the width of a scratch and the load on a diamond tool

<sup>1</sup> *Proc. Birmingham Phil. Soc.* Vol. 5, Part 2, 1886.

<sup>2</sup> "On the Relation between Width of Scratch and Load on Diamond in the Scratch Hardness Test." *Proc. Inst. Mech. Eng.*, April, 1923.

and has found that the square of the width of the scratch plotted against the load on the tool gives a straight line passing through a point with co-ordinates  $p$  and  $q$  for all the materials tested.

The conclusion is that

$$k = \frac{P - p}{w^2 - q}$$

where  $P$  is the load on the tool in grammes,  $w$  is the width of the scratch in 1/1000 mm.,  $k$  is a constant for each material. It is suggested that  $k$  may be taken as a measure of the scratch hardness. The values of  $p$  and  $q$  are small and appear to depend upon the state of the point of the diamond.

**9. Wear Test of Hardness.**—The Council of the Institution of Mechanical Engineers appointed a Committee in 1914 to report on a Hardness Test for Hardened Journals and Pins. The Report<sup>1</sup> of the Committee contains the Report of Dr. Stanton on experiments made by him for the Committee, some appendices and a discussion, all of great value and interest.

Two kinds of wear are distinguished, namely, wear by rolling and wear by sliding. A figure of merit is obtained by noting the wear of a rod rotated at a high speed inside a hard steel ring loaded through a ball bearing to produce a definite pressure between rod and ring at the line of contact.

Rolling wear is tested by rotating the rod, and this rotates the ring inside the ball bearing. Sliding wear is tested by rotating rod and ring together in such a way that there is a known amount of relative slip per revolution.

**10. Wear Test by Dry Rolling. The Saniter Test.**<sup>2</sup>—A rod  $\frac{1}{2}$  inch diameter is driven at 4000 revolutions per minute inside a hardened steel ring 1 inch inside diameter loaded with 205 lb. Dr. Stanton repeated Mr. Saniter's test with a 1 inch rod, driven at 2200 revolutions per minute in a  $1\frac{1}{2}$  inch hard steel ring loaded to 410 lb. Dr. Stanton defined the "wear" of the rod to be the reduction of its diameter, measured in ten-thousandths of an inch, after 200,000 revolutions.

**Resistance to wear by dry rolling** is defined to be the reciprocal of the wear multiplied by 1000.

Quoting the results of one experiment, a rod of nickel chromium steel (Ni 2.5 per cent. ; Cr 2.0 per cent. ; C 0.7 per cent.), hardened in oil from 850° C. and tempered in air from 600° C., was reduced in diameter 71 ten-thousandths after 200,000 revo-

<sup>1</sup> *Proc. Inst. Mech. E.*, Nov., 1916.

<sup>2</sup> *Journal of Iron and Steel Institute*, 1908. No. 3, page 75.

lutions. Its resistance to wear is then represented by the figure  $1/71 \times 1000 = 14$ .

The Brinell hardness was tested, giving for the worn surface of the rod a number 420, for the unworn surface the same. The scleroscope hardness figures were—for the worn surface 71, for the unworn surface 67.

**11. Wear Test by Dry Sliding.**—Dr. Stanton designed an ingenious machine for doing this test, particulars of which are given in the Report.

The rod is turned 1 inch diameter and the ring is bored slightly more than 1 inch, so that the difference in the lengths of the inner circumference of the ring and the circumference of the rod is  $\frac{1}{4}$  inch. An Oldham coupling connects the driving chuck with the ring, so that the ring is left free to settle down on the rod under the load it carries. Both rod and ring are driven at the same speed, so that there is  $\frac{1}{4}$  inch slip per revolution. The load, 410 lb., is applied to the ring through a ball bearing, and the combination is driven at 2000 revolutions per minute.

Wear is defined to be the thickness in mils. of the surface of the rod rubbed away during a slip of 1000 feet. With  $\frac{1}{4}$  inch slip per revolution this slip is accomplished in 48,000 revolutions, occupying twenty-four minutes of running time. No lubricant must be allowed to get between ring and rod at the line of contact.

**Resistance to wear by sliding** is defined to be the reciprocal of the wear; in Table 2 of the Report, however, this reciprocal is multiplied by 100. Quoting an example: The thickness abraded from the surface of a rod of 0.52 carbon steel after 1000 feet of slip under the load of 410 lb. was 1.3 mils. The figure of wear is therefore 1.3, and the reciprocal of this is 0.77, and multiplied by 100 is 77, the figure given in the table.

The Brinell hardness numbers are—for the worn surface of the rod 237, for the unworn surface 234. The scleroscope hardness figures are—for the worn surface 41, and for the unworn surface the same.

The following table gives some of the results in the Report, and is interesting as showing the Brinell and the scleroscope hardness numbers in comparison for steels of known composition.

**12. Hardness.**—Reviewing the test for hardness just described, the question now arises, What is hardness? Is it a single quality of material which can be measured by a single test. There is no difficulty in understanding what hardness is. A workman has clear ideas on the subject. He knows that tool steel

TABLE 1

Test No.	Marks.	Condition of Material.	Brinell Test.		Scleroscope Test.		Sliding Abrasion Test.		Ratio Brinell number to Scleros. number	Ratio Brinell number to Sliding Abrasion Resistance.	Analysis.							
			Unworn Surface.	Worn Surface.	Unworn Surface.	Worn Surface.	Thickness removed, mils. per 1000 ft. slip.	Resistance to sliding Abrasion.			C.	Si.	Mn.	S.	P.	Cr.	Ni.	
1	6	Hardened in oil at 850° C., tempered in gas muffle at 600° C.																
2	1010/2	Manganese steel	420	420	67	68	0.7	140	6.3	3.0	0.70	—	—	—	—	2.0	2.5	
7	A	Carbon steel as forged	277	284	44	46	2.2	45	6.3	6.2	1.36	0.36	13.10	—	—	—	—	
14	2250/958	rolled	234	237	41	41	1.3	77	5.7	3.0	0.52	0.10	1.26	0.05	0.09	—	—	
15	2250/955	Carbon steel	235	—	41	42	1.1	91	5.7	2.6	0.65	0.13	0.60	0.02	0.03	—	—	
17	720/1	toughened	337	—	61	61	0.3	330	5.5	1.0	0.65	0.13	0.60	0.02	0.03	—	—	
18	704/1	Mild carbon steel	115	116	21	24	5.3	19	5.5	6.0	0.21	0.02	0.46	0.05	0.06	—	—	
30	68	chemically hardened to 35 tons per sq. in.	149	144	37	37	5.5	18	4.0	8.8	0.04	0.05	0.41	0.04	0.07	—	—	
31	4789	Gauge steel, hardened	720-740*	—	107	106	0.35	290	6.8	2.5	1.02	0.31	0.45	0.02	0.03	1.43	0.03	
35	719	Ditto, ditto	675-695*	—	100	101	0.1	1000	6.8	0.7	0.86	0.18	1.34	0.02	0.03	0.05	—	
36	708	Admiralty bronze	75	82	17	26	4.9	20	4.4	3.8	—	—	—	—	—	—	—	
		Phosphor-bronze	131	137	26	29	1.0	100	5.0	1.3	—	—	—	—	—	—	—	

\* Values approximate owing to flattening of ball.



hardened will cut most metals. He knows that the blunted steel tool can be sharpened on a corundum wheel. And he knows that a corundum can be turned with a diamond-pointed tool as easily as wood can be turned with a steel tool. Diamond, corundum, hardened tool steel, other metals, stand to him in a scale of hardness, completely understood.

The difficulty is to find a form of words which will define hardness, because hardness is a property which is the sum of other properties. Hardness is related to other properties and cannot be defined without reference to them, any more than the strength of a material can be defined in absolute terms.

In the discussion of the Hardness Report, Sir Robert Hadfield says: "Efforts to establish an academic idea of hardness are limited to the resistance offered by a material free to flow up to the point where it is permanently deformed, which in brittle substances of course means fractured. In elastic materials this academic definition of hardness is nothing more than the yield-point. To measure the hardness one has therefore only to measure the yield-point."

Brinel found that for some materials the hardness number can be related to the ultimate stress. It is equally true that for other materials it can be related to the yield point. These ascertained relationships emphasise the difficulty of defining the property known as hardness.

**13. The Fatigue Test.**—The stresses within the members of a structure or within the parts of a machine are rarely constant. They vary as the load varies or as the piece moves under constant load, or from both causes combined. A variation of stress at a given point within the material, starting from a given value and finishing at the same value, may be called a **stress cycle**.

A stress cycle at a point is defined by:—

1. The range, or the amplitude of the stress.
2. The mean stress.

The amplitude of the stress in the cycle is the algebraical difference between the highest and the lowest stress. The mean stress is half the algebraical sum of the highest and the lowest stress. The frequency of the cycle is the number of times it is repeated per unit of time.

At a point in the section of a piston rod the highest stress is say  $f_t$  tons per square inch in tension during the in or pulling stroke and  $f_c$  tons in compression during the outward or push stroke. The amplitude of the stress cycle is then  $f_t - (-f_c) = f_t + f_c$ , and the mean stress is  $\frac{f_t - f_c}{2}$  tons per square inch.

If  $f_t = f_c$  then the amplitude is  $2f_t$  and the mean stress is zero. The frequency of the cycle is equal to the number of double strokes made per minute.

The rotation of a railway axle under its constant load produces a stress cycle at every point within the axle. The amplitudes at a given cross-section are greatest at the surface fibres. At a section of the axle where the bending moment produced by the load is  $M$ , the direct stress is  $M/Z$ ,  $Z$  being the modulus of the section, and this is a tensile stress  $f_t$  when the fibre turns through the highest position and an equal compressive stress when it passes through the lowest position. The fibre sustains a stress cycle of amplitude  $2f_t$  and the mean stress is zero. The frequency of the cycle is the number of revolutions made by the axle per minute.

If at a point in a machine element a stress cycle between assigned limits produces no permanent change of form of the inner structure at the point, the inner structure is undamaged and the cycle may be repeated indefinitely without fear of ultimate fracture. If, however, the stress cycle produces the minutest permanent change of form, work has been expended on the structure, and the first step has been taken to fracture the element, and it is only a question of how many repetitions of the cycle must be made to fracture it.

Wohler designed testing machines in which he sought to imitate conditions of stress variation met with in practice and to find experimentally how many repetitions of a stress cycle of given amplitude and mean stress would break a test piece. The mean stress in his experiments was zero. His researches were carried out over a long period. The results were published in *Engineering*, Vol. 11, 1871. He concluded generally that for every mean stress there is a particular stress cycle which will just not break the piece after unlimited repetition. Bauschinger (*Mittheilungen aus dem Mechanische-Technischer Laboratorium in München*, 1886) concluded that so long as the highest or the lowest stress in a cycle did not exceed the elastic limits of the material, the cycle could be repeated indefinitely without breaking the piece.

A simple form of Wohler fatigue-testing machine imitates the conditions of the railway axle. A turned test piece is held at one end in the chuck of a belt-driven spindle, and a load is hung on the free end. The test piece, in fact, forms a peg on which to hang a load. As the spindle rotates each point in the test piece is subject to a stress cycle of mean value zero. The amplitude of

the cycle is defined by the load on the end, and its distance from the section of the test piece designed for the test.

In modern machines of this type the spindle is motor-driven, so that the test can be carried out at a higher frequency. Sketches and a description of a modern machine of this type will be found in a paper by Dr. Stanton and J. R. Pannell.<sup>1</sup>

The spindle of the machine is driven by a motor at about 2000 revolutions per minute. The hanger carrying the load is attached to a ball bearing at the end of the test piece, and to prevent vibration at this high speed the hanger is at its lower end attached to a piston working in a dash pot. A form of test piece used in this machine is shown in Fig. 5. It is bored out at one end, the end held in the chuck, so that the stress cycle of maximum amplitude is applied to a tube.

The range of stress in the cycle is varied by varying the load.

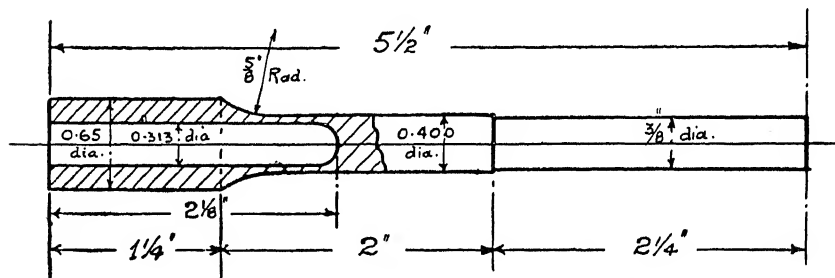


FIG. 5.—Test Piece for Wohler Fatigue-testing Machine.

To make a satisfactory test several test pieces are required. The first piece is run under a load which produces a stress cycle of wide enough range to break the piece after a few thousand repetitions of the cycle. The next piece is run under a stress cycle of narrower range, and it might take, say, 1,000,000 repetitions of the cycle to break the piece.

The test is finished when the range of a cycle has been found which will not break the test piece after 6 million repetitions, but a range which, if slightly enlarged, would break the piece in fewer than 6 million repetitions. The maximum stress in tension corresponding to this range is called the **fatigue strength** of the material.

For example, a series of tests run on 8 test pieces, turned to the dimensions given in Fig. 5, furnished the result that the fatigue limit was between  $10\frac{1}{2}$  and 13 tons per square inch for a stress

<sup>1</sup> "Strength and Fatigue Properties of Welded Joints in Iron and Steel," *Proc. Inst. C. E.*, Vol. 188, 1911-1912, Part 2.

cycle of zero mean value. This means that a stress cycle in which the highest stress was  $10\frac{3}{4}$  tons per square inch in tension, and the lowest stress  $10\frac{3}{4}$  tons per square inch in compression, would after 6 million repetitions just not break the piece.

The limiting fatigue strength is estimated from a Range-repetition Diagram, Fig. 6. The ordinates represent the range of stress and the abscissae the number of repetitions of the stress cycle. The diagram is quoted from the paper mentioned above. The dots show the results of separate experiments. A smooth curve through these points shows the value to which the range approaches as it is reduced. The material was 0.27 carbon steel.

The point  $x$  on the diagram, for example, means that a stress

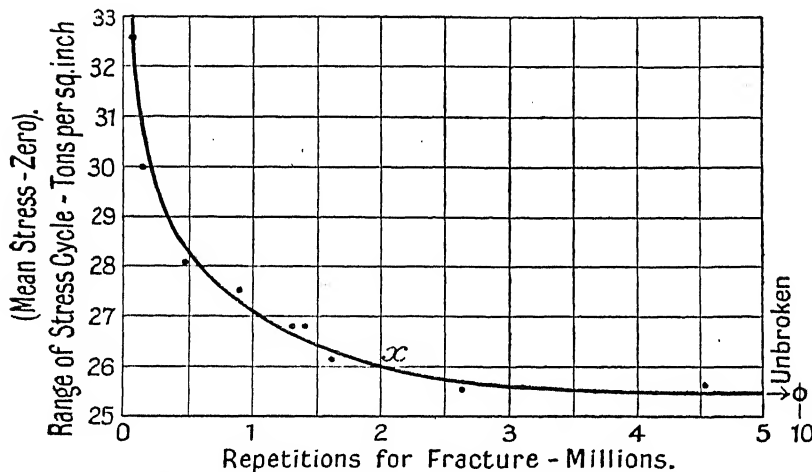


FIG. 6.—Range-repetition Curve, 0.27 Carbon Steel.

cycle of range 26 tons per square inch, and mean value zero, will break the piece after 2 million repetitions of the cycle. The diagram shows that when the range is reduced to 25.5 tons per square inch, the curve becomes parallel to the axis. The inference is that the range can be applied an unlimited number of times without producing fracture. The maximum stress of this cycle is the fatigue limit of the material, and this is usually recorded as  $\pm 12\frac{3}{4}$  tons per square inch.

A dead weight hanging on the end of a rotating test piece does not produce a uniform distribution of stress over the section on which the bending moment is a maximum, even when the test piece is bored out as shown in Fig. 5.

Dr. Stanton describes in *Engineering*, February 17, 1905, a

fatigue tester in which a stress uniformly distributed over a section is made to vary between a maximum value in tension to a maximum value in compression about 2000 times per minute. The machine is based on an earlier design of Osborne Reynolds. Essentially the machine is a crank and connecting-rod mechanism, driven from the crank shaft and used to reciprocate a heavy piston mass. The test piece is put in line with and in fact forms part of the piston rod. The test piece then transmits to the mass the force necessary to cause it to reciprocate with a motion which is substantially simple harmonic. Neglecting the small corrections for the angularity of the connecting rod, the maximum tensile load in pounds transmitted through the test piece, and equally the maximum compressive load, is  $\frac{W4\pi^2n^2r}{g}$  in which  $W$  is the weight

in pounds of the mass reciprocated by a crank of radius  $r$  feet, making  $n$  revolutions per second;  $g$  is 32.2. The range of load is twice this. The range can be varied by changing  $W$  or the speed  $n$ .

The machine is designed with two lines of parts and is balanced so that it can be run at a high rate of speed without producing vibration. Four test pieces can be tested simultaneously. Both the rotating spindle and the reciprocating-rod machines just described apply to the test piece a stress cycle of mean value zero, or very nearly so.

**The Smith Fatigue-tester** allows a stress cycle of any mean value to be applied to the test piece. It is described in the *Journal of the Iron and Steel Institute*, Vol. 82, No. 2, 1910, in the paper "Some Experiments on the Fatigue of Metals."

A test piece, a frame free to move in guides vertically, and a spring, are connected in line, like three links of a chain. The top of the test piece is secured to the fixed frame of the machine and the bottom of the spring is secured to the base of the frame. By means of a graduated hand wheel the spring can be stretched so that it puts a definite load on the three-link system. The relatively massive central frame is inappreciably stressed by this load, but the test piece, being turned to  $\frac{1}{4}$  inch diameter, can be stressed to any value between zero and yield. The central frame or link carries a motor-driven horizontal shaft, on the ends of which are placed symmetrically a pair of unbalanced masses. Rotation of the shaft then superposes a stress on the existing constant stress produced by the spring, which varies as in simple harmonic motion. The maximum value of this stress is

$f = \frac{W4\pi^2n^2r}{g}$  lb. In this expression  $W$  is the weight of the total

unbalanced mass in pounds ;  $r$  is the radius in feet of its mass centre ;  $n$  is the revolutions of the shaft per second. The simple harmonic oscillation of the central frame therefore applies to the test piece a stress cycle of range  $2f$  superposed on the mean stress applied by the spring.

The results of research with this machine are given in the paper quoted above. The ranges of the stress cycles required to produce fracture in 1 million repetitions at a frequency of 1000 repetitions per minute were determined for a variety of materials both for the conditions of cycles with mean stress zero and for cycles with the minimum stress zero.

The conclusions given in the paper are :—

(1) That if a material be subject to stress alternations of high periodicity and of fixed range, and compressive or tensile test be gradually applied, a yielding condition will be found at a definite value of the applied mean stress.

(2) That the yield is tensile if the mean stress is tensile, and is compressive if the mean stress is compressive.

(3) That for equal and opposite mean stresses the magnitude of the yield range is the same.

(4) That the Wohler limiting range for any material is a yield range.

(5) That a series of yield ranges may be determined for most materials by experiment on a single specimen.

The **Hopkinson High-speed Fatigue-tester**<sup>1</sup> applies a stress cycle of zero mean value about 7000 times per minute. The machine was designed to investigate the influence of the frequency on the range of the limiting fatigue cycle. It was not proved that the frequency had any influence, but it was found that it required a greater number of repetitions of the limiting cycle to break the piece when it was applied at high frequency.

The test piece is set vertically in a massive foundation block and carries on its upper end a mass weighing about 180 lb., suitably constrained to allow a small vertical oscillation. This mass carries on its upper surface the armature of an electro-magnet. The electro-magnet is supplied with alternating current and the conditions are so adjusted that the alternating magnetic force excites synchronous oscillation of the test piece. In these circumstances a small range of magnetic pull is able to produce a stress cycle of wider range in the test piece. The stress in the test piece is inferred from the extension produced, and it is observed by extensometers fitted to the test piece. The range

<sup>1</sup> *Proc. Roy. Soc.*, Vol. 86, Series A, 1912.

of stress is independently calculated from the observed amplitude of the oscillation. Knowing this, the mass, and the speed, and assuming simple harmonic motion, the force can be calculated.

The results of three tests are shown in Fig. 7. From these curves it will be seen that a range of magnetic pull of 0.4 tons per square inch is able to produce a stress cycle on the piece of 30 tons per square inch range in the region of synchronous speed, namely 120 cycles per second. The machine was set up on a less rigid foundation during the experiments for curve  $D_2$ . The blunter peak is probably due to a consequent change in the damping coefficient.

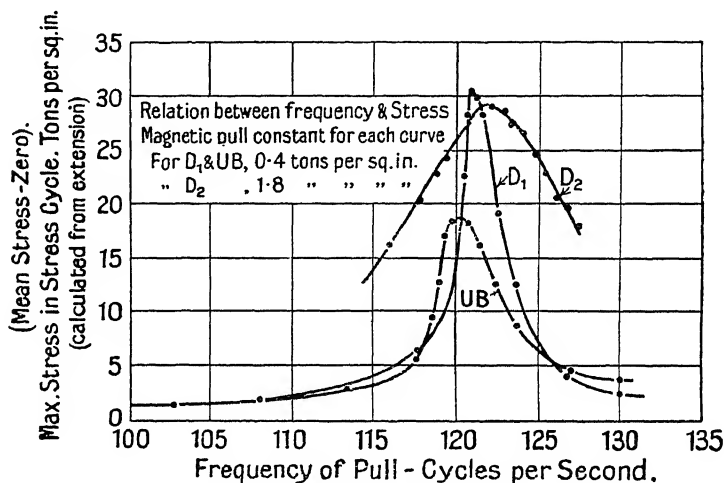


FIG. 7.—Hopkinson's High-speed Fatigue Tests.

**The Haig Fatigue-tester.** A stress cycle of any mean value can be applied to the test piece. In principle it is similar to the Smith Tester described above, except that the stress cycle is applied to the central frame, now an armature, by a magnet fixed to the frame and excited by alternating current. Test piece, central armature frame and spring are connected in line like three links of a chain. The spring can be stretched by turning a nut so that it puts an assigned mean pull on the three-link system. The relatively massive central frame carrying the armature is inappreciably stressed by this load. The spring is of the laminated type, and its length is initially adjusted so that the time of oscillation of the central frame, but with no test piece in place, is made equal to the periodic time of the magnetic pull. The magnets apply a range of stress with a frequency of 40 cycles per

second. Provision is made for adjusting the equality of the air-gaps to secure equality of magnetic pull up and down. The central armature frame is guided in its small vertical displacements by guide springs at each end of the frame. The machine is calibrated by comparing the extension of a specially made test piece with the readings of a voltmeter giving the magnetic flux through the pole pieces. In this way the voltmeter readings are converted into tons load on the test piece.

The machine is described and the results of some experiments therewith are recorded in *Engineering*, September 21, 1917, and in the *Journal of the Institute of Metals*, 1917, Vol. 2, page 55.

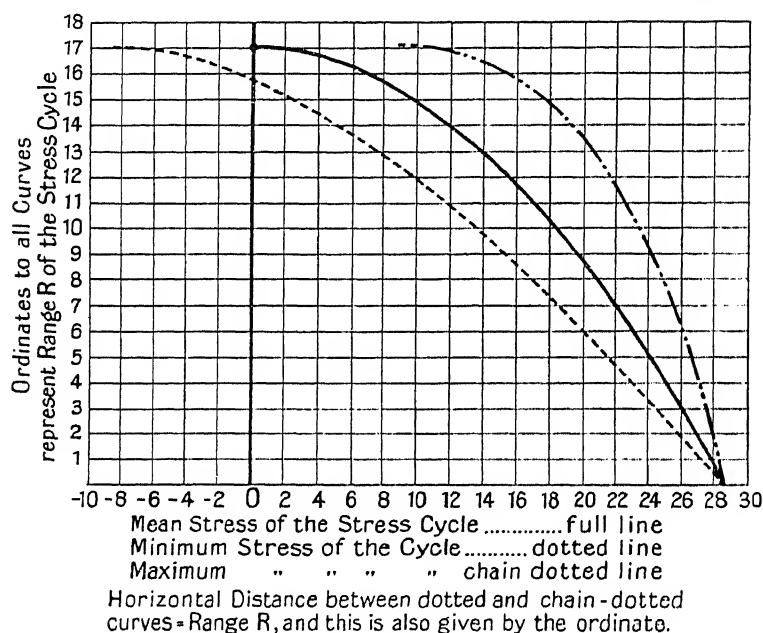


FIG. 8.

The limiting fatigue range of a stress cycle will vary with the mean value of the cycle. The results of tests in which the mean value of the cycle is varied may be plotted in a **Limiting Fatigue Range—Mean Stress Diagram**. In this diagram the ordinates are the limiting fatigue range, and the abscissæ are the corresponding values of the mean stress of the cycle. Plotted in this way, the results of many actual tests fall on a curve which is approximately parabolic in form.

By way of example such a curve is shown in Fig. 8, plotted from Bauschinger's experiments on a Bessemer steel of 28.6 tons



per square inch ultimate strength. The limiting fatigue range is 17 tons per square inch for a cycle of mean stress zero. Assuming the curve to be parabolic, its equation is of the form

$$R = R_0 - mx^2 \quad . \quad . \quad . \quad . \quad . \quad (1)$$

$R$  is the fatigue range corresponding to a stress cycle of mean value  $x$  tons per square inch.

$R_0$  is the limiting fatigue range when  $x = \text{zero}$ , that is, the cycle ranges between equal values in tension and in compression.

To find  $m$  :—

The range will be zero when the mean stress is equal to the ultimate stress  $f$ . From this

$$m = \frac{R_0}{f^2}$$

so that 
$$R = R_0 - \frac{R_0}{f^2} x^2$$

This is known as Gerber's Parabola.

For the experiments plotted,  $R_0 = 17$ ,  $f = 28.6$ , so that  $m = \frac{1}{48}$ .

The equation then becomes

$$R = 17 - \frac{x^2}{48}.$$

This equation enables the limiting fatigue range to be calculated when the mean stress  $x$  of the cycle is assigned.

The dotted curve Fig. 8 shows the minimum stress and the chain-dotted curve the maximum stress, so that the horizontal distance between these curves is the range of stress of the cycle, and this range is also given by the ordinate. It is sometimes convenient to use an expression in which the maximum stress of the cycle  $f_{\max}$  is given in terms of the range of stress  $R$ . For any cycle

$$f_{\max} = \frac{R}{2} + x.$$

Substitute for  $x$  its value from (1), namely

$$x = \sqrt{\left(\frac{R_0 - R}{m}\right)} = \sqrt{\left(\frac{mf^2 - R}{m}\right)} = \sqrt{\left(f^2 - \frac{R}{m}\right)}.$$

So that

$$f_{\max} = \frac{R}{2} + \sqrt{\left(f^2 - \frac{R}{m}\right)} \quad . \quad . \quad . \quad . \quad (2)$$

Sometimes this is written in the form

$$f_{\max} = \frac{R}{2} + \sqrt{(f^2 - nRf)}.$$

The relation between the constants is then

$$n = \frac{l}{mf} = \frac{f^2}{R_0 f} = \frac{f}{R_0}.$$

For the example above,

$$n = \frac{28.6}{17} = 1.68.$$

For a table giving values of  $f$  and  $n$  deduced from Wohler's and Bauschinger's experiments, see *The Testing of Materials of Construction*, by Unwin.

#### 14. The Examination of the Inner Structure of Metals.

—The inner structure of a metal can be seen through a microscope by light reflected from a surface or facet specially prepared for examination. The metal specimens are about the size of a dice. If the metal is in a thin sheet a piece of it can be attached to a block of wood about the size of a dice. The surface selected for examination is first polished and then it is etched with a suitable reagent. The reagent penetrates the polished surface and attacks the elements in the structure differentially so that light is unequally reflected from the various elements and thus throws up the pattern.

For example, the selected surface of a steel specimen is polished with emery of increasing fineness and is finally finished with rouge until the surface will reflect an image like a mirror. Dipped for a few seconds in a saturated solution of picric acid in alcohol, the polished surface becomes dull. After washing and drying the specimen is mounted in plasticene on a microscope slide so that the prepared surface is at right-angles to the optical axis of the microscope, when the slide is clamped on the stage. The dull surface, properly illuminated, looked at through the microscope, shows often characteristic and beautiful patterns. Fig. 106 shows the pattern given by a steel and Fig. 69 the pattern shown by brass plate.

When the magnification is high the area seen in the microscope is small compared with the area of surface prepared. A moderate magnification of 150 times corresponds to a seen area of only a few hundredths of an inch diameter, whilst a magnification of 1500 times corresponds to a seen area of only a few thousandths of an inch diameter.

The details of the inner structure are seen by light reflected from them to the eye. Magnification does not magnify the light, it only spreads the light on the object over the magnified image. The illumination of an area of a few thousandths of an inch diameter therefore must be intense in order to make the details of the image visible when the image is 1500 times the linear dimensions of the object. A magnification of 1500 times is nearly on the scale of a yard magnified to a mile; or 1 square yard to 1 square mile. One square yard must be intensely illuminated to enable it to reflect enough light to visibly illuminate a square mile.

Not only must the small area examined be intensely illuminated, but the light must be distributed over the area as uniformly as possible, so that the light is well distributed over the image. The difficulties of illumination increase greatly with the increase of the scale of magnification. But apart from the question of illumination the resolving power of the lenses has a limit, and this limit is about 1500 diameters.

The area looked at is illuminated by focusing light from a source on it. Any of the well-known methods and sources used for surface illumination in microscopy may be used for direct examination by the eye. When many specimens have to be examined and a surface searched with the microscope, it is less tiring to the eye to replace the eyepiece of the microscope with a projecting lens and so throw the image on a small screen. The screen should be made of wood and painted a dead white. The structure can then be examined by looking at the image on the screen. Alternatively the image can be thrown on the negative of a camera and the plate after development gives a permanent record of the image. Before putting the negative in the camera the image must be focused on a plane glass screen with the aid of a small eye lens to secure precise definition.

To secure sharpness of definition the specimen should be illuminated by light of one colour. To do this a colour screen is placed between the source and the specimen, so that the white light of the source is filtered and only the colour chosen allowed to proceed to the illumination of the image. The use of screens of differing colours enables part of the structure to be brought out in contrast to other parts. The colour of the screen is chosen on the principle that the colour in the object reflected in greatest proportion is the colour of the light illuminating it. A red rose glows when seen in red light, and its leaves look black, whilst in

green light the rose looks black, but the leaves shine with a vivid green.

Sharpness of definition is promoted by closing the iris diaphragms so that only the central parts of the lenses are used. This "stopping down" must not be carried to excess. The colour screen, the losses of light at the optical surfaces of the lenses and reflectors, and the stopping down, prevent a large fraction of the total light of the source from reaching the image. Therefore for projection or for photography the most intense source of light possible must be used. The most intense source is the surface of the crater on the negative carbon of an arc lamp. For low powers the incandescent tungsten bead of the "point o' light" lamp is satisfactory.

The image of the source is focused on the area of the surface to be examined by an optical system which includes in it the objective of the microscope. The beam of light from the source is brought in at the side of the microscope through an iris diaphragm and it is then reflected along the axis of the microscope through the objective, which acts as a condenser to concentrate it on the area to be examined. Bearing in mind the small area to be examined and the necessity of even illumination, it is evident that the adjustments of the lenses and the mirrors and the lamp may be tedious. I found many difficulties of a mechanical kind in the apparatus available and so designed one specially adapted for screen and high-power photographic work rather from the engineer's point of view of substantial and accurate construction, using the minimum of reflecting and refracting surfaces to conserve the light and with only the strictly necessary adjustments. Even illumination is secured in a few seconds, and the light is so conserved that an image 3 feet diameter is bright enough to be seen by a class of students even when the magnification is as high as 1000 diameters.

The general principle of the optical system of this apparatus is illustrated in Fig. 9. The diagram is not drawn to scale. The source of light A is the crater of the horizontal negative carbon of a small arc lamp. The positive carbon is set vertically and at right-angles to it. The light radiating from the crater is gathered by the short-focus lens B, and the parallel beam which this lens produces passes on through a cell C filled with alum water to filter out the heat rays. The cooled parallel beam is then focused on the iris diaphragm E by the lens D, itself fitted with an iris diaphragm.

Just inside the iris diaphragm is a totally reflecting prism F

which turns the light through a right-angle and directs it through the objective G of the microscope on to the prepared surface of the specimen H. This illuminated area is then projected by the microscope on to a camera screen or on to a white screen, both seen in Fig. 9 at J and L. When the illumination is even the centre of the crater A, the optical centre of the lens B, the optical

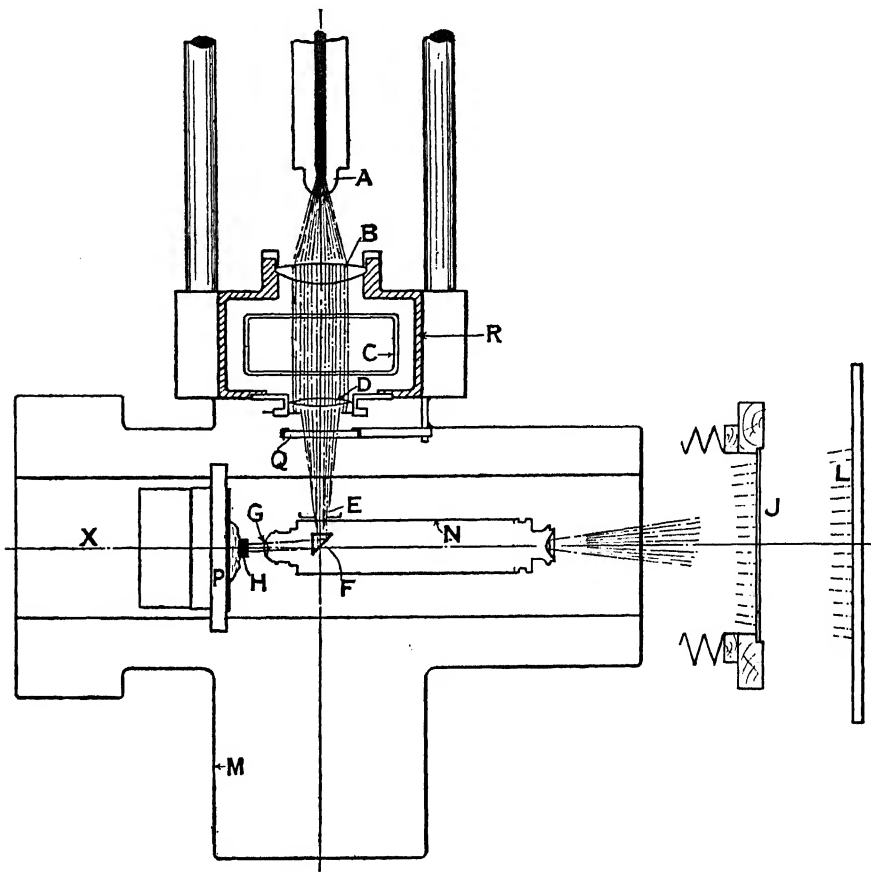


FIG. 9.—Diagram of the author's Microphotographic Apparatus. Constructed in the City and Guilds Engineering College.

centre of the lens D, and the centre of the iris diaphragm E, are in a line which, produced, cuts the optical axis of the microscope.

I secure these conditions in the apparatus which I have constructed by machining a bed M in the shape of a cross. One arm of the cross carries a miniature lathe bed, along which slide the microscope N and the stage P, each with its fine adjust-

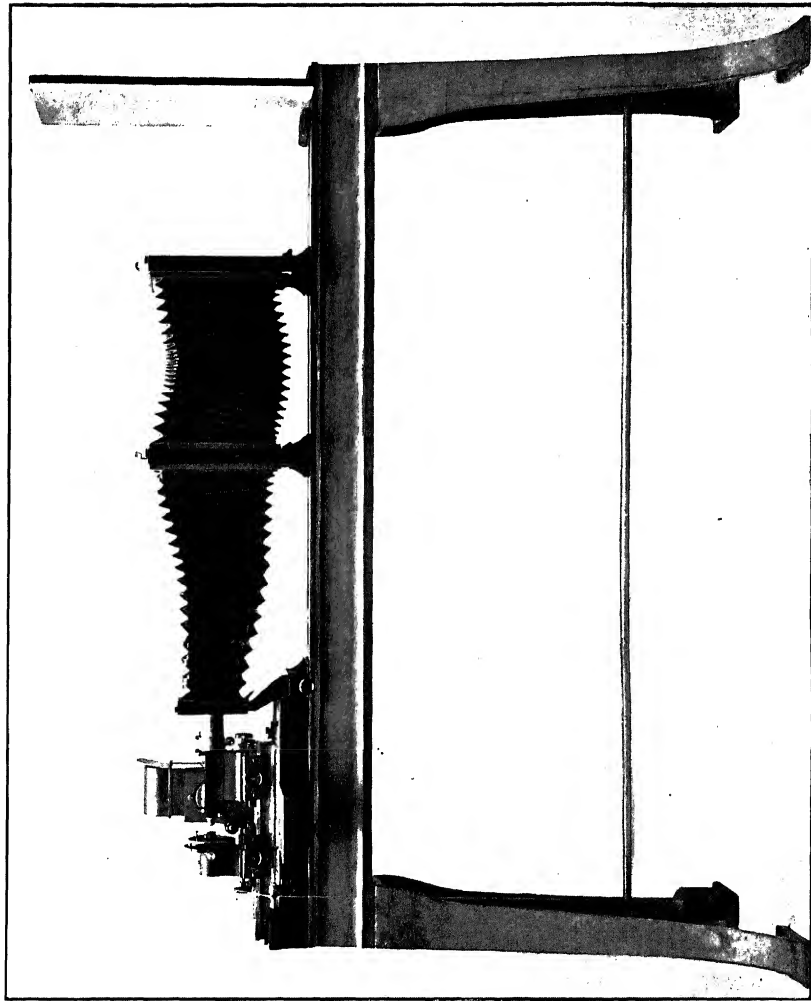


FIG. 10.

ment, like the headstock and the slide rest of a lathe. A vertical hollow pillar R, square in section, slides along an arm of the cross at right-angles to the axis of the microscope. The lenses B and D are secured to the machined faces of this pillar. The alum cell is dropped in the pillar between them. The arc lamp, constructed on strictly kinematic principles, slides along guide rods bolted to the pillar. The lamp has three degrees of freedom, so that the crater by two adjustments can be brought in the line BD, and it can also be moved along the line BD.

The pillar thus carries the arc lamp, the lenses B and D, the alum cell, and also the spectacle arm Q for the colour screens, and so forms one unit. The pillar can be unbolted and lifted out bodily and set in grooves prepared for it at X in a line with the optical axis of the microscope, so that transparent specimens, like thin sections of wood, may be illuminated by transmitted light. The total reflecting prism F has two degrees of freedom, namely a freedom to turn about its own axis and a freedom to turn as a whole about the optical axis of the microscope. These two adjustments enable the illuminating beam to be properly directed through the objective to bring the centre of the illuminated area on to the optical axis of the microscope.

A very thin disc of glass, set at 45 degrees to the axis of the microscope, may be advantageously substituted for the totally reflecting prism for low powers. The two adjustments mentioned above must be provided as for the prism. It has the advantage of perfectly axial and normal illumination, but the disadvantage that the whole beam of the reflected light passes through it to the image; and so sharpness is lost, and also the disadvantage that a small fraction only of the illuminating beam is reflected from its clear surface to the surface of the specimen. Both these disadvantages, while disqualifying for high magnifications, are negligible for low magnifications.

Fig. 10 shows a photograph of the whole apparatus. The cross-shaped bedplate, the camera and the screen are mounted on a light lathe bed. Any of the elements can be moved along the bed without sacrificing the adjustments in the optical axis. The cross-shaped headstock M can be quickly released from the bed and set up in a lecture room on the feet provided in the base, where it can be used to project on to a screen, 3 feet in diameter, images of various metals.

There is a certain amount of cultivated skill required to get good micro-photographs of metals, and the technique is better taught in a laboratory than by description. There is however

620-17  
N23

4083

much useful information as a guide to be found in books specially devoted to the microscope and in papers in the various institutions and societies who deal with microscopy and metallography.

**15. The Load-extension Diagram.**—The tensile test described above furnishes the co-ordinates of one point on a diagram of load and extension; namely the yield-point. The load is noted when the beam drops. The extension of the gauge length can be measured. The test also gives the ordinate of the point corresponding to the maximum load. The corresponding extension cannot be measured directly because the maximum load is reached and passed before it is recognized to be the maximum load when testing in the usual routine manner. The test also gives the abscissa of the extension of the gauge length at fracture. The load cannot be obtained easily. The jockey weight must be run back and an endeavour must be made to get a balanced beam from instant to instant as the piece draws out to fracture. Collecting these results, an ordinary tensile test gives the ordinate and abscissa of one point, the yield-point the ordinate of the point of maximum load, and the abscissa of the maximum extension.

Of course it is possible to obtain many simultaneous readings of load and extension by applying the load in a series of steps and then measuring the extension produced, and enough readings can be taken to plot a curve of load and extension without difficulty up to the region of the maximum load. After that, the manner of conducting the test determines the shape of the curve. It is, in fact, hardly possible to get a continuous curve by these methods after the maximum load has been passed.

The extension corresponding to any load after the elastic limit of the material has been passed depends upon the time the load is applied. The extension creeps under constant load, and the creep goes on at a greater rate as the maximum load is approached. So that the answer to the question, What is the extension corresponding to a load of  $x$  tons? requires an answer stating the extension at the end of one interval of time, and then a larger interval, and so on. The time intervals are large, so that when a bar is stretched in a machine and broken in 30 seconds the corresponding loads and extensions are substantially the same as if it were broken in 30 minutes. But if the piece is broken in 1 second the diagram differs slightly from the diagram of a five-minute break.

The practical conclusion is that when test pieces are broken at a moderate rate (the rate imposed by the testing machines



themselves when used in the ordinary manner), corresponding values of load and extension are substantially independent of the time and may be defined without reference to it.

**16. Definition of the Load-extension Diagram.**—A point describes a load-extension diagram when it moves in one direction proportionally to the load on the test piece and in a direction at right-angles proportionally to the extension of the gauge length of the test piece.

**17. Autographic Recorders.**—The point of a pencil or pen traces the load-extension diagram on a sheet of paper wrapped round a drum in most of the instruments now in use. The pencil is guided in a direction parallel to the axis of the drum, and it is connected to the jockey weight so that it moves proportionally to the jockey weight. The drum is connected to the test piece so that it turns proportionally to the extension of the gauge length. The pencil is driven by the jockey weight and the drum is driven by the extending test piece, the curve traced is therefore a diagram which strictly is the **Jockey weight-extension diagram**. It is not the load-extension diagram because the load on the test piece is the reading on the jockey weight load scale *plus* the effect of the inertia of the jockey weight and beam.

Many of the errors inherent in this type of apparatus are corrected in the automatic recorders designed by Mr. Wicksteed. Descriptions of mechanical autographic recorders are given in books and papers on the testing of materials.<sup>1</sup>

**18. The Dalby Optical Recorder.**—In this instrument the tracing-point is a spot of light, which draws the load-extension diagram on a photographic plate. The spot of light is conjugate with an illuminated pinhole. The beam of light issuing from this pinhole source is reflected successively from two mirrors, and, passing through a lens, is brought to a focus on the camera screen.

The axes of the two reflecting mirrors are set at right angles. The mirror which receives the beam of light from the source is part of an optical lever arranged on the centre line of a hollow steel

<sup>1</sup> "Autographic Test-recording Apparatus," J. H. Wicksteed (*Proc. Inst. Mech. E.*, 1886). *The Testing of the Materials of Construction*, Dr. Unwin (Longmans, Green & Co., London). "On the Use and Equipment of Engineering Laboratories," Sir A. B. W. Kennedy (*Proc. Inst. C. E.*, 1886). *The Strength of Materials*, Sir J. A. Ewing (Univ. Press. Camb. 1903). *Handbook of Testing Materials*, Martens (Chapman, Hall & Co., London, 1899).

bar called a **weigh bar**. When the weigh bar extends the mirror is proportionally tilted and the spot of light moves across the camera screen. The optical multiplication is about 300, so that an extension of the weigh bar of  $\frac{1}{100}$  inch displaces the spot 3 inches.

The second mirror receives the beam of light from the first mirror and reflects it to the camera screen. This mirror is connected through an **extensometer** with the test piece so that it tilts proportionally to the extension of the gauge length of the test piece. Its axis being at right angles with the axis of the first mirror, it moves the spot in a direction at right angles to the displacement produced by the first mirror. That is to say, the extension of the weigh bar and the extension of the gauge length produce displacements of the spot which are mutually at right angles to one another.

Weigh bar and test piece are coupled together and are stretched together as two links in a chain, so that the load on the test piece is equally the load on the weigh bar. The cross sections of the test piece and the weigh bar are proportioned so that the load which stretches the **test piece** to destruction does not stretch the weigh bar beyond its elastic limit. The stretch of the weigh bar is then a measure of the load on the test piece. The corresponding movement of the spot is therefore proportional to the load on the test piece.

The use of a weigh bar, or spring bar, or master bar, as it has been variously called, to measure the load on a test piece coupled to it, is not novel. Sir A. B. W. Kennedy and the late Prof. Ashcroft constructed recorders in which a weigh bar was used, but the small extension was multiplied mechanically, and the record was made by a stylus moving over a smoked-glass plate. An account of this instrument, together with some diagrams obtained with it, will be found in Mr. Wicksteed's paper, "Autographic Test Recorders," cited above.

The novelty of the Dalby recorder lies in the optical method of measuring the extensions of the weigh bar and the test piece and combining these extensions into a photographic record, and in novelties in the design of the apparatus to allow these optical and photographic methods to be used in spite of the shock the instrument gets every time a test piece is broken in it.

The diagrams from the Dalby recorder are free from errors caused by the inertia of the heavy beam and jockey weight of the testing machine; they are free from errors of pencil friction, and mechanical friction is reduced to a vanishing-point; they are

free from the errors of cord-stretching and from errors due to the relative movement between the instrument and the test piece. This freedom from inertia enables experiments on rapid loading to be made. Test pieces have been broken and the complete diagram obtained in a second of time. Such a performance is quite out of the range of any recorder of the mechanical type. A comparison between the shape of the diagram from a 10-second break and a 150-second break, both test pieces being cut from the same bar of mild steel, will be found in *Proceedings of the Royal Society*, Series A, Vol. 88, 1913.

The first instrument made is described in the *Proc. Roy. Soc.*, Vol. 86, Series A, 1912, and further researches are discussed in Vol. 88, 1913, of the same journal. A description of the instrument, together with some diagrams, is in the Transactions of the Institution of Naval Architects, 1912. A general description of the instrument, together with results of researches made with it, will be found in the "May Lecture" delivered by the author before the Institute of Metals in 1917. The Lecture is published in the *Journal of the Institute of Metals*, No. 2, Vol. 18, 1917. The following is a description of the standard type of the instrument.

#### 19. Description of Standard Type of Dalby Recorder.—

The instrument is self-contained. It is shown in Fig. 11 ready to go into a testing machine. It is seen in Fig. 13 in a Buckton single-lever testing machine, of the kind illustrated in Fig. 1, coupled to a test piece.

To put it in the machine the top nut N, Fig. 11, is unscrewed, the weigh bar W is pushed up through the top shackle, the nut N is replaced, and then the instrument hangs freely from the spherical seated shackle of the testing machine. The test piece T is next screwed into the muff coupling M and into the bottom shackle of the testing machine. The steelyard of the machine is not required at all during a test. It can, however, be usefully used as a safety lever. The jockey weight is run along to a load equal to the maximum load the instrument is designed for. Then, if a load is applied greater than this, the beam lifts and so gives a warning to stop the test before the weigh bar is overstrained.

The source of light is a small electric lamp held in the head H. This lamp illuminates a pinhole in the plate of which K is a trigger-like projecting end. A touch on this trigger; and the small orifice is changed to a larger one. This large orifice is convenient for finding the spot on the plate. The spot is focused

on the screen by pushing in or drawing out the draw tube S. Fine focusing is done by the milled collar U.

Extension of the weigh bar W tilts the mirror receiving the beam of light from the source, and, in consequence, the spot of light focused on the screen moves horizontally across the plate.

The **extensometer**, by which the spot is made to move vertically; proportionally with the extension of the gauge length; is seen in Figs. 11 and 13. The extensometer is permanently attached to the centre block of the instrument, but can be removed as a separate unit.

Two vertical rods VV carry sliding blocks BB, on which are pivoted arms AA. These sliding blocks are clamped to the vertical bars in positions suitable to the gauge length of the test piece. The arms AA are connected by a spring Y. In Fig. 11 a loop of string is seen connecting the forked ends of the arms. It is there to hold the arms temporarily against the tension of the spring Y.

After the test piece has been screwed into place the loop of string is removed and the spring brings the forks home on the flanges of the test piece. Each of the forks is free to turn about its axis, so that the angular motion of the arms due to the displacement of the flanges downwards as the piece extends is proportional to the mean displacement of the flanges apart.

The down-displacement of the upper flange is the stretch of the part of the test piece above the flange and the small stretch of the parts of the instrument itself up to the place where the weigh bar is clamped to the centre block. The down-displacement of the lower flange is the stretch of the part of the test piece above the flange; and again the small stretch of the parts of the instrument itself up to the place where the weigh bar is clamped to the centre block.

The difference of these down-displacements is the extension of the gauge length defined by the flanges. It is therefore the difference of these displacements which must be conveyed to the second mirror of the optical system. The necessary subtraction is done by a link. The near end of the link is seen in Fig. 11 at L. One end of the link is pivoted to the upper arm, the other end rests on a pole P, which itself rests in a cup in the lower arm. When the top arm turns down, the end of the link L pivoted to it moves up. When the bottom arm turns down the end of the link L, resting on the pole P, moves down. The centre of the link moves down proportionally to the difference of the displacements

THE DALBY RECORDER

To face p. 34.

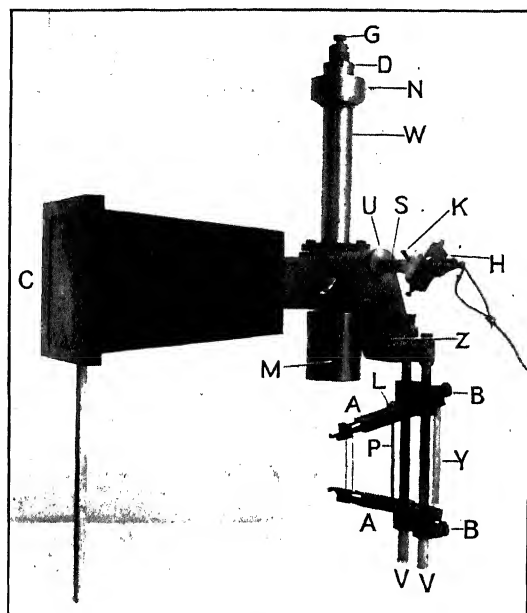


FIG. 11.

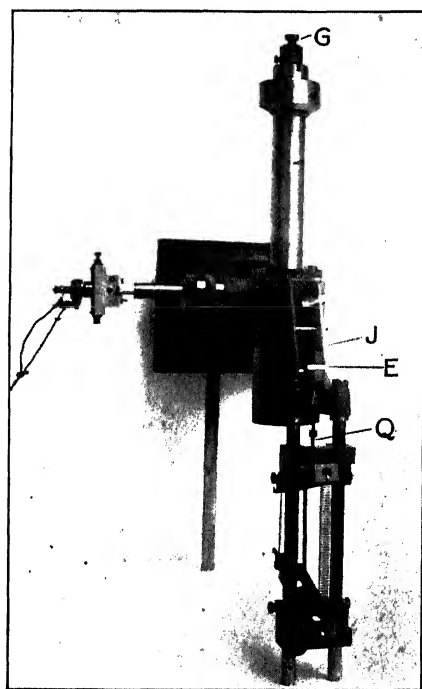


FIG. 12.—End View.

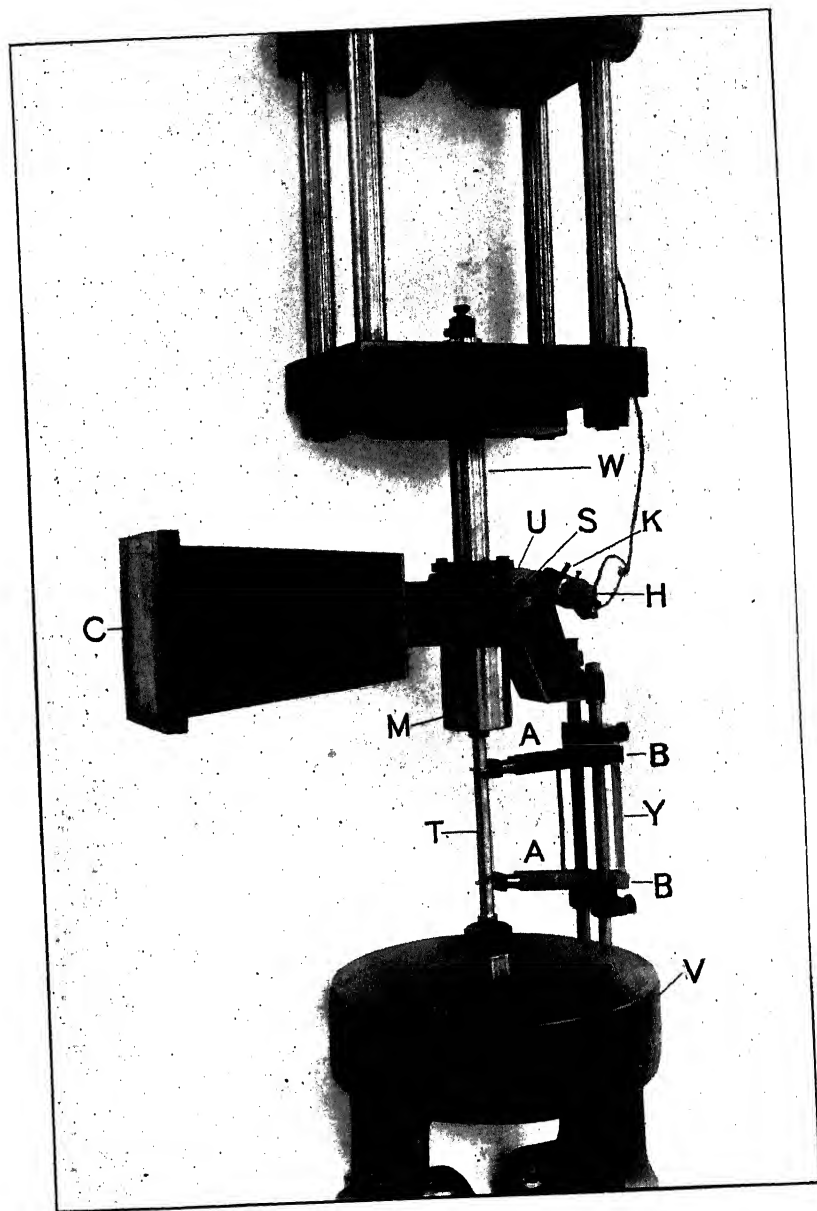


FIG. 13.—The Recorder in a Testing Machine.

of its ends, that is, proportionally to the extension of the gauge length defined by the flanges.

A pole Q seen in Fig. 12, which is an end view of the instrument, transmits the motion of the centre of the link to the horizontal arm of a bell-crank lever pivoted at Z. The vertical arm of the lever is connected by a horizontal pole with the hanging arm of the mirror mount of the second mirror within the instrument. By this system of levers the mirror gets an angular displacement proportional to the extension of the gauge length of the test piece.

**20. The Optical Cell.**<sup>1</sup>—This is a separate unit carrying the optical details of the instrument. It can be withdrawn from the weigh bar in a few seconds, examined, and replaced, without taking the instrument out of the machine. The muff coupling is taken off, and then an end nut; the optical cell then drops out of the bottom of the weigh bar after the upper horizontal pole of the extensometer has been removed. The centre pole comes away with it. The centre pole can be removed separately from the top by taking off the end nut and with it the adjusting head G.

**21. Adjusting the Zero.**—Extension of the test piece displaces the spot from the top of the plate downwards. The spot is moved independently in this direction by changing the length of the adjustable pole Q. Extension of the weigh bar moves the spot horizontally across the plate from right to left. The spot is moved independently in this direction by turning the adjusting screw G at the top of the weigh bar Fig. 13.

The origin to which the spot must be brought before beginning a test is the north-east corner of the plate, about  $\frac{1}{2}$  inch either way from the edges. It is brought to this position by adjusting the length of the pole Q, and by turning the screw G.

<sup>1</sup> Patent No. 113,008 of 1917.

**22. Calibration of the Weigh Bar.**—The load scale of the weigh bar is found experimentally. Known loads are applied to the bar and the corresponding displacements are recorded photographically. A series of known loads can be applied conveniently in a Buckton single-lever testing machine of the kind illustrated in Fig. 1. The instrument is set up in the machine as in Figs. 11, 12, 13, but the test piece is replaced by a steel bar strong enough to take without damage the maximum load of the scale to be recorded.

A typical load scale is seen in Fig. 14.

**23. Calibration of the Extensometer.**—The extensometer mechanically multiplies the extension of the gauge length by three. An extension measured from a diagram with an ordinary rule divided by three gives the corresponding actual extension. The instrument may of course be arranged to work on a different scale.

Calibrating pieces are provided with the instrument, so that the extension scale may be recorded on each diagram. These pieces are seen at E (Fig. 12). Normally they rest on the neck of the screw socket, out of the way, but are there when wanted. One piece clamped under the head screw J displaces the spot through a distance corresponding to one half inch extension. Four pieces are provided, so that four lines at intervals, corresponding to half-inch extensions, can be recorded on the plate.

The dead-stop pieces are more convenient than a micrometer head, although for some purposes the micrometer head may be useful. For example, an extension calibration plate may be made like that seen in Fig. 15. After a diagram has been taken this plate may be applied to read off the extension corresponding to any point on the load-extension curve, and afterwards the load scale may be applied to read off the corresponding load. Many examples of load-extension diagrams taken with the instrument are given in the next chapter.



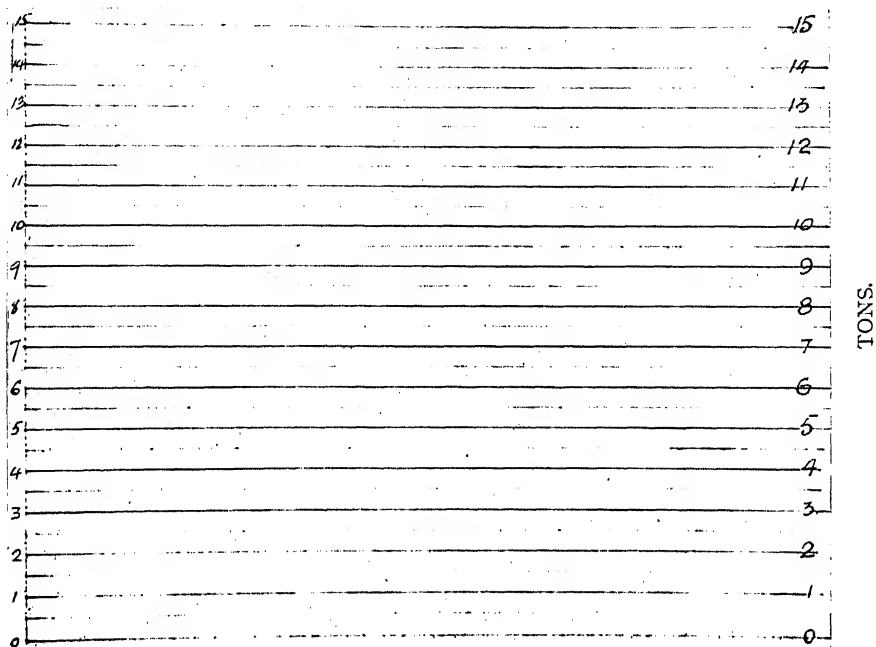


FIG. 14.—Load Scale of 15-ton Recorder.

INCHES.

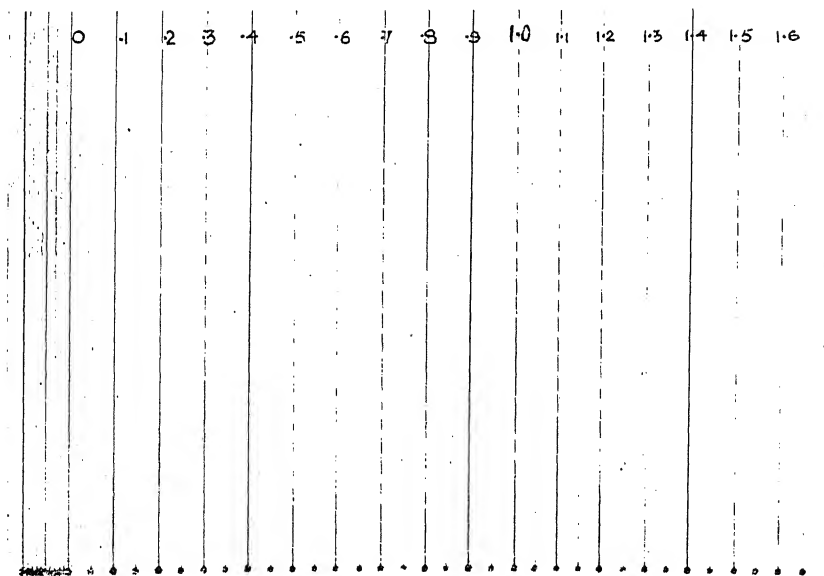


FIG. 15.—Extension Scale of 15-ton Recorder.

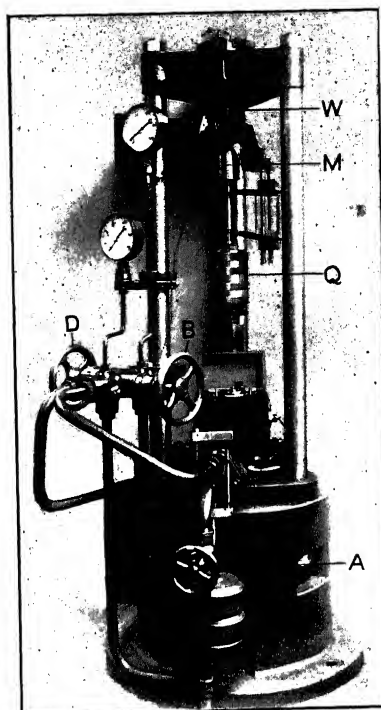


FIG. 16.—Hydraulic Machine for 15-ton Axial Pull.

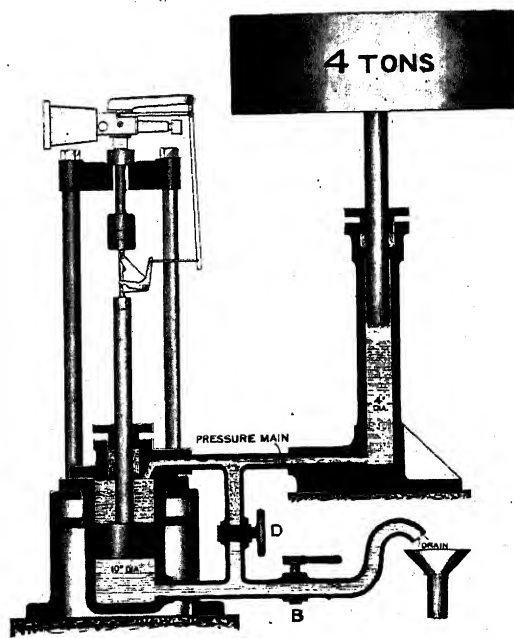


FIG. 17.—Diagram of Hydraulic Machine for use with the Dalby Recorder.

**24. Special Testing Machine for Use with the Instrument.**—The testing machine shown in Fig. 16 was designed for quick loading, but it is convenient for general testing. The instrument is shown set up in the machine with a test piece in place. The test piece is connected to the muff coupling M and directly to the piston rod of the hydraulic straining cylinder in the base of the machine through the coupling nut Q. There are no shackles. Often shackles introduce the error they are designed to prevent. A shackle turns into alignment against the friction of its pin. The line of load being coincident with the centre line, the shackles approach alignment as the load increases, but never quite get there. I have used crossed knife-edges, but prefer a machine with accurately machined guides for all ordinary work. W is the weigh bar hanging with the instrument from a spherical seat in the top casting of the machine. Alternatively crossed knife-edges can be used. The hydraulic main is connected through the valve A. Load is applied quickly by opening the valve B. An alternative small valve (hidden behind the pipes), is provided for applying load at more usual rates. Load is removed by opening the valve D. When D is opened the piston rod moves up, but is locked in position at any point of its stroke when D is closed. The machine was designed with the co-operation of Mr. Christopher James and constructed by Buckton & Co., of Leeds.

A single-lever testing machine is desirable in addition to this machine, because with it calibration of the weigh bars can be checked from time to time.

Fig. 17 is a diagrammatic illustration of the complete apparatus involved in a test and illustrates the principle of control. An accumulator whose ram is loaded with 4 tons maintains a constant pressure, through the hydraulic connecting main, on the top of the piston of the hydraulic straining cylinder. The total pressure on the piston, top side, is 4 tons multiplied by the ratio of the area of the piston less the area of the piston rod, and the area of the accumulator ram. This ratio is 5, allowing the piston rod to be 3 inches diameter, so that the maximum load on the piston is 20 tons. This load is supported by the water beneath it until the exhaust valve B is opened; then the water support flows away. If B is opened quickly it is equivalent to knocking away the support under a load. It should be noticed that water from the main has not to flow in to do the loading; the water load is there and falls on the test piece directly the supporting water pressure is relieved. The load is applied gradually by

## 38 STRENGTH AND STRUCTURE OF METALS

adjusting the valve B (or a smaller one) to relieve the pressure under the cylinder gradually.

When B is shut and D is opened the water pressure acts from the main on the bottom of the piston. The total pressure is 4 tons, multiplied by the ratio of the areas of the cylinder and accumulator, namely  $100/16 = 6\frac{1}{4}$ , so that the total upward push is 25 tons. But the total downward load is only 20 tons. The unbalanced push-up of 5 tons is available to bring the piston up against friction. It is locked in any position in its upward stroke by closing the valve D.

LOAD-EXTENSION DIAGRAMS AND INNER  
STRUCTURE OF METALS IN COMMON USE

**25. General Remarks.** — Load-extension diagrams of materials of special interest to engineers are collected together in this chapter. With each diagram is given a microphotograph taken from the polished and etched specimen piece cut from the end of the test piece, whose stretching to fracture is recorded in the diagram. These microphotographs show the inner structure of the material in its primitive state, magnified 120 times.

Therefore when looking at a load-extension diagram and studying its shape the inner structure of the material can at the same time be kept under the eye and a comparison of strength and inner structure can be made. Further, since the magnification is kept constant, the microstructures of different materials can be compared amongst themselves on the same scale. In addition there are microphotographs magnified some more than 120 times, and some less, in order to bring out details of structure.

A comparison of the load-extension curves amongst themselves will show that metals may be grouped into families, each family being characterized by the form of the load-extension curve. The curve of the iron and steel group is totally different in general shape from the curve of the gun-metal group. Difference of curvature within a group-shape distinguishes members of the same family from one another. Differences in heat treatment and in the mechanical processes of manufacture are shown by differences of curvature in the diagram and sometimes by radical differences in the shape of the curves.

For example, the group curve for iron and steel in its normal condition is quite different in shape from the group curve of overstrained iron and steel. The material appears to belong to a different family. There is thus the family group of the material in its normal state and there is the family group of the same material in its overstrained state.

The shape of the load-extension curve tells much when its

language is understood, and practical experience soon enables differences in shape to be interpreted.

**26. Swedish Iron (Fig. 18).**—The test piece was cut from a bar of special purity given to me by Sir Robert Hadfield. This is the analysis :—

	Per cent.		Per cent.
Carbon . . . .	0·047	Phosphorus . . . .	0·057
Manganese . . . .	0·005	Silicon . . . .	0·014
Sulphur . . . .	0·008		

The recording spot of light, starting from zero, describes what appears to be a vertical line. It is however slightly inclined to the vertical axis, but the inclination is too small to be clearly shown by the extension scale used.

When the spot reaches 3·75 tons the test piece suddenly yields and the load automatically falls to a little over 3·2 tons, after which the spot wanders along an irregular path for about 0·12 inches at an average load of 3·3 tons, and then climbs upwards in a smooth curve to a maximum load of 5·25 tons. Local contraction sets in, and the spot falls along a smooth curve to the point of fracture. At the instant of fracture the recorded path of the spot ends. Its return to zero load is done so quickly that no record of its passage is left on the plate.

Up to the yield-point the extension is mainly elastic. After the yield-point the extension is mainly plastic. The elastic and plastic parts of the diagram are connected by an irregular link. When the extension includes plastic extension, it reveals itself as permanent set when the load is removed. The irregular link is a family characteristic of iron and carbon steels. It does not usually develop in normally treated alloy steels. I have found no trace of such a link in the diagrams of the non-ferrous metals.

The physical constants derived from the diagram are :—

Stress at yield-point . . . .	13·27 tons per square inch.
Stress corresponding to maximum load . . . . .	18·6      "      "      "
Stress at instant of fracture . .	48·7      "      "      "
Extension on 5 inches . . . .	35 per cent.
Reduction of area . . . . .	74 per cent.

The usual practice is followed in calculating the yield-stress and the stress corresponding to the maximum load, namely, to assume no change in the area of the bar and therefore to divide the respective loads by the original area of the bar.

SWEDISH IRON

To face p. 40.

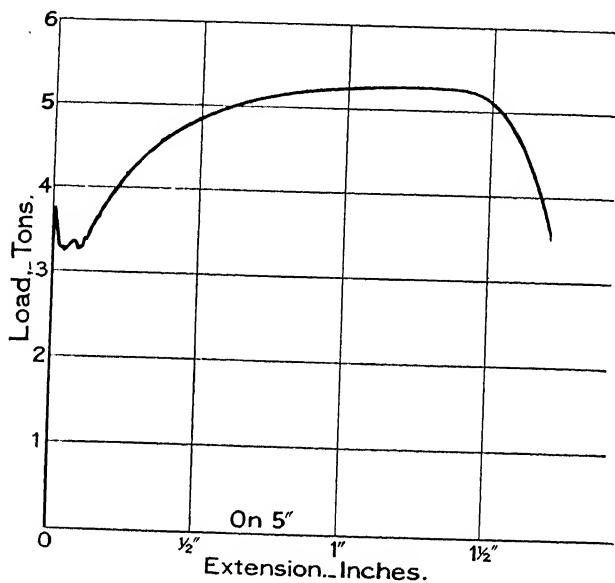


FIG. 18.



FIG. 19.—Longitudinal Section.  $\times 120$ .



FIG. 20.—Cross Section.  $\times 120$ .

In this test the area of the test piece before the application of the load was 0.2825 square inches.

The yield load measured from the diagram is 3.75 tons. The corresponding stress is then recorded as:—

$$\text{Stress at yield-point} = \frac{3.75}{0.2825} = 13.27 \text{ tons per square inch ;}$$

and for the maximum load of 5.25 tons,

$$\text{Stress corresponding} = \frac{5.25}{0.2825} = 18.6 \text{ tons per square inch.}$$

The stress at instant of fracture is calculated from the actual area of the bar at fracture. The area found by direct measurement of the fracture was 0.073 inches.

The load measured from the diagram is 3.55 tons.

$$\text{Stress at instant of fracture} = \frac{3.55}{0.073} = 48.7 \text{ tons per square inch.}$$

The extension on 5 inches can be measured directly from the diagram, and this can be checked by direct measurement from the broken halves of the test piece. These are clamped together longitudinally in an apparatus designed for the purpose in order to get the measurement accurately.

Reduction of area is the difference between the original area of the unloaded bar and the area of the fracture.

For this piece the reduction is  $0.2825 - 0.073 = 0.2095$  square inches, corresponding to 74 per cent. of the original area.

The inner structure of the metal is seen in Figs. 19 and 20. The metal is built of blocks irregular in shape and size. Each block is a crystal, and each block is itself built of atomic elements ranged in regular courses. Though the regular packing of the atoms is similar in each block, the general orientation of the atomic packing is different from block to block. Only the block arrangement is seen in the figures ; their own atomic structure is not shown.

The polished and etched plane in both samples catches the blocks of the block structure sometimes in full section and sometimes at a corner. A small area seen in the photograph may therefore correspond to the corner of a large block buried in the substance. It is therefore not easy to get the exact sizes of the blocks, but the eye looking at both sections together can get an impression of block size and shape which serves to distinguish between the inner structure of different samples. The central block in the cross-section is probably the largest block in the region photographed, being about 0.01 inch across its largest diameter. The black spots in the cross-section and the small elongated black threads in the longitudinal section are slag.



They are few and minute, a sign of good quality. The diameter of a slag spot does not exceed 0.0004 inch. Slag threads always appear in iron manufactured by the puddling process, but they are absent in steel or ingot iron which has been melted during manufacture.

**27. Yorkshire Iron (Fig. 21).** The test piece was cut from a bar of  $1\frac{1}{4}$  inches diameter, the analysis of which gives :

	Per cent.		Per cent.
Carbon . . . . .	0.049	Phosphorus . . . . .	0.083
Manganese . . . . .	0.015	Silicon . . . . .	0.145
Sulphur . . . . .	0.004		

The family likeness between the curves of Swedish iron and this curve is striking, but there are noticeable differences. Yorkshire iron is stronger than Swedish iron, but it does not stretch so much before fracture.

The physical constants derived from the diagram are :—

Yield stress on original area . . . . .	15.9 tons per square inch.
Stress corresponding to maximum load . . . . .	22    "    "    "
Actual stress at instant of fracture . . . . .	41.9    "    "    "
Extension of 5 inches . . . . .	28.4 per cent.
Reduction of area at fracture . . . . .	58.6 per cent.

The curves of both kinds of iron sweep down from the maximum load to the point of fracture in a way indicating great reduction of area before fracture. As explained above, from maximum load to fracture the extension recorded is local extension.

The inner structure of the material is seen in Figs. 22 and 23. The sections show good regular block structure, with blocks somewhat smaller than those in the Swedish iron section. The photographs were taken from samples cut from the unstrained end of the test piece. Cut sections of slag threads are seen in the cross-section and elongated pieces of the threads in the longitudinal section. The slag threads are fine, though more numerous than in the Swedish iron.

Yorkshire iron is a brand of recognized quality, and it commands a high price. It can be used with confidence where much afterwork in the smith's fire has to be done and where much welding is relied upon. It is useful where shock or vibration has to be withstood, as for draw-gear in railway vehicles, and it has many uses peculiar to itself even in the steel age.

YORKSHIRE IRON

To face p. 42.

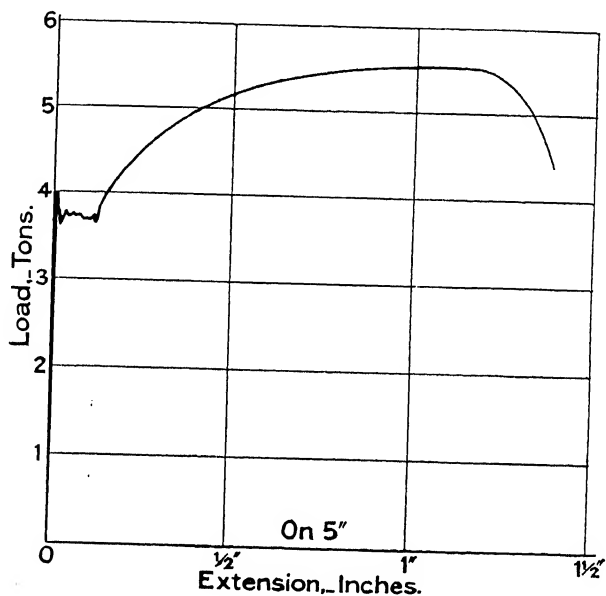


FIG. 21.

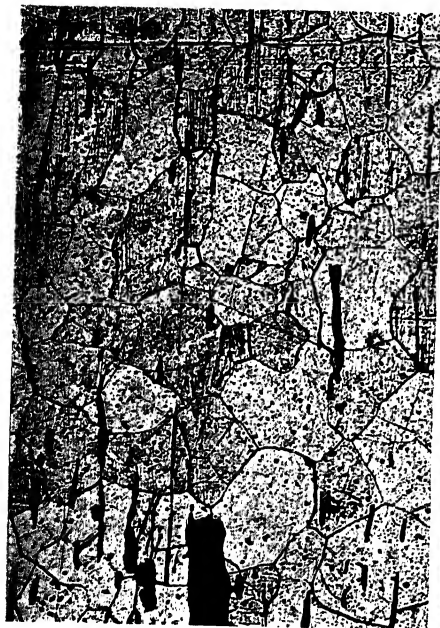


FIG. 22.—Longitudinal Section.  $\times 120$ .

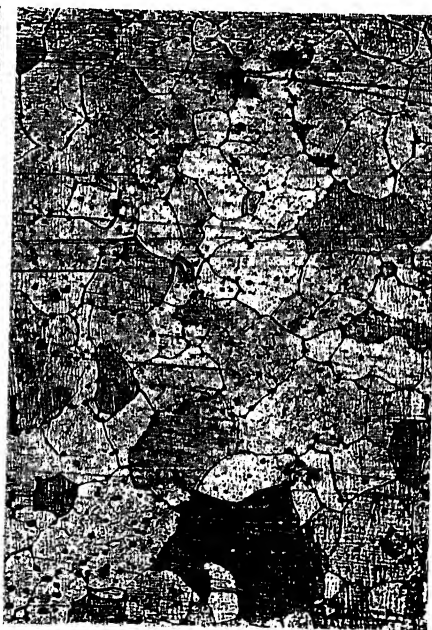


FIG. 23.—Cross Section.  $\times 120$ .

STAFFORDSHIRE IRON

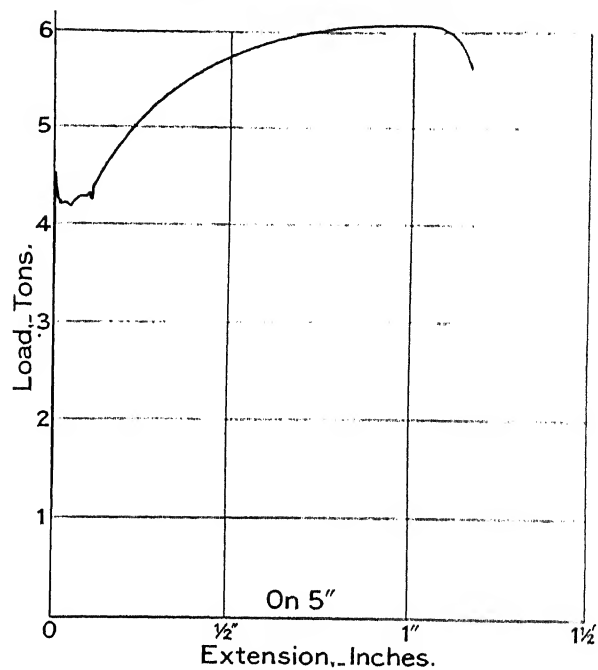


FIG. 24.



FIG. 25.—Longitudinal Section.  $\times 120$ .

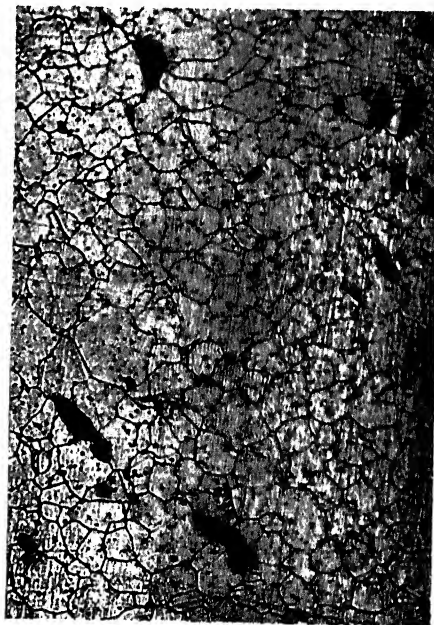


FIG. 26.—Cross Section.  $\times 120$ .

**28. Staffordshire Iron** (Fig. 24). The test piece was cut from a  $1\frac{1}{4}$  inch bar of good quality Staffordshire iron, the analysis of which gives:—

	Per cent.		Per cent.
Carbon . . . . .	0.075	Phosphorus . . . . .	0.188
Manganese . . . . .	0.050	Silicon . . . . .	0.180
Sulphur . . . . .	0.016		

The sulphur and phosphorus are not so perfectly removed as in Swedish and Yorkshire irons, and the effect, combined with differences in the process of manufacture, is seen in the load-extension diagram. There is the family likeness to Swedish and Yorkshire iron, but there is no longer the downward sweep of the curve from maximum load to fracture. Local extension and contraction of area are reduced, although the iron is stronger. The decreased ductility may be due to the phosphorus, and the slight toughening to the higher carbon and perhaps the sulphur.

The physical constants derived from the diagram are:

Yield stress . . . . .	18.02 tons per square inch.
Stress corresponding to maximum load . . . . .	23.95 „ „ „
Actual stress at fracture . . . . .	36 „ „ „
Extension of 5 inches . . . . .	23.6 per cent.
Reduction of area . . . . .	38 per cent.

The small reduction of area compared with Yorkshire Iron or Swedish Iron is very noticeable. This iron is considerably cheaper than the Yorkshire and Swedish brands.

A glance at the inner structure in Figs. 25 and 26 shows that the manufacturing process has not resulted in the uniformity of structure seen in the Yorkshire or Swedish brands, nor is the slag so completely expelled.

**29. Yorkshire Iron and the Puddling Process.** Yorkshire iron is made from ironstone mined in North Yorkshire. The fuel for smelting the ore is mined with it. In fact, the ore is found in beds sandwiched between beds of coal. The upper bed is in some districts called black bed coal and is used for boiler fuel. The lower bed is called better-bed coal and is used for smelting the ironstone above it because of its remarkable freedom from sulphur and phosphorus. Phosphorus produces brittleness in cold iron and sulphur a brittleness in hot iron. Neither is easily separated from iron when once it gets into it. Therefore ores and fuels free from these elements are specially valuable. The ideal of every iron and steel maker is an unlimited supply of

ore and fuel free from sulphur and phosphorus. In practice, as will be seen from the analyses given, the quantities present in the finished product of both iron and steel are small.

Mines, blast furnaces, and ironworks are clustered together near the deposits in the districts about Leeds, notably at Farnley and Lowmoor and Monkbridge. The ore is reduced in the blast furnace to grey pig. Grey pig is then melted with coke on the open hearth of a refinery and the molten metal is run from the hearth on to the sand floor surrounding the refinery and solidifies in shallow pools about 3 inches deep. The refining process transforms the grey pig into white iron and removes most of the silicon. The solidified slabs are broken into lumps and are transferred to the puddling shop.

The puddler removes the carbon from this white iron, together with other impurities, and produces a material which, although not carbon-free, contains small percentages only, and even smaller percentages of phosphorus and sulphur. The chemical analysis of the test pieces of Yorkshire iron given in Table 2 shows to what a state of purity the iron is brought by the puddling process.

The white iron lumps are, after a preliminary heating by the furnace gas, melted on the hearth of a furnace by heat derived from a coal fire placed on one side of the hearth. The flames from the furnace are deflected from the roof over the hearth to the metal on the hearth and pass away to the chimney on the other side of the hearth, heating the white iron lumps placed in their way as they go. When the lumps are melted some oxygen-carrying substance is added to the bath, usually bloom cinder, or even air is admitted. The puddler inserts an iron bar through the hole in the furnace door and thoroughly mixes the oxidizing substance into the melted iron. The carbon in the boiling bath then combines with the oxygen presented to it and passes away with the furnace gas as carbon monoxide, burning as it goes to carbon dioxide. With the disappearance of the carbon from the bath the iron becomes viscous. The viscous mass is manipulated by the puddler into lumps, and at the end of the operation the liquid bath of impure iron has been transformed into three or four pasty lumps, each weighing about 1 cwt.

A lump dripping with slag is removed from the hearth on the end of the rabble to the steam hammer. The hammer at first is let down gently on the dripping lump and squeezes it. Slag spurts out in every direction. The lump is turned under the hammer in all ways and squeezed until the slag is all squeezed out of it; the blows from the hammer then become firmer, and

the lump is gradually forged into a block about 14 inches square and 2 inches thick. This block is called a **Stamping**. Each lump in turn is brought from the hearth on the end of the rabble and is hammered into a stamping. Each stamping is then broken in halves.

These half-stampings are piled into cubes about 14 inches each way. A cube is piled from half-stampings selected from all the puddling furnaces in the shop, so that the material represents the average skill of all the puddlers. Each cube is bound with wire, heated in a furnace to welding heat, and then brought out and hammered and rolled into a bar about 8 feet long, 3 inches wide, and  $1\frac{1}{2}$  inches thick, or some such general dimensions.

These bars are then cut into short lengths, the short lengths are piled into cubes, and the cubes are reheated, hammered, and rolled a second time. The process is repeated a third time, and the reheated cube is hammered into a block about 18 inches long and 5 inches square. This block is called a **bloom**, and it is the final product of the ironworks. These blooms are then rolled into angle irons, bars, plates, or sections.

Staffordshire iron is produced by a similar puddling process, but the refinery operation is omitted. The Staffordshire ironstones and fuels differ in quality from those of North Yorkshire, and the pig is charged directly on to the hearth of the puddling furnace.

**Steel.** Up to the date of the invention of the puddling process by Court in 1784, malleable iron was produced in small quantities by fusing the pig iron with coke or charcoal. The invention of the puddling process made it possible to produce malleable iron in large quantities at a time, and cheapened the product. The invention gave to England a commercial supremacy during the century following and was a source of untold wealth to this country. All through the age of puddled iron Yorkshire iron held a leading place.

Steel during this period was made from puddled bar by an old process of **cementation**. Bars of good iron were packed in an iron box with charcoal or bone or some carboniferous material free from oxygen, and the box was luted up and placed in a furnace and kept there for several days. The carbon from the packing made its way into the heated iron bars and so changed them into steel. After this process of cementation the bars came out of the boxes covered with blisters, and in consequence they received the name **blister steel**. Blister steel, cut into lengths, piled, hammered, or rolled, was changed to a product called

**single-shear steel.** Single-shear steel, cut, piled, hammered, or rolled, became **double-shear steel.** But fine steel of uniform quality was made by the Huntsman process, a process still in use. Blister steel was broken into short lengths and was melted in a crucible. The steel poured from these crucibles was known as **crucible-cast steel.** It was known to early steelmakers that manganese had a beneficial effect on the quality of steel. Its voracity for oxygen exceeded the power of the iron to hold oxygen, and its presence in the iron therefore prevented the formation of oxide of iron, a substance very deleterious to the quality of the product. Whatever be the process of its preventive action it was known that the fine quality of the steels made in Styria and in Germany was due to the presence of manganese in the ore from which the iron was produced, which the steelmakers used for conversion into steel. Also Heath, an Indian Civil Servant, discovered that the excellent quality of certain Indian steels was due to manganese in the metal. He came home and patented the process of adding manganese to steel. It was added, in the form of carburet of manganese, to the crucible in which the Huntsman process was being carried out. The quality was improved and the process became general, but Heath himself did not reap the benefit of his discovery because his patents were generally infringed, and so slow is our process in the law courts that although the Lords ultimately gave a decision in his favour, it was too late to help him, for he was dead.

Manganese is now added to steel in the form of **ferro-manganese.** This substance usually contains about 80 per cent. of manganese, 14 per cent. iron, and 6 per cent. carbon. Its addition to a converter or bath of decarburized iron therefore allows the manganese to exert its influence and at the same time carburizes the bath to the particular percentage aimed at. Recarburization is also done by adding **spiegeleisen**, a natural product containing about 6 per cent. of carbon, but much less manganese than ferro-manganese.

This was the state of things up to the year 1856: iron bars, plates, and angles, made from puddled blooms, universally used for structural material; steel made by the cementation process for ordinary use; and fine steels for cutlery made by the Huntsman process.

Bessemer at the Cheltenham meeting of the British Association announced his discovery, and his discovery revolutionized the industry. His process was to melt pig iron and then to blow air through it. The oxygen of the air oxidized the impurities,

including the carbon, and at the end of the process the liquid bath was converted into iron practically devoid of carbon and other impurities found in the pig. Carbon was then added, to the degree required, by the addition of a known weight of spiegel-eisen or ferro-manganese.

The process was carried out in a vessel called a converter, mounted on trunnions and lined with ganister, a refractory substance almost pure silica. A usual converter capacity was 5 tons. The pig iron to be converted was melted in a cupola near the converter and run from it into the converter. A blowing engine then forced air through the mass of metal in the converter, the air entering through fine holes in the ganister lining at the bottom. In about twenty minutes carbon and silicon had been burnt out and the flaming gas had died down at the mouth of the converter. The addition of ferro-manganese, or of spiegel, or of both, then took place, the converter was next turned down on its trunnions and its charge of steel poured into ingot moulds ranged round the apparatus. The plant was under control by hydraulic power.

The steel age began with the introduction of this process in 1857. The process spread rapidly all over the world. There was however one limitation to the process as carried out by Bessemer. The process did not remove phosphorus from pig iron. Any phosphorus in the pig before the blow remained in the steel after the blow. Phosphorus cannot be permitted in steel except in very small percentages, because it produces brittleness.

Iron, for conversion to steel by the Bessemer process, had therefore to be free from phosphorus. This limited the choice to Swedish pigs or pigs made from hematite ore. This limitation was removed by Thomas and Gilchrist, who were cousins. Gilchrist was a student at the Royal School of Mines and took his Associateship in 1871. It was generally known that phosphorus could be removed from the melt by adding lime to the converter. The difficulty was that the products of the reaction dissolve the silica lining of the converter. Thomas and Gilchrist substituted for the silica lining a lining made from dolomite, magnesian limestone. The lining was then basic instead of acid, and the products of the reactions between the lime and phosphorus did not attack it. The discovery was announced at a meeting of the Iron and Steel Institute in 1878. The process was demonstrated in 1879 at the works of Bolckow, Vaughan & Co., Middlesbrough, and good steel was made from low-grade ore, hitherto unusable.



The process developed rapidly in Belgium, France, and America, and enabled Germany to use her deposits of low-grade ore for steel-making.

The difference, then, between acid Bessemer steel and basic Bessemer steel is that pig iron low in phosphorus is decarburized in a converter lined with ganister and that pig iron high in phosphorus is decarburized and dephosphorized in a converter lined with dolomite. Both melts are changed into steel by the addition of the assigned quantity of carbon put in with ferromanganese. The general process of blowing the charge in the converter is the same in the two processes, except that in the basic process a short after-blow is given after the addition of lime to remove the phosphorus. The **Siemens open-hearth** process grew alongside the Bessemer process, and from being a formidable rival has in many districts displaced it. The process consists in the decarburization of pig iron by melting with it iron ore, an oxide of iron, with or without steel scrap. This process is carried out in a **Siemens regenerative furnace**. In the older furnaces heat for melting the charge placed on the hearth of the furnace was obtained from a coal fire at one side of the furnace. The flames, passing over the low wall separating the furnace proper from the hearth, were deflected by the roof of the furnace down on to the ingredients on the hearth, and then, passing away to the chimney on the opposite side of the furnace, carried away to the atmosphere heat which was thus lost.

The object of the designer of the regenerator furnace is to conserve the heat thus lost. The coal fuel is first gasified in separate gas producers and is then led through flues to the furnace hearth, mingling at exit in the furnace with air brought through separate flues and delivered into the furnace in the right proportion for proper combustion of the simultaneously delivered gas. The flaming gas is reflected from the roof of the furnace on to the ingredients of the charge on the hearth and then passes away through openings on the opposite side of the hearth to the chimney. Placed in the flue, full in the way of the hot, flaming gas escaping from the furnace, are stacks of firebricks, loosely piled so that the escaping gas, flowing through the spaces between the bricks, gives up heat to the bricks. When the bricks have become heated to a state of incandescence, the whole flow of gas and air to the furnace and burnt gas from the furnace is reversed by merely turning two reversing valves in the flues, one to reverse the air-flow and the other to reverse the gas-flow.

The first Siemens regenerative furnace was erected at Chances' Glass Works, Birmingham, in 1861.

The hearth of the furnace is lined with acid or basic materials, according to the grade of pig iron to be dealt with. In the Bessemer process the pig iron to be converted is first melted in a cupola near the converter, from which it is run into the converter either along a suitable channel or is transferred in a ladle. In the open-hearth process pig iron and scrap steel are placed on the hearth of the furnace and are there melted, after which iron ore is added to decarburize the pig and to oxidize other impurities. At the end of the melting and purifying process the hearth contains limpid liquid steel containing only a small percentage of carbon. Ferro-manganese is added to bring the bath to the assigned carbon percentage, and then the charge is run off into a ladle through the taphole of the furnace. It may be let out from the ladle into ingot moulds carried on small trucks running on a railway beneath the ladle.

These few general remarks about steel manufacture may be helpful to students. For detailed knowledge of the subject the work on *The Metallurgy of Iron*, by Professor Thomas Turner (Griffin, London, 1915), should be studied, and also that on *Steel* by F. W. Harbord and J. W. Hall (Griffin, London, 1911).

We now pass on to consider typical carbon-steel diagrams.

**30. Mild Steel.**—Fig. 27 shows the diagram of a piece of mild steel. The test piece was turned from a rod 1·065 in. diameter. The chemical analysis is:—

	Per cent.		Per cent.
Carbon . . . .	0·132	Phosphorus . . . .	0·028
Manganese . . . .	0·300	Silicon . . . .	0·028
Sulphur . . . .	0·017		

The shape of the curve is similar to those of iron. There is the quick drop from the yield-point to an irregular link, and the smooth rise to maximum load, after which the load falls evenly to fracture.

The physical constants of the metal deduced from the curve are:—

Stress at yield-point . . . .	18 tons per square inch
Stress corresponding to maximum load . . . .	24·8 „ „ „ „
Stress at instant of fracture . . . .	53·8 „ „ „ „
Extension on a length of 5 inches . . . .	30·6 per cent.
Reduction of area . . . .	67·4 „ „

The inner structure, magnified 120 times, is seen in Fig. 28 (longitudinal section). Compared with the inner structure of Swedish iron (Fig. 19), or Yorkshire iron (Fig. 22), the block size is finer, and there are two kinds of blocks, black and white. The black blocks must not be confused with slag, because the steels are practically slag free. The substance of a white block is called **ferrite**. Ferrite may be regarded as pure iron from the point of view of metallography. The substance of a black block is called **pearlite**.

In order to show that the distribution of the black blocks amongst the white is not necessarily uniform, Fig. 29 shows a cross-section magnified only sixty times. This photograph shows that the pearlite blocks are by no means uniformly distributed through the metal. The bar from which the test piece was turned was annealed. Reference for further information about this particular material may be made to the Interim Report of the British Association Committee on Stress Distribution in Engineering Materials published on page 159 of the 1915 B.A. Report.

The Committee obtained a stock of 1 ton of this mild steel early in 1914. The material was from a single melt, and the preliminary tests furnished by Mr. Cook show the influence of rolling on the physical constants. For example, a bar rolled down to  $\frac{1}{16}$  inch diameter shows a yield stress as high as 23·9

MILD STEEL.

To face p. 50.

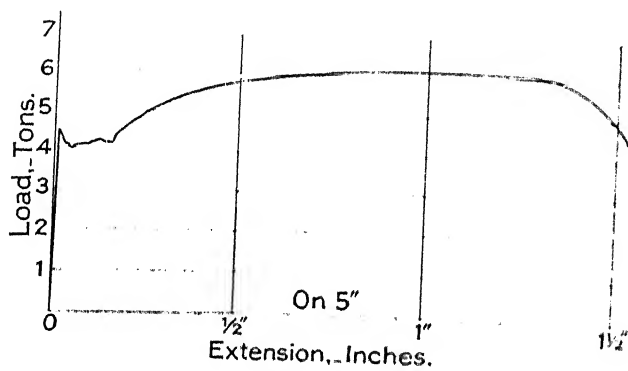


FIG. 27.

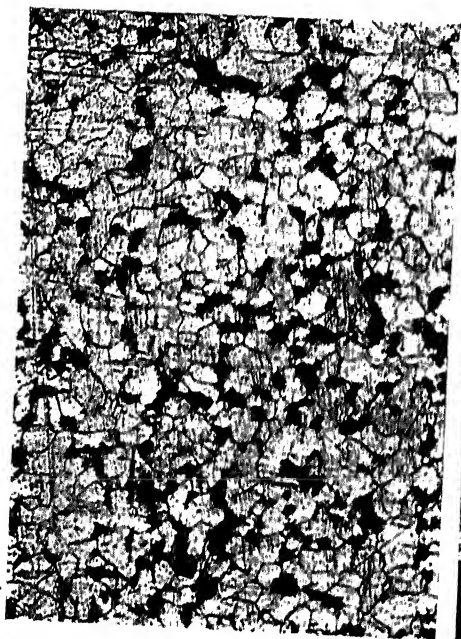


FIG. 28. Longitudinal Section. - 120.



FIG. 29. Cross Section. - 60.

STEEL

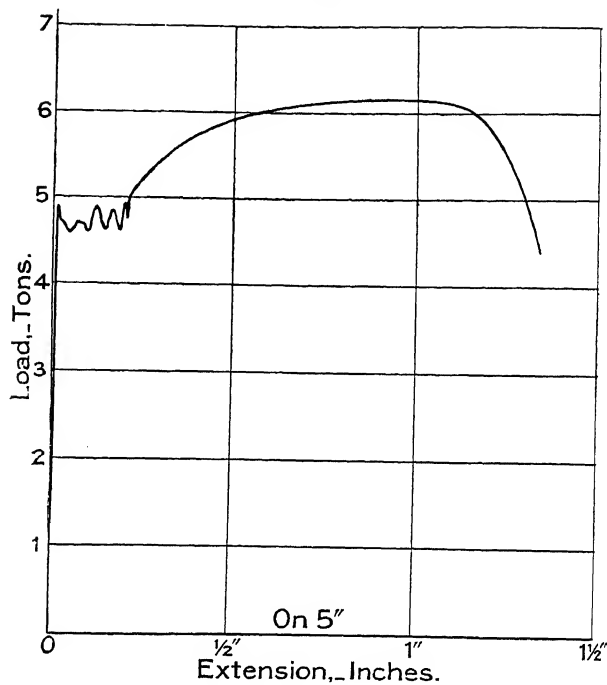


FIG. 30.



FIG. 31.—Longitudinal Section.  $\times 120$ .

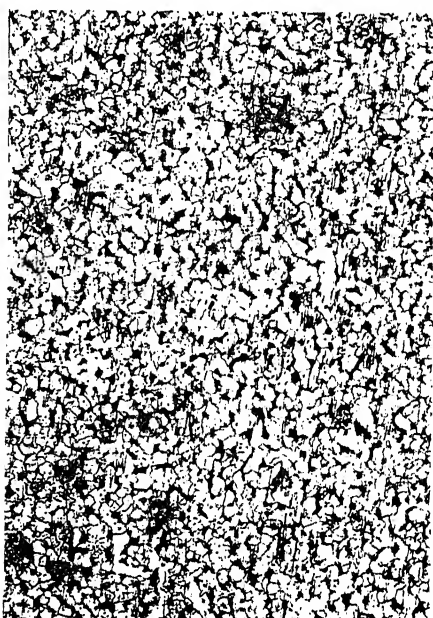


FIG. 32.—Cross Section.  $\times 120$ .

tons per square inch, whilst a bar rolled only to  $1\frac{5}{16}$  inch diameter has a yield of 13 tons per square inch. The higher yield stress is produced by the greater amount of mechanical work done upon it to reduce it to the smaller diameter. Tests by alternating loading were made by Dr. B. P. Haigh.

**31. Steel.** - Fig. 30 shows the load-extension diagram of a 0.22 carbon steel. The chemical analysis is: -

	Per cent.		Per cent.
Carbon . . . .	0.22	Phosphorus . . . .	0.03
Manganese . . . .	0.49	Silicon . . . .	0.035
Sulphur . . . .	0.02		

The curve possesses the family characteristics of the irons and steels, but with a marked individuality of the irregular link. In fact, the pronounced waves in this link give a clue to its meaning. The central peak in the link shows that the plastic curve had commenced, but that a local yield-point occurred and the load dropped. Four times the effort was made and four times the metal yielded. This indicates that the metal does not yield uniformly all along the gauge length at the same instant. When the first yield takes place, that is, when the beam drops in a lever testing machine, some of the metal along the gauge length has still to pass the yield-point. As will be seen later, iron and steel are peculiar in this respect because no irregular link is seen in the load-extension diagrams of other metals or even in alloy steels.

The physical constants obtained from the diagram are: -

Stress at yield-point . . . .	22.8 tons per square inch.
Stress corresponding to maximum load 28.65 . . . .	" " " "
Stress at instant of fracture . . . . 59.9 . . . .	" " " "
Extension on a length of 5 inches . . . . 26 . . . .	per cent.
Reduction of area . . . . . 30 . . . .	" "

The inner structure (Fig. 32) shows an even distribution of black pearlite blocks amongst the white ferrite blocks, and the longitudinal section (Fig. 31) indicates banding in the direction of rolling. Rolling does not always produce this banded effect, as will be seen by comparing the longitudinal structure of other samples. The banding is probably connected with the temperature of rolling.

**32. Bright Drawn Steel.** (Fig. 33.) The test piece was turned from a bar of bright drawn steel taken out of stock. The chemical composition of the material is as follows.

	Per cent.		Per cent.
Carbon . . . . .	0.195	Phosphorus . . . . .	0.049
Manganese . . . . .	0.570	Silicon . . . . .	0.020
Sulphur . . . . .	0.038		

The physical constants are :—

No marked yield-point.

Stress corresponding to maximum load 33.7 tons per square inch

Stress at instant of fracture . . . 50.0    "    "    "    "

Extension on 5 inches . . . 16.3 per cent.

Reduction of area . . . 54.0    "    "

The inner structure of the material is seen in Figs. 34 and 35. The distribution of black pearlite blocks in both cross and longitudinal sections is remarkably uniform. Neither the preliminary hot rolling nor the subsequent cold working in the process of producing bright drawn steel has produced banding in the pearlite. From the longitudinal section the blocks have an average diameter of about 0.001 inches.

The shape of the load-extension diagram is strikingly different from any yet illustrated of iron and steel. Yield drop, and irregular link have disappeared and the curve is smooth from origin to fracture. The diagram is however consistent. Its peculiar shape reveals that the metal is in an overstrained condition. This condition is produced by the cold work done upon it in the manufacturing processes. There is nothing in the microphotographs to indicate that the material is in the overstrained state. The structure is regular and normal and on the scale shown, namely 120 diameters, the inner structure would suggest material in the normal unstrained condition.

BRIGHT DRAWN STEEL

To face p. 52.

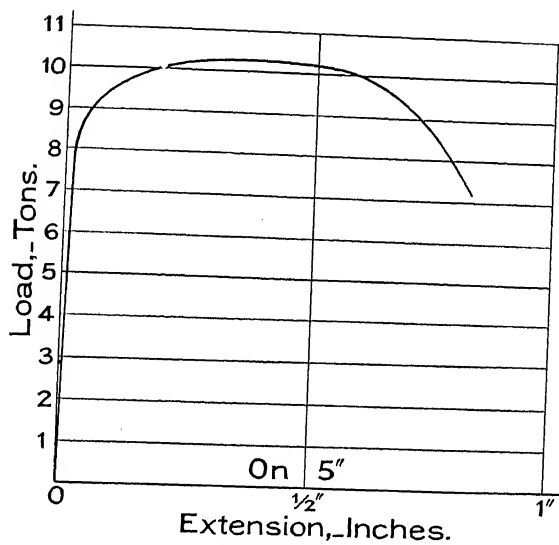


FIG. 33.

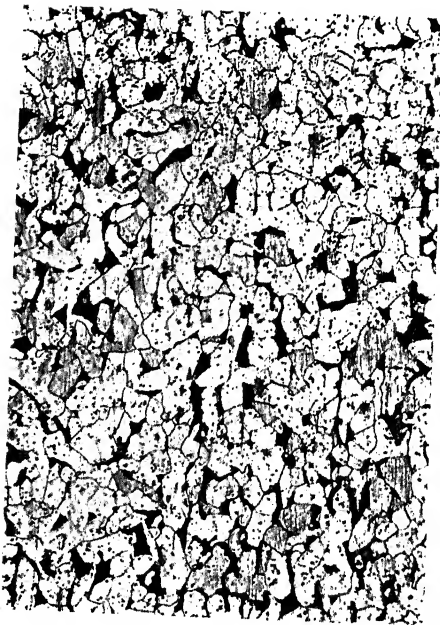


FIG. 34.—Longitudinal Section.  $\times 120$ .

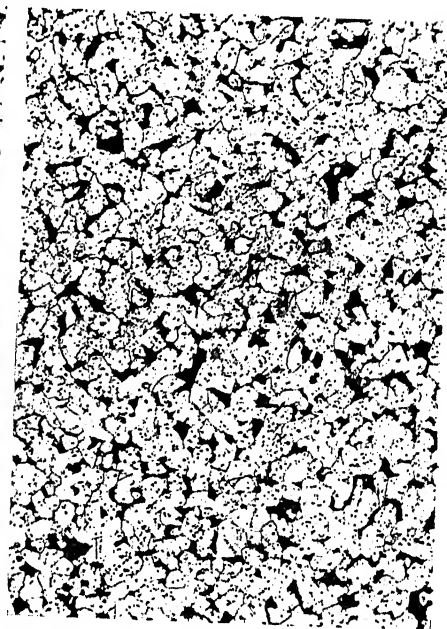


FIG. 35.—Cross Section.  $\times 120$ .



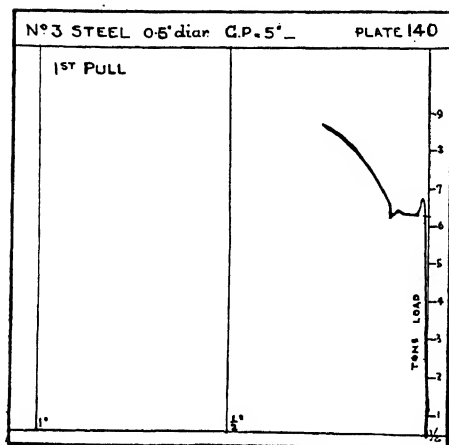


FIG. 36.

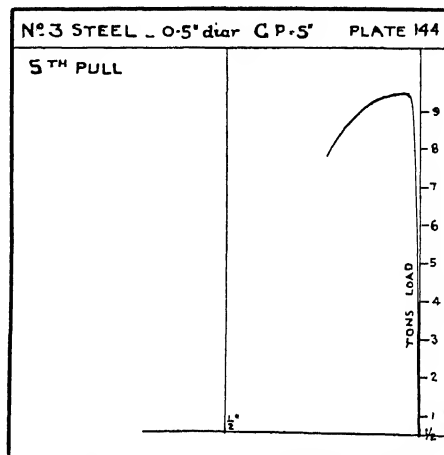


FIG. 37.

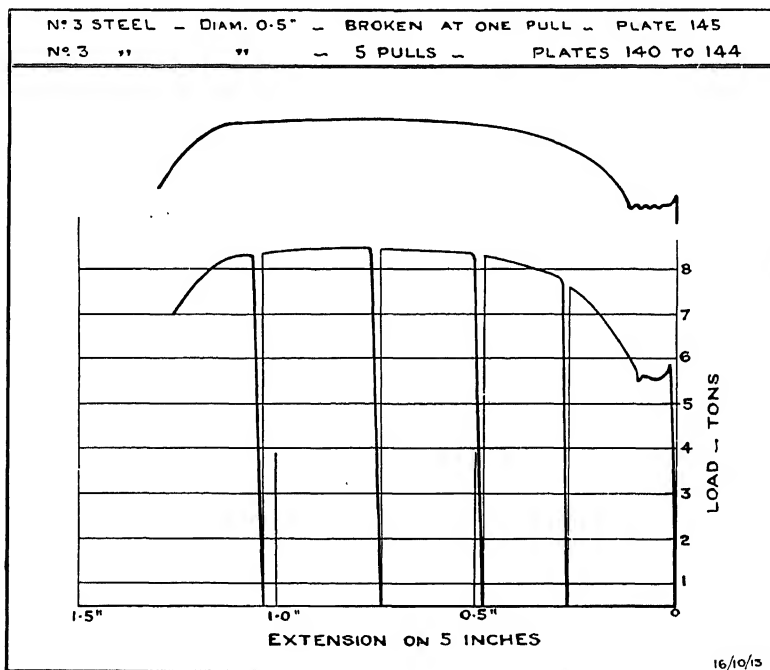


FIG. 38.

To illustrate this, consider the diagram Fig. 36. It is from a steel test piece, but stretching was stopped and the load was removed when the piece had been stretched about  $\frac{1}{4}$  inch. The load was then reapplied and the piece was stretched to a little over 1 inch. The load was again reapplied and the piece was broken, and the diagram for this operation is seen in Fig. 37. This diagram is similar in shape to the diagram Fig. 33. The inference is that the material giving diagram Fig. 33 is in a state similar to that of the material giving the diagram Fig. 37, that is, overstrained.

Fig. 38 shows the complete story of the test, of which Fig. 36 is the beginning and Fig. 37 is the end. Five plates were taken in sequence. The five plates placed in order are seen in Fig. 38. The upper contours of the diagrams run into a curve which is true to the group curve of the iron and steel family. The continuous curve in the upper part of Fig. 38 was taken in one pull from a test piece of the same material. It should be understood that each diagram of the sequence of five was taken separately on a separate negative. The time elapsing between the diagrams was only a few minutes.

**33. Bright Drawn Steel, Heat-treated.**—Fig. 39 shows the effect of heat treating the overstrained metal of Fig. 33.

Two test pieces were cut from the same bar of bright drawn steel taken out of stock. One of them, broken straight-away, gave the load-extension diagram (Fig. 33). The second test piece, annealed for forty-five minutes at 550° C. and afterwards broken, gave the diagram Fig. 39.

The annealing process has quite restored the steel to its normal state, and the load-extension curve at once falls into the group shape belonging to irons and steels. From this plate the physical constants of the annealed metal have been calculated and they are recorded in the first column below. In the second column are given the figures corresponding to Fig. 33 for comparison.

	FIG. 39.	FIG. 33.
Stress at yield . . .	33.3 tons per sq. in.	
Stress corresponding to maximum load . . .	35.2 „ „ „	33.7
Extension on 5 inches . .	17.4 per cent.	16.3 per cent.
Reduction of area . . .	55.0 „ „	54.0 „ „

The heat treatment has restored the metal to the normal state of mild steel corresponding with the carbon content.

The inner structure of the annealed material is seen in Fig. 40. It differs little from the inner structure of the overstrained material. The structure of the cross-section is very similar. Two microphotographs (Figs. 41 and 42) are added, magnified only forty times to show how regularly the pearlite constituent is distributed through the material.

**34. Mild Steel, containing 0.1 per cent. nickel.**—Fig. 43 is a diagram from a steel test piece of which the chemical analysis is :—

	Per cent.		Per cent.
Carbon . . . . .	0.13	Phosphorus . . . . .	0.01
Manganese . . . . .	0.38	Silicon . . . . .	0.27
Sulphur . . . . .	0.02	Nickel . . . . .	0.10

The physical constants derived from the diagram are :—

Stress at yield-point . . .	9.2 tons per square inch
Stress corresponding to maxi- mum load . . . . .	21.2 „ „ „ „
Stress at instant of fracture .	41.5 „ „ „ „

XIV.

# BRIGHT DRAWN STEEL, HEAT TREATED

To face p. 54.

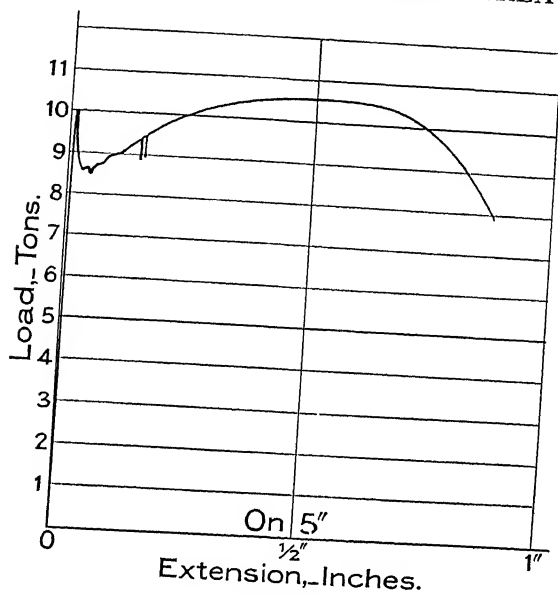
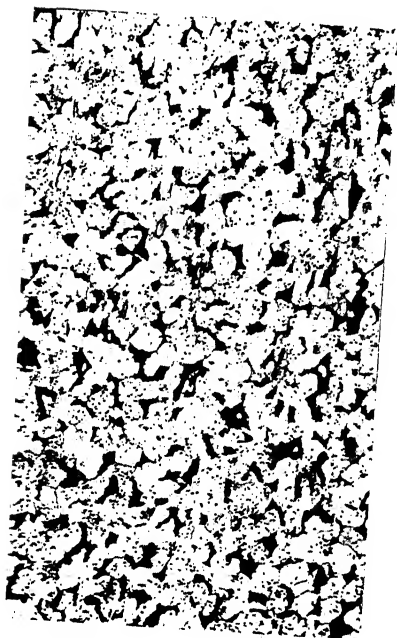


FIG. 39.



—Longitudinal Section.  $\times 120$ .

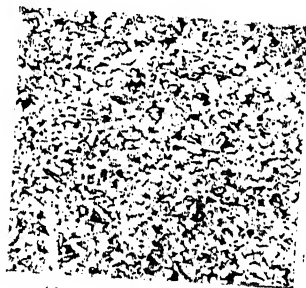


FIG. 41.—Longitudinal Section.  
 $\times 40$ .

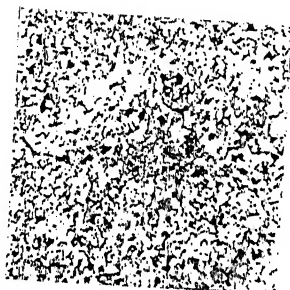


FIG. 42.—Cross Section.  $\times 40$ .

MILD STEEL  
CONTAINING 0.1 PER CENT. NICKEL

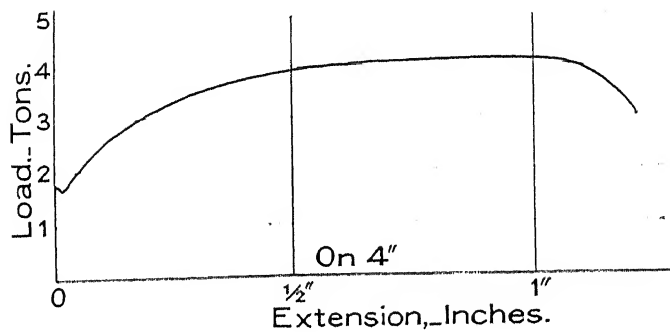


FIG. 43.



FIG. 44.

× 120.

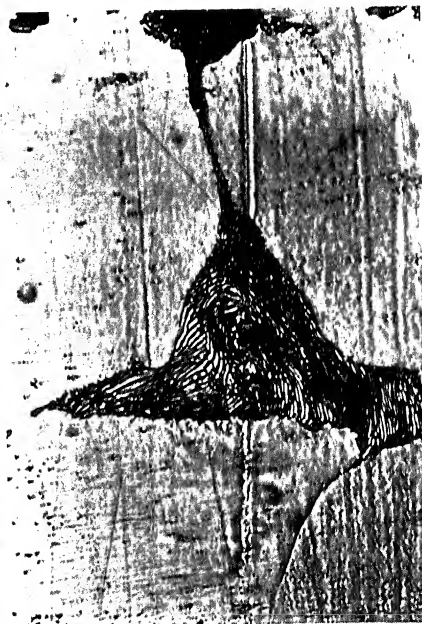


FIG. 45.

× 720.

Extension on 4 inches gauge	
length . . . . .	31 per cent.
Reduction of area . . . . .	64 „ „
Charpy impact number . . . . .	1.56
Brinell hardness . . . . .	81

The yield stress is remarkably low for steel with the carbon content of 0.13 per cent., as will be seen by comparing the results with those of mild steel of the same carbon content (§ 30).

Fig. 44 shows the inner structure magnified 120 times. Compared with Fig. 28 and with the other structures of steel (Figs. 32, 34), it will be seen that the blocks are relatively enormous in size. Very approximately these blocks, as seen on the diagram, are each of the order 1 square inch area as compared with 0.022 square inch in Fig. 34. The linear relation being 0.15 to 1, the block volumes are in the ratio of 1 to 350 approximately. Sir Robert Hadfield, who gave me the steel, described it as embrittled and told me that this large block size was brought about by prolonged annealing at about 1200° C. and slow cooling in the crucible. Block size has grown at the expense of the strength.

**35. Pearlite.**—The black pearlite blocks may now be more closely examined. Fig. 45 shows one of the black blocks of Fig. 44 magnified 720 times. The particular block seen in Fig. 45 does not appear in the field of view of 44, but it is not far from it. The structure seen is called laminated pearlite. The laminations are alternating sheets of ferrite and cementite.

**Cementite** is the chemical compound of iron and carbon,  $\text{Fe}_3\text{C}$ . Thin sheets of iron alternating with thin sheets of cementite, packed closely together about 60,000 sheets to the inch, form the substance of a pearlite block, and these packed sheets are bent in the pack into shapes which suggest that the final forms of the blocks seen in the microscope have been developed against a complicated play of internal molecular forces.

Steel containing 0.9 per cent. of carbon and suitably annealed is found to be built entirely of pearlite blocks. It is usually assumed that the whole of the carbon present is combined with iron to form the cementite sheets, and therefore that none of it is dissolved in the iron sheets or iron blocks. With this assumption the composition of a pearlite block can be deduced.

From the chemical formula  $\text{Fe}_3\text{C}$ , 0.9 per cent. of carbon requires  $\frac{0.9 \times 168}{12} = 12.6$  per cent. of iron to form cementite, assuming that the atomic weights of iron and carbon are respec-

tively 12 and 56. Therefore in 100 parts by weight of pearlite there will be  $12.6 + 0.9 = 13.5$  parts by weight of cementite, and the remaining 86.5 parts by weight of iron in the iron laminations. In general, assuming that all the carbon present in the pearlite is in the cementite sheets, and taking 0.9 as the carbon content corresponding to the all-pearlite structure,  $x$ , the percentage of pearlite contained in a steel containing  $c$  per cent. of carbon, is

$$x = 111c,$$

and the iron left over to form iron blocks after the laminated pearlite is formed is

$$100 - 111c \text{ per cent.}$$

For example, the steel of which Fig. 44 is the inner structure contains 0.13 per cent. of carbon, then the iron blocks contain  $100 - 111 \times 0.13 = 86$  per cent. of iron and the black blocks contain 14 per cent. of pearlite. This 14 per cent. of pearlite contains all the carbon, and the balance of the iron partly in chemical combination with the carbon to form  $\text{Fe}_3\text{C}$  and partly in laminations. The black blocks in Figs. 28, 32, 35 are constructed of lamellar pearlite.

The formation of lamellar pearlite takes place as the metal cools and when heat flows from it at a certain rate. Lamellar pearlite is not formed if the heat flows away too fast. It is also not formed if it is cooled too slowly, nor if other metallic alloys are present in any great proportion. Its appearance may be taken as an index of a moderate rate of cooling and absence of much alloy.

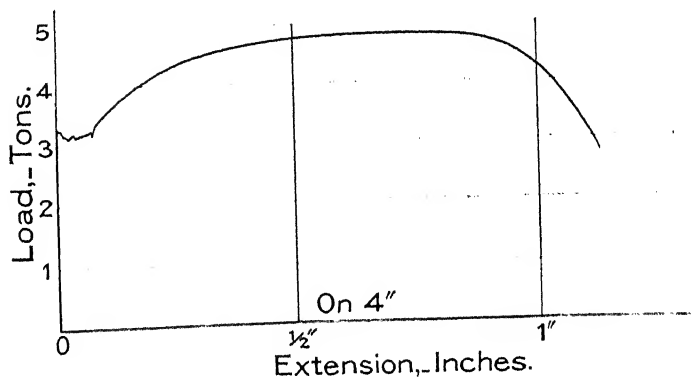


FIG. 46.





**36. Heat Treatment to reduce the Block Size of Steel.—**

As an immediate illustration, the presence of nickel and a special heat treatment increased the strength and produced a non-pearlitic structure of the embrittled steel whose load-extension curve is Fig. 43, with corresponding inner structures Figs. 44 and 45. A test piece of it was heated for thirty minutes at 880° C. and then quenched in water, after which it was reheated for two hours at 650° C. and cooled slowly. The load-extension diagram Fig. 46 shows that its yield stress has been doubled. The block size of the inner structure has been reduced. Lamellar pearlite could not be seen in any of the blocks, even under the highest powers.

The physical constants are brought together here for comparison. The peculiar behaviour of this steel is probably due to the nickel present in it. Physical constants derived from the diagrams are :—

	Embrittled State.	Heat-treated State.
Stress at yield-point	9.2	18.4 tons per square inch.
Stress corresponding to		
maximum load	21.2	24.8   "   "   "   "
Stress at fracture	41.5	71.0   "   "   "   "
Extension on 4-inch		
gauge length	31.0 per cent.	29.5 per cent.
Reduction of area	64.0   "   "	80.0   "   "
Charpy impact num-		
ber	1.56	18.67
Brinell hardness	81.0	106.0

**37. Strength and Inner Structure of Mild Steel.—**In a paper by the author published in the *Transactions of the Institution of Naval Architects*, 1917, some facts are marshalled which indicate that the strength of pure carbon steel increases uniformly with the increase of carbon provided that the heat treatment has been such as to produce lamellar pearlite in the structure.

Assuming a linear relation between the stress corresponding to the maximum load on a test piece  $f_s$  and the carbon content  $c$  of the steel, the relation deduced from these experiments is

$$f_s = 51c + 16.$$

The strength of steel in the region of 0.9 per cent. of carbon varies in a somewhat erratic manner. The formula is not reliable above about 0.7 per cent. of carbon. A steel containing 0.13 per cent. carbon from this formula should have a value of  $f_s = 22.63$  tons per square inch. The expression will be found useful in estimating to a first approximation the strength of steel

of known carbon content annealed so that lamellar pearlite is produced.

**38. Nickel Steel.**—Fig. 48 shows the normal diagram for nickel steel of the following composition :—

	Per cent.		Per cent.
Carbon . . . .	0.32	Silicon . . . .	0.09
Manganese . . . .	0.56	Nickel . . . .	3.52
Sulphur . . . .	0.037	Copper . . . .	0.042
Phosphorus . . . .	0.027		

This normal state is produced by special heat treatment on the part of the manufacturer. Sometimes the drop at yield is more pronounced and approaches a carbon steel in shape. But this difference indicates a difference of heat treatment or mechanical treatment in the process of manufacture.

Alongside is seen a diagram (Fig. 49) taken from a test piece of overstrained nickel steel. There is a total absence of drop at yield. Both these pieces were cut from the same material. The test piece from which Fig. 49 was taken was first stretched  $\frac{1}{10}$  inch to overstrain it and then the load-extension diagram was taken.

The inner structure of normal and overstrained material is seen in Figs. 50 and 51, both magnified 120 times. The structure seen is in longitudinal section, but the cross-sections showed little difference. The specimen cube, the etched surface of which is seen in Fig. 50, was cut from the end of the test piece 49 and the specimen cube, the etched surface of which is seen in Fig. 51, was cut close to the fracture of test piece 49. Both are therefore from the same test piece. The material seen in Fig. 50 has not been under load at all. The material seen in Fig. 51 has been under a stress corresponding to a direct pull of more than 60 tons per square inch. Little difference is seen in the structures. Below are two photographs (Figs. 52 and 53), in which the structure is magnified 36 times.

The physical constants derived from the diagrams are as follows :—

	FIG. 48.	FIG. 49.
Stress at yield . .	36	37.6 tons per square inch.
Ultimate stress . .	46.6	46.0    "    "    "    "
Stress at fracture .	63.0	66.5    "    "    "    "
Extension on 5 inches	16 per cent.	14.4 per cent.
Reduction of area .	36.6    "    "	39.9    "    "

NICKEL STEEL

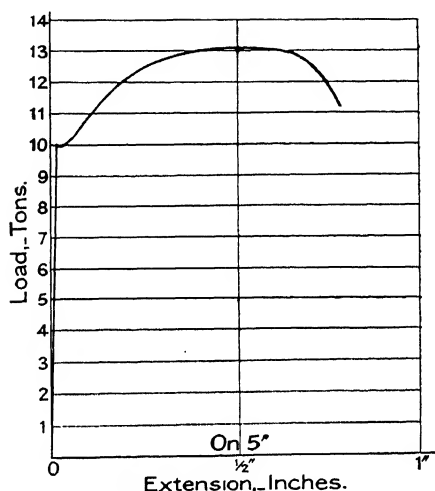


FIG. 48.

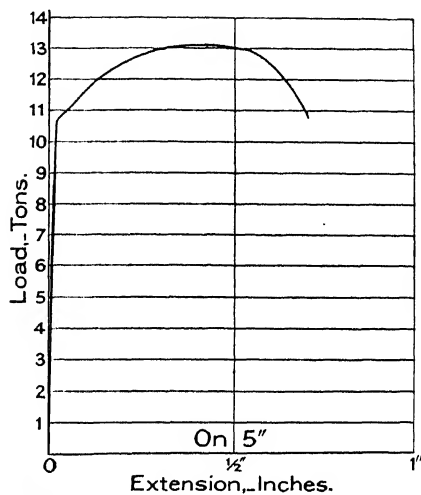


FIG. 49.



FIG. 50.—Normal.  $\times 120$ .



FIG. 51.—Overstained.  $\times 120$ .

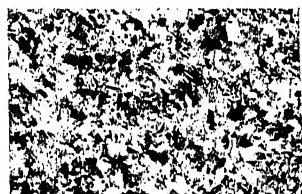


FIG. 52.  $\times 36$ .

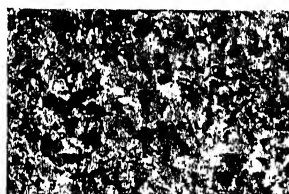


FIG. 53.  $\times 36$ .

LONGITUDINAL SECTIONS.

# CHROME NICKEL STEEL

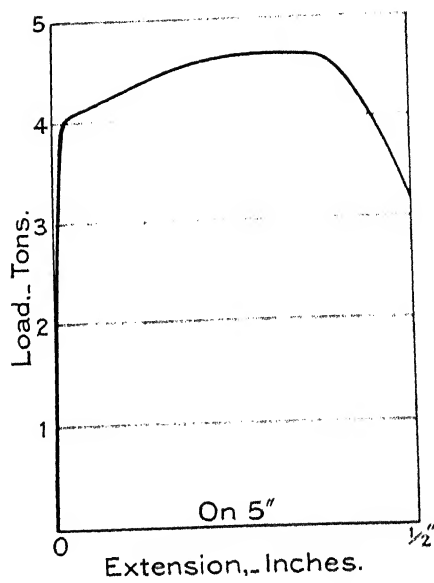


FIG. 54.



FIG. 55.— Cross Section.  $\times 120$ .

**39. Chrome Nickel Steel (Hadfield's).** The load extension diagram of this alloy steel is seen in Fig. 54. The chemical composition is

	Per cent.		Per cent.
Carbon . . . . .	0.33	Silicon . . . . .	0.13
Manganese . . . . .	0.33	Nickel . . . . .	3.73
Sulphur . . . . .	0.44	Chromium . . . . .	1.73
Phosphorus . . . . .	0.34		

There is no drop at yield point. The curve passes into the plastic state, regularly grows to a maximum, and then falls to the fracture down a long steep path, showing that there is considerable reduction of area before fracture.

The physical constants are :

Stress at yield . . . . .	53 tons per square inch.
Stress corresponding to maximum load . . . . .	61 tons " " "
Stress at instant of fracture . . . . .	100 tons " " "
Extension on 5 inches . . . . .	10 per cent.
Reduction of area . . . . .	59 " "

The inner structure is seen in Fig. 55. It is seen to be built of blocks, some dark and some light, but the effect of the nickel and chromium has been to destroy the sharp contrast between ferrite and pearlite. It is difficult to interpret the structure in the ordinary terms. The presence of nickel and chromium may have caused a more uniform distribution of the carbon through the material.

**40. Tin and Zinc.**—Load-extension diagrams of these two metals are shown side by side in Figs 56 and 57. It will be noticed that the load scale (Fig. 57) is twice the load scale in Fig. 56. Both curves exhibit a characteristic which differentiates them from the family of curves peculiar to iron and steel. The load rises rapidly to a maximum up a line which looks fairly straight and then passes an apex and falls away rapidly to fracture.

The diagram is in shape like a scythe standing on its handle. The vertical line at the end of the diagram (Fig. 56) is caused by an extensometer lever coming against a stop so that the extension is not fully recorded. The load at fracture is correctly recorded and the total extension can be measured from the halves of the broken test piece. The curve for tin shows an abrupt apex at maximum and then an almost uniform fall, ending by a curved slope to fracture.

The diagrams of inner structure shown below indicate a structure of small blocks.

The physical constants of these bars are compared below:—

	Zinc.	Tin.
Ultimate stress . .	10.4	2.8 tons per square inch.
Stress at fracture. .	24.6	5.05 " " " "
Extension on 2 inches	62 per cent.	42 per cent.
Reduction of area .	83.4 " "	80 " "

No stress at yield-point is included in the table, because, with a magnification of extension scale to show the shape of the rising load line, it is found that there is no real elastic limit. The curve begins to curve slightly almost from the origin of no load.

Comparing the size of these blocks with those of say Swedish iron, and then comparing the ultimate strengths of zinc and tin with that of Swedish iron, it will be clear that block size alone is no indication of the strength of metals generally. Tin with a small block is only one-sixth as strong as Swedish iron with a block many times larger.

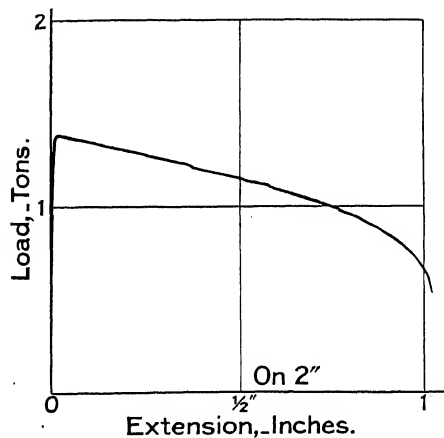


FIG. 56.

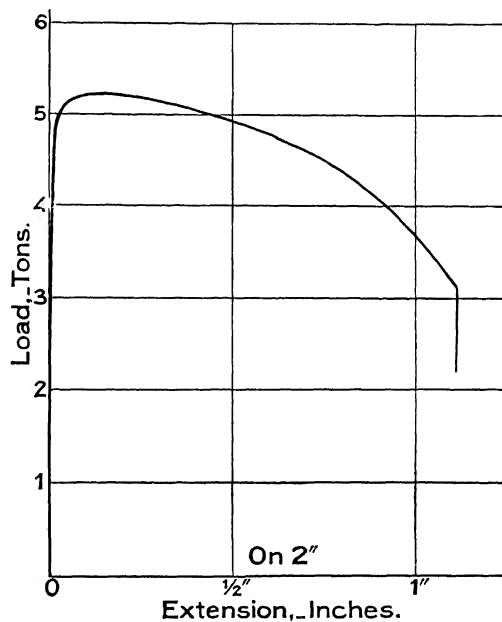


FIG. 57.

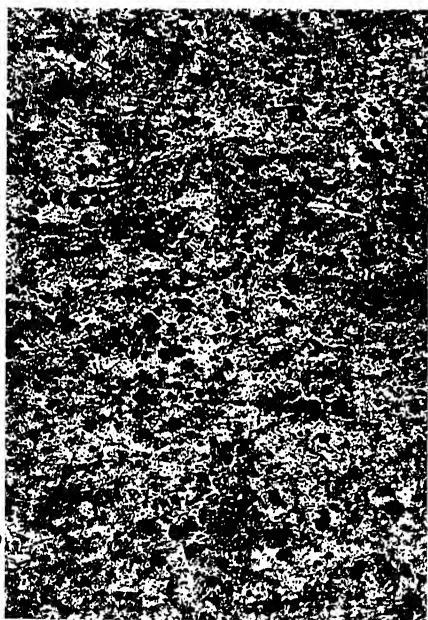


FIG. 58.—Tin. Cross Section.  $\times 120$ .

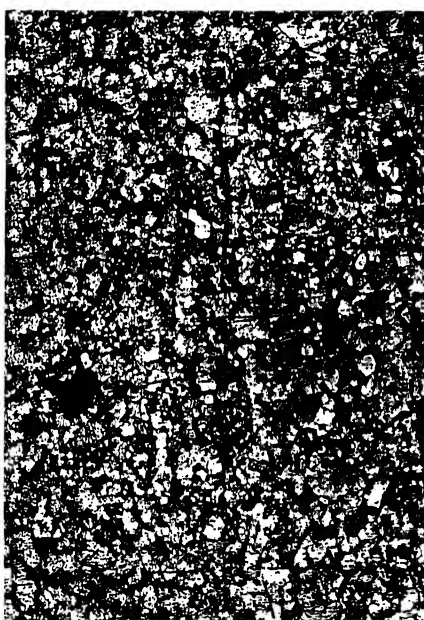


FIG. 59.—Zinc. Cross Section.  $\times 120$ .

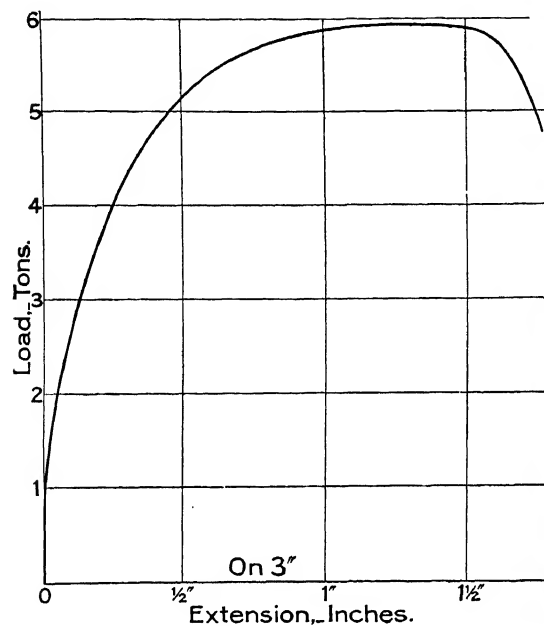


FIG. 60.—Electrolytic.

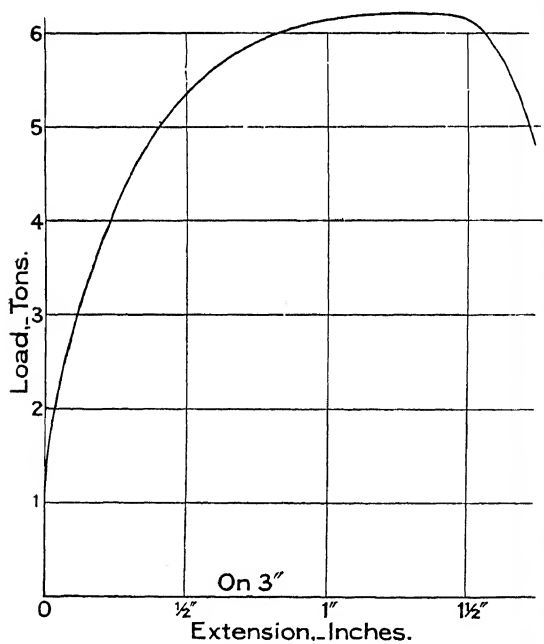


FIG. 61.—Arsenical.



FIG. 62.—Electrolytic. Cross Section.  $\times 120$ .



FIG. 63.—Arsenical. Cross Section.  $\times 120$ .



**41. Copper.** Load extension curves for electrolytic and arsenical copper are shown in Figs. 60 and 61, together with their respective inner structures, Figs 62 and 63.

These curves show a family characteristic of their own. After a short, apparently vertical, rise of load they curve away to the right in a long upward sweep to a maximum load and then fall away to fracture like iron or steel. But compared with zinc and tin the family characteristics are wide apart. The recording spot climbs a short quasi elastic line and then follows a plastic curve to a high altitude before reaching the flat upper region of the maximum load. In both tin and zinc the spot climbs quickly to its highest altitude up a path which on the scale of the diagram shows imperceptible curvature to the apex and then without lingering drops from it to the fracture. Comparing the copper curves together as members of a family, it will be seen that the soft electrolytic copper begins its upward curve sooner than the harder arsenical copper.

The physical constants from the diagram are as follows :

	Electrolytic Copper.	Arsenical Copper.
Stress at yield . . .	2.65	3.58 tons per square inch.
Ultimate stress . . .	14.12	14.82 " " " "
Stress at fracture . .	33.15	35.5 " " " "
Extension on 3 inches	58 per cent.	58 per cent.
Reduction of area . .	66 " "	68 " "

Yield stress has been tabulated, but it is not comparable in the elastic sense with the yield stress in steels and irons. It means here the point at which plastic extension becomes pronounced. Extensometer measurements of repeated loading within the yield stress would not show true elasticity.

Comparing the inner structures together, it will be seen that there is not much difference. Compared with steels and iron, the blocks are more angular.

**42. Brass.**—Two load-extension diagrams are shown in Figs. 64 and 65, taken from ordinary commercial brass rod.

The test piece in the load-extension diagram (Fig. 64) was cut from a bar sold as "naval brass." The rod of Fig. 65 was sold as A.B. brass.

The compositions of the brasses are shown in the following table :—

	Naval Brass. Per cent.	A.B. Brass. Per cent.
Copper . . . . .	60.00	59.20
Zinc . . . . .	39.00	39.70
Tin . . . . .	1.00	0.00
Lead . . . . .	Trace	Trace
Iron . . . . .	0.00	1.10
Manganese . . . . .	0.00	0.00

Both brasses are called 60-40 brass. This mixture gives high strength. The physical constants of the two brasses, determined from their load-extension diagrams, are as follows :—

	Naval Brass.	A.B. Brass.
No marked yield-point.		
Stress corresponding		
to maximum load .	29.6	32.6 tons per square inch.
Stress at fracture .	51.3	48.5 " " "
Extension on 4 inches	36 per cent.	29.7 per cent.
Reduction of area .	45.3 " "	33.5 " "

Comparing these figures, it will be seen that the material called A.B. brass is slightly stronger than naval brass, but not so ductile.

There is a marked difference between their inner structures (Figs. 66 and 67), but they have the common characteristic that two kinds of material are used in their structure. A light material which has built itself into elongated clusters of crystals in Fig. 66, and has built itself into separate and isolated blocks in Fig. 67. This is called alpha brass. Secondly, a dark material which fills the spaces between the light material. This is called beta brass. The interlaced structure of the naval brass is seen better in Fig. 68 under the smaller magnification of 36 diameters.

Brass of the 60-40 composition shows great variety of inner structure, depending not only upon the impurities in the ingredients, but upon its previous history as regards cold working and heat treatment. The structures shown above are those found in rod brass as purchased.

Brass composed of 70 per cent. copper and 30 per cent. zinc

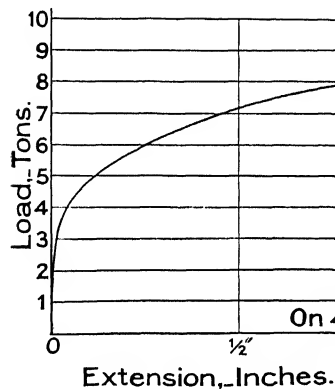


FIG. 64.—Naval Brass.

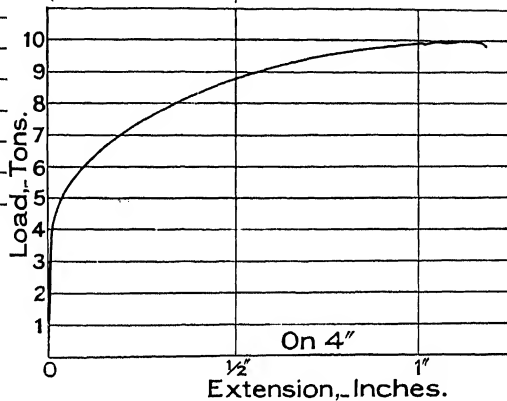


FIG. 65.—A. B. Brass.



FIG. 68.—Naval Brass.  $\times 36$ .



FIG. 66.—Cross Section Naval Brass  
Longt. Similar.  $\times 120$ .

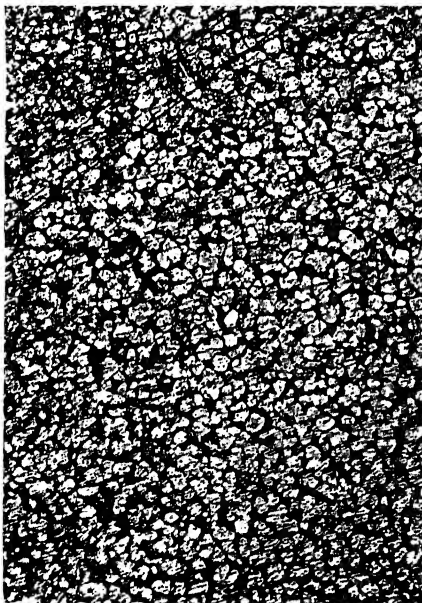


FIG. 67.—Cross Section A. B. Brass.  
Longt. Similar.  $\times 120$ .



FIG. 69.- Cross Section 70 30 Brass Rod.  
× 120.

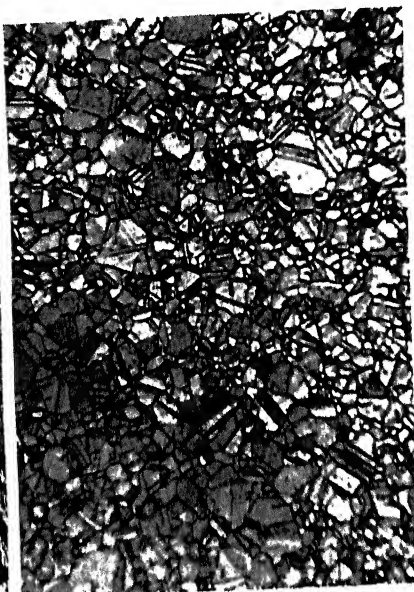


FIG. 70. Cross Section 70 30 Brass Plate.  
× 44.



FIG. 71.

× 533.



FIG. 72.

× 533.



FIG. 73.

× 533.

has greater ductility than 60-40 brass, but it is not so strong. Its ductility enables it to be used for cartridge cases. Its block crystals are elongated and distorted during the drawing and stamping processes, and frequent annealing is necessary. The inner process during annealing is a process of recrystallization. The elongated and distorted blocks recrystallize into blocks of approximate equal dimensions along the axes of crystallization.

The inner structure of a drawn and annealed rod of 70-30 brass is seen in Fig. 69, magnified 120 times. The block size depends upon the cold work done upon it before the annealing process was applied, and also on the annealing process itself. The stress corresponding to the maximum load was 21 tons per square inch. The extension was 58 per cent. on 5 inches, and the reduction of area 67 per cent. The inner structure of a sheet of this material is seen in Fig. 70, magnified 44 times. The material is in the annealed condition. Comparing this structure with that of the 60-40 brass it will be seen that there is only one material used in the building. This one kind of crystal block is alpha brass. Beta brass does not appear in the structure until the zinc reaches the proportion of about 36 per cent. i.e. a 64-36 brass would show a structure in which the beta constituent begins to appear.

Figs. 71 and 72 and 73 show the inner structure of a part of the brass plate magnified 533 times. This degree of magnification brings out markings which suggest the inner structure of the crystal blocks themselves. The units of construction are ranged in regular rows parallel to the axes of crystallization. From block to block the orientation of the crystalline axes changes. Parallel bands will be seen across many of the block crystals. This is called twinning. Twinning is a regular change in the direction of the axes of crystallization, followed by another change back to the primitive directions. The crystal blocks of annealed material which has been cold-worked show twinning freely. Fig. 69 shows twinning in almost every block in the field. It is the structure of a 70-30 bar, magnified 120 times; cf. Figs. 62 and 63.

It may be noted that although the composition of the brass rod, of which the inner structure is seen in Fig. 69, and the brass plate illustrated in Fig. 70, is identical, namely 70 copper and 30 zinc, yet the strength constants differ when the material is tested as a bar or as a thin plate.

Drawn into a thin plate 0.025 inch thick, the physical constants are given in the first column in contrast with the physical

constants of the same 70-30 material determined from a test piece turned from a bar  $1\frac{1}{4}$  inch diameter.

	Thin Plate.	$1\frac{1}{4}$ -inch Bar.
No marked yield-point.		
Stress corresponding to maximum load .	15	21 tons per square inch.
Extension on 5 inches	22.5 per cent.	58 per cent.
Reduction of area . .	30    "    "	67    "    "

This comparison incidentally illustrates the influence of the cross-section on the physical constants for the extremes of a thin plate and a circular section.

Much information about brass is given in the 4th Report of the Alloys Research Committee of the Institution of Mechanical Engineers. In the discussion on this Report Sir William Anderson contributed some interesting particulars of the details of manufacture of cartridge cases from 70-30 brass. Reference may be made to a paper by F. Johnson, M.Sc., entitled "The Alloys of Copper and Zinc: an Investigation of some of their Mechanical Properties, *Journal of the Institute of Metals*, Vol. 20, No. 2, 1918.

**43. Gun Metal and Phosphor Bronze.**—Load-extension diagrams of these metals are shown side by side in Figs. 74 and 75, the inner structures in Figs. 76 and 77. The analyses show:—

	Gun Metal. Per cent.	Phosphor Bronze. Per cent.
Copper . . . . .	86.5	94.6
Tin . . . . .	2.7	3.4
Lead . . . . .	Trace	0
Phosphorus . . . . .	0	0.3
Zinc . . . . .	10.8	1.7

The physical constants from the diagrams are:—

	Gun Metal.	Phosphor Bronze.
Stress corresponding to maximum load	30.65	31.65 tons per square inch.
Stress at fracture .	55.60	68.7    "    "    "    "
Extension on 4 inches	12 per cent.	8 per cent. on 5 inches
Reduction of area .	58.7    "    "	70    "    "

The curve of phosphor bronze resembles that of the tin constituent. It is quite unlike copper. The curve of gun metal also resembles that of this constituent.

The blocks of the phosphor bronze are large and angular, and there is twinning in nearly all of them in a marked degree. The test pieces were both cut from bars about 1 inch in diameter, purchased from stock.

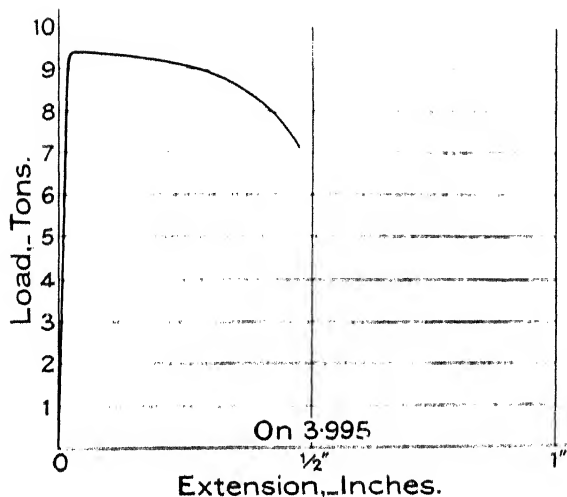


FIG. 74.

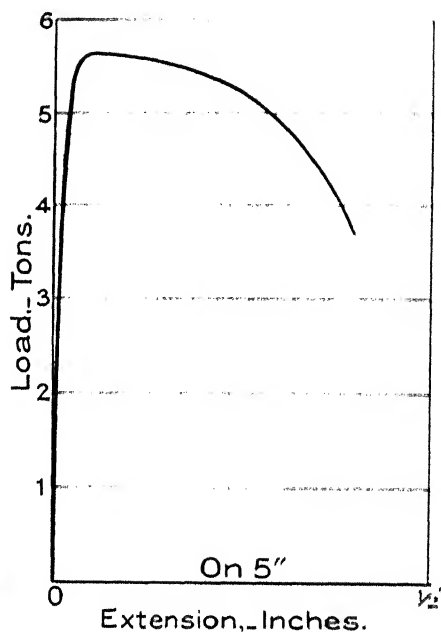


FIG. 75.



FIG. 76. Gun Metal. Longitudinal Section.  $\times 120$ .



FIG. 77. Phosphor Bronze. Longitudinal Section.  $\times 120$ .



CAST IRON

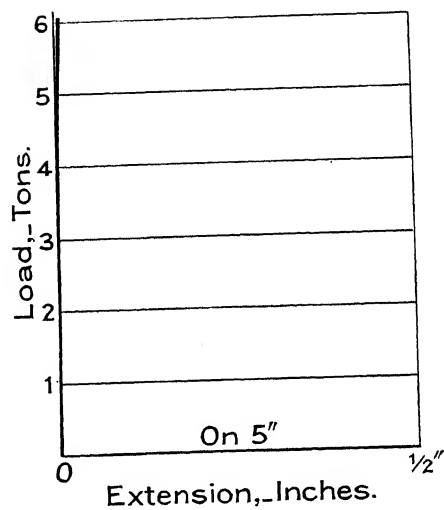


FIG. 78.



FIG. 79.—Cross Section.  $\times 120$ .



**44. Cast Iron.**—Cast iron shows no plastic yielding. As seen in the load-extension diagram (Fig. 78) the load increased to 6 tons and then the test piece broke off short. The corresponding stress is 13.4 tons per square inch. Neglecting the small reduction of area, this is the stress at fracture, so that in cast iron the stress corresponding to the maximum load and the stress at fracture are practically identical.

The extension measured on this test piece, namely 0.04 per cent. on 5 inches, is minute compared with the extension of the ductile materials iron and steel.

The inner structure is seen in Fig. 79, magnified 120 times. It is seen to be in the main a mixture of two materials, a dark and a light. The general nature of the structure will be better understood after the inner structure of pig iron has been studied.

TABLE 2

	Stress in Tons per sq. in.			Extension per cent. of Gauge Length.	Gauge Length. Ins.	Reduction of Area per cent.	Chemical Analysis.					
	At Yield.	At Maxm. Load.	At Fracture.				Carb.	Mn,	S.	P.	Si.	Ni.
Swedish Iron .	13.3	18.6	48.7	35.0	5	74.0	.047	.005	.008	.057	.014	
Yorkshire Iron.	15.9	22.0	41.9	28.4	5	58.6	.049	.015	.004	.083	.145	
Staffordshire Iron	18.0	23.9	36.0	23.6	5	38.0	.075	.050	.016	.188	.180	
B.A. Mild Steel	18.0	24.8	53.8	30.6	5	67.4	.132	.300	.017	.028	.028	
Steel . . . .	22.8	28.7	59.9	26.0	5	30.0	.220	.490	.020	.030	.035	
Bright drawn .	—	33.7	50.0	16.3	5	54.0	.195	.570	.038	.049	.020	
B.D. Steel H.T.	33.3	35.2	58.6	17.4	5	55.0	.195	.570	.038	.049	.020	
Mild Steel § 34.	9.2	21.2	41.5	31.0	4	64.0	.130	.380	.020	.010	.270	.100
Do. Heat Treated	18.4	24.8	71.0	29.5	4	80.0	.130	.380	.020	.010	.270	.100
Nickel Steel .	36.0	46.6	63.0	16.0	5	36.6	.320	.560	.037	.027	.090	3.52
Ch. Ni. Steel .	53.0	61.0	100.	10.0	5	59.0	.330	.330	.440	.340	.130	3.77
											Cu	.042
											Ch	1.73
Zinc . . . .	—	10.4	24.6	62.0	2	83.0	—	—	—	—	—	—
Tin . . . .	—	2.8	5.0	42.0	2	80.0	—	—	—	—	—	—
Copper, El.	2.6	14.1	33.1	58.0	3	66.0	—	—	—	—	—	—
Copper, Ars.	3.6	14.8	35.5	58.0	3	68.0	—	—	—	—	—	—
							Cu	Zn	Tin	Pb	Fe	Mn
Brass, Naval .	—	29.6	51.3	36.0	4	45.3	60.0	39.0	1.0	trace	.0	.0
Brass, A.B. .	—	32.6	48.5	29.7	4	33.5	59.9	39.7	0.0	trace	1.1	.0
Gun Metal .	—	26.3	33.5	14.0	4	21.6	85.4	—	12.4	2.4	—	—
Ph. Bronze .	—	31.6	68.7	8.0	5	70.0	89.7	—	8.85	1.21	Ph.	trace
Cast Iron . .	—	13.4	—	—	5	—	—	—	—	—	—	—

## CHAPTER III

### COMPARISON OF TABULATED RECORDS OF STRENGTH AND DUCTILITY

**45. Influence of Gauge Length on the Figures of Strength and Ductility.**—The results of tests discussed in the previous chapter are tabulated in Table I. Following the usual practice, the observed load at yield and the observed maximum load are each divided by the primitive area of the test piece to get the yield stress and the ultimate stress or tenacity of the material. The load at fracture is divided by the cross-sectional area of the fracture to get the stress at fracture. The extension of the gauge length, reduced to a percentage, is entered in the table, together with the gauge length on which the extension was measured. The percentage extension is commonly used as a measure of the ductility of a material. The reduction of area is also entered.

The question now arises, Can strengths of different materials be compared by comparing ultimate stresses? and can ductilities be compared by comparing percentage extensions? The answer to the first question is yes, if proper precautions are taken in the design of the test piece; but to the second question the answer is in general no, but yes if the test pieces are geometrically similar in form. The conditions which influence the answers to both these questions are brought out by the experiments about to be described.

The load-extension diagrams arranged in echelon, Fig. 80, were taken from test pieces cut from one and the same mild steel bar. The object of the record was to trace out the influence of the gauge length on strength and ductility. Therefore it was necessary to define the gauge length by shoulders in order to get down to so small a length as one-eighth of an inch. The test pieces were alike except in gauge length. This was varied from one-eighth of an inch between the shoulders to five inches between the shoulders by the steps indicated in Fig. 80. The ends of each test piece were screwed 1 inch gas, and the part to be broken was

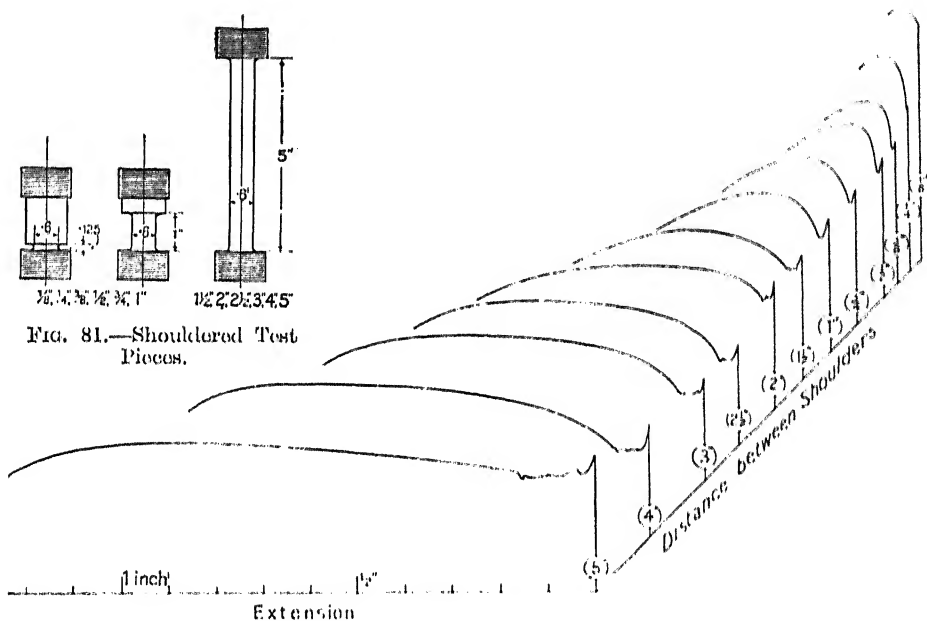


FIG. 80.—Load-extension Diagrams in Echelon.

turned down to 0.6 inch diameter. The  $\frac{1}{8}$ -inch, 1-inch, and 5-inch test pieces are seen in Fig. 81.

**Tensile Strength, Tenacity, Stress corresponding to Maximum Load.** A glance at Fig. 80 shows that the maximum load increases for very short gauge lengths, the increase beginning in the region of the  $1\frac{1}{2}$ -inch test piece. The increase is seen better in the curve of tensile strength plotted against the gauge length (Fig. 82).

The tenacity corresponding to the maximum load carried by the 5-inch test piece is about 30 tons per square inch. The tenacity corresponding to the maximum load carried by the  $\frac{1}{8}$ -inch test piece is about 49 tons per square inch. Thus one and the same material appears to vary in tenacity between 30 and 49 tons per square inch. This variation is brought about by merely varying the gauge length. Therefore tabulated tenacities of different materials are only comparable with one another when the influence of the gauge length is eliminated.

From Fig. 82 it will be seen that the tenacity is uninfluenced by the gauge length until it is shortened to about  $1\frac{1}{2}$  inches, equal to about  $2\frac{1}{2}$  diameters. Therefore, for the material of the experiment, test pieces 4 diameters between shoulders would furnish comparable values of the tenacity.

**Ductility.**—Ductility is usually measured by the percentage elongation of the gauge length.

The elongation between the shoulders of the 5-inch test piece is 30 per cent. The elongation between the shoulders of the  $\frac{1}{8}$ -inch test piece is 75 per cent. That is, one and the same material appears to vary in ductility between 30 per cent. and 75 per cent.

From Fig. 82 it will be seen that no part of the percentage elongation curve is parallel to the axis, and therefore the percentage elongation is always influenced by the gauge length. Therefore with test pieces of constant diameter the percentage elongation depends upon the gauge length. Ductilities of different

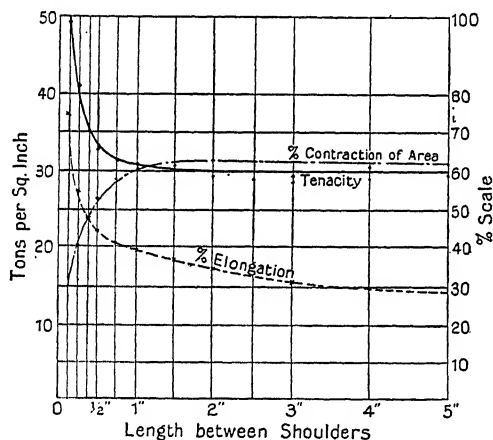


FIG. 82.—Tenacity, Percentage, Elongation, and Contraction of Area plotted against Gauge Length.

materials, therefore, cannot in general be compared by comparing tabulated figures of percentage elongation.

The percentage contraction of area is plotted in Fig. 82, and it appears to come under the influence of the gauge length at about the same point as the tenacity. Contraction of area, expressed as a percentage, may be expected therefore to be constant for the same material until the gauge length is shortened to  $2\frac{1}{2}$  diameters. As shortening proceeds the percentage contraction diminishes. It appears to be about 62 per cent. up to a gauge length of  $1\frac{1}{2}$  inches and then rapidly drops to 15 per cent. as the gauge length shortens to  $\frac{1}{8}$ -inch.

Summarizing, gauge length always influences the percentage elongation, but does not sensibly influence the tenacity or the percentage reduction of area until it is reduced below a certain limit. For the material used in these experiments the limit is  $2\frac{1}{2}$  diameters.

**46. Form of Test Piece.** The best form of test piece to use with the load-extension instrument is illustrated at A (Fig. 83). The gauge length is defined by flanges turned on the test piece itself. As the load is increased and extension proceeds these flanges move apart without themselves suffering distortion or undergoing stress. They remain at right-angles to the axis of the bar. This immunity from distortion has been tested experimentally by comparing the value of the elastic modulus derived from a flanged test piece with the elastic modulus derived from a test piece on which the gauge length was defined by dots. Any difference was within the limit of experimental error. Dr. Coker also tested the distribution of stress in the body of the bar produced by the flanges by his well-known optical method. The xylonite test piece indicated that there was no stress in the flanges themselves and that their effect on the body of the bar is to produce a very local but strictly symmetrical modification of the stress, so that as load is increased and the test piece stretches, the pull at the root of the flange upwards is equal to the pull at the root of the flange downwards, so that there is no tendency to distort the flange. The modification of the stress produced by the flanges, besides being symmetrical, is slight, and therefore it has negligible influence on the extension between the flanges and therefore on the elastic modulus  $E$ .

A flanged test piece therefore gives correctly the extension of the gauge length defined by the flanges.

A plain bar with the equivalent of a flange clipped on may equally be used for elastic testing. The loose flange is shaped like a horseshoe, and three steel-pointed screws pass radially through the flange and clip it to the bar. The screws are tightened against the elasticity of the horseshoe, and so the horseshoe is held fixed and as part of the test piece as the elastic test proceeds.

Flanges turned on the test piece are, however, preferable, notwithstanding that, although without influence in an elastic test, they have a definite influence on the ultimate extension of the gauge length. The body of the bar is hampered by the flanges in its plastic lateral contraction, and this prevents free extension just in the region of the flanges. A series of comparative tests on mild steel showed that a flanged test piece extends about 3 per cent. less than a plain one when the gauge length is 5 inches and equal to about 8 diameters. Fig. 84 shows the load-extension diagrams from the series of test pieces illustrated—all turned from mild steel.

The shouldered test piece seen at C (Fig. 83) is useful, especi-

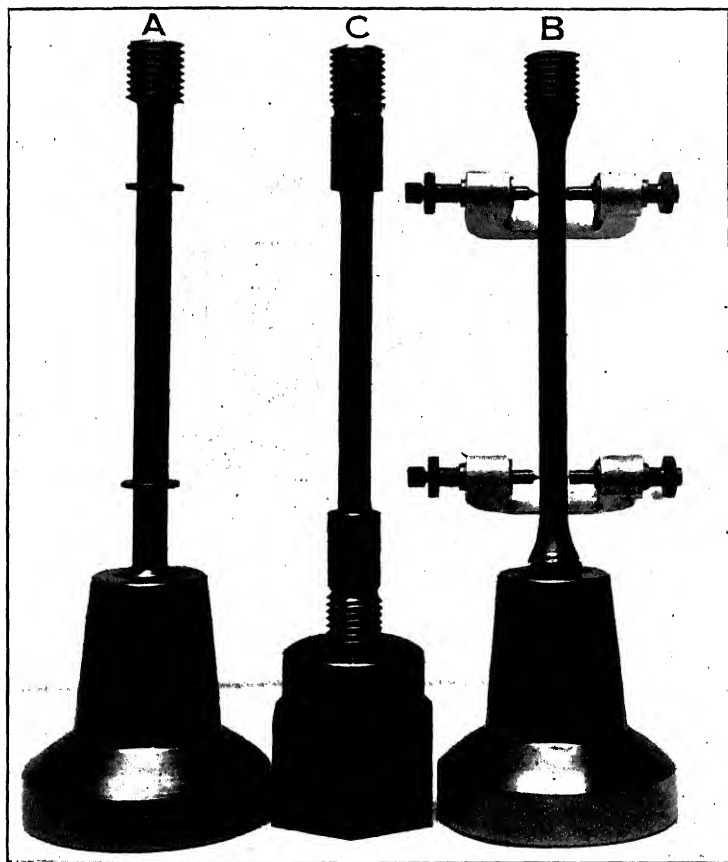
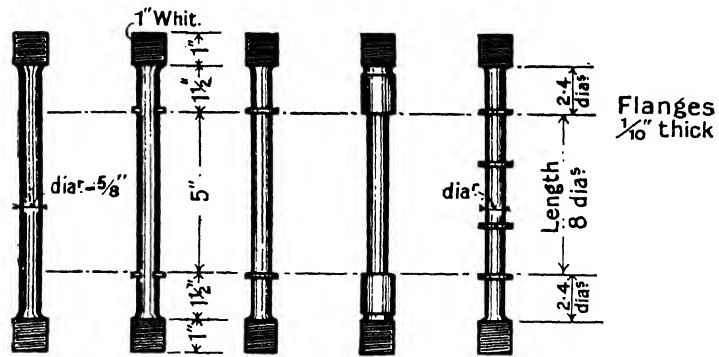
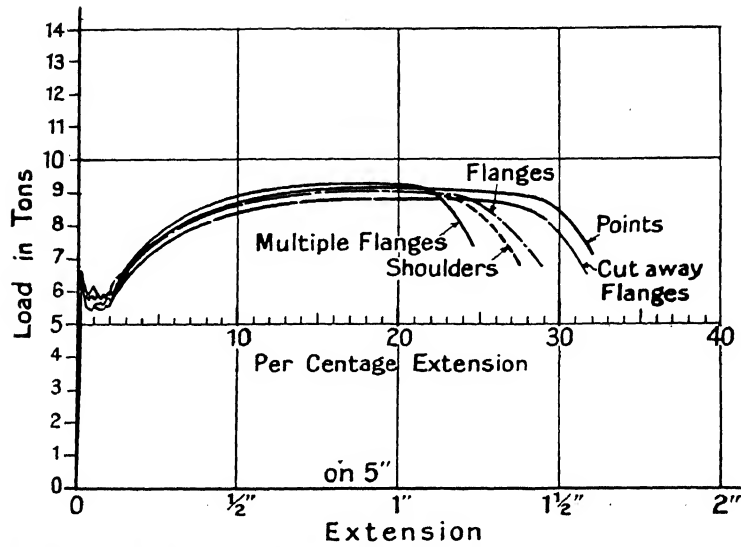


FIG. 83.—Forms of Test Pieces.



Annealed from 900° C. Carbon 0.156 %.

FIG. 84.—Effect of Flanges and Shoulders in Extension.



ally for short test pieces, but should not be used if the extension is to be multiplied very much. The shoulders distort slightly into a lenticular shape as the piece is stretched, so that the distance between them is slightly in excess of the extension of the primitive gauge length which they defined. The error is quite immaterial for ordinary testing, but is serious if an elastic measurement is to be made. The value of  $E$  derived from such a measurement would be lower than the true value.

When the gauge length is defined by centre dots on a plain bar, and the piece is to be broken, clips have to be used, each carrying a pair of pointed screws which are driven into the diametrically opposite centre dots defining each end of the gauge length. Clips for a no-load to break test are shown mounted on the test piece at B (Fig. 83). The pointed gauge screws must continue to grip the test piece as its diameter contracts under load, and the points must therefore be spring-loaded.

The practical disadvantages of clips are that the points cannot satisfactorily be driven into the hard steels which have to be tested nowadays, and that they slip during the test when the metal is soft, because the centre dots elongate; and further, the shock of fracture often breaks the points. For elastic testing the friction which the points produce is against accurate work. The only advantage of the clip is that the extension is measured on a central part of the bar of uniform diameter, uninfluenced by the flanges in any way. This advantage ceases to have value if the test pieces are made similar in form. Many difficulties of automatic testing disappear when the pointed screw disappears.

**47. Ductility and the Principle of Similarity.**—As mentioned above, comparison of the strength of different materials is made by comparing their tenacities as derived from tensile tests, it being understood that the gauge length is long enough to exclude end effects.

Comparison of the ductility of different materials cannot in general be made by merely comparing their percentage elongations. The statement of percentage elongation must be accompanied by a statement of the gauge length on which it was measured and on the proportion of gauge length to cross-section. It will be recalled that no part of the "percentage elongation—gauge length" curve (Fig. 82) is parallel to the axis, differing markedly in this respect to the tenacity curve, which, as mentioned above, is independent of local contraction, and of the end-flow, when the gauge length exceeds a definite number of diameters of the cross-section. But when the test pieces are similar in form

the Principle of Similarity applies to ductile materials, and comparison of ductility can be made by comparing percentage elongations.

The Principle of Similarity, which in its relation to the testing of materials is known as Barba's<sup>1</sup> Law, may be stated as follows :—

Geometrically similar test pieces of different sizes deform similarly and are geometrically similar after deformation.

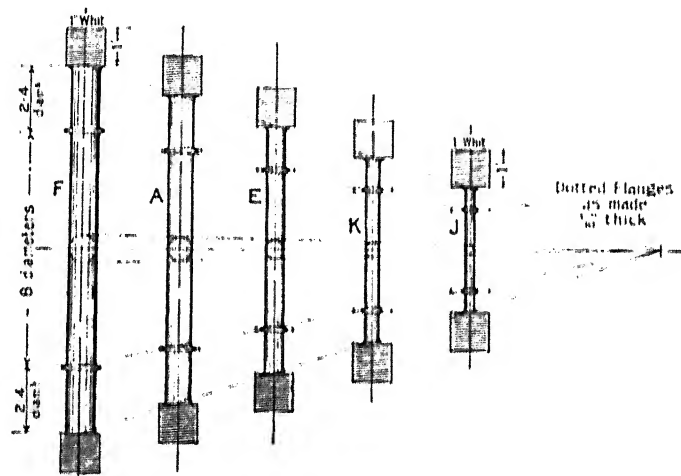


FIG. 85.—Series of Similar Bars. Annealed from 900° C.  
Carbon 0.156 per cent.

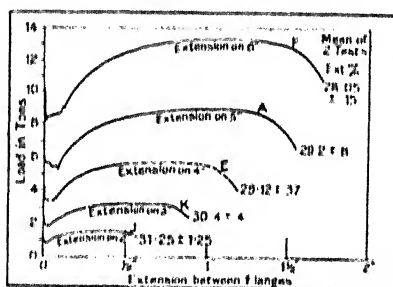


FIG. 86.—Load-extension Diagram.

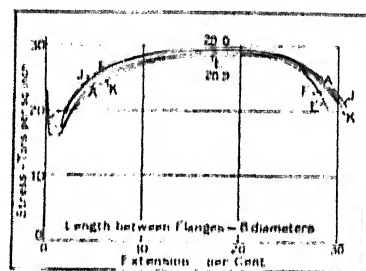


FIG. 87. Stress Extension, per cent.

One test piece is "similar" to a second test piece when all its dimensions are the same multiple or fraction of the dimensions of the second test piece.

In practice the ends of the test pieces must be made of constant dimensions to fit the sockets or grips, but in a properly

<sup>1</sup> "Résistance des Matériaux. Étude sur les allongements des métaux après rupture," *Mémoires de la Société des Ingénieurs Civils*, 1880, 1, p. 682.

designed test piece the parts in the sockets are so far removed from the gauge length that the effect on the flow of metal is negligible.

The principle of similarity, its validity, and its utility are illustrated and tested in Figs. 85, 86, and 87. The material is mild steel. A bar was annealed, and then the test pieces shown in Fig. 85 were made. The gauge length is in all of them 8 times the diameter. The diameter of the smallest test piece was  $\frac{1}{4}$  inch; of the largest,  $\frac{3}{4}$  inch. Strict similarity is departed from only in the flanges and ends. The flanges were of constant dimensions, 1 inch diameter and  $\frac{1}{10}$  inch thick. The ends were all screwed 1 inch Whitworth. The test pieces are ranged together to show that lines through the corresponding dimensions radiate to a point, a simple test of the similarity in form required by the principle.

The corresponding load-extension diagrams are seen in Fig. 86. They differ widely in form, but only by about 3 per cent. in the percentage elongation. The load-extension diagrams are reduced to "stress extension per cent." diagrams in Fig. 87. The diagrams of Fig. 87 should be coincident if the material were uniform in quality.

The test pieces were turned from a bar about  $1\frac{1}{4}$  inch diameter. The smallest test piece therefore represents the quality of the core of the bar. It is well known that there is a variation of quality in rolled bars from the centre outwards. The complete figures of these tests show that from the centre outwards there is a gradual decrease of ductility as measured by the percentage elongation, and by the contraction of area. The mean figures of the test are given in the following table:—

TABLE 3

Diameter of Test Piece.	Percentage Elongation.	Reduction of Area, per cent.	Tons per square inch.		
			Yield.	Tenacity.	Fracture.
$\frac{1}{4}$ in.	31.25	64	20.9	29.55	57.5
$\frac{3}{8}$ in.	30.40	64	20.32	28.82	57.7
$\frac{1}{2}$ in.	29.12	61.5	21.4	28.93	54.7
$\frac{5}{8}$ in.	29.20	60.1	21.27	29.67	54.1
$\frac{3}{4}$ in.	28.05	57.35	22.63	29.67	53.95

If the material were of uniform quality throughout, and assuming the Principle of Similarity to apply accurately, then the percentage elongation would be the same regardless of the difference in

the size of the test pieces. The gradual change in the percentage reduction of area shows that the quality of the material is not uniform throughout. It is changing from the centre outwards. It is safe to conclude, therefore, that the Principle of Similarity applies within the limits of the variation in quality of the material, and therefore that it is of great utility in practical testing.

The Principle of Similarity is easily applied when the test bars are turned. It is not so easy to apply it generally, because the cross-sections of test pieces vary in shape, and for similarity only one form of cross-section is admissible. An approach to the principle is made by making the gauge length a multiple of the square root of the area of the test piece.

A standard proportion which has been used in many laboratories is a gauge length of 20 units and an area 3.1416 square units. No account is taken of the form of the section. It may be circular or rectangular. The gauge length to be marked off on the test piece or otherwise defined is then calculated from

$$L : \sqrt{A} = 20 : \sqrt{3.1416} \quad . \quad . \quad . \quad (1)$$

In this expression  $L$  is the gauge length in inches, and  $A$  is the area of the cross-section of the test piece in square inches. The expression reduces to

$$L = 11.3 \sqrt{A} \quad . \quad . \quad . \quad . \quad (2)$$

If the bar is circular in form and its diameter is  $d$  inches, (2) becomes

$$L = 10d.$$

It may not be possible to get material long enough to make test pieces to give a gauge length of 10 diameters.

Then a suitable standard form may be defined for any particular research and the test pieces are made in scale sizes of it. If the form of the cross-section is kept constant, the Principle of Similarity is strictly observed. If the cross-section of the test pieces varies in form, then a near approach is made to the principle by making the gauge length proportional to the square root of the area of the cross-section.

**48. Ductility measured by the Percentage Extension produced by the Maximum Load.**—After the yield-point has been passed the plastic extension proceeds uniformly along the bar as the load increases to its maximum value. This is not strictly true, but it is substantially true. Therefore on a plain bar each inch extends by the same amount, and the percentage extension is the same, whether it is reckoned from 1 inch or from

any number of inches within the gauge length, or from the whole gauge length. The ductility calculated from the extension produced by the maximum load is thus comparable with the ductility similarly calculated from another material.

The flanges of the test piece introduce a slight error in the uniformity of extension, but it is inconsiderable in comparison with the effect of the local extension. The ductility calculated from the extension produced by the maximum load on a flanged test piece thus provides a good figure of comparison.

The extension corresponding to the maximum load is measured from the load-extension diagram. The process is to draw a horizontal tangent to the load-extension curve and then to project the point of contact to the horizontal scale. The reading on the scale is the extension required. This measurement excludes the local contraction. It is, in fact, the extension just before the metal begins to flow to a waist.

**49. Approximate Expression for the Extension.**—The total extension  $e$  of a gauge length  $L$  on a plain bar may with fair accuracy be represented by the empirical expression

$$e = a + bL.$$

It is here assumed that extension proceeds uniformly until local contraction begins and then continues locally until the test piece breaks. The uniform extension of  $b$  inches per inch contributes the amount  $bL$  inches to the whole extension. The local extension is independent of the gauge length and contributes the amount  $a$ . The constant  $a$  may be regarded as including the slight local effect of the flanges where a flanged test piece is used.

Theoretically two tests are necessary and sufficient to find the constants  $a$  and  $b$  for a given material. The test piece is marked off in equal intervals, say in half-inches. The usual practice is to start from the interval, including the fracture, and then reckon each way and so find an extension  $e$  of a gauge length  $L$  with the fracture at its centre.

From two measurements of this kind on different gauge lengths a pair of simultaneous equations may be formed with different values of  $e$  and  $L$  from which the values of  $a$  and  $b$  can be calculated, or several measurements may be made from the bar, and then the method of least squares applied to find the most probable values of  $a$  and  $b$ .

Dividing the expression  $e$  by the length  $L$ , and multiplying by 100, the corresponding expression for the percentage extension

## 76 STRENGTH AND STRUCTURE OF METALS

of a gauge length  $L$  is found in terms of two constants  $A$  and  $B$ , thus :—

$$\frac{100e}{L} = \frac{100a}{L} + 100b = \frac{A}{L} + B \quad . \quad . \quad . \quad (2)$$

It is clear from this expression that the percentage extension is expressed by a different number according to the gauge length taken. The expression, though not strictly accurate, has been tested by experimental evidence, and the constants  $A$  and  $B$  have been tabulated for various kinds of materials.<sup>1</sup>

<sup>1</sup> "Tensile Tests of Mild Steel and the Relation of Elongation to the Size of the Test Piece." Dr. W. C. Unwin, *Proc. Inst. C. E.*, Part I, Vol. 155, 1903-4.

## CHAPTER IV

### THE INNER STRUCTURE OF METALS

**50. The Block Structure.**—The illustrations of inner structure distributed through Chapter II show that metal is built of separate blocks. Each of these blocks is itself a crystal. These crystal blocks are sometimes called crystallites. The blocks differ in shape and in size, but generally the shape may be described as polyhedral. Marked contrast in shape is seen by comparing the structure of a metal built of polyhedral blocks, like manufactured iron and steel, with the structure of pig iron (Fig. 111), where black blocks shaped like fir trees are seen to occupy the centre of the field. Under a higher magnification, however, these black fir trees are seen to be themselves built of pearlite blocks. The fir tree was the shape of the first crystal growth taking place as the metal solidified. The pearlite structure seen in Fig. 114 is that into which the fir tree builds itself as it cools to the ordinary temperature. The fir-tree shape is the ghost of a vanished single crystal.

The angles of the blocks may be sharp and acute, as in phosphor bronze (Fig. 77), or blunt and obtuse as in manufactured iron (Fig. 23), or filamental as in brass (Fig. 66). The shape of the blocks, their size, in fact the whole kind of structure, depends upon the manufacturing process which has produced the metal, and particularly upon the heat treatment through which the metal has passed. For example, the blocks in the mild steel (Fig. 44) are of enormous size compared with the blocks found in steel manufactured by a normal process. This large block size was produced by keeping the metal at about  $1200^{\circ}\text{C}$ . for a long time, and then cooling gradually. The same metal builds itself into the quite different structure seen in Fig. 47, after the following heat treatment: heat to and maintain at  $880^{\circ}\text{C}$ . for thirty minutes, and quench in water, and then reheat to and maintain at  $650^{\circ}\text{C}$ . for two hours, and cool slowly.

Notwithstanding the varieties in shape and block size seen in Chapter II, the physical properties of metal may change

widely without producing a change in the block structure, which, after polishing and etching, can be seen in a microscope. That is to say, the strength and condition of a metal cannot be deduced from its inner structure alone, although the inner structure in some conditions gives valuable information of present state and previous history, especially as regards heat treatment.

**51. The Structure of the Blocks themselves.**—Each block is a crystal built from atomic bricks laid in regular courses. When molten metal falls to its solidifying temperature, block growth starts from innumerable points or nuclei distributed through the liquid. Each block grows or crystallizes in the system peculiar to the metal and to the temperature. But the orientation of the crystalline axes is not the same from block to block. When block growth starts, the directions of growth, that is, the directions of the crystalline axes centred in the nucleus, seem to be determined by influences which act in a haphazard manner. Looking at a structure which has solidified from a molten metal there is nothing to indicate the directions of the crystalline axes from block to block, except in such definite formations as are seen in the fir-tree crystals of pig iron. Even when these indications can be seen there is still nothing to indicate what determined the primitive axial direction of growth. It requires careful etching to bring out the regular coursed structure of a block. It also requires much patience. There is an indication of regular coursed structure in Figs. 71, 72 and 73. The etching process has thrown up markings which, examined under a high power, 533 diameters, reveals a coursed structure of rectangular blocks, the largest of which measures about  $1/70,000$  of an inch square. This is not a single atomic element, but is probably an indication of a cubical group of atomic elements. These cubical groups are ranged in parallel directions. The block in which they are seen measures about  $1/160$  of an inch by  $1/300$  of an inch.

The growth of a crystal block is ultimately arrested in all directions by its growing neighbours butting into it. The final shape of the crystal is therefore irregular. The liquid metal on which the growing crystals feed is gradually reduced until finally it becomes a thin, film-like network trapped between the walls of the solid crystals. A layer of unincorporated atoms may be imagined condensed from the residue of the liquid, and held in equilibrium between the walls by the attractive forces from crystals competing to build them into their own structure.



**52. Crystalline and Amorphous Material.**—Atomic material unincorporated into a crystal block is called amorphous material. Seen in the microscope it is non-crystalline, formless, and structureless. Liquid metal is amorphous. Solid metal may be described as crystal blocks separated by thin layers of amorphous material. Metal solidifying from the liquid crystallizes with extreme rapidity. The most rapid cooling fails to prevent crystallization. The rate of cooling has a profound influence on the size and even on the kind of crystal block. Slow cooling produces a coarse structure, rapid cooling a finer structure ; but whatever the structure may look like it is built of crystal blocks.

Cold-working a metal, like hammering it, or rolling it, or wire-drawing it, or stamping it, reduces part of the crystal structure to amorphous material. The crystal blocks themselves become distorted, slip-bands develop along the crystalline interfaces, and crystal debris and amorphous material are produced through the metal. But this amorphous material and crystal debris recrystallize into a normal structure when the metal is heated to a suitable temperature. This process of recrystallization is the key to the annealing processes and the heat treatment of metals used by the engineer.

Amorphous material is harder and stronger than crystalline material. The hardening of metal by overstraining it, that is by cold-working it, is regarded as due to the production of amorphous material at the expense of the crystalline material. The term "amorphous cement" is used by metallurgists to describe the thin layers of amorphous material left between the crystal blocks at the end of the solidifying process.

**53. Permanence of the Crystalline Structure.**—However severely a metal is cold-worked it is impossible to reduce the crystals entirely to amorphous material. The crystal blocks of a metal are not destroyed even when the metal is stretched to fracture. They are elongated, and no doubt amorphous material is produced along planes where relative motion takes place; but the microscope reveals mainly distorted blocks and markings on them which indicate planes along which slipping has taken place. Two photographs are shown on Plate XXVII. Fig. 88 is reproduced from Fig. 19. It shows the inner structure of a Swedish iron test piece in its normal condition. Fig. 89 shows the inner structure of the same test piece at the fracture. The polyhedral blocks of the normal structure have become elongated, but they have not been destroyed.

Sir George Boilby<sup>1</sup> gives interesting illustrations of the persistence of crystalline structure in severely cold-worked metal. A gold wire, cold-drawn to  $13\frac{1}{2}$  times its original length, showed on an etched and polished longitudinal section much amorphous material, but, notwithstanding the severe cold-working, debris of the original crystal-block structure persisted, especially along the core.

A gold leaf hammered into a thin film, and then floated on the surface of cyanide of potassium, was changed into a crystal skeleton, the amorphous material being dissolved in the liquid. Even cold-working so severe that hardly a molecule in the structure could have escaped failed to entirely reduce the crystal to the amorphous state.

**54. Recrystallization. Annealing.**—Cold-working leaves a metal in a state of inner strain and with its normal crystal-block structure partly disintegrated into amorphous material. The deformed crystals have within their own crystal structure planes of slip along which amorphous material has been reduced, and in this amorphous material crystal debris may be embedded.

But metal possesses the power of recrystallization in the solid at temperatures far below the melting-point of the metal, and therefore it is not necessary to remelt a metal in order to recrystallize it. It is only necessary to raise it to a suitable temperature and then to keep it at that temperature long enough to allow the crystallizing process to complete itself.

When the overstrained metal reaches the recrystallizing temperature the broken fragments of the crystalline blocks and

<sup>1</sup> "Hard and Soft State of Metals." *Proc. Roy. Soc.*, Vol 79, Series A, 1907, p. 465.



FIG. 88.—Longitudinal Section of Unstrained Material.  $\times 120$ .



FIG. 89.—Longitudinal Section near the Fracture of a Test Piece.  
 $\times 120$ .



FIG. 93.—Result of Maintaining Test Piece B at 550° C. for 30 minutes.  $\times 120$ .

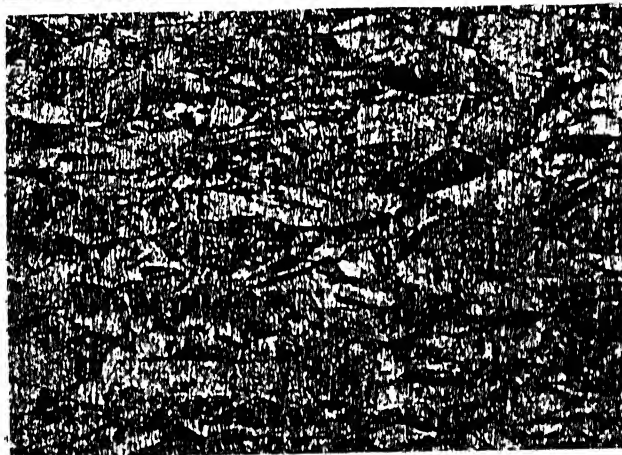


FIG. 92.—Cylindrical Part of a Brass Cap Test Piece cut at B (Fig. 90).  $\times 120$ .



FIG. 91.—Crown of a Brass Cap Test Piece cut at A (Fig. 90).  $\times 120$ .

other nuclei begin to grow into crystal blocks, incorporating the amorphous material produced by overstrain into themselves, and at the end of the process a normal crystal-block structure is reproduced, together with the normal elastic state of the metal. The hardness produced by overstrain has gone and normal material is produced.

It has been mentioned above that the elastic property of iron and mild steel is quickly recovered even by heating to  $100^{\circ}\text{C}$ . This restoration of elastic property corresponds with an inner process of recrystallization. This is a general property of metals. An example may be given. The brass cap sketched in Fig. 90 was stamped from a thin flat sheet of 70-30 brass. The process necessitates severe cold-working of the cylindrical skirt without however materially cold-working the crown.

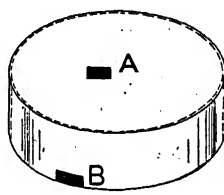


FIG 90.

The inner structure of the crown should therefore show a normal structure, whilst the inner structure of the skirt might be expected to show the peculiarities of overstrained material.

Fig. 91 shows the inner structure of a specimen cut from the crown at A. It is quite normal. Fig. 92 shows the inner structure of a specimen cut from the skirt at B. It is seen to be severely overstrained. The crystal blocks are elongated, and slip-bands are seen in all directions. Any further cold-working would probably split the material.

Fig. 93 shows the inner structure of the specimen cut from B, after maintaining it at a temperature of  $550^{\circ}\text{C}$ . for thirty minutes. The deformed crystals and the crystal debris have recrystallized into a normal structure. Cold-working can now be continued on the skirt if necessary. In fact, cold-working alternating with recrystallization can go on until the metal is reduced to any thinness desired.

In the Fourth Report of the Alloys Research Committee, (*Proc. Inst. Mech. E.*, February, 1897, p. 71), Sir William Anderson gives particulars of the process of manufacturing a brass cartridge case for 6-inch gun ammunition. A brass disc  $12\frac{1}{2}$  inches diameter and  $\frac{3}{4}$  inch thick is transformed into a thin cylinder about 14 inches long and 6 inches diameter, with a thick base, by pressing and drawing operations alternating with recrystallizing processes. The material was composed of 70 per cent. copper and 30 per cent. zinc.

Referring to Figs. 76 and 77, showing respectively the inner

structures of gun metal and phosphor bronze, it will now be recognized that each shows overstrained material. The test pieces were cut from bars finished to size by cold-working and not afterwards annealed. Fig. 94 shows the change of inner structure produced by recrystallization of the gun metal at  $550^{\circ}\text{C}$ ., and Fig. 95 the change of inner structure produced by recrystallization of the phosphor bronze at  $550^{\circ}\text{C}$ .

Sir George Beilby, in the lecture mentioned above, describes some interesting experiments correlating recrystallization with mechanical property. As mentioned above, the object of the experiments was to transform the crystal-block structure entirely into the amorphous state by the severe cold-work done by wire-drawing. This could not be done, but the experiments lead the way to others of great interest. The cold-work done on a gold wire hardened it greatly, and its inner crystalline structure was deformed and considerably broken down to amorphous material. Test lengths were cut from the overstrained wire and were annealed at different temperatures.

The "mechanical stability," to use Sir George Beilby's term, of the inner structure was measured by the load required to produce 1 per cent. extension on the gauge length of a test piece.

The overstrained gold-wire test piece stretched 0.3 per cent. and then stopped stretching under a dead load of 12 lb., corresponding to a stress of 14.6 tons per square inch; 12 lb. produced exactly the same extension on the test wire annealed at  $30^{\circ}$ , on the wire annealed at  $100^{\circ}$ , and on the wire annealed at  $200^{\circ}\text{C}$ ., showing that annealing at these temperatures had not changed the mechanical stability of the inner structure. But there was a change in the wire annealed at  $280^{\circ}\text{C}$ . A load of 11 lb. was sufficient to stretch it 1 per cent., and the microscopic examination of the structure revealed that recrystallization of the metal had just begun. The wire annealed at  $355^{\circ}\text{C}$ . stretched 1 per cent. under a load of only 4 lb., corresponding to 4.55 tons per square inch. The inference from these experiments is that the physical properties corresponding to the normal structure of crystal blocks are reproduced from the hardened state, where these physical properties are different, by a regrowth of the crystal blocks in the solid at a temperature not below  $280^{\circ}\text{C}$ .

It is now possible to distinguish between the terms **annealing** and **recrystallizing**. Annealing is merely the process of maintaining metal at a definite temperature for a definite time. This process however accomplishes nothing except the relief of internal stresses unless the temperature is maintained above a

GUN METAL AND PHOSPHOR BRONZE



FIG. 94.—Gun Metal.  $\times 120$ .

Recrystallized at  $550^{\circ}\text{C}$ . from the Structure of Fig. 76.

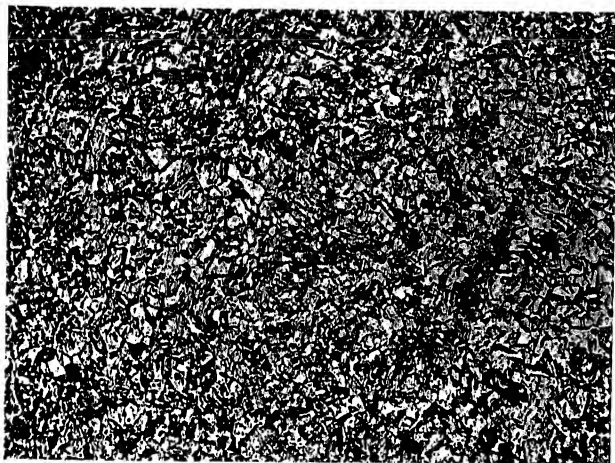


FIG. 95.—Phosphor Bronze.  $\times 120$ .

Recrystallized at  $550^{\circ}\text{C}$ . from the Structure of Fig. 77.

certain value. Then the annealing process becomes a process of recrystallization.

A question of great practical importance arises immediately. What is the temperature at which an overstrained metal will begin to recrystallize. There is no definite answer to this question. The effect of a given temperature upon a given material depends upon the time during which the material is maintained at that temperature. It also depends upon the degree of destruction done to the crystal blocks by the cold-working. The size to which the blocks grow depends upon temperature and time and previous disintegration. The subject has been treated at length by Mr. Zay Jeffries in a paper in the *Journal of the Institute of Metals*, No. 2, Vol. 20, 1918. Reference may also be made to a paper in the same journal by Dr. Hanson entitled "Rapid Recrystallization in Deformed Non-ferrous Metals."

The general conclusion is that if a metal be strained, and then heated, large crystals form at points distant from the point of greatest strain.

Professor Carpenter describes a process in *Proc. Roy. Soc.* Vol. 100, Series A, 1921, by means of which an aluminium test piece, either in plate or bar form, is transformed from its normal multi-crystal structure into a single crystal. The amorphous network surrounding and connecting the crystal blocks is eliminated from the structure. Let us consider in more detail the process Professor Carpenter applied to test pieces cut from a plate. Each piece was 1 inch wide and 0.125 inch thick, with enlarged ends, so that a length of 4 inches of the central part was, in volume,  $\frac{1}{2}$  of a cubic inch.

First, each test piece was heated to 550° C. for six hours. This produced about 150 uniform equi-axed crystals per linear inch, corresponding to 1,687,000 in a length of 4 inches. Next, a load of 0.3 tons was applied to each test piece. This load produced a stress of 2.4 tons per square inch and an elongation of an average value of 1.6 per cent. reckoned on 3 inches. Finally each test piece was placed in a furnace heated to 450° C. and the temperature was raised 15° to 20° per day up to 550° C., after which the temperature was maintained at 600° C. for one hour.

On the average this process converted the 1,687,000 crystals in the length of 4 inches into a single crystal in one test piece out of four. The tensile strength of this single crystal test piece varied from 2.8 to 4.08 tons per square inch. The extension varied from 34 to 86 per cent., reckoned on 3 inches. The multi-crystal test pieces, after 6 hours heating at 550°, gave tensile



strength from 4.5 to 4.7 tons per square inch, with from 36 to 38 per cent. extension on 3 inches.

The condition laid down for the transformation of a multi-crystal piece of metal into a single crystal is that every crystal shall be strained a small amount, but that one of them shall be strained more than all the rest. Then, on suitable heating, crystal growth begins in the region of maximum stress and may finally result in a single crystal. Bars were transformed into single crystals by a similar process. The paper entitled "The Production of Single Crystals of Aluminium and their Tensile Properties"<sup>1</sup> is a record of a remarkable series of researches. The results have a bearing on the load-extension records and will be referred to again below.

**55. Change of Inner Structure. Allotropic Modifications of Iron.** Pure metals ordinarily crystallize from the liquid and cool down without change in their inner structure. But some pure metals change their inner structure at definite temperatures during the cooling process. Iron is a metal of this kind.

After crystallization from the liquid at 1505° C., iron changes its inner structure as it passes through the temperature 900° C., and again as it passes through 768° C. The reverse is true. Heated, it changes structure as it passes through 768° C., and again as it passes through 900° C. What is called alpha-iron is the iron structure stable up to 768° C. It is the structure seen in the microscope. Beta-iron is the iron crystalline structure stable between 768° C. and 900° C. Gamma-iron is the iron crystalline structure stable between 900° C. and 1505° C., the melting-point.<sup>2</sup>

The terms alpha-iron, beta-iron, gamma-iron serve, as it were, to define the limits of climate in which each particular kind of iron can exist.

Difference of inner structure corresponds with difference of physical property. Gamma-iron can dissolve a limited amount of carbon in it, forming with carbon a solid solution, as it is called; that is to say, if at any two points in the solid metal, samples are taken, then there would be equal numbers of carbon atoms distributed through equal numbers of iron atoms, and the distribution of each would be uniform. For example, a cubic milli-

<sup>1</sup> By H. C. H. Carpenter and Constance F. Elam. *Proc. R.S.*, Series A, Vol. C, 1922.

<sup>2</sup> Recently a delta form has been detected at 1425° C. by X-ray analysis. See a paper entitled "X-ray Studies on the Crystal Structure of Steel," by Westgren & Phragmén. *Journal of the Iron and Steel Institute*, No. 1, 1922.

metre taken anywhere from a solid solution would contain equal numbers of carbon atoms and equal numbers of iron atoms uniformly distributed. The greatest proportion of carbon atoms which gamma-iron can hold in solid solution is 1.8 per cent.

Alpha-iron cannot dissolve carbon in this way. It is generally agreed that beta-iron has not the same power of dissolving carbon that gamma-iron has, and it is a matter of controversy whether it can dissolve it at all.

By far the strangest change in physical property occurs when beta-iron changes into alpha-iron or vice versa. Beta-iron, that is, iron above  $768^{\circ}\text{C}$ ., is not susceptible to magnetism. Alpha-iron can be magnetized until its temperature reaches  $768^{\circ}\text{C}$ . and it passes into beta-iron. These different kinds of iron are called allotropic modifications of iron.

Other pure metals show allotropic modifications, as, for example, antimony and tin; and allotropic modifications of oxygen and sulphur are well known. Probably the best known of all is the allotropic modification of carbon in the forms graphite and diamond. Both graphite and diamond are identical in chemical composition, but are different in their inner structure and are vastly different in their physical properties.

The temperatures at which the inner structure of iron changes have received identification letters. During the process of heating,  $\text{Ac}_2$  stands for the temperature at which alpha-iron changes to beta-iron; and  $\text{Ac}_3$  stands for the temperature at which beta-iron changes to gamma-iron. Conversely, on cooling  $\text{Ar}_3$  stands for the temperature at which gamma-iron changes to beta-iron, and  $\text{Ar}_2$  for the temperature at which beta-iron changes to alpha-iron.

If the heating and cooling processes are carried out slowly enough to give time for the inner changes to fully establish themselves, the points  $\text{Ar}_3$  and  $\text{Ac}_3$  coincide at  $900^{\circ}\text{C}$ ., and the points  $\text{Ac}_2$  and  $\text{Ar}_2$  coincide at  $768^{\circ}\text{C}$ . In practice, conversion at each point lags behind the cause, so that  $\text{Ac}_2$  and  $\text{Ac}_3$  are slightly higher than  $\text{Ar}_2$  and  $\text{Ar}_3$ .

In Volume 10 of the *Bulletin of the Bureau of Standards, Washington*, 1914, is a paper by G. K. Burgess and J. J. Crowe, entitled "Critical Ranges  $\text{A}_2$  and  $\text{A}_3$  of Pure Iron," which gives experimental results.

**56. Cooling Curves. Recalescence.** The fact that solid metal changes its inner structure during cooling is ascertained by means of the thermometer and with the microscope.

The structure corresponding to a high temperature is maintained, at any rate in part, by rapid cooling, so that a rapidly

cooled specimen, polished and etched, shows in the microscope, not the structure corresponding to the temperature at which it is examined but the structure belonging to the temperature from which it was quenched. The specimen should be small to secure rapid chilling all through and it should be heated and quenched in a vacuum if possible. Dr. Rosenhain has described an ingenious method of doing this in the *Journal of the Iron and Steel Institute*, Vol. 1, 1908, p. 87.

The thermal analysis of a metal is as useful as the microscopic examination. Some metals solidify and cool steadily to the ordinary temperature. Others solidify, and it is observed that the steady fall of temperature is arrested through particular ranges of temperature by heat evolution within the metal itself. The inference is that this heat evolution is the result of a change of inner structure, a rearrangement of atoms which involves the rejection of heat. Confirmation of the inference is obtained by the microscope on specimens prepared as mentioned above. Reversing the process, the steady increase of temperature on heating is arrested at the critical ranges by the absorption of heat.

The process is analogous to the rejection or absorption of latent heat when a liquid solidifies or when the solid liquefies. In a solid metal the change in either direction is from one kind of solid structure to another kind of solid structure with heat absorbed or evolved during the change.

The identification letters used specially with iron and steel and mentioned above, namely Ar and Ae, were invented by Osmond to signify arrest of temperature change during heat evolution or absorption. The capital letter A stands for arrêt, an arrest of steady cooling and heating, Ar (r = refroidissement) stands for an arrest during cooling, and Ae (e = chauffage) for an arrest during heating.

The quantity of heat evolved during solidification from liquid to solid is greater as a rule than the quantity evolved during an inner change in the solid state. Steel containing about 0.9 per cent. of carbon, however, evolves so much heat when cooling through the temperature 725° C. that it raises the metal to momentary incandescence if the conditions are suitable. This is the celebrated recalescence experiment described by Barrett in the *Phil. Mag.*, Vol. 46, Series IV, 1873, p. 472. The experiment can be shown with a steel wire containing about the percentage of carbon mentioned above. Suspend the wire between two supports so that it hangs freely like the chain of a suspension bridge. Heat it to incandescence by passing through it an electric current.

Cut the current off and watch the wire in the dark. It cools from bright red to blackness, shortening as it cools, but a few instants after it has cooled to blackness it suddenly reglows and momentarily elongates and then rapidly cools to blackness again. Before the reglow the metal was not susceptible to magnetic force. After the reglow the internal structure is changed and the metal is susceptible to magnetic force. This remarkable change from the non-magnetic to the magnetic state is accompanied by heat evolution in considerable quantity. The inner structure is wholly pearlite, as illustrated in Fig. 107.

Data for plotting a cooling curve are obtained from simultaneous observations of temperature and time made on a specimen heated in a furnace and then allowed to cool down with the furnace. Temperature is measured with a thermocouple in contact with the cooling metal and in circuit with a mirror galvanometer. The observer watches the spot of light, focused from the galvanometer mirror, on a scale and presses the key of a chronograph as the spot passes selected divisions of the scale. The deflections of the galvanometer are reduced to temperature by the constant of the instrument and then the data are plotted in the temperature-time diagram. The curve is smooth if the specimen has cooled without heat evolution, but if there is heat evolution a discontinuity or protuberance appears in the curve. The small protuberances may be made more pronounced by plotting the slope of the time-temperature curve against the temperature as done by Osmond in 1887. This is called the "Inverse Rate Curve."

This direct method is, however, not susceptible of bringing out small evolutions of heat such as are sought for in a cooling solid, and even in recording the process of solidification from the liquid melt a more sensitive method is desirable. The direct method with the potentiometer and the difference method, devised by Dr. Stansfield and by Sir Roberts-Austen and described in the Fifth Report of the Alloys Research Committee, *Proc. Inst. Mech. E.*, Feb., 1899, and in the *Phil. Mag.*, Vol. 46, pp. 59 and 82, enable data for a cooling curve from liquid melt to solid to be determined with great accuracy, and the smallest evolutions of heat from a cooling solid can be detected by the difference method.

In the potentiometer method the greater part of the current produced in the circuit by the thermocouple is balanced by a current from a standard cell, and this can be accurately measured on a potentiometer. Only a fraction of the whole current thus passes through the galvanometer, so that it can be adjusted to

be sensitive over a small range of temperature. Fig. 96 shows a diagram of this type of apparatus as used by Carpenter and Keeling in their classical researches on the range of solidification of steels of varying carbon content.

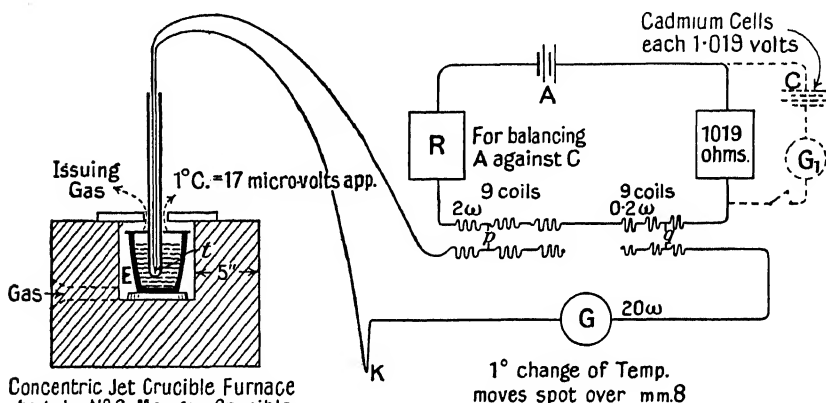


FIG. 96.—Diagram of Apparatus for measuring Heat evolved during Solidification.

Three to four pounds of the metal under test were melted in a crucible E placed in a gas furnace. After melting, the thermocouple was placed in the liquid through the fireclay lid, the gas was turned off, and furnace, crucible, and metal cooled together. The couples used were platinum and platinum-rhodium, or platinum and platinum-iridium. Temperatures from 1500° C. down to about 1000° C. were measured with these couples. Part of the current was balanced by the potentiometer. The accumulators A in the potentiometer circuit were tested from time to time by the standard cadmium cells C. K is the cold junction kept at 0° C. Adjustments were made so that 1° C. change in temperature of the

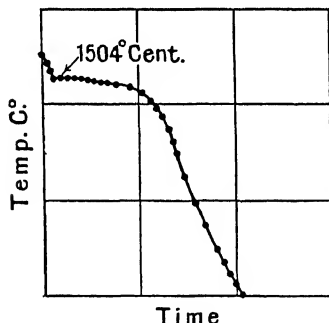


FIG. 97.—Cooling Curve during Solidification of a Melt of 0.02 Carbon Steel.

metal moved the spot over 8 mm. on the galvanometer scale. The range of the galvanometer readings was 27°. The current was then balanced on 27° steps by the potentiometer. Fig. 97 shows a cooling curve plotted from the data observed with this apparatus.

The difference method devised by Sir Roberts-Austen is used to detect the small evolutions of heat in a cooling solid. The solid-metal test piece is cooled with a compensating test piece made of a material which cools steadily without heat evolution. A thermocouple is placed in a hole drilled in the metal test piece, and a second thermocouple is placed in a hole drilled in the compensator. Both couples are included in the circuit of a sensitive galvanometer, but connected in opposition. The deflection of the galvanometer is thus proportional to the difference of temperature between metal and compensator. If both cooled together at the same rate without heat evolution the record would be a straight line. In practice, owing to difference in specific heat and emissivity, the line would be a sloping one without heat evolution from either metal, but with heat evolution

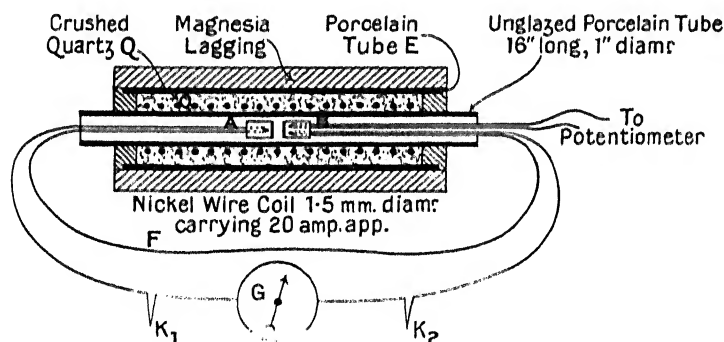


FIG. 98. Diagram of Apparatus for measuring Heat Evolution during the Cooling of a Solid.

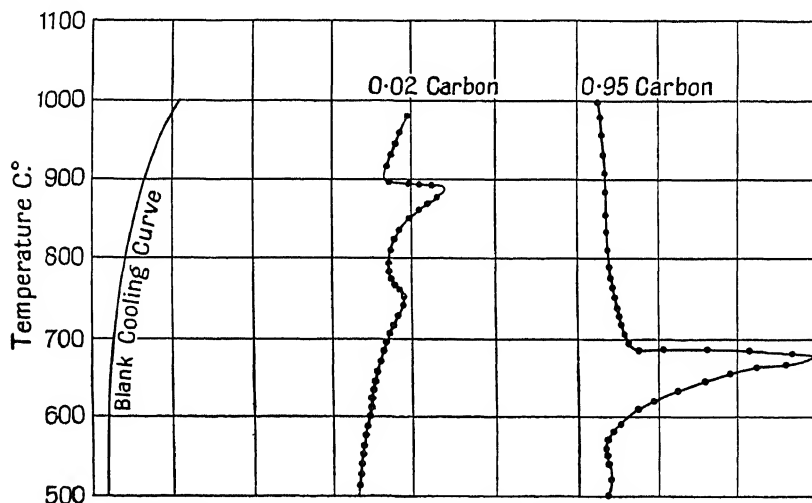
from the metal this sloping line would show marked lateral peaks and blunter protuberances according to the suddenness, quantity, and range of temperature over which heat evolution took place.

The heat evolutions are made still more pronounced if the slope of the difference curve is plotted against the temperature of the metal in the way devised by Rosenhain and described in *Proc. Physical Soc.*, Vol. 21, 1908, p. 180, giving the "Derived Differential Curve."

The temperature of the cooling test piece is measured by an independent thermocouple inserted in a second hole drilled in it and connected with a galvanometer and potentiometer. Fig. 98 gives a diagram of the apparatus as used by Carpenter and Keeling. The furnace was a porcelain tube, unglazed, 16 inches long and 1 inch diameter, heated electrically by a coil of nickel

wire and insulated by crushed quartz Q contained in a wide porcelain tube E closed at the ends. The whole was lagged with magnesia steam-pipe lagging.

Cylinders  $\frac{5}{8}$  inch diameter and  $\frac{5}{8}$  inch long were turned of the metal to be tested. A platinum cylinder A, the compensator, was placed in the furnace with the metal test piece B. Circuit F contains the sensitive galvanometer G and the opposed thermocouples inserted, the one in the compensator A, the other in the specimen B. The second thermocouple in B goes to the potentiometer and is used to measure the temperature of the test piece. Thus the galvanometer G gives the difference of temperature of test piece and compensator and the galvanometer in the



Deflections of the Differential Galvanometer,  $\frac{1}{10}$  full size.  
Fig. 99.—Cooling Curves from Steel (Carpenter and Keeling).

potentiometer circuit gives the temperature of the test piece.  $K_1$ ,  $K_2$  are the cold junctions maintained at  $0^\circ$  C. The furnace is heated to a temperature well below the melting-point of the test piece and is kept at this temperature for about half an hour. Then the current is cut off and the whole furnace cools down. Fig. 99 shows a cooling curve taken with this apparatus.

Further details of apparatus for the thermal work should be studied in textbooks specially devoted to the subject and in the publications of scientific-instrument makers. For a detailed comparison of the various methods reference may be made to a paper, entitled "On Methods of obtaining Cooling Curves," by G. K. Burgess in the *Bulletin of the Bureau of Standards*, Vol. 5, 1908-9.

The interest to the engineer lies rather in the use made of cooling curves than in the actual manner of obtaining them. A cooling curve is to an engineer a chart showing him the temperatures at which molecular changes take place and is of immense service in guiding him towards correct processes of heat treatment and giving him general information about the inner state of the metal. The great importance of cooling curves lies in their power, when marshalled together in a series and ranged in order of alloy composition, to give to the metallurgist a view of the general principles underlying the processes of solidification and cooling of alloys. They enable the **temperature concentration diagram** to be constructed from which so much is learned and in which so much is recorded.

#### 57. Temperature-concentration Diagram of Alloys.—

When two metals are melted together to form an alloy, cooling curve and microscope show that solidification of the melt does not take place at one temperature like a pure metal or pure water, but that the melt begins to solidify at one temperature and ends the process at a lower temperature. The alloy has therefore no one solidifying temperature identified with it, but instead it has a definite temperature range belonging to it through which solidification takes place. At the higher temperature of the range the melt is all liquid. At the lower temperature of the range it is all solid.

At any temperature within the range it is partly liquid and partly solid. The higher temperature of the solidifying range of a given pair does not coincide with the melting-point of either of the metals in the mixture, but it depends upon the composition of the alloy.

Two ways of crystallization from the liquid may be distinguished. In the first, each metal of the pair crystallizes out pure without contamination from the other. In the second, each crystal as it builds selects its material partly from one metal and partly from the other, so that the crystals have each almost the same composition as the composition of the liquid. Given sufficient time and suitable temperature, diffusion in the solid takes place until it may be said that each separate crystal block finally attains the original composition of the liquid from which it solidified. The solid crystalline structure is called a solid solution of one metal within the other.

Pairs of metals crystallizing in the first way, though mutually soluble in all proportions in liquid form, are said to be mutually insoluble in the solid form. Pairs of metals crystallizing in the



second way are mutually soluble in the liquid form and are said to be mutually soluble in all proportions in the solid form.

No pair of metals crystallizes exactly in the first way. But some pairs have such a limited solubility one in the other in the solid state that they may be regarded as solidifying in the first way. Thallium and gold are such a pair.

In order to follow the process of solidification of a pair crystallizing in the first way, consider therefore the experimental results obtained from the thermal analysis of thallium and gold and plotted in the temperature concentration diagram (Fig. 100).

Thallium will build crystals from the liquid melt of the alloy without using a single atomic brick of gold. And gold will build its crystals without using a single atomic brick of thallium, supposing the solidifying process to follow strictly the first but ideal method. But each hampers the other in the building process, as the diagram will soon show.

There are two ways of defining the composition of a mixture. One way is by the weight proportion of the metals present. The second is by the atomic proportion. It is often convenient to plot the temperature concentration diagram to show the composition in atomic proportion.

Let  $x : y$  be the weight proportion of the metals in a mixture. Then if the atomic weight of the  $x$  metal is  $a_1$ , and the atomic weight of the  $y$  metal is  $a_2$ , the atomic proportion of the mixture is

$$\frac{x}{a_1} : \frac{y}{a_2}$$

from which the percentage atomic proportion of the metal  $y$  in the mixture is

$$100 \frac{\frac{y}{a_2}}{\frac{x}{a_1} + \frac{y}{a_2}}$$

Suppose, for example, that a mixture of 90 per cent. by weight of thallium and 10 per cent. of gold is to be reduced to atomic proportion.

The atomic weight of thallium is 204, and of gold 197. Then the atomic proportion of gold in the mixture is

$$\frac{100 \times 10/197}{90/204 + 10/197} = 10.3 \text{ per cent.}$$

The atomic proportion is then 89.7 per cent. thallium and 10.3 per cent. gold.

There is then no difficulty in passing from weight proportion to atomic proportion and vice versa. Assume that a cooling curve has been taken for an alloy of thallium and gold containing 10 per cent. of gold in atomic proportion, and then a curve for an alloy containing 20 per cent. of gold in atomic proportion, and so on for each increase of gold in the mixture by 10 per cent.

Set up an ordinate at each change of 10 per cent. in the mixture Fig. 100, and mark off on each ordinate the corresponding

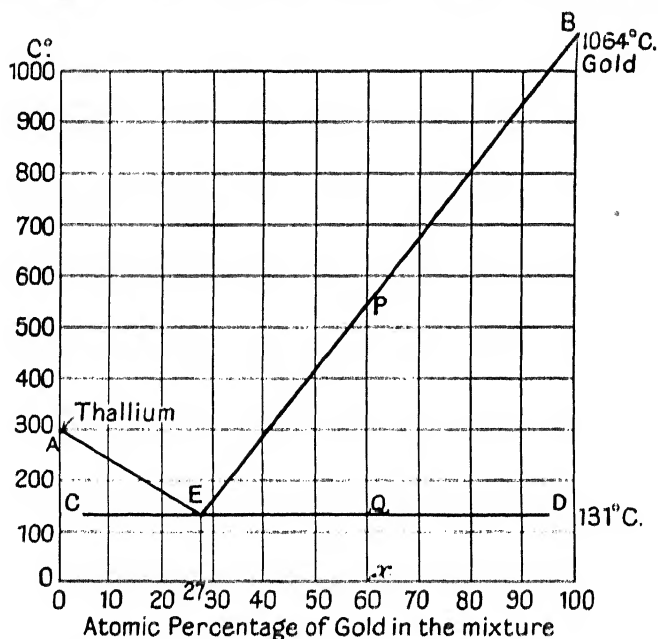


FIG. 100. Temperature-concentration Diagram: Thallium and Gold.<sup>1</sup>

temperatures of the arrests shown on the cooling curves. The ordinate through the zero of the horizontal scale represents a melt of pure thallium. There is only one arrest point on this ordinate, namely at 300° C., the temperature of solidification of thallium. The next ordinate marks a composition of 10 per cent. gold and 90 per cent. thallium in atomic proportion. The cooling curve furnishes two temperatures on this ordinate; one on the line AE, and one on the line CE. The ordinate at 27 per cent. gold shows one arrest at temperature 131° C. As the percentage of gold increases each ordinate is found marked with two temperatures which get wider and wider apart until the experi-

<sup>1</sup> M. Levin, *Zeitschrift für Anorganische Chemie*, 1905, Vol. 45, page 31.

mental melt is wholly gold. One arrest only is plotted, namely at  $1064^{\circ}\text{C.}$ , the temperature of solidification of pure gold.

The diagram as it stands is merely a record of the temperatures of arrests plotted against composition. The microscope enables the temperatures on an ordinate to be identified with the beginning and the end of solidification of an alloy of the composition defined by the position of the ordinate.

Joining the points together, there results a horizontal line at the temperature  $131^{\circ}\text{C.}$  and two inclined lines meeting this horizontal at E. The diagram as it now stands illustrates some fundamental principles in metallography.

First selecting any mixture and erecting an ordinate, as at  $x$ , the intercept on this ordinate PQ is the solidifying range of temperature for the alloy of that composition. Secondly, if the mixture at E is selected the range of temperature is nil. This mixture solidifies at one temperature, namely  $131^{\circ}\text{C.}$  This is the most fusible mixture that can be made of this pair of metals. It is called the **eutectic mixture**, meaning the most fusible mixture. The name was introduced by Prof. Guthrie.

The process of solidification may now be followed on this diagram. Consider the solidification of a mixture of 10 per cent. of gold. The metal in the melt in excess of the eutectic proportion begins to crystallize first and goes on crystallizing at falling temperature until the liquid melt is reduced to the eutectic proportion, and then the gold begins to crystallize and both metals then go on crystallizing at constant temperature until the whole melt has solidified. The eutectic structure often exhibits a beautiful stratified appearance in the microscope.

The metal in excess of the eutectic proportion crystallizes at a falling temperature because as it is withdrawn from the melt in crystal form the metal left liquid is changed in composition and therefore its solidifying range has changed. For example, in the 10 per cent. mixture of gold and thallium there is an excess of thallium above the eutectic proportion which is 27 per cent. of thallium, and this excess begins to crystallize at  $255^{\circ}\text{C.}$  Suppose 20 per cent. of it has crystallized out; then at the moment the composition of the remaining liquid is 10 parts gold and 70 parts thallium, corresponding to 15 per cent. gold nearly. The ordinate at this mixture shows that the temperature of crystallization is  $206^{\circ}\text{C.}$

Therefore, the ordinate which marks the composition of the liquid mixture moves slowly towards the eutectic point during the process of crystallization of thallium. As it moves, its foot

shows the instantaneous composition of the liquid and its intersection with the line AEB defines the corresponding instantaneous temperature of the liquid. When it arrives at the eutectic point the liquid has been reduced to eutectic composition, the gold begins to crystallize, and then thallium and gold crystallize side by side but separately at the constant temperature until the whole of the liquid has become solid.

Summarizing, the characteristics of pairs of metals which, although mutually soluble in one another in all proportions as liquids, are insoluble in one another as solids, are:—

1. That they form a eutectic mixture.
2. That this mixture solidifies at constant temperature.
3. That this temperature is below the solidifying temperature of either of the metals in the pair.
4. That an alloy of any composition but the eutectic composition has a solidifying range.
5. That the upper temperature of this range increases from the eutectic temperature in proportion to the excess of either metal present when the mixture is defined by atomic proportion.
6. That the lower temperature of the range is the same for all mixtures and is equal to the eutectic temperature.

So long as the temperature of an alloy lies above the line AEB it is all liquid. This line is called the **liquidus**. If the temperature is below the line CED it is all solid. The line CED is called the **solidus**.

If the temperature falls within the triangular area AEC the alloy is liquid, with crystals of thallium in it. If the temperature falls within the triangular area BED the alloy is liquid with crystals of gold in it.

It can easily be predicted from this what the general appearance of the solid alloy will be in the microscope. Assuming that the eutectic mixture has solidified in a stratified form so that it is easily recognized, an alloy whose composition lies between 0 and 27 per cent. gold will show crystals of thallium embedded in the eutectic. An alloy whose composition lies between 27 and 100 per cent. gold will show crystals of gold embedded in eutectic. The eutectic itself will consist of alternating layers of gold and thallium bent and distorted into most beautiful patterns.

Silver and copper, silver and lead, bismuth and tin, cadmium and zinc, zinc and tin, are pairs of metals which solidify in the way above described, and there are many other binary pairs, as they are called, which follow the same process, remembering

always that separate crystallization without contamination from either is an ideal process. The contamination is a question of degree only.

Separate crystallization of the two constituents of a mixture is not confined to crystallization from the liquid. An analogous process takes place from a solid solution of two constituents as well as from a liquid solution. One of the most interesting examples of this is steel.

When carbon is added to a bath of liquid iron it immediately combines chemically with so much of the iron as it requires to form  $\text{Fe}_3\text{C}$ , that is cementite, and then the cementite is dissolved in the remainder of the iron. Assume that 0.5 per cent. of carbon is added to a bath of liquid iron. From the formula it follows that this quantity of carbon will combine with 7 per cent. of iron to form  $7\frac{1}{2}$  per cent. of cementite, leaving  $92\frac{1}{2}$  per cent. of iron. The bath may now be regarded as a liquid solution of  $92\frac{1}{2}$  per cent. iron and  $7\frac{1}{2}$  per cent. cementite. This solidifies as a solid solution, so that, given time for diffusion in the solid, a crystal block of the solid solution will ultimately contain  $7\frac{1}{2}$  per cent. cementite and  $92\frac{1}{2}$  per cent. iron. This solid solution of iron and cementite is called **austenite** from the discoverer of it, Sir Roberts-Austen. As the austenite cools a temperature is reached, at about  $768^\circ\text{C}$ ., at which the austenite begins to deposit crystals of alpha-iron. This goes on, the austenite increasing in strength as the temperature falls until the austenite has increased in strength to  $13\frac{1}{2}$  per cent. cementite in  $86\frac{1}{2}$  per cent. iron, corresponding to 0.9 per cent. carbon in 99.1 per cent. iron at a temperature of  $725^\circ\text{C}$ . Below this temperature the austenite breaks up into alpha-iron and cementite. The solid solution has separated into a mechanical mixture of its constituents called pearlite. The form of the pearlite depends upon the rate at which cooling takes place through this change-point. It may be laminated or it may be granular or some other form.

Part of the temperature concentration diagram of the iron-carbon system of alloys is plotted in Fig. 101 to illustrate this and to show by comparison the similarity of the diagram to the diagram of thallium and gold crystallizing from a liquid solution.

The ordinate corresponding to 0.5 per cent. of carbon, equivalent to  $7\frac{1}{2}$  per cent. of cementite, shows a range, beginning at  $768^\circ\text{C}$ . and ending at  $725^\circ\text{C}$ ., through which the austenite deposits crystals of alpha-iron. Alpha-iron crystallizes out from the austenite whilst the ordinate moves towards the eutectic point E, its foot showing at any instant the composition of the austenite

and its upper temperature the temperature of the solid. Arriving at E, alpha-iron and cementite separate from the austenite and recrystallize into a mechanical mixture which is called the **eutectoid** of alpha-iron and cementite. This goes by the general name of **pearlite**.

The term Eutectoid denotes the most fusible mixture of two solids in the sense that a higher temperature transforms them into a solid solution. The term Eutectic implies that the most fusible mixture is transformed by heating into a liquid solution.

Steel containing 0.9 per cent. carbon should therefore show the eutectoid structure alone. Steel containing less carbon should show ferrite embedded in the eutectoid, steel containing more carbon than 0.9 per cent. should show cementite embedded in the eutectoid.

Fig. 107 shows the eutectoid structure produced under the thermal conditions in which the simultaneous but separate crystal building of ferrite and cementite produce the laminated alternations of either called pearlite. Fig. 106 shows ferrite in pearlite, the structure of a 0.57 carbon steel. Fig. 108 shows cementite in pearlite, the structure of a 1.4 carbon steel.

The change in inner structure corresponding to increased carbon content can be traced easily on one specimen by case-hardening a piece of iron and then polishing and etching a cross-section. The case-hardened shell appears as a dark frame round the section if viewed under a low power. The carbon makes its way into the metal during the case-hardening process so that the carbon content along a direction perpendicular to the surface decreases from a maximum at the surface to a minimum at the inner depth of penetration. By merely moving the test piece across the field of the microscope the various structures determined by varying carbon content can be passed in review.

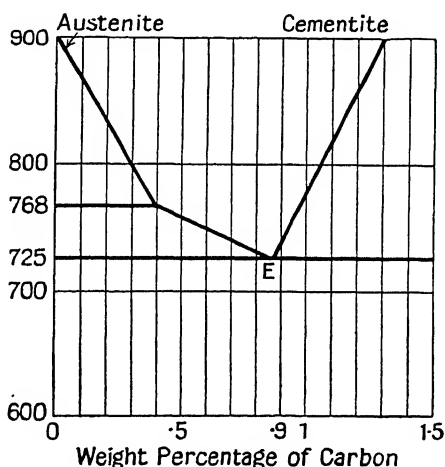


FIG. 101.—Temperature-concentration Diagram: Iron and Carbon in the Solid.

Starting from the centre of the piece and using a suitably high power, there will be seen in succession ferrite, then ferrite in pearlite, then pearlite only, and finally cementite in pearlite. These structures can be seen merging one into the other as the specimen is moved across the field.

Let us now consider the temperature-concentration diagram belonging to an alloy of two metals which are mutually soluble in all proportions both in the liquid and in the solid states. It might be expected that a melt of given composition of such a pair would solidify at constant temperature, building crystals of identical composition with the liquid. The cooling curves show, however, that solidification takes place through a range of temperature.

The power of crystal-building appears to be controlled by the temperature so that when crystals begin to build themselves from the liquid melt they select material, not in proportion to the composition of the melt, but in a proportion determined by the temperature of the liquid. In consequence of this the composition of the liquid left as solidification proceeds is continually changing, and with it the temperature at which crystals build themselves, and the crystals themselves build with varying proportion.

The full lines in Fig. 102 show the temperature-concentration diagram of copper and nickel. A series of cooling curves marshalled along the axis in order of atomic composition of the melts from which they were taken show arrests which, joined, give the curved lens-like diagram seen. Consider the alloy containing about 40 per cent. nickel. It begins to solidify at about 1280° C. It has finished solidifying at about 1210° C. The composition of its initial crystal structure is determined by the temperature at which solidification begins, and it is inferred that the proportion in which the initial crystals select their material from the liquid is defined by the ordinate corresponding to the solid state at that temperature. Draw therefore a horizontal line through the point T to cut the solidus in B. An ordinate through B cuts the base in *b*, showing that the composition of the crystals first formed is 58 per cent. nickel and 42 per cent. copper.

At *t*, the temperature at which the melt is wholly solid, draw a horizontal to cut the liquidus in G. Then at the moment of solidification the last liquid drop has the composition defined by an ordinate dropped from G, namely 25 per cent. of nickel and 75 per cent. of copper. The crystals formed during the process of solidification thus have a varying composition from within outwards. The core has the composition *b*, the outer

sheath the composition  $g$ , and the average composition is  $x$ . Given time and a suitable temperature, this inequality of composition is redressed by the process of diffusion in the solid towards the average composition  $x$ .

Thus in a liquid melt of composition  $x$ , crystals begin to build of composition  $b$  at temperature  $T$ , and finish building with composition  $g$  at temperature  $t$ , and then tend to the average composition  $x$ , corresponding to the range  $Tt$  by the process of solid diffusion. During the process of solidification the ordinate  $Ttx$ , representing the original composition of the liquid, moves into coincidence with  $Gg$ , and the ordinate  $bB$ , showing the

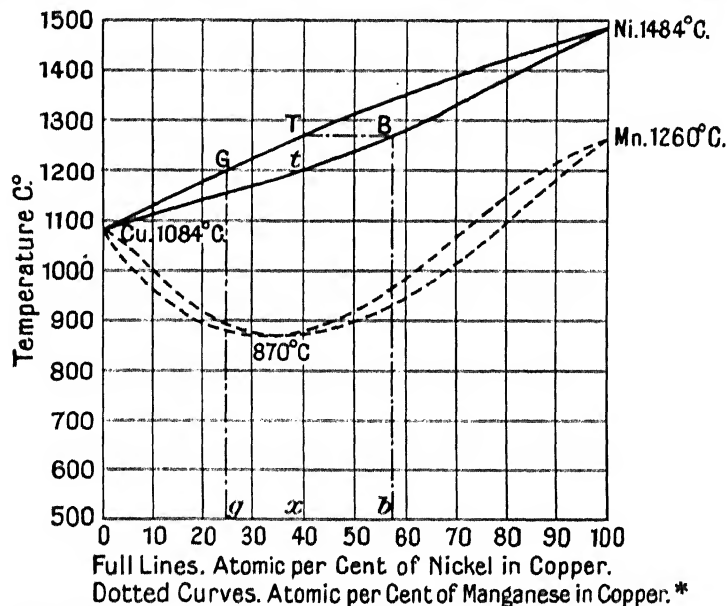


FIG. 102.—Temperature-concentration Diagrams of Nickel in Copper and of Manganese in Copper.†

composition of the initial crystal structure, moves also into coincidence with  $Gg$ . Both  $Ttx$  and  $bB$  meet in  $Gg$  at the moment of solidification of the last drop of the liquid.

The crystal structure of a solid solution seen in the microscope has not usually the sharpness of outline exhibited in the structure of alloys which do not form solid solutions. Owing to the varying composition of the crystals the etching fluid produces blurred edges and softened and rounded outlines. The sharpness will

\* W. Guertler and G. Tamman. *Zeitschrift für Anorganische Chemie*, 1907, vol. 52, page 25.

† S. F. Shermitschuy and T. T. Urasow, A. E. Rykowski, *Z. A. C.*, 1908, vol. 57, page 20.



depend upon the extent to which diffusion has brought the crystals towards a uniform composition.

The peculiarities of pairs of metals which are mutually soluble in the solid in all proportions are :

1. That they form no eutectic mixture.
2. That the solidifying range of a mixture lies between the solidifying temperatures of the pair.
3. That the micro-structure depends upon the extent to which diffusion in the solid has brought the crystals towards a constant composition.

Other pairs give an assemblage of arrest points, which when joined show a solidus and liquidus coinciding at a point of minimum temperature lower than the solidifying temperatures of either metal in the pair. At this point of minimum temperature the crystals select their materials from the liquid in exactly the proportion in which they are present in the liquid. Growing crystals and diminishing liquid keep the same proportion during the whole process of solidification at the constant minimum temperature. An alloy of the pair in any other proportion than that corresponding to the minimum temperature has a solidifying range and the crystals build in varying proportion. No eutectic is formed.

Copper and manganese furnish a diagram of this kind. Copper solidifies at  $1084^{\circ}\text{C}.$ ; manganese at  $1260^{\circ}\text{C}.$  But a mixture of 35 per cent. manganese and 65 per cent. copper, atomic proportion, solidifies at the constant temperature  $870^{\circ}\text{C}.$ , and the crystals select manganese and copper from the liquid for building in the proportion 35 to 65.

Insolubility in the solid as exemplified by the thallium-gold diagram (Fig. 100) is an ideal condition never quite realized in practice. Metals usually possess the property of mutual solubility in the solid to some, even if to a very limited, extent.

The diagram of silver and copper may be used to illustrate the general form of diagram belonging to pairs which form eutectic mixtures and at the same time possess the property of a limited mutual solubility in the solid.

Silver can dissolve up to about 7 atomic per cent. of copper in solid solution. A crystal block of this structure analysed would show this atomic proportion. The ordinate *cCf* marks this alloy in the diagram (Fig. 103). Its solidifying range is *Cf* degrees. Again, copper can dissolve up to about 15 atomic per cent. of silver in solid solution. The ordinate *dDg* marks this alloy on the diagram. Its solidifying range is *Dg*. An

alloy of silver containing less than 7 per cent. of copper solidifies like a solid solution, and the curves of the diagram Fig. 103 show the solidifying ranges.

An alloy of silver containing more than 85 atomic per cent. of copper solidifies as a solid solution, and the curves of the diagram show the solidifying ranges. An alloy of silver containing more than 7 and less than 40 atomic per cent. of copper forms a saturated solution of 7 atomic per cent. copper in silver, and then the excess copper in the mixture behaves as a separate metal to the saturated solution. The ordinate marking the original mixture moves towards the eutectic point at E, and then excess copper begins to solidify and the silver-saturated

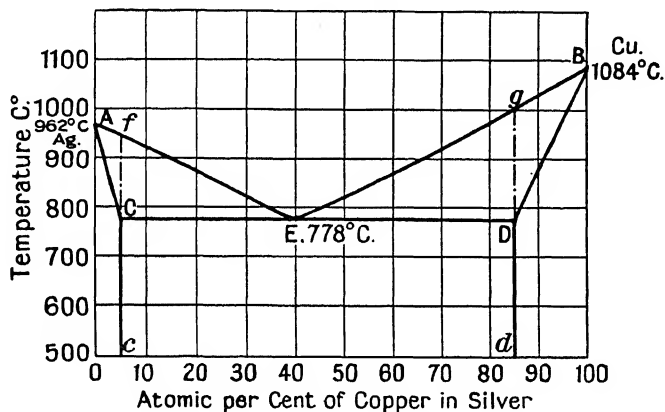


FIG. 103.—Temperature-concentration Diagram: Silver and Copper. \*

solution and the excess copper solidify separately side by side at common temperature 778° C.

An alloy of silver containing more than 40 and less than 85 atomic per cent. of copper—or perhaps it is better to say an alloy of copper containing more than 15 and less than 60 atomic per cent. of silver—forms a saturated solution of 15 atomic per cent. silver in copper, and then the excess silver in the mixture behaves as a separate metal to the saturated solution of copper. The ordinate marking the mixture moves towards the eutectic point E as the saturated solution crystallizes at falling temperature, and then the excess silver begins to solidify and excess silver and copper-saturated solution crystallize separately side by side at common temperature 778° C.

These percentages are given to illustrate the type of diagram and are only approximately accurate. The arrest points defining

\* W. von Lepkowski. *Zeitschrift für Anorganische Chemie*, 1908, vol. 59, page 290.

the lines of the diagram were determined by Heycock and Neville (see *Phil. Trans.*, 1897, 189A, 25), and the limits of solubility marked by the points C and D were investigated by Friedrich and Leroux (*Metallurgie*, 1907, 4, 293), but according to Desch there is still a little doubt about their exact values.

The general type of diagram for a pair of metals possessing limited mutual solubility in the solid shows a horizontal through the eutectic point E, terminated either way by points C and D. The ordinates through these points mark the composition of either alloy when saturated with the other. Lines from the temperature limits of the solidifying ranges of these saturated solutions meet in the solidifying temperatures of the pure metals. For example, lines from C and *f* meet in A and from D and *g* meet in B.

When the alloy has the eutectic composition the melt solidifies at constant temperature and the inner structure may be regarded as produced by a pair of saturated solutions behaving towards each other as a pair of pure metals.

Solid solutions generally alter their composition as the temperature changes. This point has been illustrated by the diagram of the carbon-iron alloys Fig. 105. Iron at 1139° C. can dissolve up to 27 per cent. of cementite corresponding to 1.8 per cent. of carbon, but at 725° C. it can only dissolve 13½ per cent. of cementite, corresponding to 0.9 per cent. of carbon. During the cooling of the solid from 1139° C. to 725° C. the excess cementite gradually separates out.

The behaviour of solid solutions may be further illustrated by alloys of copper and zinc. These metals form a complicated series of solid solutions whose limiting proportions change as the temperature changes. Part of the temperature-concentration diagram of the copper-zinc series is shown in Fig. 104.

A melt containing 30 per cent. of zinc and 70 per cent. of copper solidifies in the way described above for a pair of metals forming solid solutions. The ordinate  $xT$  marks this alloy in the diagram.  $T$  is the range of solidification and  $x$  is the average composition. This material is called the alpha-solution. Its structure is like that of a pure metal and is seen in Fig. 91 above. Each crystalline block there seen is built of atoms in the average proportion of 30 zinc to 70 copper. As mentioned above, if cooled too quickly so that diffusion is prevented, the  $\alpha$ -material may appear to be built of two separate constituents because the rich inner cores of the blocks and the poorer outer sheaths are differentially etched and therefore the alpha-solution

is non-homogeneous and appears in the microscope as two blurred but different structures. The curved line AB marks the limiting conditions of composition and temperature in which the inner structure is entirely built of alpha-material. At ordinary temperatures the alpha-solution may contain as much as 37 per cent. of zinc. A melt containing 40 per cent. of zinc solidifies through the range  $T_1t_1$  forming what is called the beta-solution. This solution is stable until the temperature falls to  $750^\circ\text{C.}$ , and then alpha-solution begins to separate from it.

According to Carpenter this beta-solution is only stable above  $470^\circ\text{C.}$  Below this temperature it breaks up into alpha-solution and another called gamma-solution. Thus the inner structure of brass containing 40 per cent. zinc shows two definite materials, namely the alpha-blocks and the gamma-blocks. An example of this is seen in Figs. 66 and 67 above. The two structures appear very different, and this is no doubt due to a different history of cooling rates and mechanical working. The rate of cooling influences the final structure greatly. Rapid cooling of a 40 per cent. alloy may retain the beta-structure. Less rapid may give an alpha- and beta-structure.

But with a rate suitable to the conditions of the diagram the final structure will be alpha-solution and gamma-solution.

The diagram shows that the ductile 30-70 brass consists entirely of alpha-solution. And the strong 40-60 brass consists of a mixture of alpha- and gamma-solution when cooled slowly enough to allow diffusion to establish equilibrium.

Summarizing, the thallium-gold diagram Fig. 100 is typical of a pair of metals each of which crystallizes from the liquid separately. In these circumstances there is one mixture of them which solidifies at a constant temperature lower than the melting-point of either, and the structure produced is a mechanical mixture of the separate crystals of the two metals. The mixture is called the eutectic mixture and the structure the eutectic

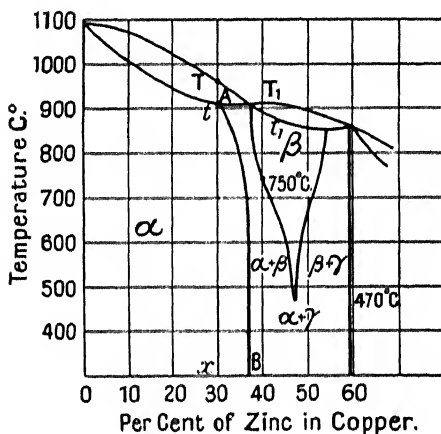


FIG. 104.—Part of Temperature-concentration Diagram: Copper and Zinc (Brass).

structure. Mixtures of the metals in any other but the eutectic proportion solidify through a range of temperature and the inner structure shows pure crystals of the excess metal distributed through the eutectic structure.

The copper-nickel diagram Fig. 102 is typical of a pair of metals which crystallize from the liquid in quite the opposite way. Solidification takes place through a temperature range, but each crystal as it grows selects material from each metal in the liquid in a proportion which changes as solidification proceeds through the temperature range, but finally, by diffusion in the solid, the crystals adjust themselves to the composition of the liquid from which they solidified. Each crystal block may then be regarded as a solidified part of the liquid solution and the resulting structure is called a solid solution. Pairs of metals forming solid solution in all proportions do not form eutectic mixtures. Their structure, after diffusion in the solid to uniform composition, is like the block structure of a pure metal.

The copper-manganese diagram Fig. 102 is typical of pairs which form solid solutions and at a particular composition solidify at a constant minimum temperature. The solid separating at this minimum temperature is not an eutectic mixture but a solid solution separating in the same proportion as the liquid. The crystal as it builds incorporates the material from the liquid in the exact proportion in which it is present in the liquid.

The copper-silver diagram Fig. 103 is typical of many pairs of metals. It shows a pair each of which can dissolve a little of the other in the solid. The saturated solution of either metal then behaves as a separate metal to the metal in excess of that which it can dissolve. The saturated solutions forms eutectic mixtures with one another.

A metal after solidification may not retain its structure as it cools. It may rebuild in the solid. The solid solution formed from the liquid then stands to the structure at a lower temperature in a similar way to that in which the liquid stands to the solid formed at the solidifying temperature or through the solidifying range. The pair of metals in solid solution may recrystallize separately from the solid solution and give a eutectic diagram like thallium and gold or like silver and copper. This is illustrated by the recrystallization of austenite, and a part of the iron-carbon diagram is shown in Fig. 101. The pair of metals in the solid solution recrystallizes separately into an eutectic of cementite and ferrite containing pure crystals of ferrite or of cementite according to the composition of the material. Again, solid

solutions may break up into other solid solutions, and this is exemplified by part of the copper-zinc diagram.

These diagrams do not by any means exhaust the types that are to be found in practice. Some metals when mixed act chemically on one another, just as exemplified by carbon in iron. Then it may be necessary to consider three constituents in a melt of a pair of metals, namely the separate metals themselves and the chemical compound formed from them. There may even be a series of definite compounds formed with limited solubilities in the solid, one in the other. Whatever may be the complexities, the temperature-concentration diagram is established step-by-step from the temperature arrests observed on cooling and heating curves, aided by the microscope and supplemented by other physical data such as density, magnetic hysteresis, electrical conductivity, specific heat, chemical data, electrochemical, and also the measurement of mechanical properties.

These few notes on the temperature-concentration diagram may be useful to engineers and may serve to show what a wide field of research has been covered by metallographers to establish the properties of possible pairs of metals. Metals taken three at a time offer a field of research of almost illimitable extent. The subject may be pursued in the excellent textbooks of Rosenhain or Desch, both pioneer workers in these subjects.

The diagram is by some called the Constitutional Diagram and by others the Equilibrium Diagram. The term equilibrium is used to signify that the thermal phenomena recorded in the diagram are those corresponding to thermal equilibrium. Mention has already been made that the temperature of an arrest is slightly different, according as the observation is made on a cooling curve or on a heating curve, but that if the rate of cooling or heating is very slow the temperatures coincide. The temperature recorded in the diagrams is that which it is assumed would be found either from a heating or from a cooling curve along which the change of temperature was made with infinite slowness.

**58. Temperature-concentration Diagram of the Iron-carbon Alloys.**—Sir Roberts-Austen, in the Fourth and Fifth Reports of the Alloys Research Committee,<sup>1</sup> demonstrated that carbon formed a series of alloys with iron comparable with other pairs of metals and furnished data from which a preliminary diagram was constructed. Roozeboom, applying the principles of thermodynamics to the data, extended the curves of the diagram, and many workers have contributed experimental data

<sup>1</sup> *Proc. Inst. Mech. E.* 1897, Fourth Report, and 1899, Fifth Report.

in the endeavour to fix the shapes of the lines and curves drawn through the arrest points.

The iron-carbon diagram now generally accepted is based on the later experimental work of Carpenter and Keeling. Their work covered a range of alloys from 0.01 to 4.5 per cent. of carbon. Details of their investigations, together with the diagram, are published in the *Journal of the Iron and Steel Institute*, No. 1,

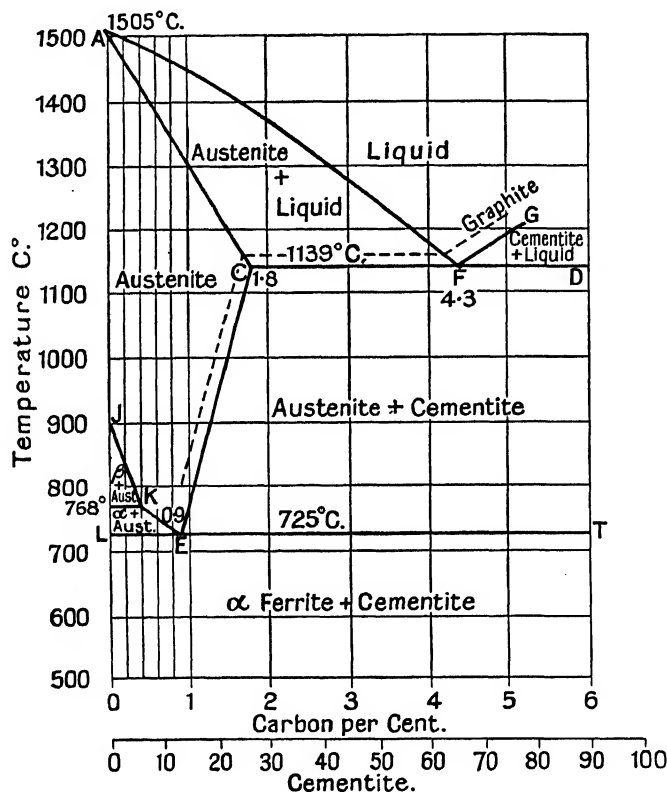


FIG. 105.—Temperature-concentration Diagrams: Iron-carbon Alloys.  
(Carpenter and Keeling.)

1904. Reference has already been made to the paper to illustrate the general method of thermal analysis. The Carpenter-Keeling diagram is shown in Fig. 105. This figure corresponds with the diagram published by Professor Carpenter in his paper, "The Iron-carbon Equilibrium Diagram and its Practical Usefulness," *Trans. Inst. of Naval Arch.*, 1918. The range, beginning with pure iron, covers all the carbon steels and varieties of cast irons.

It will be noticed at once that, although the percentage of

carbon in the iron is set out along the base; the areas of the diagram bear names which indicate that equilibrium is not between iron and carbon but between austenite and cementite. A cementite scale is therefore added. Cementite, as mentioned above, is the chemical combination of carbon with iron represented by the formula  $\text{Fe}_3\text{C}$ . Cementite, or carbide of iron as it is alternatively called, was discovered by the late Sir Frederick Abel in 1885. The formula shows that 1 part by weight of carbon combines with 14 parts by weight of iron to form 15 parts of cementite. Cementite has been supposed to be an unstable compound, splitting up easily into ferrite and graphite. The question was exhaustively considered by Dr. Stead in his Presidential Address to the British Association at Sheffield in 1910. Briefly Dr. Stead, after recapitulating the work of others, goes on to describe the results of his own researches. He concludes that a small quantity of sulphur present with cementite makes it stable, but that silicon has the opposite effect. Quoting three of Dr. Stead's conclusions at the end of his address:—

1. The experimental results advanced show proof that carbide of iron,  $\text{Fe}_3\text{C}$ , in presence of iron sulphide crystallizes with a minute quantity of sulphur not exceeding about the one-thousandth part of the weight of the carbide, but the nature of the iron-carbon-sulphur compound has not yet been determined.

2. It seems almost, if not absolutely, certain that it is the sulphur crystallized with the carbide which makes the latter stable.

3. Silicide of iron, when heated at  $1000^\circ \text{C}$ . with pure white iron free from silicon, effects the decomposition of the carbide of the white iron. Based on this observation the hypothesis seems justifiable, in cases where all the silicon present in hypo-eutectic alloys crystallizes out with the primary austenite, that after the carbide has solidified diffusion of the silicide follows, and this leads to the decomposition of the carbide of iron into graphite and iron.

From this it is safe to conclude that the full lines of the iron-carbon diagram (Fig. 105) show the equilibrium of austenite and cementite which has been made stable by sulphur.

The dotted lines on the diagram marked graphite show the modification brought about by unstable cementite. Equilibrium is then between austenite and graphite.

**Austenite** is a solid solution of carbon in gamma-iron. As already mentioned, gamma-iron possesses the property of dissolving carbon. The quantity which can be dissolved depends



upon the temperature. The greatest quantity is 1.8 per cent. at  $1139^{\circ}\text{C}$ . When the temperature of this solid solution is reduced, it is found that cementite separates from the solution, not carbon; it seems therefore reasonable to suppose that originally the carbon first formed cementite and then this cementite dissolved in the gamma-iron. The maximum solubility is then expressed by saying that gamma-iron dissolves 27 per cent. of cementite at  $1139^{\circ}\text{C}$ . Whichever view is taken of the matter the crystals of the solid solution when analysed would show 1.8 atoms of carbon mingled with 98.2 atoms of ferrite, always assuming that time has been given for all parts of the solution to be brought to a uniform composition by diffusion in the solid.

Turning now to the full-line diagram, the lines AFG form the liquidus. A temperature above this line defines an alloy which is wholly liquid. ACD is the solidus. A temperature below this line defines an alloy which is wholly solid. A temperature within the area AFC defines an alloy which is a liquid containing crystals of austenite. A temperature within the area GFD defines an alloy which is a liquid containing crystals of cementite.

A temperature within the area DFCEFT defines an alloy showing a groundwork of a eutectic mixture of austenite and cementite with crystals of austenite or cementite embedded in it according as the carbon content is less or greater than 4.3 per cent.

A temperature below  $725^{\circ}\text{C}$ . defines an alloy in which the austenite has decomposed into ferrite and cementite and the structure shows a groundwork of the eutectic of ferrite and cementite, usually laminated pearlite, in which is embedded crystals of ferrite or cementite according as the carbon content is less or greater than 0.9 per cent.

A temperature within the area ACEKJ defines an alloy built wholly of austenite crystals. As described above, this solid solution of austenite when cooled behaves as if the two metals ferrite and cementite were solidifying from a liquid solution of ferrite and cementite of which JKEC is the liquidus and LET the solidus. If through the presence of silicon or any other cause the cementite is decomposed, then the dotted lines of the diagram marked graphite define the equilibrium conditions between ferrite and graphite.

The presence of impurities, manganese, phosphorus, silicon, sulphur, and other substances in the melt introduce complexities in the solidification and cooling processes and modify the temperature of the arrests, as will be well understood from Dr. Stead's address. Special steels and special irons must be studied by

special cooling curves. The diagram as it stands is a guide to the correct interpretation of microphotographs and to the correct heat treatment of pure carbon steels containing the usual small quantities of impurities.

We now use the diagram to aid in the interpretation of the microphotographs of iron and steel distributed through Chapter II, together with others introduced to illustrate the structure of the pig irons.

### 59. Interpretation of Microphotographs.

**Iron.**—The structure of commercial irons is seen in Figs. 19, 20, 22, 23, 25, 26. From the diagrams we infer, although the iron is not quite carbon-free, that we are looking at alpha-iron, which, when heated, changes to beta-iron at  $768^{\circ}\text{C}$ . and to gamma-iron at  $900^{\circ}\text{C}$ . and finally melts at about  $1505^{\circ}\text{C}$ . Since no other structure is seen we assume that the carbon and other constituents shown in the analysis are dissolved in the iron. The black threads and spots are slag inclusions.

**Mild Steel.**—The structure is seen in Figs. 28, 29, 31, 32, 34, 35, 40, 44, and 45. Looking at Fig. 44 we see two structures, ferrite and pearlite, and Fig. 45 shows that the pearlite is of the laminated kind. This steel contains 0.13 per cent. of carbon. The ordinate in Fig. 105 corresponding to this carbon content indicates that this steel would show temperature arrests at  $725^{\circ}\text{C}$ .,  $768^{\circ}\text{C}$ .,  $867^{\circ}\text{C}$ .,  $1470^{\circ}\text{C}$ ., and  $1498^{\circ}\text{C}$ . These are equilibrium temperatures. The actual temperatures observed in an experiment would differ from these by amounts depending upon the rate of heating or cooling.

A liquid melt of this steel begins to solidify at  $1498^{\circ}\text{C}$ . and the process is finished at  $1470^{\circ}\text{C}$ . The solid is austenite containing 0.13 per cent. of carbon, equal to 19.5 per cent. of cementite in solid solution. When the temperature has fallen to  $867^{\circ}\text{C}$ . the austenite begins to deposit crystals of beta-iron and the composition ordinate moves towards the eutectic point E. When the temperature has fallen to  $768^{\circ}\text{C}$ ., the beta-crystals deposited change to alpha-iron and the austenite then deposits alpha-iron crystals as the temperature continues to fall. The foot of the ordinate shows the composition of the austenite, and the intersection with the line KE the corresponding temperature, as the strength of the austenite increases with rejection of iron crystals at falling temperature. When the ordinate reaches E the temperature has fallen to  $725^{\circ}\text{C}$ . and the austenite has reached its saturation strength of 0.9 per cent. carbon. It then

reverts to pearlite of a kind which depends upon the rate of cooling through the temperature. No further change takes place as the solid cools. What we see in Fig. 45 is then the end of a complex process of crystallization.

To follow the reverse process imagine an ordinate to pass through the point E, because it is the element of this composition, pearlite, that first responds to heat applied to the structure. When the rising temperature reaches  $725^{\circ}\text{C}$ . the pearlite changes to austenite, and as the temperature increases this austenite begins to absorb first alpha-iron up to  $768^{\circ}\text{C}$ . and then beta-iron up to  $867^{\circ}\text{C}$ ., the ordinate showing the average composition of the austenite, moving to the left. When it reaches the composition 0.13 it stops: the temperature of the austenite increases until at  $1470^{\circ}\text{C}$ . it begins to melt, the melting process being ended at  $1498^{\circ}\text{C}$ . The melt is then wholly a liquid solution of austenite consisting of 19.5 per cent. of cementite dissolved in iron.

**Steel containing 0.5 per cent. of Carbon.**—The change produced by falling temperature has been described for this particular steel. It differs from mild steel only in that the cooling austenite deposits no beta-iron and the solidifying range is increased to  $66^{\circ}$ . Solidification begins at  $1470^{\circ}\text{C}$ . and ends at  $1404^{\circ}\text{C}$ .

Fig. 106 shows the inner structure of a steel of this kind when cooled through the reversion temperature  $725^{\circ}\text{C}$ . at the rate necessary to cause reversion of the austenite to lamellar pearlite. The white areas are the alpha-iron blocks. The structure is described as a groundwork of the eutectoid in which is embedded alpha-iron blocks. The boundaries of the blocks are not brought out because the etching of the test piece was specially directed to bring out the pearlite.

**The Eutectoid Steel containing 0.9 per cent. of Carbon.**—The temperature at which solidification begins is  $1443^{\circ}\text{C}$ . and the process ends at  $1332^{\circ}\text{C}$ ., a range of  $111^{\circ}\text{C}$ . The austenite cools without change to  $725^{\circ}\text{C}$ . and then reverts to pearlite.

The inner structure is seen in Fig. 107, where the rate of cooling has been adjusted to produce lamellar pearlite. This steel, when heated, changes its pearlite to austenite when passing through  $725^{\circ}\text{C}$ . and then begins to melt at  $1332^{\circ}\text{C}$ . and finally becomes liquid at  $1443^{\circ}\text{C}$ .

**Steel containing 1.4 per cent. of Carbon.**—This begins to solidify at  $1420^{\circ}\text{C}$ . and is solid austenite at  $1220^{\circ}\text{C}$ . The solidifying range is therefore  $200^{\circ}\text{C}$ . The first formed and



FIG. 106.—0.57 Carbon Steel.  $\times 1066$ .



FIG. 107.—0.9 Carbon Steel.  $\times 533$ .



FIG. 108.—1.4 Carbon Steel. Deeply etched.  $\times 120$ .



FIG. 109.—1.4 Carbon Steel. Lightly etched.  $\times 400$ .



FIG. 110.  $\times$  533.

poorer austenite crystals, by diffusion from the later-formed richer crystals, will get slowly to the average composition. The cooling austenite begins to deposit crystals of cementite when the temperature has fallen to about  $950^{\circ}\text{C}$ ., and continues to do so until, at  $725^{\circ}\text{C}$ ., the strength of the austenite has been reduced to 13.5 per cent. cementite dissolved in solid solution, that is, 0.9 per cent. carbon. Cooling through this temperature, the austenite inverts to pearlite with cementite crystals formed into a sort of network marking out the boundaries of the pearlite blocks.

Such a structure is seen in Fig. 108, magnified 120 diameters. This photograph was taken from a sample of 1.4 carbon steel free from alloy elements and shows the structure resulting from slow cooling. It was deeply etched to bring out the boundaries. The dark blocks are laminated pearlite, as will be seen from Fig. 109, which shows the structure of the same sample lightly etched to bring out the detail, and magnified 400 diameters. The cementite veins are clearly seen running through the structure and defining the boundaries of blocks of pearlite.

Reheated, the laminated pearlite would fade into a saturated solution of 0.9 per cent. austenite when the temperature reached  $725^{\circ}\text{C}$ ., and then as the temperature rose the austenite would gradually absorb the cementite boundaries until at about  $950^{\circ}\text{C}$ . there would be only a solid solution of austenite containing 1.4 per cent. of carbon. Melting would begin at  $1200^{\circ}\text{C}$ . and would be complete at  $1420^{\circ}\text{C}$ .

**Pig Iron containing 3 per cent. Carbon. White Iron.**—Solidification begins at about  $1270^{\circ}\text{C}$ . and ends at  $1139^{\circ}\text{C}$ . Austenite, containing 1.2 per cent. of carbon, equal to 18 per cent. of cementite, begins to crystallize from the melt, and as explained above the austenite gets richer and richer as crystallization proceeds until it reaches the average composition 1.8 per cent. carbon, equal to 27 per cent. cementite.

When the melt has fallen to the temperature  $1139^{\circ}\text{C}$ . it contains therefore crystals of saturated austenite and a liquid mixture of saturated austenite and cementite such that the carbon content is 4.3, the eutectic proportion. Saturated austenite and cementite then solidify separately at constant temperature. The resulting structure is a groundwork of eutectic with saturated austenite crystals embedded in it. As this cools the austenite crystals deposit cementite until the strength is reduced at  $725^{\circ}\text{C}$ . to 0.9 per cent. carbon, and then, passing through this temperature, the austenite reverts to pearlite. An example of this "reverted austenite" is seen in the pearlite

peninsula, Fig. 114, facing page 114. The cementite in this structure is stable so that the iron was probably a high-sulphur, low-silicon iron.

**Grey Iron.**—If the iron had been high in silica and low in sulphur the cementite would have decomposed and the inner structure would show, at ordinary temperature, reverted primitive crystals of austenite and graphite. The dotted line in the diagram Fig. 105 shows the temperature corresponding to these conditions. An inner structure of this type is seen in Fig. 110, facing page 111. The groundwork of laminated pearlite, reverted austenite, shows black graphite areas distributed through it. The left side of the photograph shows a finer distribution than the right side.

**Pig Iron, 4.3 per cent. Carbon.**—This solidifies at  $1139^{\circ}\text{C}$ . into an eutectic structure of saturated austenite and cementite. The structure seen in the microscope is a laminated form of cementite, as if strands of macaroni had been folded backwards and forwards on themselves and dark austenite had been caught between the folds.

If less than 4.3 per cent. of carbon is contained in a pig, then the structure seen is the 4.3 per cent. eutectic containing crystal forms of primitive austenite which have reverted to pearlite. If more than 4.3 per cent. of carbon is in the pig, then the structure seen is the 4.3 per cent. eutectic, containing large plates of primary cementite crystals.



**Mottled Pig Iron.**—A blast furnace may produce pig iron which when broken across shows either a grey fracture, or a white fracture, or a fracture of mottled appearance in which grey iron appears as definite areas distributed evenly through white iron. This is known as mottled pig. There are many grades of grey iron, but all of them contain carbon mainly in the form of graphite. There are various grades of white iron, and these contain carbon mainly in the combined form as cementite. In the mottled pigs, therefore, the grey areas show structures typical of grey pig and the white areas show structures typical of white pig. The study of a section of mottled pig iron is therefore instructive in that it shows on one section types of several structures.

Typical chemical analyses of white iron, grey iron, and mottled pig iron are given in the following table taken from the Presidential Address of Dr. Stead at the British Association meeting at Sheffield.

	White Iron.	Grey Iron.	Mottled Pig Iron.	
			White Parts.	Grey Parts.
Combined carbon . .	2.98	Nil	3.88	0.98
Graphite . . . .	traces	2.65	0.45	3.68
Manganese . . . .	0.29	0.72	1.63	1.60
Silicon . . . . .	1.89	5.21	0.65	0.85
Sulphur . . . . .	0.27	0.03	} Not given	
Phosphorus . . . .	1.62	1.56		
			} 4.33	
			} 4.66	

Comparing the white with the grey, it will be noticed that the white iron is high in sulphur and low in silicon, the condition necessary to keep cementite stable; and the grey iron is high in silicon and low in sulphur. The analysis of mottled pig, published by Mr. Hogg of Newburn Steel Works and quoted by Dr. Stead, shows that the white areas contain the eutectic proportion of carbon. This part of the field would in the microscope show the eutectic structure. The grey part contains more than the eutectic proportion, so that the structure seen would be the eutectic groundwork of austenite and graphite with cementite crystals embedded in it.

The following microphotographs were taken from a sample broken off a pig which had just cooled and which showed a mottled fracture. It represents the product of a blast furnace at a Middlesborough ironworks.



## 114 STRENGTH AND STRUCTURE OF METALS

Fig. 111 shows the general structure seen under the moderate magnification of 28 diameters. The central part of the photograph looks like a group of black fir trees. These "dendritic" crystals are the primitive forms in which the austenite solidified. Each crystal fir tree began growth from a nucleus, shooting out branches as it grew so that at one period the cooling metal consisted of forests of growing crystals feeding on the liquid round them until the supply was exhausted. All the black areas seen are the forms of the primitive austenite crystals, and they correspond to the grey areas of the fracture. The white areas between them represent a structure mainly of cementite, as will be seen from Fig. 112, which shows the structure magnified 100 diameters. Now the white areas resolve into gleaming crystals of primitive cementite set in a shaded groundwork between the dark areas. Under the higher magnification of 400 diameters (Fig. 113) the full geometric beauty of this shaded groundwork is brought out. It is phosphorus-iron-carbon eutectic. The section of a large crystal of primitive cementite is seen sloping diagonally across the centre of the figure. The dark areas, the ghostly forms of primitive austenite crystals, resolve into pearlite under higher magnification.

The austenite reverts to this as the temperature falls through  $725^{\circ}\text{C}$ ., rejecting cementite, until the strength is reduced to 0.9 per cent. carbon. The pearlite mass (Fig. 114) shows the tip of a fir-tree crystal, a peninsula, which crystallized originally as a solid solution of austenite, and then, depositing cementite as the temperature fell, reverted to laminated pearlite as it passed through  $725^{\circ}\text{C}$ . The phosphorus-iron-carbon eutectic can be seen distributed in the cementite.

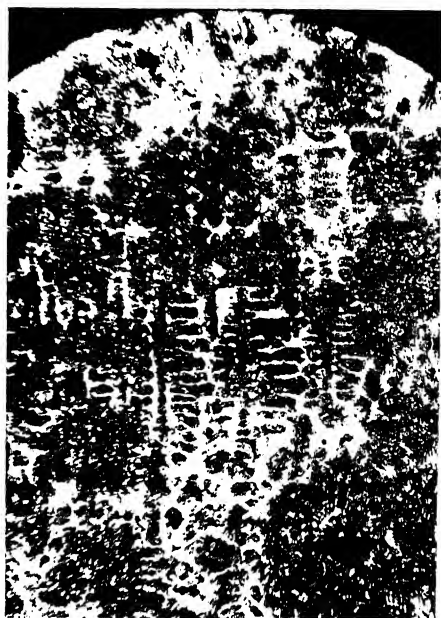


FIG. 111.

× 28.



FIG. 112.

× 100.

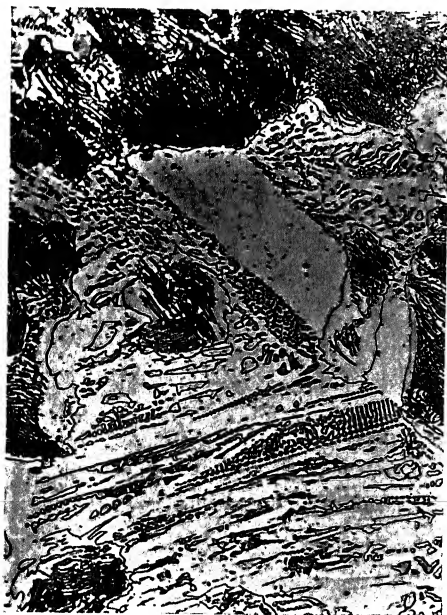


FIG. 113.

× 400.



FIG. 114.

× 533.



FIG. 115.

× 800.



FIG. 116.

× 533

Fig. 115 shows a dark area, a boulder, magnified 800 diameters. This shows the internal pearlite structure, and in the centre is seen a succession of the plates of which the pearlite is built, almost like a stairway. The section has caught the group of plates obliquely.

Fig. 116 shows a pearlite boulder set in a eutectic of reverted austenite and graphite. The dark areas in the right-hand top corner of the photograph are probably crystals of manganese sulphide.

These photographs show what a complex play of forces must operate between the atoms and molecules during the solidification and cooling of a piece of pig iron. It may be noticed that the pearlitic constituent seen is really an eutectoid steel embedded in other things. Steel-making may be regarded as a cleaning process. It cleans out the unwanted structures and aims at the 0.9 per cent. eutectoid, with ferrite embedded in it for mild steels, and cementite embedded in it for the harder steels.

A remarkable series of changes takes place in the solid before the metal is actually melted. Imagine that a piece of the metal can be placed in a crucible in circumstances which enable its inner structure to be projected as a picture on a screen, so that we can look at the picture during the process of heating and liquefaction. We should see one picture dissolve into another as the temperature increased, until finally we should look at the picture of a structureless liquid consisting of melted iron with carbon dissolved in it. If we could in reality look at such a series of pictures many questions of controversy might be settled, but the researches of Dr. Stead enable us to form a very good idea of the pictures we should see.

The first picture on the screen would be like Fig. 12, and this would remain until the temperature reached about  $725^{\circ}\text{C.}$ , when the pearlite would fade away. The sheets of cementite would, though solid, dissolve into sheets of solid iron and produce a homogeneous mixture of cementite and iron: the mixture called austenite. The geography of the picture would remain the same, but from this point onwards the cementite crystals (seen clearly in Fig. 13) round about the grey masses of austenite would in part be absorbed into them, because iron is able to dissolve increasing quantities of cementite as the temperature rises. At about  $953^{\circ}\text{C.}$ , the iron-phosphorus-carbon mixture (seen plainly in Fig. 13) would melt, and, the temperature rising, there would be pockets of liquid material distributed through the still solid mass of austenite and cementite crystals. At about  $1100^{\circ}\text{C.}$  the

## 116 STRENGTH AND STRUCTURE OF METALS

cementite crystals would melt and the austenite would begin to melt, and would go on melting with rising temperature until the mass was wholly liquid.

If now the temperature were allowed to fall again, the operations would take place in the reverse order. First crystals of the solution of iron and cementite would grow in the fir-tree form, and not until the temperature had fallen to about  $1100^{\circ}\text{C}$ . would the cementite begin to form crystals on its own account. The cooling mass would then appear as a conglomerate of fir-tree blocks or crystallites, the crystal elements of which are formed of a solution of cementite in iron, austenite and separate crystals of pure cementite, and these would by now be solid; but distributed through the solid mass would be liquid pockets of the iron-phosphorus-carbon mixture about to form the crystal net-like structure when the temperature has fallen to  $953^{\circ}\text{C}$ . The picture would now show a mass completely solid; but probably much change in the geography would be noticed as the mass cooled, because the cool structure exhibits the crushed and distorted remains of the fir-tree crystallites, and they appear to have been subject to great pressure during the cooling process.



FIG. 117.—1.46 Carbon Steel Quenched in Water from 1100° C.  $\times 120$ .

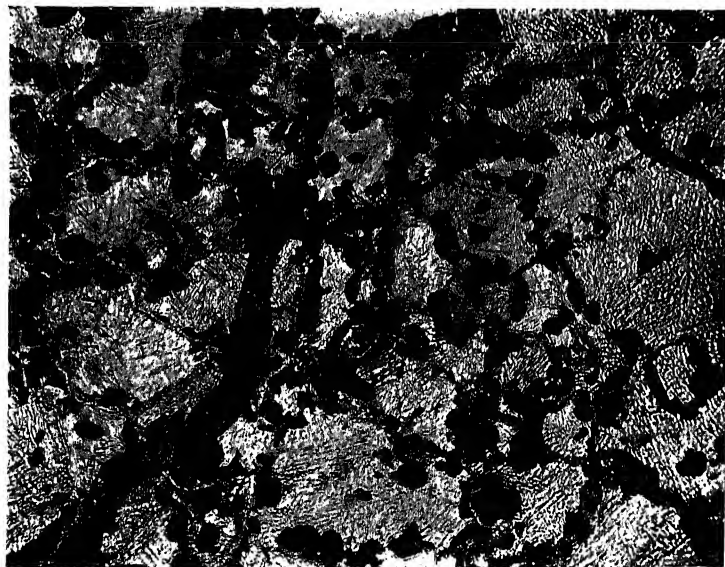


FIG. 118.—1.28 Carbon Steel. Quenched in Water from 1100° C.  $\times 120$ .

**60. The Rate of Cooling.**—The rate at which a hot piece of metal cools has a profound influence on its inner structure. As mentioned above, § 56, the structure corresponding to a high temperature is maintained, at any rate in part, by rapid cooling. It might be expected, therefore, that a mass of steel cooled with sufficient rapidity to prevent austenite reverting to pearlite would show an inner structure of austenite itself. When, however, steel is quenched from a temperature at which austenite exists, a structure is produced the blocks of which appear to be made up of bundles of needle-like fibres. This acicular structure is called martensite. Professor Carpenter holds the view that martensite is principally if not wholly austenite and that the acicular markings seen are due to the violent internal stresses set up by rapid quenching.

A piece of 1.46 carbon steel heated to about 1100° C. and then quenched in water is seen in Fig. 117. The needle-like fibres are clearly seen. Whatever be the actual mechanism of the change we can say that rapid quenching of austenite maintains the cementite in solid solution and produces a structure called martensite.

Variation of the slow rate of cooling required to produce laminated pearlite gives structures called sorbite and troostite. If austenite is cooled a little more rapidly than the rate which produces laminated pearlite, the cementite does not separate from the ferrite in thin sheets but in granules, and the structure seen is granulated pearlite, called sorbite. More rapid cooling is required to produce the structure called troostite.

Dark bands of troostite are seen in Fig. 118 marking out areas of martensite. The structure seen was produced in a sample of 1.28 carbon steel by fairly rapid cooling from a temperature of 1100° C. Troostite has the appearance of a carbon deposit. It may be that the steel is low in sulphur and high in silicon, so that the cementite is, in part at any rate, unstable. The formation of troostite is somewhat capricious. The same heat treatment on different carbon steels will produce troostite in some of them and not in others.

Control of the rate of cooling is a matter of experience, because a method suitable to a small piece of metal is often quite unsuitable for a large piece. The means adopted must have some relation to the size and even the shape of the piece.

A mass of metal cools in air at a definite rate, in oil at a quicker rate, and in water at a quicker rate still. When a mass is plunged into a liquid, either oil or water, at first evaporation of the liquid



takes place so that contact between liquid and metal is for a time prevented by a gaseous film of the liquid itself. Heat must then flow from the metal across a film of gas into the liquid and the rate of cooling is therefore determined mainly by the rate of transmission across this film.

The problem of producing a definite inner structure by the control of the rate of cooling is essentially a problem of heat transmission from the hot piece of metal to its surroundings. Moreover, the problem is complicated by the condition that it is not sufficient to get the heat out of the mass at a definite average rate; the rate of cooling through the mass of the metal must be uniform in order to produce a uniform structure. Industrial processes involving the control of the rate of cooling are necessarily therefore based on experience. The equilibrium diagram, however, gives useful information about the temperature to cool from, or the temperature to heat to, in various processes, and a few notes on the kind of assistance possible may be useful.

**61. Heat Treatment.**—The heat treatment of steel is an art, but the temperature-concentration diagram gives considerable guidance in its practice.

The most familiar process of heat treatment is the hardening of a cutting tool. The tool is first heated to a bright red and is then quenched in water. The metal is then glass-hard and too brittle to use. The tool is tempered by heating it to a temperature considerably lower than red heat, and then it is quenched from this temperature. Interpreting this process in terms of the temperature-concentration diagram, the tool is first heated to a temperature at which its inner structure dissolves into austenite, and then this austenite is maintained in the form of martensite by sudden quenching.

The inner state is one of great stress and the metal is hard and brittle. The higher the temperature from which quenching is done, the greater the internal stress which results from sudden quenching. The tool should therefore be heated only to the lowest temperature at which austenite is formed. This temperature can be found from the diagram when the carbon content of the steel is known. For example, if the tool steel contains 1.25 per cent. carbon the equilibrium temperature at which austenite forms is about 900° C. The material should not be heated much above this temperature, say to 950° C. For 0.9 per cent. carbon the temperature might be 750°, and for 1.5 per cent. carbon it must be over 1000° C. to secure conversion to austenite. These wide variations in hardening temperatures between 0.9



per cent. carbon steel, shear steel, and 1.5 per cent. carbon, show what useful guidance can be given by the diagram.

In the tempering process the tool must not be heated above the temperature at which inversion takes place, namely  $725^{\circ}\text{C}$ . As the material is warmed the stresses in the martensite are relieved and the structure passes through some transition forms until at  $725^{\circ}\text{C}$ . it passes into lamellar pearlite if the conditions are suitable.

Metallurgists distinguish two of these transition structures as troostite and sorbite. Between  $200^{\circ}\text{C}$ . and  $400^{\circ}\text{C}$ . the martensite transforms into troostite. It is a matter of workshop experience that tool steel cooled from this temperature after quenching is suitably tempered to cut the harder metals like gun metal. The inference is that a hard cutting tool consists of troostite. Between  $400^{\circ}\text{C}$ . and  $600^{\circ}\text{C}$ . the troostite transforms into sorbite. Cooled from this temperature, the tool is suitably tempered for cutting iron and mild steel. The inference is that this less hard cutting tool is built mainly of sorbite. If cooled from temperatures above  $600^{\circ}$  and  $725^{\circ}$  it is too soft to cut.

This process involves first the production of martensite and a state of great internal stress and a subsequent annealing of this stress and the formation of a definite structure. The formation of this structure can be done by a single properly regulated cooling process. Troostite, for example, could be formed by slowly cooling from the high temperature until a temperature between  $400^{\circ}\text{C}$ . and  $200^{\circ}\text{C}$ . was established, and then quenching out from this temperature. This single process is not so easily managed as the ancient double process, but its great advantage is that the necessary cutting temper is obtained without first subjecting the tool to a state of inner stress, stress which may easily crack some tools like milling cutters and tools of complicated shape.

Methods of cooling by oils and salts have for their object a definite regulation of the rate of cooling and therefore a definite control on the inner structure into which the crystals build themselves.

The temperatures obtained from the diagram relate only to straight carbon steels. The transformation of austenite to pearlite is delayed if not altogether prevented by the introduction of alloys. Alloy steels all contain carbon, in fact it is the carbon which gives them the properties of steel. The alloy added seems to influence the crystallization so that harder structures are kept in being. The temperatures of the arrests are altered and must

be separately determined for a given steel from cooling and heating curves.

An interesting example of the effect of an alloy may be quoted from a valuable paper by Dr. W. H. Hatfield entitled "Cutlery: Stainless and Otherwise." On the left of Fig. 119 are seen the cooling and heating curves of a sample of 0.9 carbon steel. The arrests are fairly close together and have a mean value of about 725 degrees. Heating and cooling curves of a sample of stainless steel are seen on the right of the figure. The arrest is at 380° C., but the arrest during heating, that is the

inversion point where the austenite solid solution is formed is considerably above 800° C. The composition of the stainless steel is —

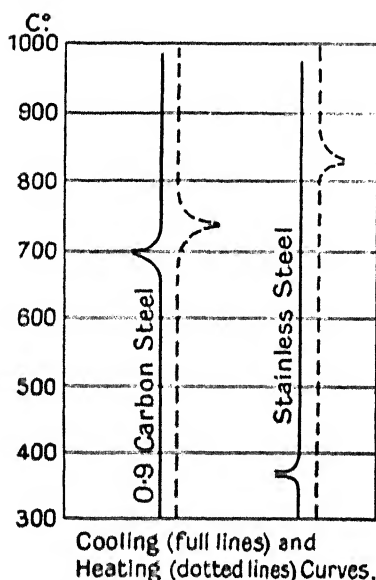


FIG. 119.

	Per cent.
Carbon . . . . .	0.30
Manganese . . . . .	0.30
Silicon . . . . .	0.12
Sulphur . . . . .	0.02
Phosphorus . . . . .	0.02
Chromium . . . . .	13.00

Chromium acts to delay the inversion processes, and at the same time confers on the steel the valuable property of stainlessness.

From the curves it will be seen that, allowing say 45° above the arrest temperature, the temperature to which the 0.9 per cent.

shear steel should be heated before quenching is about 770° C., whilst the hardening temperature for the stainless steel should not be lower than 870° C. Dr. Hatfield recommends 950° C. to 1000° C. as the limits between which it is desirable to heat stainless steel before quenching in order to secure the reversion of the structure to austenite. The tempering operation for stainless steel is 5 minutes immersion in an oil bath at 180° C.

Annealing processes are also usefully interpreted by the diagram. When steel has been transformed to austenite by heating to a temperature about 50° C. above the temperature defined by the line JKE, Fig. 105, and is then cooled to the ordinary temperature, the blocks are small whatever may

have been the general sizes of the blocks in the inner structure before heating. The process refines the structure. This process, by refining the structure, increases the strength.

If the temperature defined by the line JKE is too much exceeded the austenite blocks increase in size and the subsequent cooling does not produce the refined structure.

Attention must be given to the rate of cooling. Too slow a rate results in a coarse structure and the mechanical properties corresponding to the refined structure are lost. Steel raised to a temperature above the line AC begins to liquefy. It is then called burnt steel. Burnt steel cannot be restored to a normal state by any annealing process. It must be remelted.

Tool steels, with carbon content between 0.9 and 1.5 per cent., can be relieved of internal strain and can be softened by heating and slow cooling from temperatures somewhat below the inversion temperature. To refine the structure it may be necessary to heat it sufficiently to dissolve the structure into austenite and then to cool quickly. This produces martensite and keeps the cementite in solution. Then heat for a time to 750° C. just above the inversion point.

This refines the steel, but does not precipitate the cementite out of solution, as the steel is not heated for too long a period. If the cementite is precipitated from the solution as spines or as a network it is hard to machine.

## CHAPTER V

### THE ELASTIC AND THE PLASTIC STATES OF METALS

**62. General Properties.**—Each load-extension diagram shown in Chapter II records the history of a stretch from no-load to fracture. The microphotographs shown with them illustrate the inner structure of the metal before the stretching commenced. During the process of stretching the metal passes from a state in which stretch is proportional to the load into a state in which stretch increases more rapidly than the load. It may be said to pass from a state of perfect elasticity into a state of imperfect elasticity. In this section it is proposed to consider the elastic state and the imperfectly elastic state into which the metal is transformed by stretching.

The term **elasticity** means in a general sense the power of a metal to recover its primitive form after loading has been applied and removed. The recovery may be partial or complete. The power of complete recovery is lost when loading has once been applied above a certain limiting value peculiar to the material. Below this limiting value stretch is proportional to load. Above this limiting value stretch increases at a greater rate than the load. The stress at the limit is called the limit of proportionality. The limit of proportionality is not sharply defined. The metal merges gradually from a state of proportional stretch into a state of unproportional stretch.

No metal is, however, quite perfect in its recovery, but the term perfect, used in the sense defined above, is convenient and substantially expresses the experimental results.

The investigation of elastic property requires a high multiplication of the extension. Consequently in the "elastic recorder" which I have designed and constructed the extension is multiplied 150 times.

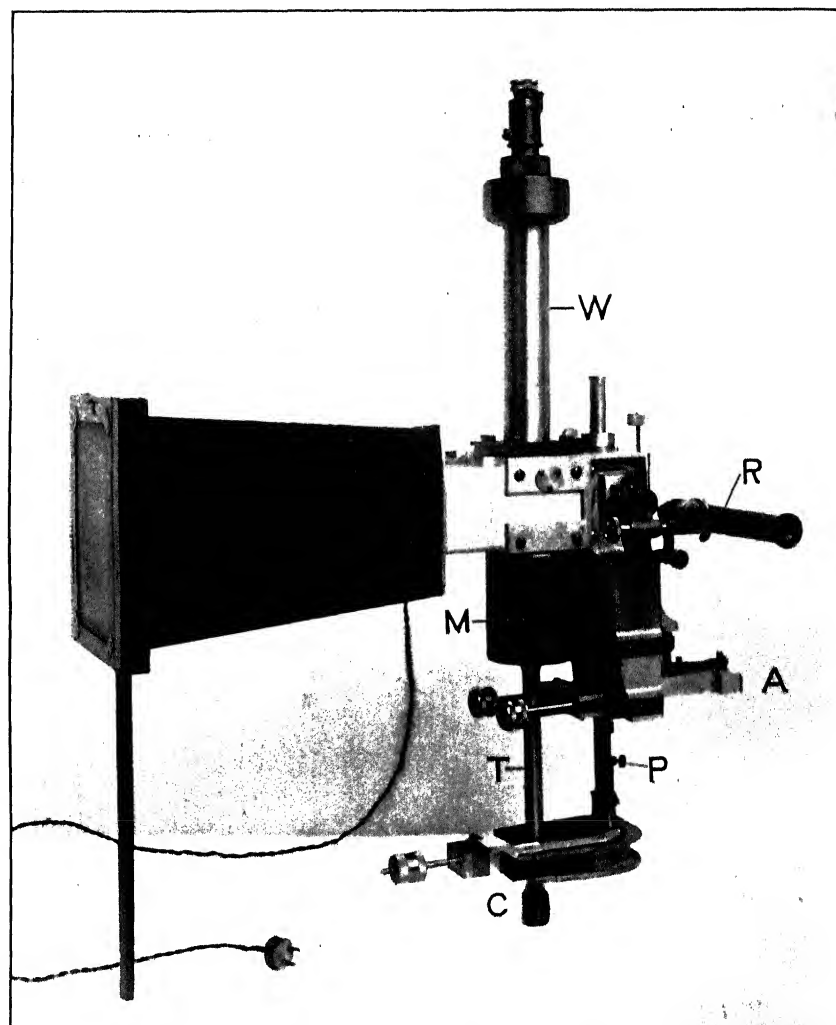


FIG. 120.—The Dalby Optical Recorder of Load and Elastic Extension.

**63. The Dalby Optical Recorder of Load and Elastic Extension.**—The recorder is shown in Fig. 120. The weigh bar *W* is coupled to the test piece *T* by the muff-coupling *M*, and the camera and light source are combined with them just as described above in section 19, Chapter I. There are slight differences in the optical arrangements inside the weigh bar, but the main difference is in the extensometer. The pivoted arms of the "breaking recorder" are replaced by arms balanced on knife-edges, and there is a difference in the arrangement of the levers and poles. A lower lever *C*, carried in a horseshoe support, transmits the downward motion of the lower flange of the test piece upward, through the adjustable pole *P*, to a floating link lying under and jointed with the upper lever *A*. The centre of the floating lever transmits the motion upward to the horizontal arm of a bell crank, not seen in the figure, and the vertical arm of the bell crank transmits the motion to the optical system within the bar. The chain of levers and poles is seen in the figure *in situ* and ready for an experiment.

A microscope *R* is added to the instrument so that the process of extension can be watched. It is focused on an index attached to one of the moving links, and the movement of this index is watched against a micrometer scale within the eyepiece, so that the stretch can be observed from the commencement through the range of the spot down the plate, which corresponds to a stretch of about  $\frac{1}{100}$  of an inch.

When the index is seen to move over the eyepiece scale from 0 to 1 the spot of light has moved vertically  $1\frac{1}{2}$  inch down the plate and the gauge length of the test piece has stretched approximately  $\frac{1}{100}$  of an inch. When used in the hydraulic machine described in section 24 the water power may be regulated to control the speed at which the index moves across the scale. If the power is shut off the index stops dead. When the load is removed the index moves back and stops at a point on the scale corresponding to no load.

If the load has not exceeded the limit of proportionality the index will move back to the primitive zero. If the load has exceeded the limit of proportionality the index will come back to a new zero. The distance between the primitive zero and the new zero represents to some scale the permanent set of the material. The control valves fitted to the machine enable the loading to be stopped, to be removed, and to be reapplied as may be desired. The operator works the valves in obedience to the movement of the index seen in the eyepiece of the microscope, which he watches all the time.

The apparatus is easily and quickly operated. A complete diagram showing not only the elastic line, but the effect of several removals and reapplications of the load, can be taken in a few minutes. The work of hours by apparatus hitherto available is done by the recorder in a few minutes.

**64. Typical Looped Diagram.**—A diagram taken with the elastic recorder is shown in Fig. 121. The spot of light, starting from the origin O, traced a straight line up to the point A, and then curved away to the yield at B.

The point A marks the limit of proportionality. The point B marks the yield.

The spot continued along its path after yield to C. At C the

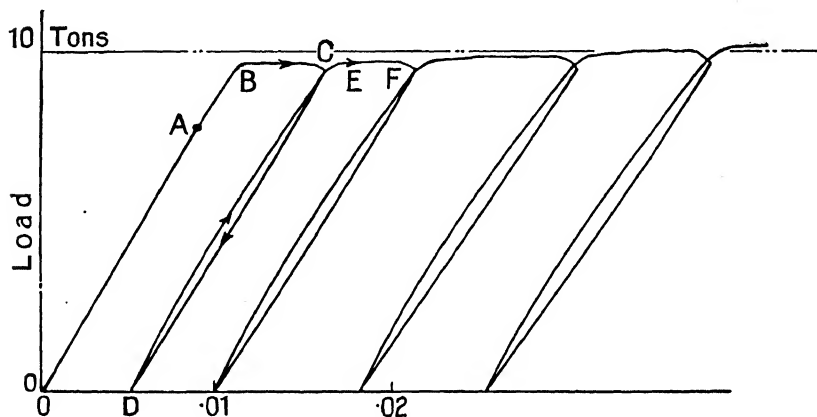


FIG. 121.—Nickel Steel.  
0.33 per cent. C., 3.68 per cent. Ni.

power valve was closed and the exhaust valve was opened slightly. The load leaked off and the spot descended along the curved path from C to D. The spot stopped dead at D when the piece was free from load. The power valve was then opened gradually and the spot moved upwards along the curved path from D to C, where yield occurred again, and then the spot continued along the approximately constant load-path to F. Another loop was described, and a third and a fourth, before the range of the plate was exhausted.

Comparing the lines OA and DC, both described from no load, it will be seen that the metal is in two different states. The path from O to A is practically straight. The stretch is proportional to the load. If the load is removed whilst the spot is travelling up this path the spot will travel down its own upward track and

come to rest at O. It recovers its primitive form after the load is removed. Its elasticity is perfect.

But starting from D, the path is curved. The stretch increases at a greater rate than the load. If the load is removed the spot no longer travels down its own tracks, but strikes out a new path. It does not recover its form at D after the load is removed.

This point may be illustrated immediately by means of Fig. 122. In this record the test-piece, in an overstrained and therefore in the imperfect elastic state, was stretched to C, and then the load was removed and reapplied, but loading was stopped when the piece stretched again to C. This was seen in the microscope. The index was allowed to move up to a definite

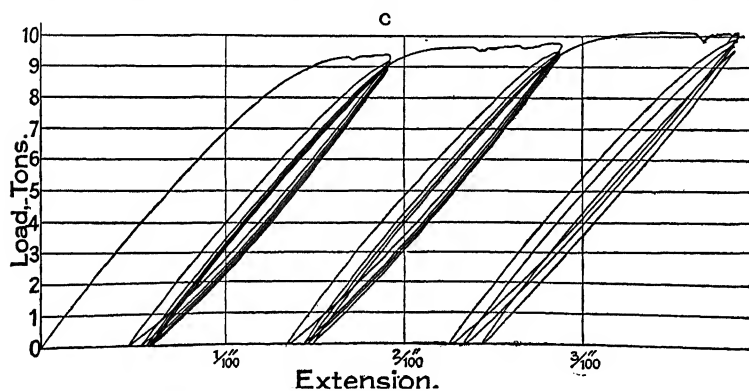


FIG. 122.

line on the scale and then the power was shut off and the load removed. The process was repeated several times.

Each time the loop described was smaller. There was a slightly increasing permanent set.

The diagrams bring out the difference between the two elastic states, namely, the state in which the metal exists before it has been loaded beyond its limit of proportionality and the state produced by the overloading.

But the diagram, Fig. 121, illustrates something more. When the piece has been stretched to C, although the metal is described as in the plastic state, it is not plastic in the sense that putty is plastic, but still possesses elastic property, though in an imperfect way. For when the load is removed at C the test piece shrinks to the dimension OD. A glance at the diagram will show that the imperfect elastic shrink is roughly equal to the perfect elastic stretch. Or more accurately:—



## 126 STRENGTH AND STRUCTURE OF METALS

The proportionate elastic extension + the plastic extension after the limit of proportionality has been passed is about equal to the imperfect elastic shrink + the permanent set OD.

Measuring from the diagram, we have approximately :—

Proportionate elastic extension	=	0.009 inch.
Plastic stretch	=	0.007    "
Total	=	0.016    "

Also

Unproportionate elastic shrink	=	0.011 inch.
Permanent set	=	0.005    "
Total	=	0.016    "

The metal retains this imperfect elastic property right up to the

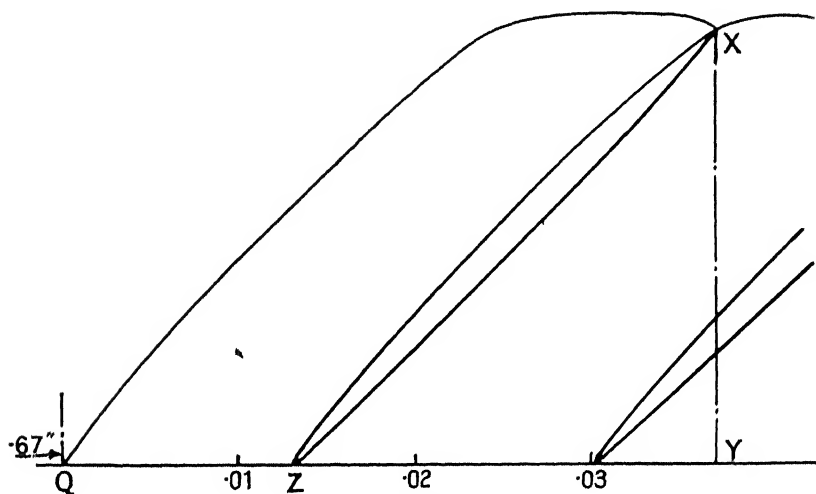


FIG. 123.—Nickel Steel.  
0.33 per cent C., 3.68 per cent Ni.

point where local contraction begins. This point is illustrated by Fig. 123, which is the last of a series of plates, of which Fig. 121 is the first. The piece had been stretched until its original gauge length of 5 inches had increased to 5.67 inches. The spot of light starting from Q (Fig. 123) described the curved path typical of overstrained material, and then at X stretching was stopped, and the loop drawn. A part of the last loop before local contraction set in is just seen on the diagram.

The imperfect elastic shrink YZ is 0.0244 inch and the permanent set QZ is 0.0127 inch.

The load scales are identical in the two diagrams.

65. **Information to be gained from a Looped Diagram of Material in its Normal State.**—To illustrate this, Fig. 124 shows a diagram of a piece of 0.8 carbon steel calibrated with its load scale. The elastic line and three complete loops were traced by the spot on the plate, and a loop within the second loop, and again a loop within the third loop, were traced by the partial removal and reapplication of the load.

The extension scale of the original diagram is  $1\frac{1}{2}$  inch =  $\frac{1}{100}$  inch extension of the gauge length.

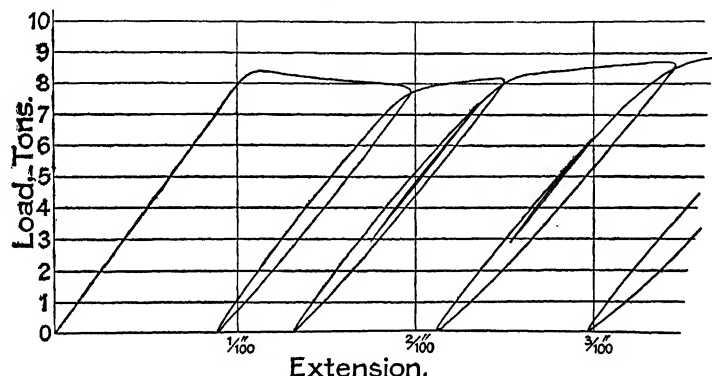


FIG. 124. Carbon Steel.

#### DATA MEASURED FROM THE DIAGRAM

Limit of proportionality . . . . .	about 7 tons.
Yield . . . . .	8.44 tons.
Area of first loop . . . . .	0.22 square inch.
Area of second loop . . . . .	0.26     "     "
Area of third loop . . . . .	0.42     "     "

In this instrument 1 square inch of loop area represents 5 foot-pounds. A load of 7 tons produces an extension of the gauge length of 0.00865 inch.

#### DATA MEASURED FROM THE TEST PIECE

Diameter . . . . .	0.6255 inch.
Area . . . . .	0.307 square inch.
Gauge length . . . . .	5 inches.
Volume of gauge length . . . . .	1.535 cubic inches.

#### DEDUCED RESULTS

Stress at the limit of proportion-	
ality . . . . .	22.8 tons per square inch.
Stress at yield . . . . .	27.5     "     "     "     "

Since a stress of  $7/0.307$  tons per square inch produces an extension of  $0.00865/5 = 0.00173$  inch per inch of gauge length, the modulus of elasticity,  $E$ , is in round numbers 13,200 tons per square inch.

Work done in elastic hysteresis during the description of the first loop  $= 0.22 \times 5 = 1.1$  foot-pounds.

This may be reduced for comparison to work done per cubic inch of gauge length, which is 0.70 foot-pound.

The results of the calculations may be arranged in tabular form thus:—

	Foot-pounds of Work Done per cubic inch of Gauge Length.
First loop . . . . .	0.70
Second loop . . . . .	0.85
Third loop . . . . .	1.37

This material has an ultimate strength of about 57 tons per square inch with a reduction of area at fracture of about 30 per cent. and an extension of 15 per cent. on the primitive gauge length of 5 inches. The stress at fracture was 74 tons per square inch. These data are obtained from a record taken with another instrument, the instrument seen in Fig. 11.

It requires many plates to exhaust the extension of a piece when only a few hundredths of an inch can be shown on each plate, but, as will be seen below, this has been done for a few materials, so that the further consideration of these loops will be for the moment deferred.

The shape of the loop, its area, and rate of increase are severally characteristic of a material. The next step in the enquiry is therefore to pass in review the looped diagrams taken from different kinds of material.

**66. Looped Diagrams of Various Metals.**—Records from various metals are reproduced in the following series of diagrams. The load scale is varied so that the diagrams from the weaker metals may be seen on a suitably large scale. The extension scale on all the diagrams was originally,  $1\frac{1}{2}$  inches measured horizontally on the diagram represented an extension of  $\frac{1}{100}$  of an inch of the gauge length.

**Yorkshire Iron (Fig. 125).**—The limit of proportionality occurs at 2.5 tons (8.1 tons per square inch) and the yield at 4.2 tons (13.7 tons per square inch). There is a slight drop at yield,

and then the load goes on increasing to its maximum value, which for this material is between 21 and 22 tons per square inch. The

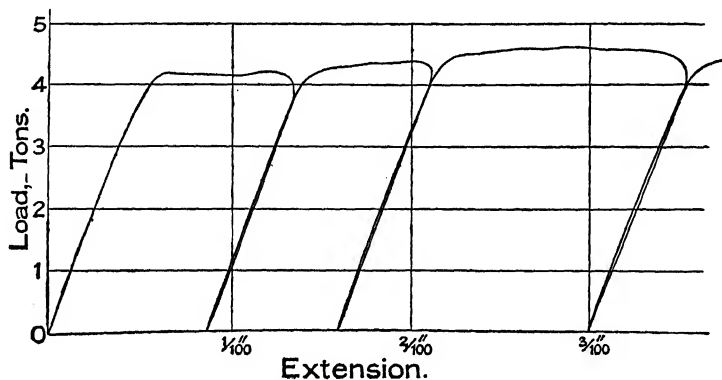


FIG. 125.—Yorkshire Iron.

area of each of the first two loops is small. This small loop area is characteristic of good-quality iron.

**Staffordshire Iron** (Fig. 126).—The limit of proportionality

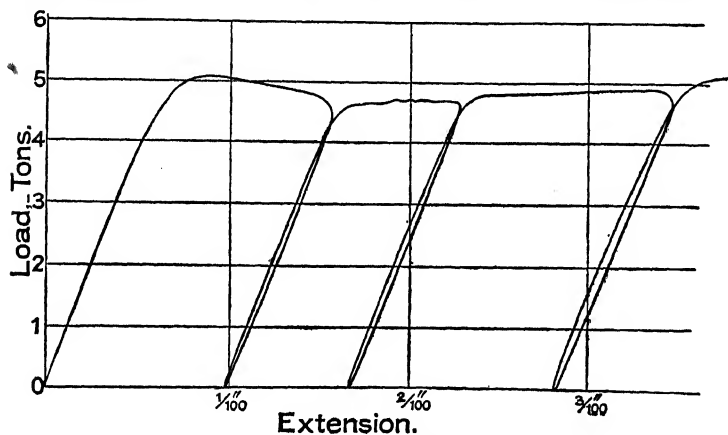


FIG. 126.—Staffordshire Iron.

is reached at about  $3\frac{1}{2}$  tons (11.4 tons per square inch), and the yield at 5.1 tons (16.6 tons per square inch). The load then drops to about 4.7 tons. The loop area is distinctly larger than in Yorkshire iron. This means that the hysteresis loss caused by the removal and the reapplication of the load is greater than in Yorkshire iron.

**Carbon Steel : Carbon 0.8 per cent.**—Fig. 124 above shows the diagram from a piece of this steel of normal quality. A

subsequent delivery of the same steel was expected to give a diagram of the same type, but the record actually obtained is seen in Fig. 127. The limit of proportionality is reached in this material at 3 tons (10 tons per square inch instead of 22.8 found

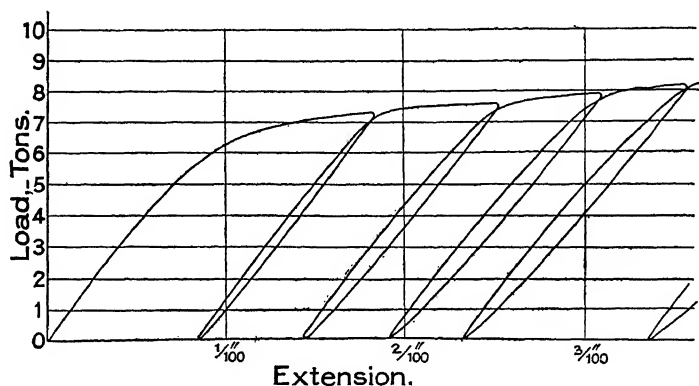


FIG. 127.—Carbon Steel.

in steel of the normal quality) and there is no definite yield-point. Clearly the diagrams establish the fact of a grave difference in quality of metal nominally the same. Between the two deliveries there must have been some change in the manufacturing process.

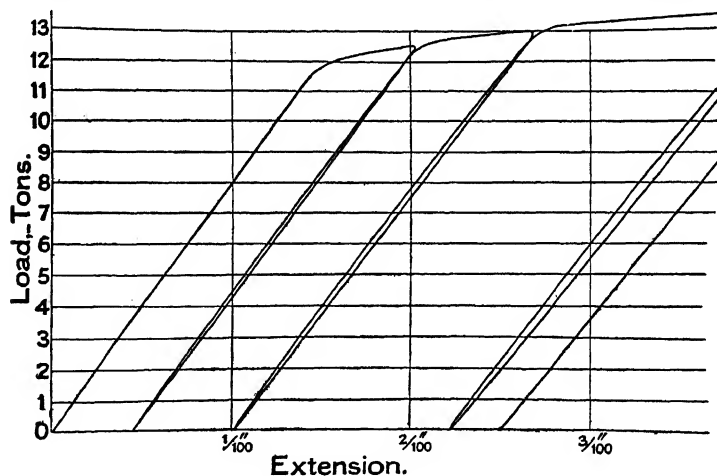


FIG. 128.—Nickel-chrome Steel.

**Nickel Chrome Steel (Fig. 128).**—The yield is gradual and the loop area is small, but the rate of increase of loop area is rapid. The ultimate strength of this material found (from a test piece 1 inch diameter) is 54 tons per square inch with an exten-

sion of 14 per cent. on 8 inches and a reduction of area of 55 per cent. The limit of proportionality occurs at a load of 10 tons (32.5 tons per square inch), and yield sets in at 11 tons (36 tons per square inch).

**Nickel Steel.**—The ultimate strength of this material is about 48 tons per square inch with an elongation of 20 per cent. on 5 inches and a contraction of area of 47 per cent. The limit of proportionality is at 30 tons per square inch and yield at 32 tons per square inch. Fig. 121 above shows a looped diagram of this material.

**Zinc (Fig. 129).**—Diameter of test piece, 0.8 inch. Gauge

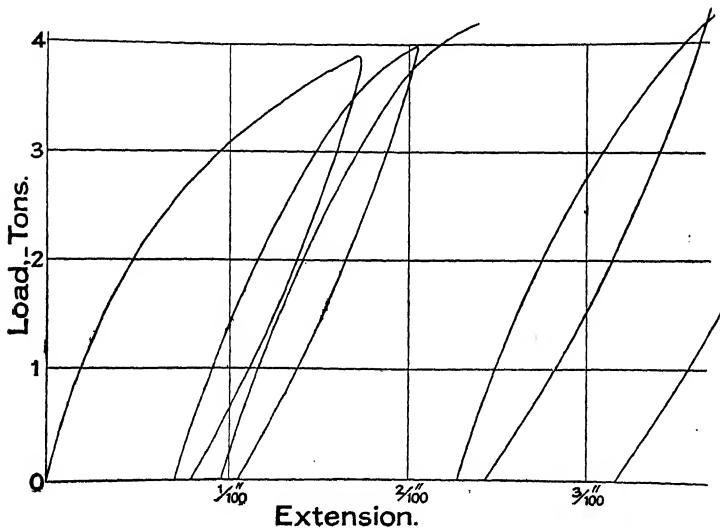


FIG. 129.—Zinc.

length, 5 inches. The material was cut from a zinc rod. The line curves away from the origin, and there is no limit of proportionality. The loops are large and show relatively great hysteresis loss. The material continues shrinking after the load has been removed. This is shown by the flat base of each loop. It is shrinking under the action of its own molecular forces because it is entirely free from external load. Immediately after the removal of the load the shrinking continues at a rapid but decreasing rate. In 1 minute the rate has become almost imperceptible. In  $1\frac{1}{2}$  minutes shrinking stops. The material has found internal equilibrium.

**Tin** (Fig. 130). Diameter of test piece, 0.8 inch. Gauge length, 5 inches. The material was cut from a tin rod. The diagram is like the diagram for zinc, but on a smaller scale. It is

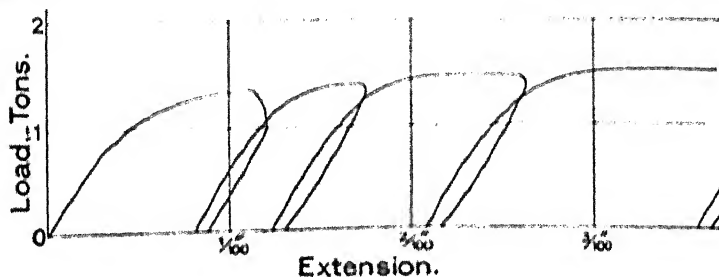


FIG. 130. Tin.

a weaker material. It shrinks, as seen in the diagram, after the load has been entirely removed.

**Copper : Pure and Free from Arsenic** (Fig. 131).—Dia-

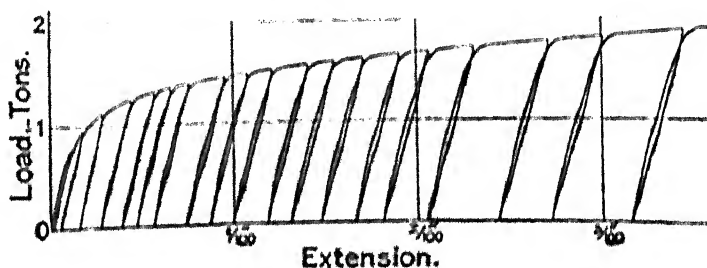


FIG. 131.—Pure Copper.

meter of test piece, 0.8 inch. Gauge length, 5 inches. There is no distinguishable limit of proportionality. The loop area is small and the rate of increase is small. This is a general characteristic of all the copper samples which I have tested. The small hysteresis loss appears to be identified with the quality of toughness.

**Copper : Arsenical** (Fig. 132).—Diameter of test piece, 0.8 inch. Gauge length, 5 inches. The effect of the arsenic is remarkable. It seems to give to the copper an elastic line with a limit of proportionality at about 1.4 tons (2.8 tons per square inch). There is no sudden yield. The loop area is small, and the rate of increase small. The load was removed and reapplied three times before increasing the load beyond 1.1 tons. The spot returned each time accurately in its own tracks, showing that the

limit of proportionality had not been reached. Comparing this with the previous diagram, it will be seen that with pure copper

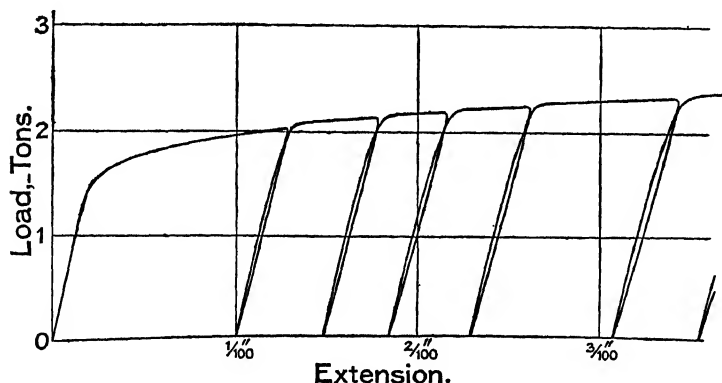


FIG. 132.—Arsenical Copper.

looping begins when the load is removed and reapplied from even a small value.

**Brass (Fig. 133).**—Test piece of normal dimensions. The

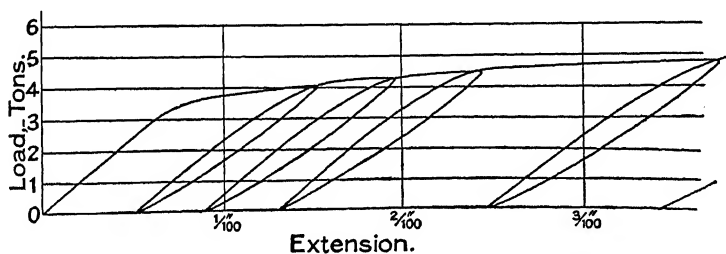


FIG. 133.—Brass.

material was cut from a brass rod. The composition was found to be about 60 per cent. copper and 40 per cent. zinc, with small traces of iron and lead. There is a definite limit of proportionality at  $2\frac{1}{4}$  tons (7.33 tons per square inch), and yield continues gradually to the maximum load. The loop area is relatively large. There is no shrinking at no-load, although the material contains such a large proportion of zinc. The ultimate strength of this material is about 33 tons per square inch.



**Phosphor Bronze** (Fig. 134).—Test piece of normal dimensions. The curve in this diagram shows a limit of proportionality at about 2 tons (6.5 tons per square inch), although it is difficult to locate the point exactly because the yield begins so imperceptibly and continues so gradually. The loop area is small and the rate of increase definite.

Examined under a larger scale, it is doubtful if any true limit

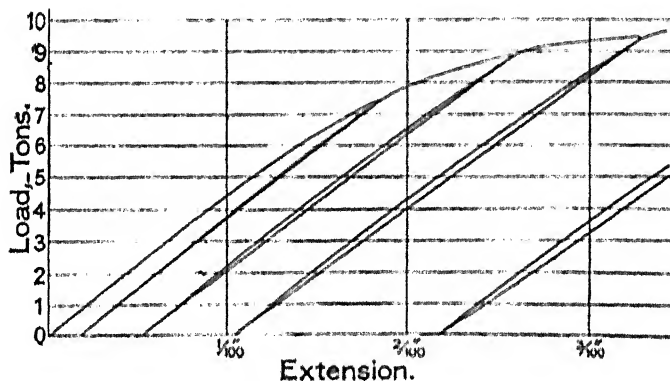


FIG. 134.—Phosphor Bronze.

of proportionality would be found. Strictly, the modulus of elasticity of alloys can only be defined as the slope of the tangent to the curve at the origin.

**67. Loop Area and Permanent Set.**—As mentioned above, it requires many plates to exhaust the extension of a normal test piece when only about  $\frac{1}{100}$  of an inch can be shown on one plate. The experiments have however been made for a few materials, including 0.8 carbon steel, nickel steel, mild steel and iron. The experiment is stopped when local contraction sets in.

The result of such an experiment is seen in Fig. 135. The material is 0.8 carbon steel. The capital letters along the procession of loops in Fig. 135 refer to the sequence of negatives. The usual time interval between successive plates is the time required to change the plate in the camera. A scale is placed under the loops so that the permanent set of the primitive 5-inch gauge length can be read off at any point in the procession of loops. For example, the permanent set at the end of looping operation recorded on the sequence of plates ABCD is the distance  $O_k$  — 0.137 inch.

Selected loops from the procession are shown in Figs. 136 to 139. The elastic line and the first and second loops are seen in

Fig. 136. The area of the first loop represents an energy loss of 0.42 foot-pounds; of the second loop, 1.15 foot-pounds.

After taking plate F the experiment was stopped. The test piece was removed from the machine and was laid aside. After six days rest it was put back, and the stretching was continued. The first line after the rest is seen in plate G, Fig. 138. There is no elastic recovery. The inner state of the metal is as it was. Fig. 139 shows the last plate of the procession. The gauge length had stretched about 0.8 inch, and the experiment was stopped because there were signs that fracture was imminent.

**68. Curves of Loop Area and Permanent Set.**—It will be noticed in Fig. 135 that the loop area increases with the stretch at first rapidly, and then at a slower rate.

In Fig. 140 the area of each loop in the procession is plotted vertically against the corresponding permanent set. A capital letter identifies the first loop area on the plate corresponding to the letter. For example, the point close to D shows that the area of the first loop on plate D is 0.92 square inch, and that the corresponding permanent set is 0.105 inch.

The dotted curves are drawn through the ends of the ordinates, giving the loop areas on the plate identified by the capital letter near its first loop. These dotted curves do not run into one another to form a continuous curve. There is some process going on within the metal which, in the short time required to change the plates, results in the first loop on the new plate being slightly smaller in area than the last loop recorded on the preceding plate. Whatever the process may be it soon exhausts itself, as will be understood from a consideration of the place in the diagram occupied by the group of areas measured on plate G. Although there was an interval of six days between the taking of plate F and G, the group of areas recorded on plate G have not lost their place in the diagram. They range with the others.

Curve No. 1 is drawn through the upper ends of the dotted curves and towards the end through the average position of the dots. This curve brings out the trend of the loop areas and in fact establishes :—

- 1, that there is a general rate of increase of loop area peculiar to the material;
- 2, that the loop area tends to a maximum value as stretching proceeds.

A scrutiny of the loops of the diagrams Fig. 125 to 134 shows that the rate of increase of loop area differs considerably in different materials.

Curve 1 (Fig. 140) adds the additional information, that loop

area may be expected to tend to a maximum value. This value for the 0.8 steel of curve 1 is 7.51 foot-pounds per loop per cubic inch of the material in the primitive gauge length.

**Nickel Steel.** Curve 2 shows the results of a series of experiments on nickel steel. The general rate of increase of area differs and the maximum value of the loop area is smaller. Its value is 2.9 foot-pounds per cubic inch of material in the primitive gauge length.

**Mild Steel containing 0.15 Carbon.** The sequence of plates A, B, C, D, E, F, was taken in twenty-three minutes. After taking F, the experiment was stopped and resumed in fifteen days time. The sequence was then plates G, H, I, J, K, and then a stretch to 5.83 inches; plates L and M, and then a stretch to 6.12 inches; finally plate N.

It will be seen from Curve 3 that after fifteen days rest the loop area has vanished. The material left in the imperfectly elastic state has been transformed into the perfectly elastic state by mere lapse of time. The spot moved away from the origin in a straight line, and to all appearances the material of the test piece was fresh, and had never been strained beyond its elastic limit.

But the rapid increase of loop area to the normal area on plate K revealed that the material had been previously over-strained.

The rate of increase of loop area is thus able to give valuable information of the previous history of the steel, provided a normal curve of **loop area and permanent set** is available for comparison. The maximum loop area of this material is 1.9 foot-pounds per cubic inch of material in the primitive gauge length.

The results of experiments on iron are plotted in curves 4 and 5.\*

**69. Influence of Time.**—When a metal has been overstrained its power of recovering its original form is lost. After the load is removed it returns partly towards its primitive form, but stops short of it by the permanent set.

It is found that metals differ remarkably in this respect. If the metal is iron or mild steel, proportional elasticity is slowly recovered with lapse of time and the recovery is accelerated by boiling. This is exemplified by Curve 3, which shows that a piece of mild steel, overstrained, and then left to itself for fifteen days, was found to be perfectly elastic when testing was recommenced. This property of irons and mild steels is however well known and was established by Sir Alfred Ewing. See *Phil. Trans.*, 1899.

In a paper by the author† it is shown that this slow

\* "Researches on the Elastic Properties and the Plastic Extension of Metals," *Phil. Trans.*, Series A, Vol. 221, pp. 117-138.

† *Phil. Trans.*, Series A, Vol. 221, 1920.

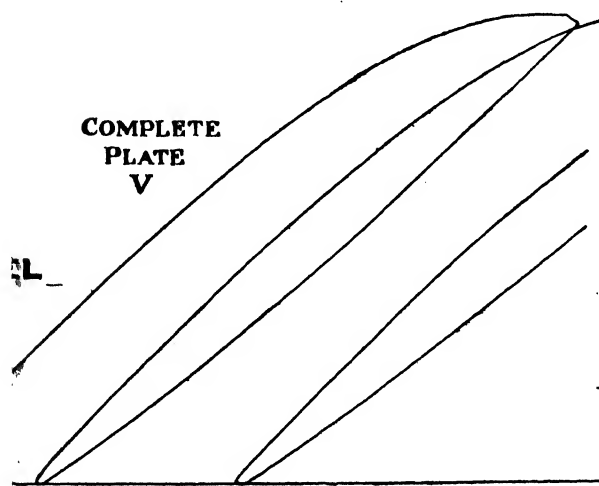
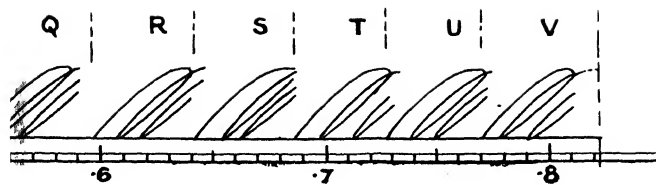
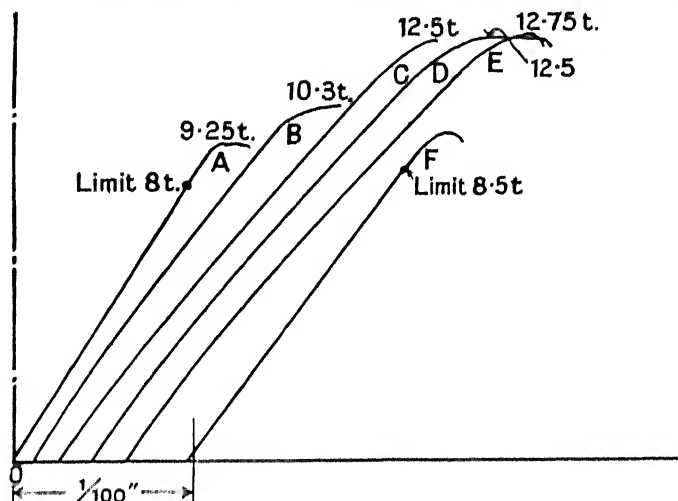


FIG. 139.

*To face p. 136.*

recovery by lapse of time or by moderate heating is by no means true for all materials. The diagrams, Fig. 137 and 138, illustrate this point. They show that a lapse of time of six days had negligible influence on the overstrained state of a piece of 0.8 carbon steel. It was left imperfectly elastic after a test and it remained in that state until testing was resumed six days later. A time-interval of six days may not seem sufficient to test the point, but other tests with an interval of rest of about a year confirm the result.

Nickel steel fails to recover its elasticity by lapse of time or by moderate heating. Details of one experiment with a 3.6 nickel steel containing 0.33 per cent. of carbon are recorded in Fig. 141. The first pull on a normal test piece of this material



		Limit.	Yield.
		Tons/sq. in.	
July 4, 1918	1st Pull E. 13,500 6.01 tons = 10.58 t./sq. inch } stretch a G.L. of 5 inch 0.00724 in.	26	30.01
" "	2nd Pull, after 2 per cent. stretch		
" "	3rd Pull, after 6 per cent. stretch		
July 5, 1918	4th Pull, after 6.01 per cent. stretch		
July 10, 1918	5th Pull, after 6.2 per cent. stretch and boiling 1 hour in water		
July 11, 1918	6th Pull, after 7 per cent. stretch, and annealing at 550° C. E 13,500	30.5	33.6

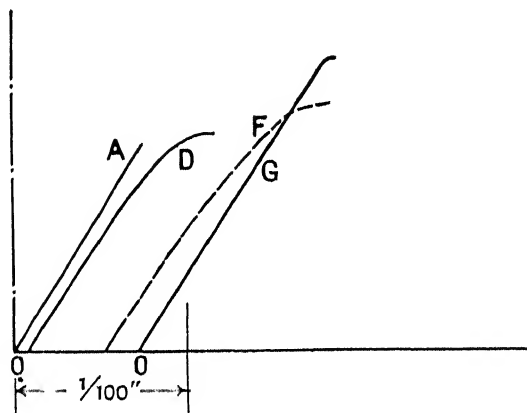
Fig. 141.—Nickel Steel, 0.33 per cent. C, 3.68 per cent. Ni.  
Gauge Length 5 inch, diam.  $\frac{1}{8}$  inch.

is marked by the letter A. The limit of proportionality is reached at 8 tons, 26 tons per square inch, and the yield at 9.25 tons, 30 tons per square inch.

The test piece was stretched 2 per cent. and then a second pull was taken, and the result is shown by curve B. Proportional elasticity had disappeared. Curve C is the record of a pull after a 6 per cent. stretch. Curve D is a repetition test after turning the bar to a slightly reduced diameter. The time interval between C and D is twenty-four hours. No restoration of elasticity has taken place. And it has been established by other experiments on the same material that a lapse of several months has no effect. The piece was then boiled for one hour, and the test curve E shows that the boiling has not produced elastic recovery.

Finally the piece was heated in a muffle furnace to 550° C., and was kept there for half an hour, and was then cooled with the furnace. Line F, taken immediately after this treatment, shows perfect elastic recovery with a slight raising of the limit and the yield-point.

Contrast the curves of Fig. 141 just considered with those of Fig. 142, showing the results of tests made on a test piece of mild steel carbon 0.15 per cent. A is the record of the first pull; D



July 22, 1918	1st Pull
" "	4th " after 2 per cent. stretch
" "	6th " " 4.2 per cent. "
Aug. 7, 1918	7th " " 15 days' rest.

FIG. 142—Mild Steel, 0.156 per cent. C.  
Gauge Length 5 inch, diam.  $\frac{1}{4}$  inch.

is the record after the piece had been stretched 2 per cent. ; F the record after a stretch of 4.2 per cent. Then the piece was taken out of the apparatus and laid aside. After fifteen days rest it was retested and G shows the result. The elastic recovery is complete. Lapse of time alone has transformed the imperfectly elastic line F into the perfectly elastic line G.

The influence of time on the elastic recovery thus depends upon the metal. Iron and mild steels are influenced profoundly. Alloy steels and high-carbon steels are hardly influenced at all. These materials must be heated to a relatively high temperature to restore imperfect to perfect elasticity.

**70. Looping under Constant Load.**—The diagram, Fig. 143,

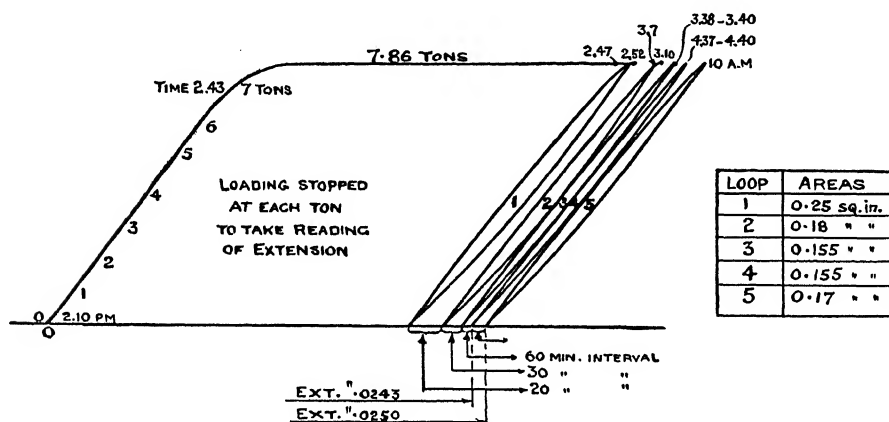


FIG. 143.—Looping under Constant Load. 0.8 Carbon Steel.

shows the effect of looping under constant load, the material used being 0.8 carbon steel.

The test piece was placed in a Buckton testing machine and the load was applied gradually until yield began at 7.86 tons, and then loading was stopped. Extension was allowed to proceed under this load for four minutes, and then the load was removed and reapplied to the same value. The spot of light traced out the loop marked 1 in the figure.

Extension under the load, still 7.86 tons, went on slowly, and loops 2, 3 and 4 were taken at intervals of twenty, thirty, and sixty minutes respectively. The load was then maintained during an interval of seventeen hours twenty minutes, and then loop 5 was taken. During this long interval the gauge length stretched about  $\frac{1}{1000}$  of an inch.

Comparing these loops, it will be seen that there is no recovery

of proportional elasticity during a gradual stretch of about twenty hours under the yield load of 7.86 tons. The inference is that if the yield load is kept on the test piece until it has stopped extending, a process which may take a long time, the material does not recover its elastic state but continues in its state of imperfect elasticity. The behaviour of iron or mild steel under this test would probably be different.

#### 71. The Practical Utility of the Looped Diagram.—

A record showing the elastic line and a few loops may be of great practical utility in industrial applications. The diagram, from normal material satisfying known conditions of composition and manufacture, may be used as a diagram of comparison. The form of the curve, the loop area, and the rate of increase are all sensitive to changes in the material and to changes in the inner state of the material. The effect of subjecting a material to different processes of heat treatment can be studied by means of a diagram of this kind.

The diagram is also useful in showing the load at the limit of proportionality, for this load bears neither a constant relation to the yield-point, when there is one, nor to the ultimate load. Consequently factors of safety reckoned against either the yield load or against the ultimate load are ambiguous.

The diagram may be found useful to the engineer and metallurgist, especially when used in conjunction with a no-load to break diagram, in co-ordinating the results of the many different tests now made to ascertain the quality of metals. In Chapter II it has been shown that the form of the no-load to break curve quite definitely discovers whether the metal is in the overstrained condition. The elastic and looped diagram gives additional aid in this respect.

But it promises help in another direction, which has not yet been fully explored. It is probable that the limiting range of stress in fatigue has for its positive value the stress equal to the limit of proportionality, at any rate to a first approximation, belonging to a material in its normal state. If this can be established then the upper fatigue limit can be discovered by an inspection of the elastic record.

For example, referring to the diagram for iron (Fig. 126), it will be seen that the limit of proportionality is about  $3\frac{1}{2}$  tons, corresponding to 11.4 tons per square inch. Eight test pieces of the same material were independently tested for fatigue limits at the National Physical Laboratory by Dr. Stanton, and it was found that after applying in the aggregate 24,000,000 alternations



of load, the limiting range of stress in fatigue fell between  $\pm 10\frac{1}{2}$  and  $\pm 13$  tons per square inch.

The average value of the upper limit in fatigue is therefore 11.75 tons per square inch. The limit of proportionality found by inspection of the elastic diagram, namely, 11.4 tons per square inch, is thus within the limits actually found and approximates closely to the mean value.

If this result could be generalized it could be asserted that a load elastic extension record shows the positive value of the fatigue limit. The long and tedious experiments with alternating loads, although necessary for scientific research, would be unnecessary in practice. Such an assertion requires to be fortified by

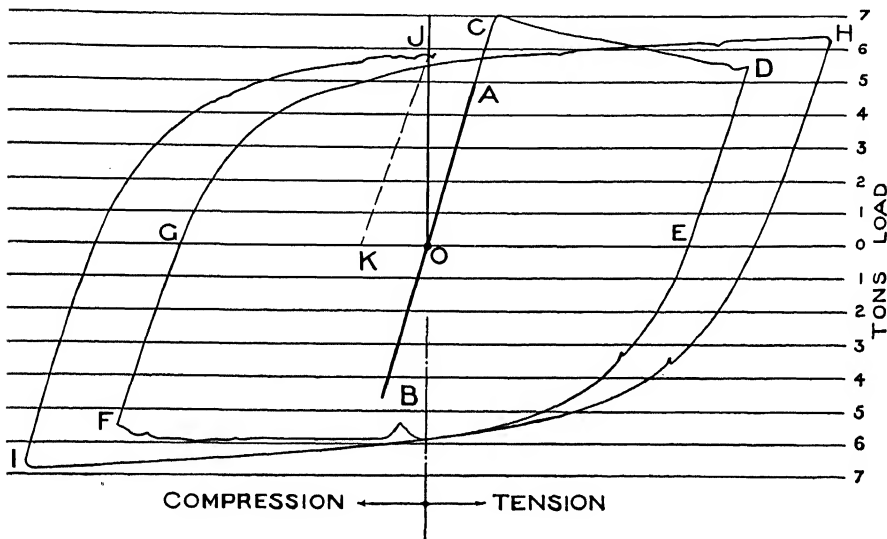


**FIG. 144.**

satisfactory comparisons over a wide range of materials. This therefore is a promising field of research.

**72. Push-and-pull Diagrams.**—A useful type of diagram is shown in Fig. 144. It may conveniently be referred to as a push-and-pull diagram, because the test piece is alternately compressed and stretched.

The diagram is taken with the instrument shown in Fig. 120, fitted in a hydraulic machine like that seen in Fig. 16, except that the hydraulic cylinder is made to be double-acting and the control valves are suitably altered. The weigh bar is secured in a top mounting so that it can take either a push or a pull. The test piece from which the diagram, Fig. 144, was taken is

shown in Fig. 145. The diameter of the cylindrical part is 0.625 inch and the gauge length between the flanges is 2 inches. After the test the piece ran between lathe centres with almost

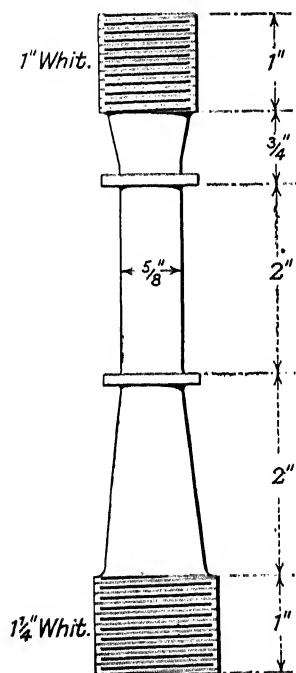


FIG. 145.—Test Piece.

perfect truth, showing that there had been no lateral bending. In fact, the error was not more than may be found when a test piece is run between centres after a test wholly tensile.

The test is applied in this way. Looking into the microscope attached to the instrument, a field of view is seen like that shown in Fig. 146. When the adjustments are correct the spot of light is in the centre of the camera plate when the index is at the centre of the field.

Watching the index through the microscope the tension valve is slowly opened and the index is seen to creep to the left. When it reaches a pre-determined value on the stretch scale the valve is closed and the stretching stops and the test piece is held in tension under the load corresponding to the stretch.

The pressure is then relieved and the compression valve is opened and it is kept open until the index has reached an assigned value on the compression scale to the right of the zero. The valve is then closed and compression stops and the test piece is held under the load corresponding to the compression. The pressure is then again relieved and the tension valve is opened for a second time and kept open until the index reaches an assigned value on the stretch scale.

The test piece can thus be loaded between increasingly wide limits in tension and compression. The test is ended by bringing the index back to the central zero, and finally removing the load.

When the index is at zero, the test piece has been brought back to its primitive dimensions in respect of gauge length, but

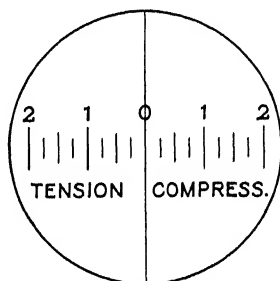


FIG. 146.

it is still in a state of stress. When the load is relieved the piece returns to a state of no stress and its primitive form changes to dimensions corresponding with the amount of load removed.

Turning now to the diagram, Fig. 144, the test cycle was designed to stretch and compress the test piece within the elastic limit and then to stretch and compress it after the elastic limit had been passed and the metal had become plastic.

In looking at the diagram it may be remembered that the total stretch shown is about  $\frac{1}{10}$  of an inch and the total compression shown is the same.

The first pull displaced the spot of light from zero to A and produced a load of 5 tons, 16.3 tons per square inch. The removal of the load displaced the spot down the same path back to zero. There is no trace of looping.

The first push displaced the spot from zero to B. The removal of the load displaced the spot back along the same path to zero. There is no trace of looping. The spot has moved between the approximate limits of +5 tons and -5 tons along a straight line showing that the modulus of elasticity is the same in tension as in compression and that the range of stress applied is well within the limits of elasticity.

The second pull carried the load beyond the yield at C and displaced the spot from zero through A and C to D. The removal of the load displaced the spot from D along an imperfectly elastic line to E.

The second push displaced the spot from E to F. The mere reversal of the stress has provoked an altogether different response from the test piece. From D to E the path is nearly straight. From E to F the path bends and shows a compression approaching the perfectly plastic conditions.

The removal of the load displaced the spot from F to G and the kind of response changed from the plastic to the imperfectly elastic.

The third pull displaced the spot from G to H and the path shows a stretch approaching the perfectly plastic condition.

Removal of the load and the third push displaced the spot from H to I.

Removal of the load and the fourth pull displaced the spot back to J.

The gauge length then had returned to its primitive dimension. The removal of the load displaced the spot to K. The distance OK is the permanent set produced by the cycle imposed on the test piece.

**73. The Yield in Compression.**—Fig. 147 shows a push-and-pull diagram from a test piece of equal dimension with and of the same material as the test piece from which the diagram Fig. 144 was taken.

The loading was applied so that the material was broken down in compression.

The first push displaced the spot from zero to A, and produced a load of  $4\frac{1}{2}$  tons, 15.5 tons per square inch.

The relief of the load and the first pull displaced the spot through zero to B, producing a load of 5 tons.

The relief of the load and the second push carried the load

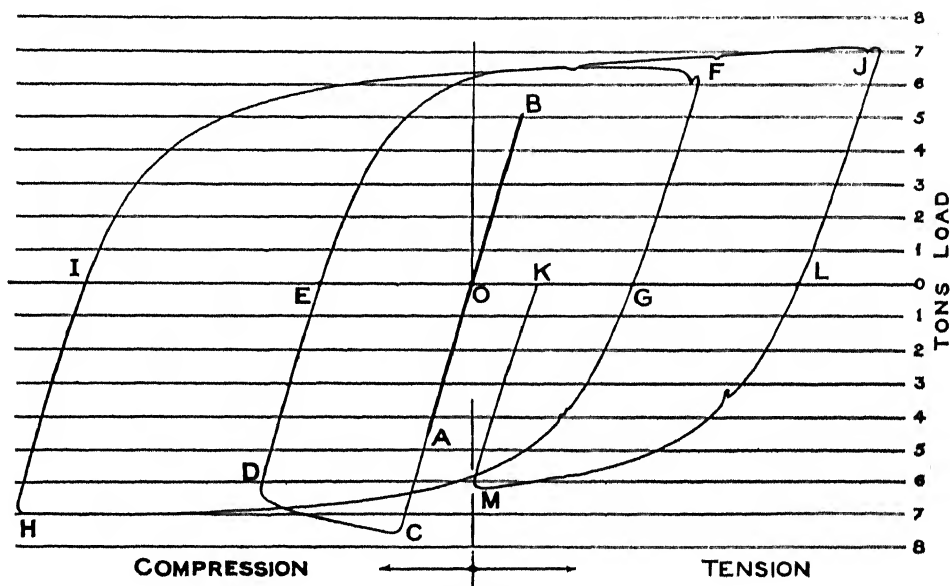


FIG. 147.

beyond the yield at C and displaced the spot through the zero A and C to D.

The relief of the load and the second pull displaced the spot from D through E to F.

The relief of the load and the third push displaced the spot from F through G to H.

The relief of the load and the third pull displaced the spot from H through I to J.

The relief of the load and the fourth push displaced the spot from J through L to M, the centre of the scale, and therefore the gauge length was reduced to its primitive dimension.

The relief of the load displaced the spot from M to K. OK is the permanent set of the gauge length produced by the cycle imposed on the test piece.

Comparing the original plates together the slope of each elastic line is the same and corresponds to a modulus of elasticity of 13,200 tons per square inch both in tension and compression.

The yield in tension took place at 7.2 tons, 23.4 tons per square inch. The yield in compression took place at 7.75 tons, about 25 tons per square inch.

Comparing the diagrams, it will be seen that the phenomena of yield is much the same in tension as in compression, except that the breakdown is not quite so sharp in compression. After the yield has been passed both diagrams show the characteristic that an increasing load provokes a plastic response from the material, while a decreasing load is nearly elastic in the sense that the path is nearly a straight line.

**74. Torque Twist Diagram.**—A diagram showing the relation between torque and twist is shown in Fig. 148. The

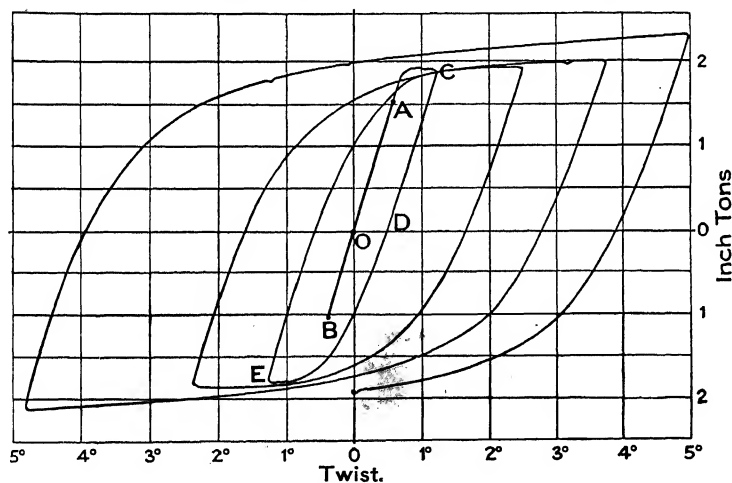


FIG. 148.

describing point of light moves proportionally to the torque, vertically, and proportionally to the twist of the gauge length, horizontally. Any point on the curve therefore fixes by its ordinate the torque on the test piece and by its abscissa the twist which that torque has produced on the gauge length.

The diagram was taken with the apparatus described below from a mild-steel test piece  $\frac{7}{8}$  inch diameter. The gauge length on which the twist was measured was 2 inches. Starting from

zero the spot of light first moved along the straight path to A as the torque was gradually increased from zero to about 1.5 inch-tons. The torque was then removed and the spot retraced its path back to zero. A negative torque, increasing gradually to -1 inch-ton approximately, displaced the spot down the straight path to B; and its removal displaced the spot back along the same path to zero.

So far the twist is proportional to the torque. Measuring from the original plates, it was found that a torque of 1.2 inch-tons produces a twist of 0.475 degrees on the gauge length of 2 inches.

Let  $T$  be the torque in inch-tons which produces the twist  $\theta$  degrees on a gauge length of  $L$  inches.

Let  $I$  be the polar moment of inertia of the section of the test piece. If  $d$  is the diameter of the test piece, then

$$I = \frac{\pi d^4}{32} = 0.0575 \text{ when the diameter is } \frac{7}{8} \text{ inch.}$$

Let  $C$  be the modulus of rigidity of the material, tons-inch units.

Then  $C$  can be calculated from the well-known relation,

$$C = \frac{57.3TL}{\theta I}$$

This reduces to  $C = 5030$  with  $T = 1.2$ ,  $\theta = 0.475$ ,  $L = 2$ , and  $I = 0.0575$ .

Reapplying the torque, the material yields at 1.83 inch-tons and the spot is displaced to C through the point A.

Let  $f$  be the maximum shearing stress in the material corresponding to the yield torque 1.83 inch-tons.

Let  $Z$  be the modulus of the section, which for the circular section of the test piece is  $\frac{\pi d^3}{16} = 0.1315$  when  $d$  is  $\frac{7}{8}$  inch.

Then  $f$  can be calculated from the well-known relation,

$$f = \frac{T}{Z}$$

This reduces to  $f = 13.9$  tons per square inch with  $T = 1.83$  and  $Z = 0.1315$ .

This is a measure of the yield of the material in shear.

Removal of the torque displaced the spot along the almost straight path to D. The operations so far have produced a permanent twist OD. A negative torque displaces the spot from D to E, the material again breaking down at about 1.8 inch-tons torque. The twisting of the test piece between increas-

ingly wide limits by alternately removing and reapplying positive and negative torques is continued until the diagram seen in the figure is complete.

Comparing this diagram with a push-and-pull diagram, there is a striking similarity in form. Both show an elastic line and a limit of proportionality. Both show a definite yield of the material, followed by a plastic flow. Both, after yield, show an imperfectly elastic line when load or torque is removed. And both show an imperfectly elastic line merging rapidly into a plastic curve and a new yield with increase of load or torque.

Torque-twist diagrams from cast iron, brass, high-carbon steel, copper, are similar in general form to that shown for mild steel.

The following data have been deduced from such diagrams.

	C, Tons per Square Inch.	$f$ , Tons per Square Inch.
Mild steel . . . . .	5030	13.9
0.8 carbon steel . . . . .	5400	17.0
Cast iron . . . . .	2240	2.4 doubtful
Brass rod . . . . .	1282	4.8 doubtful

The values under  $f$  are not the ultimate shearing strengths of the materials, but the shearing stress corresponding to the yield torque.

**75. The Dalby Torque Twist Recorder.**—A general view of the instrument is shown in Fig. 149. A test piece T is seen standing on end in front of the apparatus. To the right is a torque tube W on end. The torque tube is provided with a jaw at one end and a flange at the other, both solid with it.

A test piece T and a torque tube W are in place in the apparatus and ready for a test. The test piece is secured to the torque tube by the set screws shown. When secured together any torque applied to one is equally applied to the other. The torque on the torque tube is thus a measure of the torque on the test piece, since it is so proportioned that its limit of proportionality in shear is never exceeded. The torque tube is permanently secured to the frame by its flange. It is carefully set up so that the cylindrical sliding poppet head F is accurately in line with it.

To put in a test piece, the sliding head F is drawn back and one end of the test piece is pushed into the jaws of the torque tube registering there by the turned spigot on its end. Then the sliding piece is pushed up until the turned spigot on the other end of the test piece registers in it. In this way the axis of the test piece is placed accurately in line with the axes of the torque bar and the sliding head F. The set screws are then tightened up on the flats of the test piece.

Torque is applied to the test piece by turning the handwheel H. The twist produced is watched in the microscope M on a scale like that shown in Fig. 146.

The spot of light focused on the camera plate P from the source S describes the torque-twist diagram as the torque is applied and varied. The beam from the source S is reflected successively from two mirrors of an optical cell of the same type as that used with the load-extension instruments. The optical cell is dropped in place after removal of the cap O.

The lower mirror of the optical cell is connected by a system of levers to the torque tube so that an angular twist of the tube produces an angular displacement of the mirror and therefore a linear displacement of the spot across the plate proportional to the torque. The connecting levers are so designed that only the torque is transmitted to the mirror. Any bending of the torque tube is cut out and does not affect the mirror. The upper mirror of the optical cell receives an angular displacement proportional to the twist of the gauge length.

The gauge length is defined by two flanges turned on the test piece. A hole is drilled in one flange and a slot in line with it



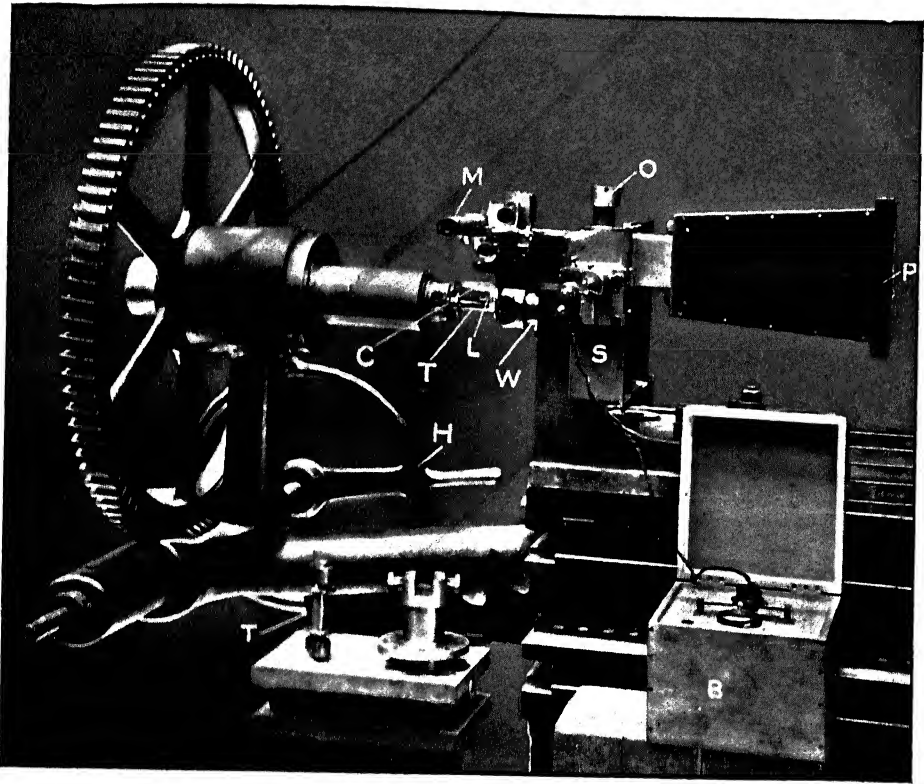


FIG. 140. The Dalby Torque Twist Recorder.

is cut in the other flange. A triangular plate C (Fig. 149) with three pointed legs is used to transmit the relative twist of the flanges to the vertical lever L, which by means of a light pole engages the upper mirror of the optical cell.

The plan of the plate on the test piece is shown in the normal and in a displaced position in Fig. 150.

Leg No. 2 rests in the hole in the flange. Leg No. 1 rests in the slot of the other flange. Leg No. 3 rests in the slot in the bottom end of the lever L. This slot is at right-angles to the slot in the flange of the test piece. Any small twist of the

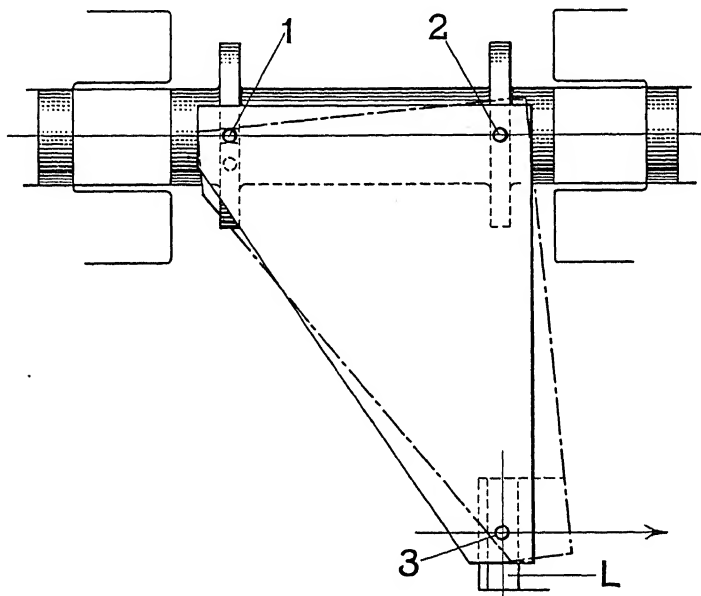


FIG. 150.—Plan of Triangular Plate.

gauge length is by means of this plate transmitted to the upper mirror of the optical cell and so moves the spot of light up or down the plate proportionally.

The whole of the recording apparatus, the camera and the source of light and the microscope, are carried by a framework secured to the end of the torque bar projecting beyond the flange. All these parts are therefore free from strain when the torque is applied because it is passed from the bar to the frame through the flange and bolts securing it to the main frame of the apparatus.

The torque bar is calibrated directly. A bar is placed across the end of the tube in its slotted end and is secured there by the

set screws. The sliding head F is fitted with a centre, like a lathe centre, and is pushed up so that this centre engages a centre hole drilled in the face of the cross-bar. Known loads are applied in succession to the bar at a known radius, and for each load the displaced spot is moved across the plate and so traces out a line of known torque value. The torque scale printed with the diagrams was found in this way.

The twist scale is found from a specially prepared test piece. Instead of one slot being milled in the left flange, several are cut at a known angular distance apart. The cutting of these slots in a modern milling machine is an operation of ease and accuracy. Then No. 1 leg of the triangular plate is placed in these slots in succession and the spot is moved so that it traces out a line on the plate corresponding to each slot.

The apparatus is easily worked. A torque-twist diagram like those illustrated can be taken in about two minutes. The torque may be applied by any method which may be found convenient. In Fig. 149 a single worm and worm-wheel is shown. A double-gearred worm-gear may be fitted, hand-operated, or it may be operated by a motor.

Many types of diagram may be taken. The type shown is a continuously widening limit of twist. This is a useful type, since it enables the elastic characteristic of the material in shear to be deduced from it with quickness and ease. It shows the limit of proportionality in shear, the yield torque, and the slope of the elastic line gives the modulus of rigidity as illustrated above.

**76. Comparisons and Conclusions.**—Glancing at the looped diagrams, Figs. 121 to 134, one property of metal is revealed by all of them. And this is, that after the limit of proportionality has been passed, the response of the metal to the removal and the reapplication of a load is an absorption of energy represented by an area. Other things being equal, the magnitude of the area depends upon the kind of metal. The loops vary from small sizes in soft iron to large sizes in high-carbon steels and to even larger sizes in zinc and other metals. The curved boundaries of the area follow generally the slope of the elastic line of the metal, and this remains true up to the moment of fracture.

Compare these looped diagrams with the push-and-pull diagrams (Figs. 144 and 147). The response to the removal of load of either sign is the same as in the looped diagrams, namely imperfectly elastic. But there is a remarkable difference when a load is reapplied of opposite sign to the load removed. Whereas,

as shown in the looped diagram, the response to the reapplication of a load of the same sign as that removed is an imperfectly elastic line, the response shown in the push-and-pull diagrams to the application of a load of opposite sign to that removed is mainly plastic. Thus we may say that an alternating load is met by an alternating response from the material. Response to removal is elastic, though imperfectly elastic; response to an application of load of opposite sign to that removed is mainly plastic.

Similar characteristics are exhibited in the torque-twist diagram (Fig. 148). Response to removal of a torque of either sign is imperfectly elastic; response to an application of torque of opposite sign to that removed is mainly plastic.

What is the explanation of this alternative response? How is it that up nearly to fracture the metals keep elastic property?

Even when fracture is imminent elastic shortening is visible to the eye when the load is removed. What is seen is the shortening corresponding to the distance YZ (Fig. 123). The explanation rests on the researches of Ewing and Rosenhain and on the recent researches of Carpenter published in *Proc. Roy. Soc.*, Vol. 100, Series A, 1921.

Ewing and Rosenhain established facts of primary importance to the science of metallography, and a full account of their work will be found in the Bakerian Lecture delivered at the Royal Society in 1889 and published in *Phil. Trans.*, Vol. 193, Series A, under the title "The Crystalline Structure of Metals." The particular part of their work which bears upon the question of the alternating response to an alternating load is that part in which they show that a crystal-block structure responds elastically to loading so long as the stress is within the limit of proportionality, but when this limit is exceeded the crystal structure slips along gliding planes within the blocks themselves. They recorded that when a polished and etched section is watched in the microscope the appearance of a particular block remains unchanged so long as the stress applied is below the limit of proportionality, but when this limit is exceeded, fine lines, and then, as straining proceeds, systems of lines crossing one another, appear in the field of view. These lines are held to indicate a serrated or stepped surface, the steps being produced by relative slipping along gliding planes within the blocks themselves. The authors named these fine lines **slip-bands**.\* Slip bands occur in all metals as soon as plastic deformation takes place.

\* *Proc. Roy. Soc.* Vol. 65, March 16, 1899, page 85.

I have repeated these observations on a piece of Swedish iron kindly given to me by Sir Robert Hadfield. A thin flat test piece is fitted into a straining frame small enough to be carried on the stage of a microscope. One surface of this test piece is polished and etched. The normal unstrained structure is seen in Fig. 151. A turn of the straining screw and fine lines, the slip-bands (Fig. 152), appear across the blocks. A block near the centre of the photograph, Fig. 152, is seen under a magnification of 640 diameters in Fig. 153. This block measures approximately  $\frac{3}{8}\frac{0}{0}\frac{0}{0}$  inch long and  $\frac{2}{8}\frac{0}{0}\frac{0}{0}$  inch wide. The average distance between the slip-bands crossing this block is of the order  $\frac{1}{12}\frac{0}{0}\frac{0}{0}\frac{0}{0}$  of an inch. The shadows cast by the ridges suggest the stepped edges of the slipped layers. In cross-section the surface would be seen on edge, and this edge would look like the teeth of a saw, but somewhat unevenly spaced. The actual inclination of the slipped layers to the polished surface cannot be calculated without a section showing these teeth.

Proceeding with the straining, the systems of lines seen in Fig. 154 appear crossing one another like a network. The magnification is here 120 diameters only, in order to give a general view of the strained inner structure on the standard scale. The structure seen in Fig. 154 is the result of straining the gauge length of the test piece about 6 per cent.

Turning now to the recent researches of Professor Carpenter and Miss C. F. Elam, described in a paper entitled "The Production of Single Crystals of Aluminium and their Tensile Properties," *Proc. Roy. Soc.*, Vol. 100, Series A, December, 1921, and already referred to in Chapter IV, Carpenter has succeeded in producing crystals of aluminium large enough to furnish test pieces 0.57 inch diameter with a gauge length of 5 inches. Tested in the elastic recorder these single-crystal test pieces gave diagrams of the same kind as those from multi-crystal test pieces. There was the elastic line merging at yield into a plastic line, and loops were formed whenever the load was removed and reapplied. The value of the elastic modulus, calculated from the elastic line of the single-crystal test piece, was 4460 tons per square inch. The yield load of the single-crystal test piece was lower than that of the multi-crystal test piece. This is perhaps due to the fact that the amorphous network binds together a multitude of crystal blocks whose axial orientations are infinitely varied, so that the tendency to slip along planes of gliding in a given direction is shared by comparatively few only of the total number of crystals. The remainder present their planes of gliding at angles

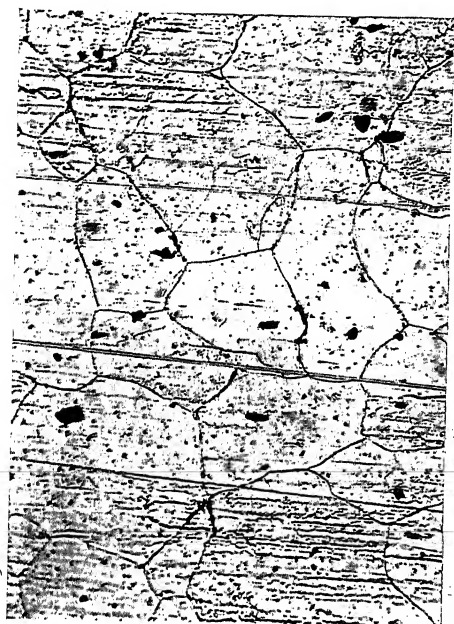


FIG. 151.—Unstrained.  $\times 240$



FIG. 152.—Strained, showing slip bands.  $\times 240$ .



FIG. 153.—Strained, showing central block of Fig. 152.  $\times 640$ .



FIG. 154.—Strained, and showing system of crossed slip bands.  $\times 120$ .

to the applied forces, so that the components of stress along the planes are below the slipping values.

It may therefore be inferred from Carpenter's researches that elastic response and plastic yield are properties of the crystalline structure itself and that these properties are independent of the amorphous structure which binds the crystals together.

There is one striking difference between the shapes of the fractures of single and multi-crystal test pieces. Although the single-crystal test pieces were circular in section and therefore, by analogy with multi-crystal test pieces of circular form, might be expected to show a cup-and-cone fracture, without exception the single-crystal test pieces drew out at fracture to the shape of a wedge. The inference from this is that a single-crystal test piece draws out to fracture along gliding planes. This is a singular confirmation of Ewing and Rosenhain's work on slip-bands and it indicates that the cup-and-cone fracture so often seen in the circular test piece is a consequence of its multi-crystal structure.

Carpenter's work therefore enables us to base the discussion of alternating response to alternating loads on the ascertained fact that the elastic property of the metal resides mainly in the crystalline structure. The amorphous network is eliminated from the discussion.

Let us now consider briefly the stresses which are brought to bear upon a crystal block forming part of a test piece. An axial load on the test piece produces on a section inclined to the axis a direct stress and a shearing stress. The shearing stress is a maximum on each of a pair of planes inclined about  $45^\circ$  to the axis of the test piece. Any crystal so situated within the mass of the test piece that gliding planes within its substance coincide with these directions of maximum shear is in danger of slipping along these gliding planes. If we isolate such a crystal block the stresses on its faces are equivalent to a pair of equal and opposite couples, together with the components of the direct forces as indicated in Z (Fig. 155). Each force and couple produces its appropriate action. Let us assume that the gliding plane along which the shearing resistance is the least coincides in direction with the forces of one of the couples, and let us consider the component distortion produced by the forces of this couple alone. This distortion will be typical of the resultant distortion of the crystal as a whole.

Then *a*, Fig. 155, represents the unstrained crystal, whilst *b* shows the crystal deformed elastically by the shearing forces. Perfect elastic recovery is shown at *c* when the forces are



removed and elastic deformation of opposite sign at *d*, followed by elastic recovery *e* after the removal of the load. This

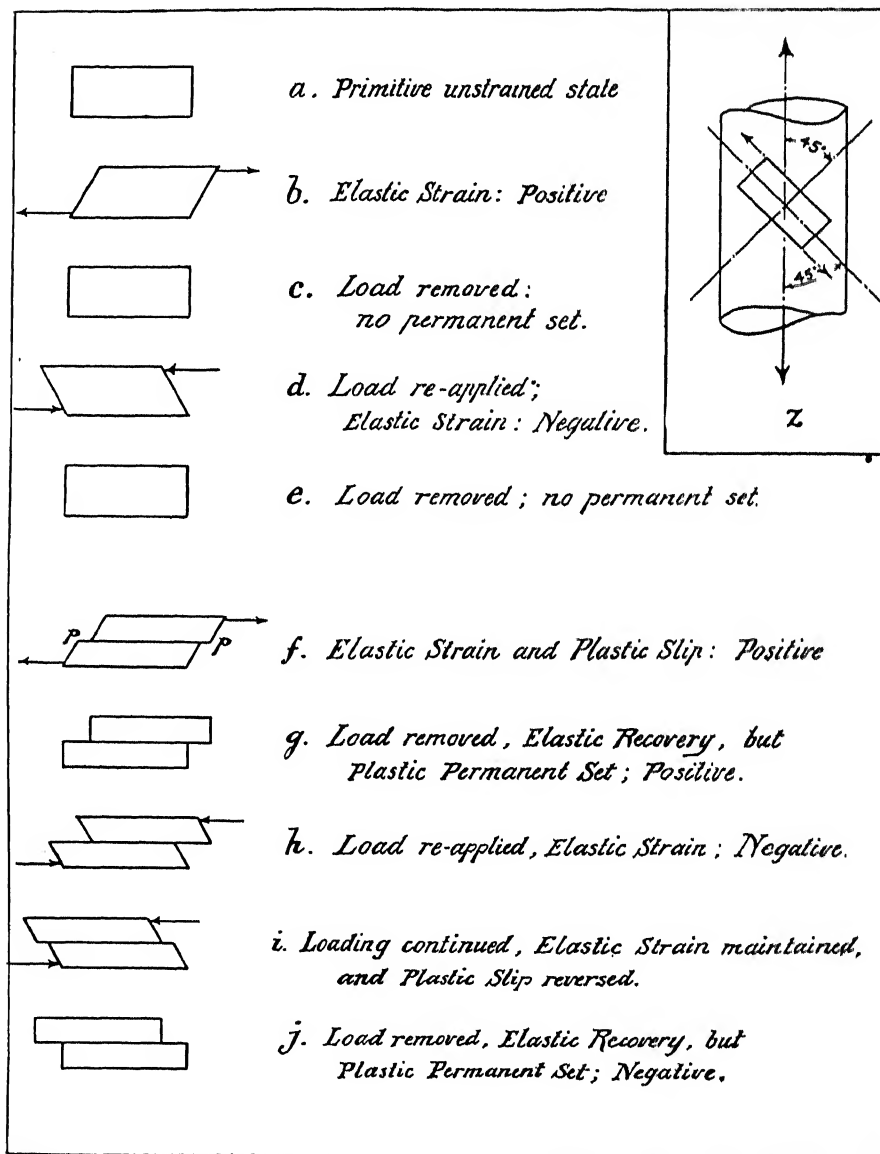


FIG. 155.

imaginary cycle corresponds to the actual cycle O to A, A to O, O to B, and B to O in Fig. 144.



The group of sketches *f g h i j* represent the deformations produced when the forces increase to values capable of producing slip along the gliding planes. The forces first produce elastic deformation like *b*, and then a slip along a gliding plane *pp* as indicated in *f*. Removal of the forces relieves the elastic strain but leaves the parts of the crystal in their displaced positions as indicated in *g*. Reversal of force produces first an imperfectly elastic deformation *h* and slip of opposite sign. Removal of the load again relieves the elastic strain but leaves the layers in their displaced positions. The imaginary cycle may be regarded as equivalent to the actual cycle *OCD, DE, EF, FG* of Fig. 144. The combination of elastic deformation with plastic slip thus explains the shape of the diagrams Figs. 144 and 147, and also the torque-twist diagram Fig. 148.

We may therefore conclude that an elastic strain is a deformation of the crystalline structure, but when this slip occurs the stress has reached the yield stress and the visible sign is plastic yield. Slipping comes on gradually, and this is shown by the difficulty of ascertaining exactly when it commences. A load on the test piece well below the yield load corresponding to the peak of the diagrams will produce slow yielding or creeping if left on long enough. The term limit of proportionality might be defined as the limiting load which is just insufficient to produce creep if maintained indefinitely.

It is generally assumed that relative sliding along a slip plane breaks down the crystalline structure, in the immediate neighbourhood of the glide, into amorphous material. As shown above, some materials, notably iron and mild steels, have the power at ordinary temperature, of recovering their elasticity after overstrain, and it is inferred that they possess the power of healing the injury along the slip planes.

Some metals require to be heated to high temperatures to bring back the elastic state after plastic deformation as shown above. It is still a matter of investigation why mild steel will, after overstrain, slowly heal itself at ordinary temperatures, or rapidly if boiled in water, whilst high carbon and nickel steels cannot do so unless the temperature is raised considerably. There are many other questions which require investigation, assuming always that the slip theory is true. For example, when a slip has taken place, is the debris of the crystal structure along the slip plane identical in quality with the so-called amorphous material which forms the solid network in which the crystal blocks are embedded and bound together? Does the

debris when it recrystallizes unite the slipped parts along the plane by a crystalline mortar indistinguishable from the crystalline structure of the parts, or does it rebuild itself into the amorphous network, leaving the slipped parts of the crystal as individual but now smaller crystal blocks? Or do the crystal boundaries of the slipped parts themselves become active along the plane and become the active rebuilding material? Experimental data on these points are wanting.

Reviewing the experimental data available, however, it is a fair conclusion that an overstrain is a combination of elastic deformation and plastic slip along gliding planes within the crystals themselves, complicated by the power of recrystallization of the broken-down material at temperatures peculiar to the metal itself. And since it has been found, as explained above in Chapter IV that the severest cold-working fails to reduce the crystalline structure entirely to amorphous material, elastic property of an imperfect kind may be expected to persist in overstrained material right up to the point of fracture, as in fact is actually found.

**77. Working Stress and Factors of Safety.**—The practical value of the load and elastic-extension diagram of a material lies in its power to assist in the selection of a working stress which leaves a known margin of safety.

It is usual in practice to fix the working stress as a fraction of the ultimate stress or tenacity. This leaves the margin of safety uncertain because the stress at which the inner structure begins to fail is not a definite fraction of the ultimate stress. The stress at which looping begins is a safer guide because it defines a stress cycle which if repeatedly applied will ultimately destroy the material. Whether after such a load cycle has been applied the material begins to heal itself, or substantially to repair the damage done, either by lapse of time or by heating, is not a question of immediate importance to the designer. The fact of paramount importance is that a stress cycle has been defined which has begun to destroy the structure. The upper value of this cycle is not the yield stress as usually understood, nor is it any definite fraction of it; neither is the upper value of the cycle a definite fraction of the ultimate stress. It is a somewhat indefinite point called the limit of proportionality, and it requires accurate testing to identify it. When this point is identified on the diagram, then a stress cycle has been found which must never be exceeded. The working stress should be chosen sufficiently below this to ensure a reasonable margin of safety.

For example, consider the diagram Fig. 125. The stress at which looping would begin is about 11 tons per square inch. Therefore at this stress slip begins and the crystalline structure begins to break down, and every application of the stress cycle continues the destructive process.

The working stress to ensure a factor of safety of 3 is in this material  $11/3 = 3.6$  tons per square inch. This is a real factor of safety and leaves an ample margin for contingencies between the working stress and the stress at which failure begins. The ultimate strength of this material is 22 tons per square inch, so that, reckoned on this, the apparent factor of safety is 6.

A study of looped diagrams shows that it is not possible to formulate any general rule for the determination of the working stress beyond the rule that the load cycle which causes looping to begin is a safe guide to a working stress which will be consistent with a fairly well defined margin of safety.

## CHAPTER VI

### STRENGTH OF SCREW THREADS

**78. The Scope of the Research.**—The experiments described in this chapter were communicated in 1918 to the British Engineering Standards Association. There was much discussion in Committee about the form of thread to be adopted in the Services, and the relation of strength to form was one of the questions raised.

These experiments were devised by the author to make comparison of strength between threads of different lengths, of different forms, and of different materials, and also to investigate their modes of failure. A special extensometer was designed for measuring the extension of short test pieces, and this was combined with a weigh bar and camera to make a self-contained instrument for getting autographic records.

The form of screw pair used in these experiments is shown in Fig. 156. The experimental part of the screw is a thread 0.625 inch diameter and 14 threads per inch, trimmed to an even number of threads. This thread is turned on the end of a shank  $\frac{1}{2}$  inch diameter and  $\frac{7}{8}$  inch long. The shank is turned solid with the enlarged end. The enlarged end is screwed 1 inch gas. This end is screwed directly into a connector in the head of the piston rod of the testing machine shown in Fig. 16. The nut of the pair screws directly into the muff-coupling of the load-extension instrument.

The prongs of the fork of the extensometer span the shank and rest on the upper surface of the enlarged end of the screw. The extension of the shank and the yielding of the thread is measured by the vertical downward displacement of this annular surface, since the stretch of the massive parts of the nut is negligible compared with the stretch of shank and thread.

The screw pair fails either by the destruction of the thread, as in Fig. 157, or by the fracture of the shank, as in Fig. 158. The strength of the thread is thus always compared with the strength of a shank of constant dimensions, so that the load-extension

diagrams are strictly comparable amongst themselves when the pairs are made from the same material.

Firstly, test pairs of mild steel were turned in order to compare the strengths of threads of the Whitworth form, but of different lengths. Secondly, test pairs of hard steel were turned for a similar set of experiments. Thirdly, test pairs of brass were prepared for a similar set of experiments. Fourthly, test pairs were prepared, all of mild steel. Some of the plugs were trimmed to two complete threads and some to three complete threads, and the thread form was varied. Fifthly, the modes of failure of two of the test threads were investigated. Lastly the effect of thread deformation on the inner structure was examined microscopically.

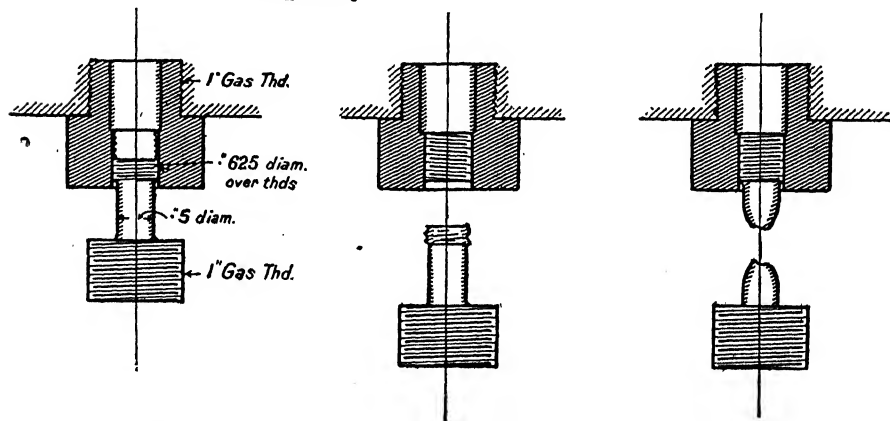


FIG. 156.—Screw Pair. FIG. 157.—Thread Failure. FIG. 158.—Shank Failure.

### 79. Comparison of the Strengths of Threads of different Lengths : Whitworth Form.

**Mild-steel Series.**—The mild steel used had the composition :—

	Per cent.		Per cent.
Carbon . . . .	0.15	Phosphorus . . . .	0.052
Silicon . . . .	0.057	Manganese . . . .	0.99
Sulphur . . . .	0.064		

The results of a test on a 5-inch gauge length are tabulated below.

Ultimate strength . . . .	30 tons per square inch.
Yield . . . . .	23 " " "
Elongation . . . . .	30 per cent.
Contraction of area . . . .	64 "
Stress at fracture . . . .	55 tons per square inch.

Pairs were cut with Whitworth threads, 14 per inch, and the plug threads were trimmed on end to form a series of 1, 2, 3, 4, and 5 complete threads on five of the plugs respectively. The load-extension diagrams of the five pairs are shown together in Fig. 159, each plotted from a separate zero of extension to facilitate comparison. The diagrams in the figure are reproduced  $1\frac{1}{2}$  times the actual size of the diagrams developed on the negative taken with the instrument.

Consider the diagram from the two-thread pair. The length *ab*

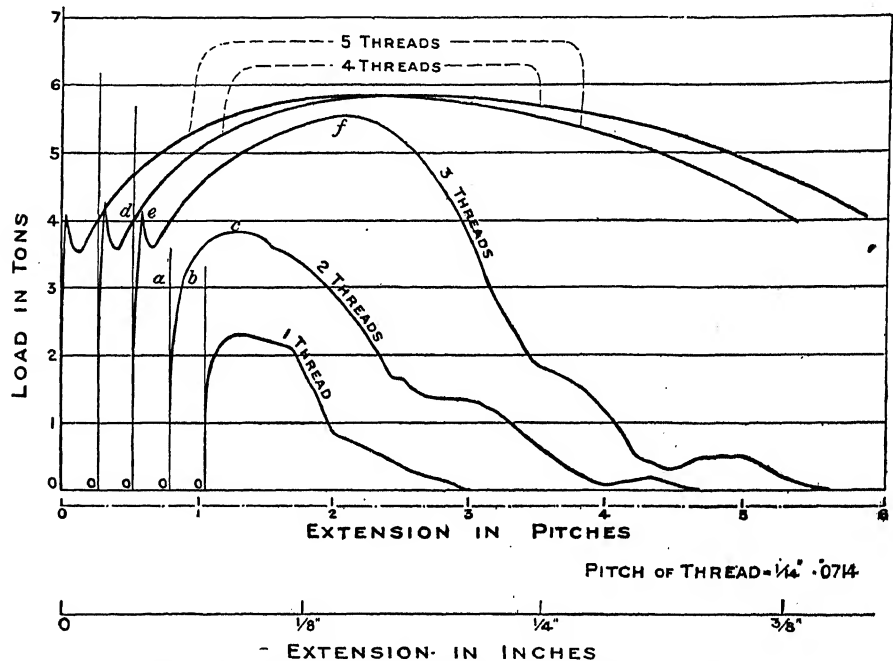


FIG. 159.—Load-extension Diagrams of Five Mild-steel Pairs (Whitworth Thread).

represents the extension of the shank and the yielding of the threads in contact, produced by a load of three tons. The yielding of the two threads in contact is large in comparison with the elastic yielding of the shank. For when the pair is screwed together by hand, contact takes place between the thread of the plug and the thread of the nut at five separate points. The load produces a stress at these points, causing local compression, and this compression extends the area of contact about the five initial points of contact, and thus brings additional points into contact in other places along the thread, until finally a combina-

tion of plastic and elastic yielding results in the bedding of one thread on the other throughout the length of the plug thread. The yielding corresponding to this bedding process in the two-thread plug is greater than the elastic extension of the shank, and the yielding increases rapidly as the load increases to *c*. The threads of the plug fail at this load, and are drawn out against the resistance of the deformed thread of the nut. The point *c* shows that the two-thread plug failed under a load of  $3\frac{3}{4}$  tons, yielding 0.037 inches, or about half a pitch.

The three-thread plug gives a diagram of a different kind. The yield stress in the shank is reached and passed before the three threads give way. They have yielded considerably under a load of four tons, as the length *de* shows, and they hold up very nearly to the maximum load the shank can carry, but not quite. The three threads definitely fail at *f*, and the plug draws out, with the shank still unbroken, but strained almost to its breaking-point. The point *f* shows that the three-thread plug failed under a load of  $5\frac{1}{2}$  tons, yielding 0.114 inch or about 1.6 pitches. The rest of the curve merely records the resistance against which the deformed threads of the plug are drawn out across the deformed threads of the nut.

The two-thread and the three-thread diagrams are typical of two classes of diagram obtained for mild steel: one in which the threads fail before the stress in the shank reaches the yield stress; the other, in which the threads hold up until the yield stress in the shank is passed, but fail before the ultimate stress in the shank is reached. Some diagrams will be seen below in which the threads give way just in the region of the yield load of the shank.

From the diagrams it will be seen that the four-thread pair failed by the breaking of the shank. The threads just held to the maximum shank load of  $5\frac{3}{4}$  tons, but they were considerably deformed.

The five-thread pair failed by the breaking of the shank with only slight deformation of the five threads.

The curve giving the history of the shank failure with negligible deformation of the experimental thread is used as a control curve in these diagrams. The control curve is generally obtained from a ten-thread pair, so that the thread deformation shall be negligible.

**Hard-steel Series.**—The hard steel used had the composition:—

	Per cent.		Per cent.
Carbon . . . . .	0.8	Phosphorus . . . . .	0.01
Silicon . . . . .	0.2	Manganese . . . . .	1.48
Sulphur . . . . .	0.013		

## 162 STRENGTH AND STRUCTURE OF METALS

The results of a test on a three-inch gauge length are tabulated below:—

Ultimate strength . . .	39.9 tons per square inch.
Yield stress . . . . .	24.4 „ „ „ „
Stress at fracture . . .	65.6 „ „ „ „
Elongation . . . . .	17.33 per cent.
Reduction of area at fracture . . . . .	50.25 „

Pairs were cut with Whitworth threads, 14 per inch, and the

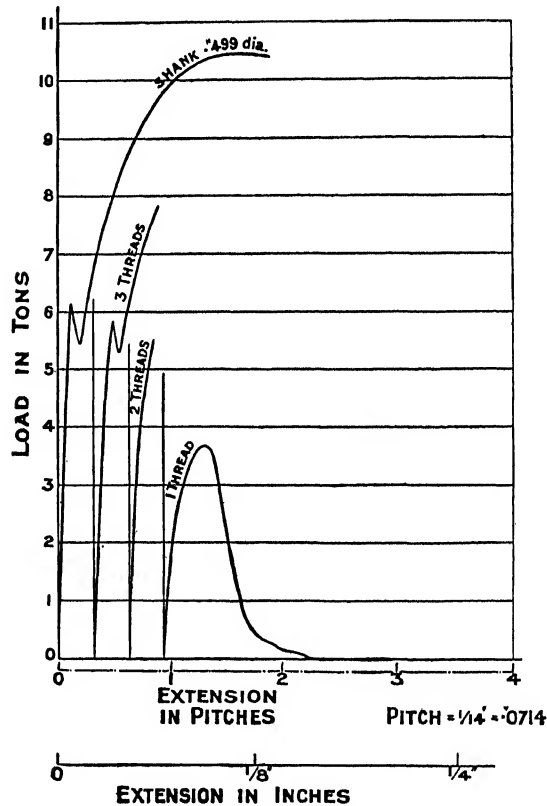


FIG. 160.—Load-extension Diagram, of 0.8 Carbon Steel, 4 pairs (Whitworth Thread).

plugs were trimmed on end to form a 1, 2, 3, complete threads on three of the plugs respectively; a fourth plug was cut with 10 threads from which to get the control diagram. The load-extension diagrams of the four pairs are shown together in Fig. 160, each plotted from a separate extension zero to facilitate



comparison. The diagrams in the figure are reproduced  $1\frac{2}{3}$  times the actual size of the diagrams developed on the negatives taken with the instrument.

The single-thread pair broke when the load reached  $3\frac{1}{2}$  tons. The thread of the plug sheared off clean along its base and was left in the nut complete.

The two-thread plug broke across the section at the beginning of the thread when the load reached 5.5 tons, corresponding to 26.2 tons per square inch of the section actually broken. The fracture was slightly conical, sloping up to an apex coincident with the point of the hole drilled for the lathe centre.

The three-thread plug broke across a section at the beginning of the thread when the load reached 7.8 tons, corresponding to a stress of 37.3 tons per square inch on the area actually broken. The fracture was slightly conical and sloped up as in the two-thread specimen, but it ended well below the lathe centre hole.

The ten-thread plug giving the control curve broke at the root of the shank. The maximum load carried by the shank was 10.45 tons, corresponding to a maximum stress of 53.4 tons per square inch. The yield load was 6.1 tons, corresponding to 31.2 tons per square inch on the area of the shank. The load at fracture was 10.4 tons, corresponding to 62.5 tons per square inch. In this plug the centre of the shank diminished in diameter to 0.461 inch, but did not break there. The diameter of the fractured area measured 0.488 inch.

**Brass Series.**—The brass used had the composition:—

	Per cent.
Cu . . . . .	59.7
Zn . . . . .	40.3

The results of a test on a 5-inch gauge length are tabulated below:—

Ultimate strength . . .	29.2 tons per square inch.
Stress at fracture . . .	43    "    "    "
Elongation . . . . .	20 per cent.
Reduction of area . . .	19    "

Pairs were cut with Whitworth threads, 14 per inch, and the plugs were trimmed on end to give 2 and 3 complete threads respectively, and a third plug was cut with 10 threads from which to get the control curve. The load-extension diagrams of the three pairs are shown together in Fig. 161, each plotted from a

separate extension zero to facilitate comparison. The diagrams in the figure are reproduced approximately  $1\frac{1}{2}$  times the actual size of the diagrams developed on the negatives taken with the instrument.

The two-thread plug failed at 3.4 tons. The threads deformed as cantilevers and allowed the plug to be pulled clean away against the friction of the deformed threads. The total extension of threads and shank at the maximum load measured 0.036 inch, equivalent to about 0.5 of the pitch.

The three-thread plug held up to a maximum load of 4.6 tons,

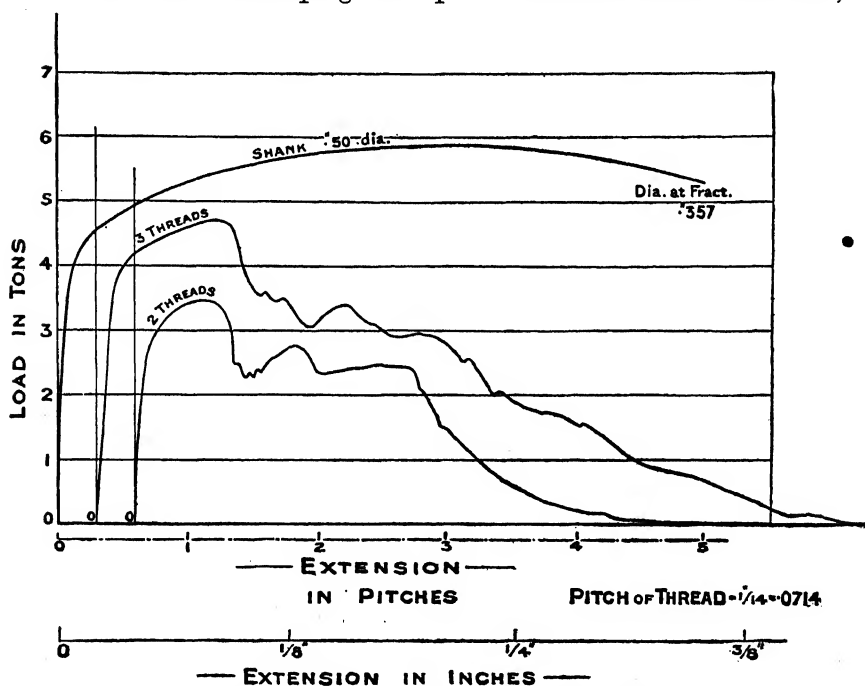


FIG. 161.—Load-extension Diagram of Brass Pairs (Whitworth Thread).

and then the threads failed as cantilevers and the plug pulled out. Total extension corresponding with the maximum load 0.07 inch, equivalent to about 0.96 of the pitch.

The control curves indicate that four threads would have been amply sufficient to carry a load equal to the maximum load which the shank could carry. The control plug broke through the shank, giving :—

Ultimate strength . . .	29.5 tons per square inch.
Stress at fracture . . .	52    "    "    "    "

80. Comparison of the Control Curves.—These curves, Fig. 162, are the load-extension curves of the shanks. The shank is essentially a short specimen originating from an abrupt change of section from  $1\frac{1}{4}$  inch to  $\frac{1}{2}$  inch with a slight radius in the corner, 0.06 inch, and ending with a screw thread, 0.625 external diameter, 14 threads per inch, Whitworth. The plain part of

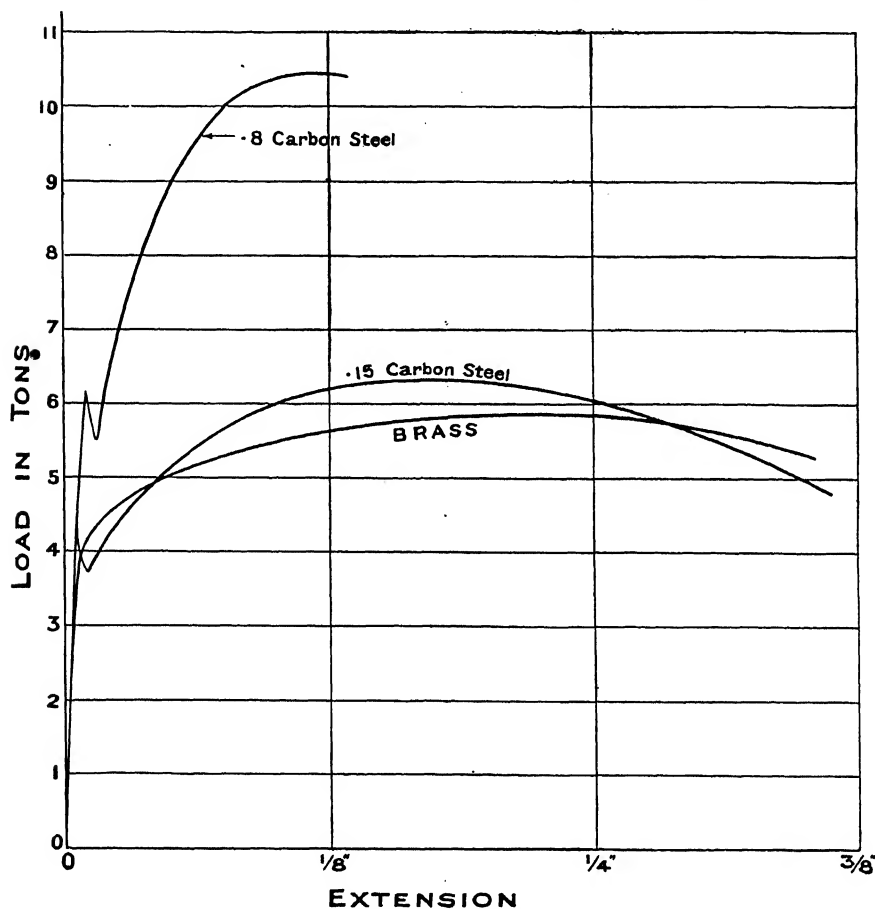


FIG. 162.—Comparison of Control Curves.

the shank is  $\frac{1}{2}$  inch diameter and  $\frac{7}{8}$  inch long. The interest in these diagrams lies in the fact that the material is free to deform and flow at the screw end, whilst at the root of the shank, flow under stress is conditioned by an abrupt change of section from  $1\frac{1}{4}$  inch to  $\frac{1}{2}$  inch.

The effect of this constraint on the flow is to increase the ulti-

mate strength of the hard material, and to increase the flow stress at fracture of the soft materials. The flow stress of the harder material and the ultimate stress of the softer materials are only slightly affected. The following comparative table brings out these points. The heading "Tested normally" means the results of a test on a long specimen where end effects are eliminated.

	Tested normally.	From Shanks. Fig. 158.				
HARD STEEL.						
Ultimate strength	39.9	53.4	tons per square inch.			
Yield stress . .	24.4	31.2	”	”	”	”
At fracture . .	65.6	62.5	”	”	”	”
MILD STEEL.						
Ultimate strength	30.0	32.8	”	”	”	”
Yield stress . .	23.0	22.8	”	”	”	”
At fracture . .	55.0	70.0	”	”	”	”
BRASS.						
Ultimate strength	29.2	29.5	”	”	”	”
At fracture . .	43.0	52.0	”	”	”	”

**81. Influence of the Form of Thread on Strength.**—To obtain information on this point, two-thread pairs with threads of the forms shown in Fig. 163 were constructed together with an equal number of three-thread pairs. The thread-forms used in the comparison are shown in the following table:—

Form of Thread.	External Diameter.	Core Diameter.
Whitworth standard. Angle 55° . . .	0.625	0.5335
Whitworth truncated. Angle 55° . . .	0.614	0.5335
Whitworth deepened. Angle 55° . . .	0.625	0.5235
Whitworth 60°, i.e. $\frac{1}{4}$ off top and bottom	0.625	0.5434
Metric. Angle 60° . . . . .	0.625	0.5260
Sellers. Angle 60° . . . . .	0.625	0.5322

In all pairs the thread in the nut is cut of exactly the same form as the thread on the plug. In order to secure uniformity of quality of the material, the material for the pairs was cut from the same bar of steel, the analysis of which is given in § 79,

and all the pieces were annealed together in a gas furnace at a temperature of 900° C. for one hour and were then allowed to cool down with the furnace.

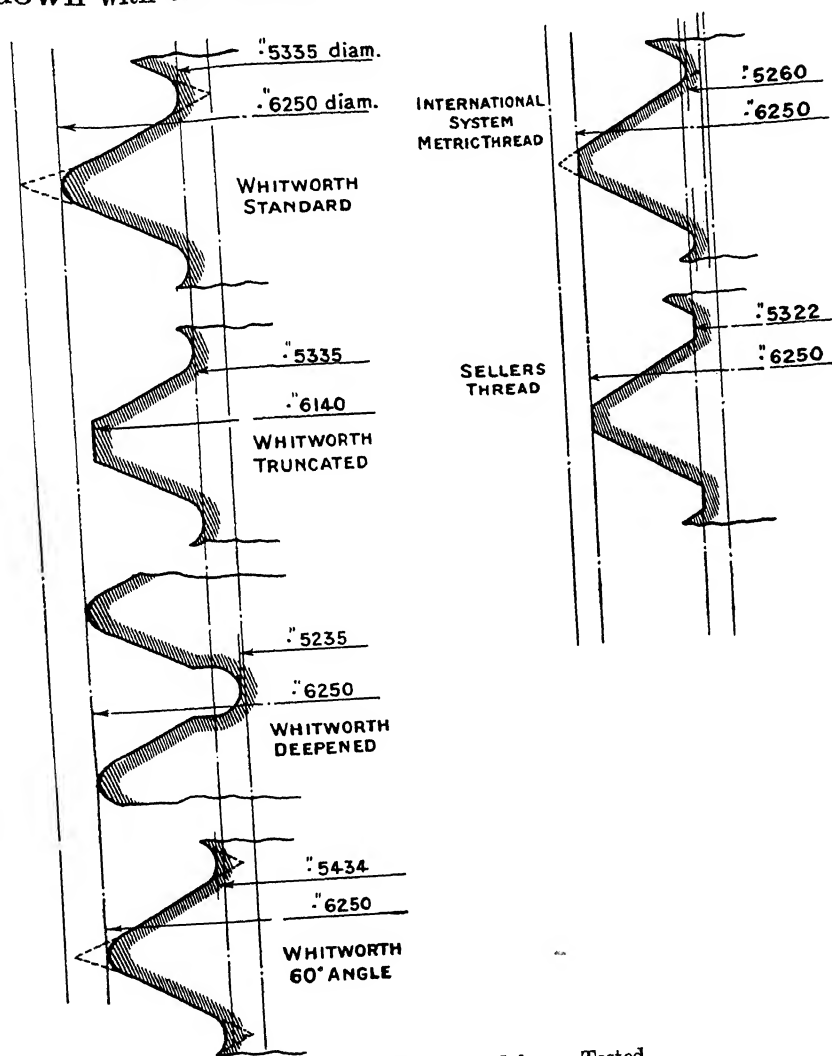


FIG. 163.—Thread-forms Tested.

The curves, Fig. 164, show the result of the tests on the two-thread pairs. The upper curve is a control curve obtained from a ten-thread specimen. The curves fall into two groups, namely a 55° group and a 60° group. The comparison shows that the 60° threads are about 12 per cent. stronger than the 55° threads. The

60° plugs show, with remarkable similarity, that the threads were just failing when the stress in the shank reached the yield stress. The effect of the superposition of the extension of the threads on the extension of the shank is to change the abrupt peak and quick recovery of the shank seen in the control diagram, into a more gradual drop and a more gradual recovery to the slightly increased load at which the thread fails.

Fig. 165 shows the load-extension curves for the three-thread series. The upper curve is a control curve obtained from a ten-thread plug. It will be seen that the 60° threads hold whilst the stress in the shank reaches and passes the yield-point, but

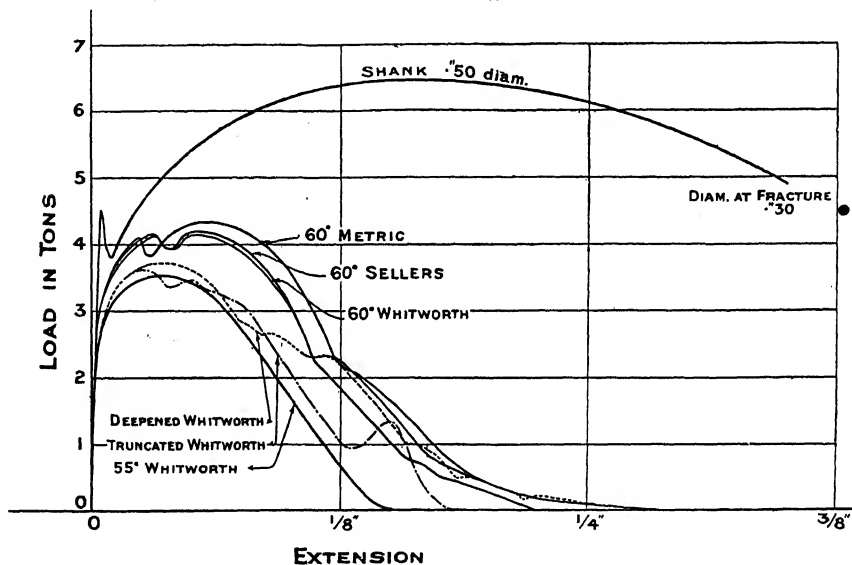


FIG. 164.—Load-extension Diagrams of two-thread Pairs (Mild Steel). Nominal Diam. .625 inches over Threads, but Truncated Whit. .614 inches over Threads.

that they give way before the stress in the shank can reach its ultimate value. The 55° group, although holding until the stress in the shank has passed the yield-point, give way at lower loads than the 60° threads.

The deepened Whitworth is the weakest, but on the diagram it appears to be weaker than it really is, because instead of getting three full threads under load it was found after the test that the plug had not been screwed into the nut quite far enough, so that the test really was a test on 2.8 threads instead of three threads. The truncated Whitworth is weaker than the standard Whitworth, but there is very little to choose between the different

forms of the 60° group. It may be repeated here to avoid confusion that the 60° Whitworth is a thread cut with a tool ground to 60° and having  $\frac{1}{6}$  of the angular depth rounded off top and bottom. It is thus shallower than the standard Whitworth thread.

Comparing these curves together, both from the two-thread group and the three-thread group, it will be seen that the advantage of the 60° over the 55° thread is so slight that the argument for changing the form for the sake of strength has no weight. It is only necessary slightly to increase the length of the thread of any one of the plugs in the 55° groups to bring their strengths equal

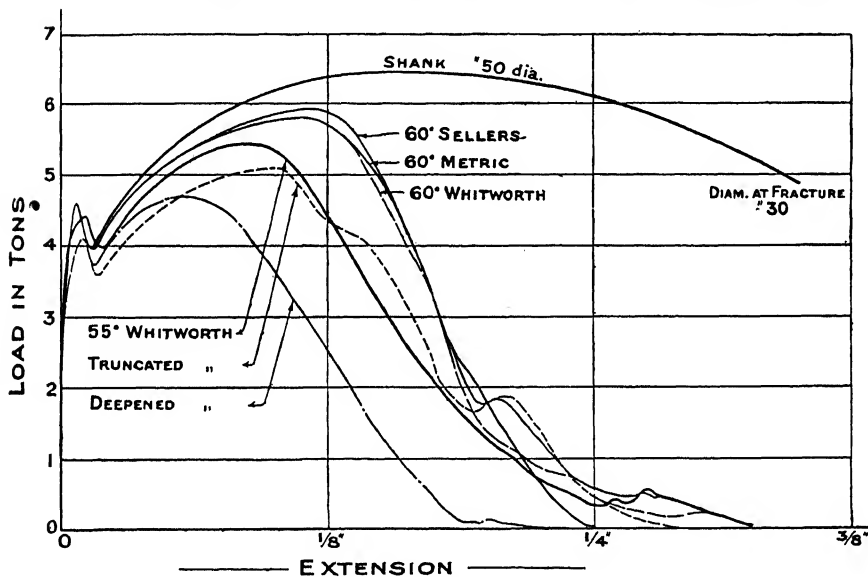


FIG. 165.—Load-extension Diagrams of three-thread Pairs (Mild Steel). Nominal Diam. .625 inches over Threads, but Truncated Whit. .614.

to the strengths of the 60° group. The 60° thread is blunter and therefore puts a greater bursting stress on the nut, a disadvantage if the screw has to stand great longitudinal force as in the screwed pair of a gun breech. Frequently the thread angle is sharpened until a square thread or a buttress thread is formed in order to avoid this bursting action.

**82. Manner of Thread Failure.**—The way in which a thread fails depends upon the material of which it is made. In hard steel the plug thread shears off near the root of the thread. In soft steels and plastic material generally the threads fail as cantilevers, the plug threads turning up and the nut threads

turning down until the deformed plug threads can be pulled out by sliding over the deformed nut threads. Many examples of the kind of resistance against which this sliding takes place are seen in the load-extension diagrams of thread failures above.

The one-thread sample of the hard steel series, seen in Fig. 160, failed by a clean shear of the thread. The thread was left coiled in the nut. The diameter of the sheared surface measured 0.536 inch, whilst the diameter of the turned core was 0.5335. Allowing for the roughness of the sheared surface and the influence of this roughness on the accuracy of the measurement, the diameter of the sheared surface may be taken equal to the core diameter.

The sheared area reckoned from this diameter and the pitch is  $3.1416 \times 0.5335 \times \frac{1}{4} = 0.12$  square inch. The load at which the thread failed, measuring from the diagram Fig. 160, is 3.75 tons, so that the shearing stress at the instant of failure is 31.3 tons per square inch, a value which is quite reasonable for the material.

Turning now to the soft steel threads, Fig. 166 shows the section of the plug and nut after the threads have been deformed, so that the plug can be pulled out over the deformed threads of the nut. This diagram was obtained by tracing a composite photograph of the threads. The photographs were taken about 25 times full size in a microphotographic apparatus, from a plug and nut milled down to a diametral plane. Fig. 166, as printed, has been reduced from the original diagram in order to fit into the printed page.

The figure shows clearly that the threads have failed as cantilevers. Thread A is undeformed. The remaining three threads of both nut and plug have deformed similarly. The relative displacement of plug and nut seen in the figure is about 0.09 inch, so that the figure shows the internal shape of the thread pairs when the plug has been pulled down by this amount. The tangents at the roots of the threads have been drawn in and their distance apart is 0.0464 inch, equal to the depth of the Sellers thread.

This profile form is typical of the thread forms in all of the soft steel specimens and in the brass specimens, except that in some of them the threads have been partially sheared, and in one three-thread specimen the thread was sheared completely off the plug and left in the nut. But, unlike the thread of the hard steel plug mentioned above, the thread sheared in a cylindrical surface considerably greater than the cylindrical surface corresponding to the core diameter. In the truncated Whitworth thread, where there was some shearing, the radius of the cylindrical surface in



which shear took place was about one-quarter the depth of the thread greater than the core radius.

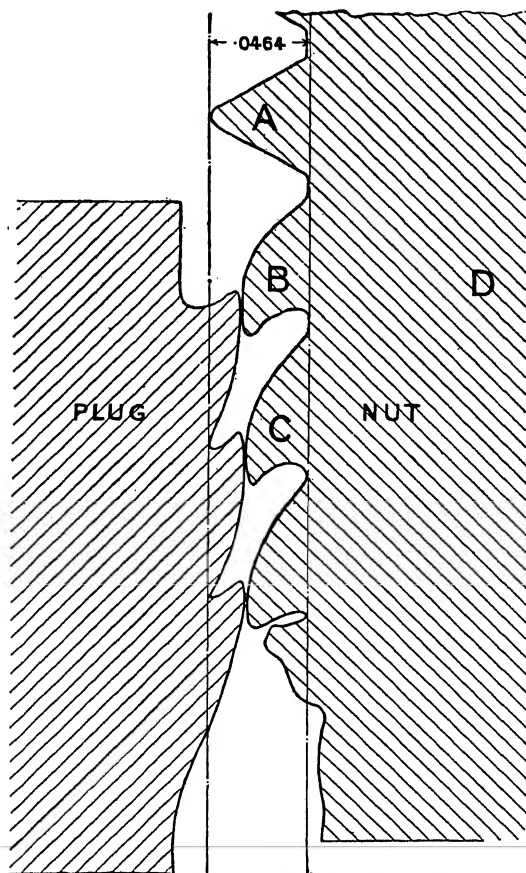
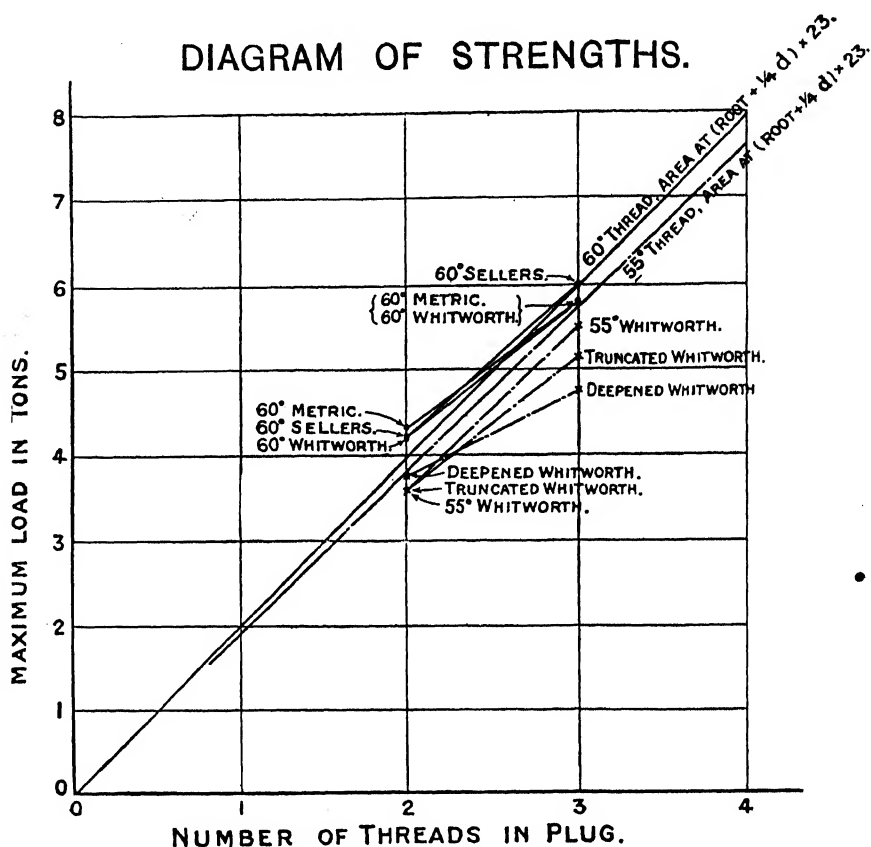


FIG. 166.—Section of Nut and Plug after Failure of Thread.

Fig. 167 shows the strengths of the two- and three-thread specimens of the mild steel series, all of which failed by threads giving way, plotted against the number of threads. Also two lines are drawn starting from the origin, the upper showing the strength of the threads reckoned on a shearing area cut off by a cylinder one-quarter the depth of the thread greater in radius than the radius of the core of a 60° Sellers thread, and taking the shearing strength of the material 23 tons per square inch, the lower line being drawn similarly for a 55° thread. The diagram indicates that the strength of a thread in mild steel may be reckoned from the shearing strength of the material taken as acting uni-

## DIAGRAM OF STRENGTHS.



## DETAILS OF CALCULATIONS

GIVING AREA OF METAL CUT BY CYLINDRICAL SURFACE WHOSE RADIUS IS  $\frac{1}{4}$  THE DEPTH OF THE THREAD LARGER THAN THE CORE RADIUS.

Whitworth.			Sellers and Metric.	
Depth of Thread (in.)	'6403 p. =	'0457	'6495 p. =	'0464
Diam. of Core (in.) ...	...	'5335		
Circum. of Core (in.)...	...	1.6750		
Area of 1 Thread at Root (sq. in.)...		'1196		
Width of Thread at $\frac{1}{4}$ depth (in.) ...		'0474		'0493
Diam. of " " " " " ...		'5565		'5554
Circum. of 1 Thread " " " ...		1.7490		1.7450
Area of 1 Thread " " (sq. in.)		'0828		'0860

FIG. 167.

formly over the area of the threads cut off by a cylindrical surface one-quarter the depth of the thread greater than the radius of the core of the plug.

INNER STRUCTURE OF THE DEFORMED THREAD

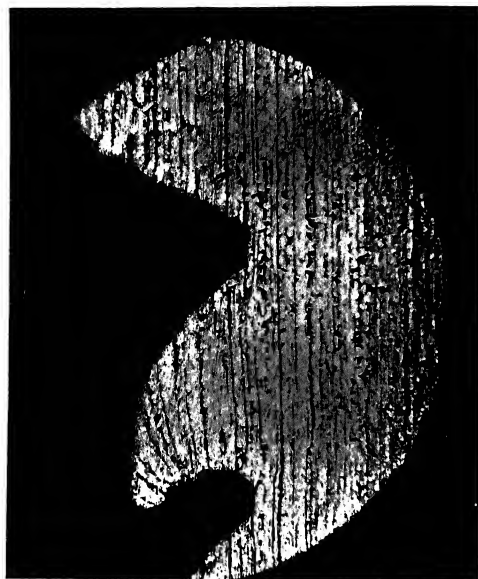


Fig. 168.—Thread A and B. Fig. 166.  $\times 20$ .



Fig. 169.—Normal Structure as in Region D. Fig. 166.  $\times 120$ .

83.  
shows a  
(Fig. 1  
magnifi  
the nut  
The  
bands.  
pearlite  
thread.  
by the

**83. Inner Structure of the deformed Thread.**—Fig. 168 shows a microphotograph 20 times full size of the threads A and B (Fig. 166). Fig. 169 shows the normal state of the material magnified 120 times. It was actually taken from the body of a nut corresponding to the region D, Fig. 166.

The structure is seen to be ferrite bands separated by black bands. These black bands are pearlite. These black bands of pearlite serve to show the distribution of stress in the deformed thread. The average distance apart of these bands is increased by the tensile stress and is reduced by the compressive stress.

4083

## INDEX

- Abel, Sir F., 107
- Allotropic modifications of iron, 84
- Alloys, temperature-concentration diagrams of, 91, 93, 97, 99, 101, 103, 106
  - composition of, by atomic proportion, 92
- Aluminium, single crystal of, 83, 84
- Amorphous material, 79
  - cement, 79
- Annealing, 80, 82
- Area, reduction of, 5, 67
- Ashcroft, Prof., 32
- Austenite, 96, 107
- Barba's law, 72
- Batson, R. G. C., 10
- Bauschinger, 17, 25
- Beilby, Sir G., 80, 82
- Brass, 62
  - looped diagram of, 133
  - structure of before and after annealing, 81
  - temperature-concentration diagram of, 103
  - threads, strength of, 163
- Calibration of weigh bar, 36
  - extensometer, 36
- Carpenter, Prof. H. C. H., 83, 88, 106, 117, 152, 153
- Case-hardening, structures produced by, 97
- Cementation process, 45
- Cementite, 55, 96
- Coker, Prof. E. G., 70
- Constitutional diagram, 105
- Cook, G., 50
- Cooling curves, 85
  - of steel, 88, 90
  - plotting of, 87
- Copper, 61
  - looped diagrams of, 132, 133
- Crowe, J. J., 85
- Crystalline material, 79
  - structure, permanence of, 80
- Curves :
  - control curves of screw threads, 165
  - cooling curves, 85, 87, 88, 90
  - derived differential curve, 89
  - difference method of obtaining cooling curves, 89
  - inverse-rate curve, 87
  - loop area and permanent set, 134
- Dalby optical recorders, description of :
  - elastic recorder, 123
  - no-load-to-break recorder, 31
  - special testing machine for use with, 37
  - torque-twist recorder, 145
- Desch, Dr. C. H., 102, 105
- Diagrams :
  - constitutional, 105
  - deformation, elastic and plastic, 154
  - limiting fatigue-range diagram, 23
  - load-extension in echelon, 68
  - looped diagram, data to be obtained from, 127
    - practical utility of, 140
  - looped diagrams of brass, 133
  - copper, 132, 133
  - iron, 129
  - phosphor bronze, 134
  - steels, 124, 125, 126, 127, 130, 131, and Figs. 135 and 139
  - tin, 132
  - zinc, 131
  - push-and-pull diagram, 141
  - screw threads, strength of, 160, 162, 164, 168, 169, 172
  - torque twist, 145
- Ductility, 69
  - influence of gauge length on strength and, 67
- Elam, Miss C. F., 84, 152
- Elastic diagrams (*see* Looped diagrams)
- Elastic recorder, 123
- Elasticity, 122
  - imperfect, 122
- Etching specimens, 25
- Eutectic mixture, definition of, 94
- Eutectoid, definition of, 97
- Ewing, Sir J. A., 136, 153
- Extension, 5, 67
- Extension, percentage, corresponding to maximum load, 74
  - approximate expression for, 75
- Extensometer for Dalby automatic recorder, 32, 34
- Factors of safety, 156
- Fatigue strength, definition of, 18
- Ferrite, 50
- Form of test-piece, 70
- Furnace, Siemen's regenerative, 48
- Gauge-length and its influence on strength and ductility, 67, 69, 72

- Gerber's parabola, 24  
 Gilchrist process, 47  
 Gold wire, experiments on, 82  
 Guertler, W., 99  
 Gunmetal, 64  
   recrystallization of, 82  
 Hadfield, Sir R., 12, 40, 55, 152  
 Hall, J. W., 49  
 Hankins, G. A., 12  
 Hanson, Dr. D., 83  
 Harbord, F. W., 49  
 Hardness, 14  
   tests for, 9, 11, 12, 13, 14  
 Hardness number, 9  
   relation between hardness number  
   and ultimate strength, 10  
 Hardness scale, Moh, 12  
 Hatfield, Dr. W. H., 120  
 Heat treatment of metals, 54, 57, 118,  
   137  
 Heycock, C. T., 102  
 Impact number, 8  
 Inverse-rate curve, 87  
 Iron:  
   allotropic modifications of, 84  
   alpha, 84  
   beta, 84  
   cast, 65  
   delta, 84  
   gamma, 84  
   puddling process, 43  
   Staffordshire, 43, 129  
   Swedish, 40  
   temperature-concentration diagrams  
   for iron-carbon alloys, 96, 105  
   Yorkshire, 42, 43, 129  
 James, C., 37  
 Jeffries, Zay, 83  
 Jude, A., 8  
 Keeling, B. F. E., 88, 106  
 Kennedy, Sir A. B. W., 32  
 Lepkowski, W. von, 101  
 Levin, M., 93  
 Limit of proportionality, 122  
 Liquidus, 95  
 Load-extension diagrams (*see* pages  
   xi, xii)  
 Loop area and permanent set, 134-136  
 Looped diagram, information to be  
   obtained from, 127  
   practical utility of, 140  
 Looped diagrams (*see* under Diagrams)  
 Looping under constant load, 139  
 Manganese, in copper, temperature-  
   concentration diagram of, 99  
 Martensite, 117, 119  
 Maximum loads, percentage extension  
   corresponding to, 74  
 Mechanical Engineers, Institution of,  
   13  
   Alloys Research Committee, 4th  
   report, 81  
 Mechanical stability, 82  
 Metals:  
   crystallization of pairs of metals  
   from liquid, 91  
   heat treatment of, 54, 57, 109, 118,  
   137  
   inner structure of, 77  
   table of strength and composition  
   of, 66  
   thermal analysis of, 86  
 Microphotographs corresponding to  
   load-extension diagrams (*see* pages  
   xi, xii)  
 Microphotographs, interpretation of,  
   109  
 Moh hardness scale, 12  
 Moore, H., 10  
 Neville, 102  
 No-load-to-break recorder, 31  
 Optical cell, 35  
 Osmond's identification letters, 85, 86  
 Overstrain, influence of time on, 136,  
   137, 138  
 Pannel, J. R., 18  
 Pearlite, 50, 55, 96  
 Phosphor bronze, 64, 134  
   recrystallization of, 82  
 Phragmén, G., 84  
 Polishing specimens, 25  
 Proportionality, limit of, 122  
 Puddling process, 43  
 Rail-testing, 6  
 Range-repetition diagram, 19  
 Recalescence, 85  
   Barrett's experiments on, 86  
 Recorders, autographic, 31  
 Recrystallization, 79, 80  
   brass, 81  
   gunmetal, 82  
   phosphor bronze, 82  
 Reduction of area, 5, 67  
 Reynolds, Osborne, 20  
 Roberts-Austen, W. C., 87, 89, 96, 105  
 Roozeboom, H. B., 105  
 Rosenhain, Dr. W., 86, 89, 105, 151, 153  
 Rykowski, A. E., 99  
 Sankey, Capt. R., 8  
 Scale, Moh hardness, 12  
 Scleroscope, Shaw, 11  
 Screw threads:  
   brass, strength of, 164  
   control curves, 165  
   diagram comparing strengths of  
   metric, Sellers, and Whitworth  
   threads, 169  
   forms of screw-threads, 167  
   influence of form on strength, 166  
   inner structure of, 173  
   relative strength, diagram of, 172  
   screw pair, 159  
   steel, strength of, 160, 162, 168, 169  
   strength of, 158

- Screw threads :  
 thread failures, manner of, 169, 170  
 Whitworth threads, tests on, 159
- Seaton, A. E., 8
- Shaw scleroscope, 11
- Shemtschushy, S. F., 99
- Siemens regenerative furnace, 48
- Siemens open-hearth process, 48
- Similarity, principle of, 71
- Slip-bands, 151
- Solid solution, definition of, 84
- Solidus, 95
- Stansfield, Dr. A., 87
- Stanton, Dr. T. E., 13
- Stead, Dr. J. E., 107, 115
- Steel :  
 blister, 45  
 bright drawn, 52  
 bright drawn, heat-treated, 54  
 chrome, 59  
 cooling curves from, 88, 90  
 crucible cast, 46  
 eutectoid, 110  
 ferro-manganese, 46  
 hardening, 118  
 loop diagrams of (*see* under Diagrams)  
 manufacturing process, 47  
 microphotographs of, 110  
 mild, 50  
 nickel, 58  
 nickel chrome, 59, 130  
 overstrain, recovery after, 137, 138  
 refining, 121  
 relation between strength and inner  
   structure of, 57  
 stainless, 120  
 tempering, 119  
 0.22% carbon, 51  
 0.5% carbon, 110  
 0.8% carbon, 127, 130, Figs. 136-139  
 1% nickel, 54  
 1.4% carbon, 110  
 3% nickel, 124, 126
- Strength, relation between strength  
 and inner structure of steel, 57
- Stress-cycle, definition of, 16
- Stress, working, 156
- Tamman, G., 99
- Temperature-concentration diagrams :  
 alloys, 91  
 brass, 103
- Temperature-concentration diagrams :  
 definition of, 91  
 iron-carbon alloys, 106  
 manganese in copper, 99  
 nickel in copper, 99  
 silver in copper, 101  
 thallium and gold, 93
- Tests :  
 ball, 10  
 Brinell, 9  
 fatigue, 16  
 Haigh fatigue, 22, 51  
 Hopkinson high-speed fatigue, 21  
 reduction of usual tensile test, 5  
 Saniter, 13  
 scratch, 12  
 shock, 5  
 tensile, 2, 5  
 wear—  
   hardness, 13  
   rolling, 13  
   sliding, 14
- Test pieces :  
 British standard notched, 7  
 Dalby flanged, 70, 141  
 forms of, 70  
 Sharpy notched, 6  
 shouldered, 70  
 Wohler fatigue-testing machine, 18
- Testing machines :  
 Buckton 30-ton single lever, 2, 5, 37  
 Isod shock, 8  
 Sharpy shock, 7  
 Shaw scleroscope for hardness, 11  
 special testing machine for use with  
   Dalby recorders, 37
- Thermal analysis of metals, 86
- Thread forms, 167
- Tin, 60, 132
- Torque-twist recorder, 148
- Troostite, 117, 119
- Turner, Prof. T., 12, 49
- Unwin, Dr. W. C., 11, 25
- Urasow, T. T., 99
- Weigh bar, 32
- Westgren, A., 84
- Wicksteed, 32
- Wohler, F., 17, 25
- Zinc, 60, 131